(2)

AFWAL-TR-86-2055

TRACTION MODELING OF MILITARY OILS

Pradeep K. Gupta Inc
117 Southbury Road
Clifton Park, New York 12065

October 1986

Final Report for Period July 1985 - January 1986

Approved for public release; distribution unlimited

AERO PROPULSION LABORATORY
AIR FORCE WRIGHT AERONAUTICAL LABORATORIES
AIR FORCE SYSTEMS COMMAND
WRIGHT-PATTERSON AIR FORCE BASE, OHIO 45433

NOTICE

When Government drawings, specifications, or other data are used for any purpose other than in connection with a definitely related Government procurement operation, the United States Government thereby incurs no responsibility nor any obligation whatsoever, and the fact that the government may have formulated, furnished, or in any way supplied the said drawings, specifications, or other data, is not to be regarded by implication or otherwise as in any manner licensing the holder or any other person or corporation, or conveying any rights or permission to manufacture, use, or sell any patented invention that may in any way be related thereto.

This report has been reviewed by the Office of Public Affairs (ASD/PA) and is releasable to the National Technical Information Service (NTIS). At NTIS, it will be available to the general public, including foreign nations.

The technical report has been reviewed and is approved for publication.

Nelson H. Forster

NELSON H. FORSTER
Project Engineer
Lubrication Branch

Howard F. Jones

HOWARD F. JONES
Chief, Lubrication Branch
Fuels and Lubrication Division

FOR THE COMMANDER:

Robert D. Sherrill

ROBERT D. SHERRILL, Chief
Fuels and Lubrication Division
Aero Propulsion Laboratory

"If your address has changed, if you wish to be removed from our mailing list, or if the addressee is no longer employed by your organization please notify AFWAL/POSL, WPAFB OH, 45433 to help maintain a current mailing list."

Copies of this report should not be returned unless return is required by security considerations, contractual obligations, or notice on a specific document.

DISCLAIMER NOTICE

THIS DOCUMENT IS BEST QUALITY PRACTICABLE. THE COPY FURNISHED TO DTIC CONTAINED A SIGNIFICANT NUMBER OF PAGES WHICH DO NOT REPRODUCE LEGIBLY.

UNCLASSIFIED

SECURITY CLASSIFICATION OF THIS PAGE

AD-A178303

REPORT DOCUMENTATION PAGE

1a. REPORT SECURITY CLASSIFICATION Unclassified	1b. RESTRICTIVE MARKINGS
2a. SECURITY CLASSIFICATION AUTHORITY	3. DISTRIBUTION/AVAILABILITY OF REPORT Approved for public release; distribution unlimited
2b. DECLASSIFICATION/DOWNGRADING SCHEDULE	
4. PERFORMING ORGANIZATION REPORT NUMBER(S) G-104-86-TR	5. MONITORING ORGANIZATION REPORT NUMBER(S) AFWAL-TR-86-2055
6a. NAME OF PERFORMING ORGANIZATION Pradeep K Gupta Inc 6b. OFFICE SYMBOL (If applicable)	7a. NAME OF MONITORING ORGANIZATION Aero Propulsion Laboratory (AFWAL/POSL) Air Force Wright Aeronautical Laboratories
6c. ADDRESS (City, State and ZIP Code) 117 Southbury Road Clifton Park, New York 12065	7b. ADDRESS (City, State and ZIP Code) Wright-Patterson AFB, OH 45433-6563
8a. NAME OF FUNDING/SPONSORING ORGANIZATION Aero Propulsion Laboratory 8b. OFFICE SYMBOL (If applicable) AFWAL/POSL	9. PROCUREMENT INSTRUMENT IDENTIFICATION NUMBER F33615-85-C-2581
8c. ADDRESS (City, State and ZIP Code) Air Force Wright Aeronautical Laboratories (AFSC) Wright-Patterson AFB, OH 45433-6563	10. SOURCE OF FUNDING NOS. PROGRAM ELEMENT NO.: 65502F PROJECT NO.: 3005 TASK NO.: 20 WORK UNIT NO.: 34
11. TITLE (Include Security Classification) Traction Modeling of Military Oils	
12. PERSONAL AUTHOR(S) Pradeep K. Gupta	
13a. TYPE OF REPORT Final 13b. TIME COVERED FROM 01Jul85 TO 31Jan86	14. DATE OF REPORT (Yr., Mo., Day) 1986 October 15. PAGE COUNT 132
16. SUPPLEMENTARY NOTATION Small Business Innovation Research Program - Phase I	

17. COSATI CODES		
FIELD	GROUP	SUB. GR.
21	05	
20	04	

18. SUBJECT TERMS (Continue on reverse if necessary and identify by block number)
Traction, Lubricant Modeling, Elastohydrodynamic, Lubrication, ~~[illegible]~~, ~~[illegible]~~, Rolling Element Bearings, oils

19. ABSTRACT (Continue on reverse if necessary and identify by block number)

A semi-empirical approach to modeling the traction behavior of turbine engine lubricants in concentrated contacts is presented. Coefficients for the model are determined by carrying out a nonlinear least-square analysis of available traction data. The effectiveness of the modeling approach is demonstrated by incorporating the lubricant traction model in a bearing dynamics computer code and by carrying out bearing performance simulations as a function of the coefficients of the traction model.

(Keywords:

20. DISTRIBUTION/AVAILABILITY OF ABSTRACT UNCLASSIFIED/UNLIMITED ☒ SAME AS RPT. ☐ DTIC USERS ☐	21. ABSTRACT SECURITY CLASSIFICATION Unclassified
22a. NAME OF RESPONSIBLE INDIVIDUAL Nelson H. Forster	22b. TELEPHONE NUMBER (Include Area Code) (513) 255-4347 22c. OFFICE SYMBOL AFWAL/POSL

DD FORM 1473, 83 APR EDITION OF 1 JAN 73 IS OBSOLETE.

UNCLASSIFIED

SECURITY CLASSIFICATION OF THIS PAGE

SUMMARY

With the objective of developing analytical traction models for the simulation of rheological behavior of lubricating oils used in practical applications, such as rolling bearings, gears, cams and similar mechanical components, the feasibility of a traction model, based on viscosity-pressure-temperature relations in elastohydrodynamic contacts, is demonstrated for two military lubricants with the MIL-L-23699 and MIL-L-7808 specifications. It is shown that the model predictions agree fairly well with the experimental data, and the practical utility of the model is demonstrated by incorporating the traction model in the advanced bearing dynamics computer model, ADORE, and by evaluating the roller slip and skid behavior in a cylindrical roller bearing as a function of the lubricant traction parameters.

Two types of rheological models are considered: type I where the viscosity varies exponentially with pressure and temperature, and type II where the variation in viscosity is exponential with pressure and inverse temperature. With the prescribed general form of the viscosity behavior the energy equation is solved through the lubricant film, with appropriate boundary conditions, and the shear stress is integrated to compute the total traction in the contact. The computed traction is compared to the experimental data and a nonlinear regression analysis is carried out to determine the model coefficients by minimizing the squared deviation between model predictions and experimental observations.

Experimental data obtained at the AFWAL Aero Propulsion Laboratory for two types of contacts is considered for determining the model coefficients: an elliptical contact with a set of cylindrical disk specimens with a rolling radius of 38.10 mm and a crown radius of 914.40 mm, and a circular contact with a set of disk with spherical surfaces with a radius of 38.10 mm. The lubricant temperature at inlet varied from 294° to 366 °K, the rolling velocity ranged between 21 and 46 M/Sec, and the Hertz contact pressures varied between 500 and 2000 MPa. The elliptical contacts represent the low end while the circular contacts correspond to the high end of Hertz contact pressures.

Both the type I and type II viscosity relations fit the experimental data obtained with the elliptical contact configuration for both the MIL-L-23699 and MIL-L-7808-type lubricants fairly well. For the type I model the regression coefficients indicate that the entire variation may be represented by a variation in a reference viscosity parameter; thus a greatly simplified relation for traction may be obtained. Also, since the the mathematical simplicity of the type I relation allows for an effective incorporation of the traction model in sophisticated component models, such as the advanced bearing dynamics computer code ADORE, it offers significant potential in the design and performance optimization of advanced mechanical components.

In the case of circular contacts with relatively high pressures, there is noticeable scatter between the model predictions and experimental observations, particularly in terms of the very high traction slope in the very low

slip region. Further model refinements to allow for the viscoelastic behavior of the lubricant are required for a more realistic modeling of the lubricants under such high pressures.

The practical significance of the traction model is demonstrated by carrying out a simulation of roller slip or skid in a cylindrical roller bearing by incorporating the traction model in the bearing dynamics computer program, ADORE. The very low traction coefficients with the MIL-L-7808 lubricant result in substantial slip of the roller as it travels through the contact zone in a radially loaded bearing. The viscous heating in the lubricant film, resulting from excessive slip, results in a significant reduction in lubricant film thickness, and a metal contact is eminent under the maximum load point. Such a close coupling between the bearing performance and traction behavior of the lubricant is further demonstrated by simulating a hypothetical lubricant with somewhat increased traction and by showing that the roller slip behavior may be significantly improved by a careful alteration of the lubricant traction behavior. Thus the feasibility of developing the optimum lubricant behavior for advanced applications, through traction modeling and dynamic simulation of component behavior, is demonstrated.

Table of Contents

1.	INTRODUCTION	5
2.	ANALYTICAL APPROACH	9
2.1	Computation of Lubricant Film Thickness	9
2.2	Computation of Traction	12
2.3	Regression Analysis for Model Coefficients	14
3.	RESULTS	19
3.1	General Traction Behavior	19
3.2	Traction Sensitivity to Model Coefficients	22
3.3	MIL-L-23699-Type Lubricant	22
3.4	MIL-L-7808-Type Lubricant	30
3.5	Effect of Contact Geometry	38
3.6	Rolling Bearing Performance Modeling	46
4.	CONCLUSIONS	56
5.	RECOMMENDATIONS FOR FUTURE DEVELOPMENTS	57
6.	REFERENCES	60
	APPENDIX A TRACTION DATA	63

1. INTRODUCTION

The significance of lubricant behavior in the performance of intricate mechanical components, such as, rolling bearings, gears and transmissions, has been well established. It is well-known that proper lubrication prevents excessive metallic contacts and reduces friction and wear of interacting elements, and serves as an effective cooling media. The traction behavior of the lubricant has proven to be a key factor in determining the stability and the overall dynamic performance of a mechanical system. For example, in rolling bearings the tractive forces at the rolling element/race interface greatly influence the orbital acceleration of rolling elements which, in turn, determines the extent of rolling element/cage collisions and associated cage instabilities. Thus, cage instabilities, ball and roller skid, roller skew and excessive wear associated with the highly dynamic interaction between the bearing elements are often attributed to the traction behavior of the lubricant.

The need for a clear understanding of the rheological behavior of the lubricant, and the development of realistic models which can accurately predict the lubricart behavior for a prescribed application, is further demonstrated by apparently conflicting requirements. For example, in order to minimize direct metal contact and wear, the lubricant film thickness between the interacting elements should be maximized, which requires the lubricant to have a relatively high viscosity; but the requirements of low traction, heat generation and torque lead to a low-viscosity lubricant. In order to simultaneously satisfy such performance requirements, an intricate coupling between the lubricant behavior and the performance of a machine element under consideration is necessary. In other words, the lubricant model must be incorporated in the component model which simulates the overall performance of the mechanical component, such as a rolling bearing. From a practical standpoint, this leads to a dual significance of lubricant traction modeling: first, the model can provide realistic designs of machine components; and second, the parametric performance evaluations, which can be obtained by the combined lubricant and component models, can help identify crucial lubricant properties required for a given performance specification. Thus for the military applications of rolling bearings, where the stability of the bearing elements and an acceptable performance of the bearing has to be ensured under the most adverse operating conditions, a realistic modeling of the traction behavior of the lubricant is extremely important. Furthermore, the required understanding of lubricant behavior and the development of predictive models is vital to future DOD needs that are beyond the current technological limits.

Over the past three decades a significant fraction of the mechanical engineering literature has been devoted to elastohydrodynamic lubrication and lubricant rheology. Investigations have ranged from the most fundamental problem of lubricant behavior at a molecular level to very applied problems where the global hydrodynamics intricately couples with the elastic distortion of the load-bearing contacts in a rolling bearing. The rolling-disk type of test rigs, such as those at the AFWAL

Aero Propulsion (AFWAL/POSL) and Materials (AFWAL/MLBT) laboratories, have proven to effectively simulate a concentrated contact and to provide a means for evaluating the tractive behavior of a lubricant. With the use of such test rigs, traction data for a number of military lubricants have been obtained [1-4]*. The commonly used military oil, with MIL-L-7808 specification, has been tested by a number of investigators. However, due to both the complexities in lubricant behavior and the experimental difficulties in traction measurement, the range of operating conditions over which the data have been obtained is limited and the repeatability of the data has often been questionable. In view of these difficulties the development of a realistic model has been extremely difficult, and the available models [1,3,5-10,25,26] need further experimental validation before they can be adopted for military applications. Also, the analytical formulations require substantial refinement before the models can be effectively used in bearing dynamics computer models. With significant improvements in the experimental techniques, the recent data obtained at the AFWAL Aero Propulsion Laboratory for the MIL-L-7808-type lubricant probably provides the most extended and reliable data base for the development of traction model for such military lubricants.

Correlations of the traction data to the fundamental properties of the lubricant, requires that the rheological behavior be measured at very high pressures, typical of a concentrated contact in a rolling bearing. This, also, is an extremely difficult task, and the available lubricant rheology data at high pressures is very scarce. Again, the facilities at the AFWAL Aero Propulsion Laboratory, such as the high-pressure viscometer, indeed, offer the most unique and advanced experimental apparatus for investigating the fundamental behavior of lubricants in concentrated contacts.

Along with the advances in lubrication theories, the computer modeling of rolling bearing dynamics has significantly advanced over the past few years. The computer models BASDAP [11], BDYN [12], DREB [13,14], RAPIDREB [15-17], TRIBO1 [18] and more recently ADORE [19] have become well known, and their capability in modeling truly dynamic behavior of the bearing under the most sophisticated and adverse operating conditions has been greatly demonstrated [19-22]. For an effective simulation of bearing behavior, the lubricant traction model has been identified as a key input to these bearing dynamics computer models [14,17,19,21]. This further emphasizes the need for the development of realistic traction models for various lubricants.

With particular emphasis on advanced DOD applications of rolling bearings, the practical significance of a traction model must be evaluated in terms of its utility in the bearing dynamics computer models. Due to the complexities associated with the dynamic interaction between bearing elements, the computer models which simulate the real-time dynamic performance of a bearing, such as the ones listed above, are quite complex, and they very often require a substantial computational effort. Since the lubricant model operates in the inner-most loop of these computer codes, a slight computational complexity in the lubricant model greatly amplifies the overall computational effort, and it imposes a severe restriction on the effective and economical use of both the bearing dynamics and the lubricant traction models. It is, therefore,

necessary that the lubricant behavior be modeled such that, along with a very realistic prediction of traction, the model offers a high computational efficiency. It is this practical requirement which leads to a rather limited utility of the available traction models, and the need for further development becomes quite clear.

The general approach to modeling the lubricant behavior has been a two-step process. The traction behavior is first experimentally measured over the expected range of operating conditions and then "curve fitted" to a mathematical model. Some of the models may essentially provide an interpolation of the actual data while the others may lead to certain constitutive equations which have a physical significance. The ultimate requirement is that the model be computationally "simple" and yet provide a realistic prediction of the traction behavior. With such guidelines the objective of the present program is to develop effective traction models for military oils, with the available traction data as a starting point.

2. ANALYTICAL APPROACH

The mechanics of an elastohydrodynamic contact is schematically described in figure 1. Since the size of the contact is generally quite small compared to the radius of the interacting elements, the assumption of a relatively flat contact, as shown in figure 1, is quite realistic. There are essentially three zones in the contact region: inlet zone, high-pressure contact zone and the exit zone. The lubricant flows from the inlet to exit through the high-pressure contact. The properties of the lubricant in the inlet zone, which is essentially at ambient pressure, determine the nominal thickness of the lubricant film in the contact, while the tractive behavior is determined by the lubricant properties under the high pressure exerted in the contact. In the exit zone, phenomena, such as cavitation, are significant, but for the computation of lubricant film thickness and traction it is reasonable to restrict the modeling to the inlet and high-pressure contact zones.

A realistic simulation of traction, therefore, demands that the lubricant properties be known both under ambient and high-pressure conditions. Although the viscosity-temperature relations under ambient or very low pressures can be easily measured, high-pressure viscometry still requires considerable development; perhaps, the high-pressure viscometer at the AFWAL Aero Propulsion Laboratory, will provide such data in the near future. For the present it may be reasonable to assume a certain type of viscosity-pressure-temperature relation in the high-pressure contact and calculate the traction as a function of the coefficients in the constitutive relation. The computed traction can be compared to the experimental data, and the coefficients which provide a reasonable fit can be determined by carrying out a regression analysis. Such an approach is very complementary to the high-pressure viscometry research. The computed coefficients, when compared with those derived for the high-pressure viscometry data, as and when it becomes available, shall provide significant insight into the fundamental behavior of the lubricant in a concentrated rolling-sliding contact.

The general approach to traction model development in the present investigation, therefore, consists of the following steps:

1. Computation of lubricant film thickness.
2. Computation of traction.
3. Regression analysis.

2.1 Computation of Lubricant Film Thickness

The lubricant film thickness, h, in an elastohydrodynamic contact is generally defined as

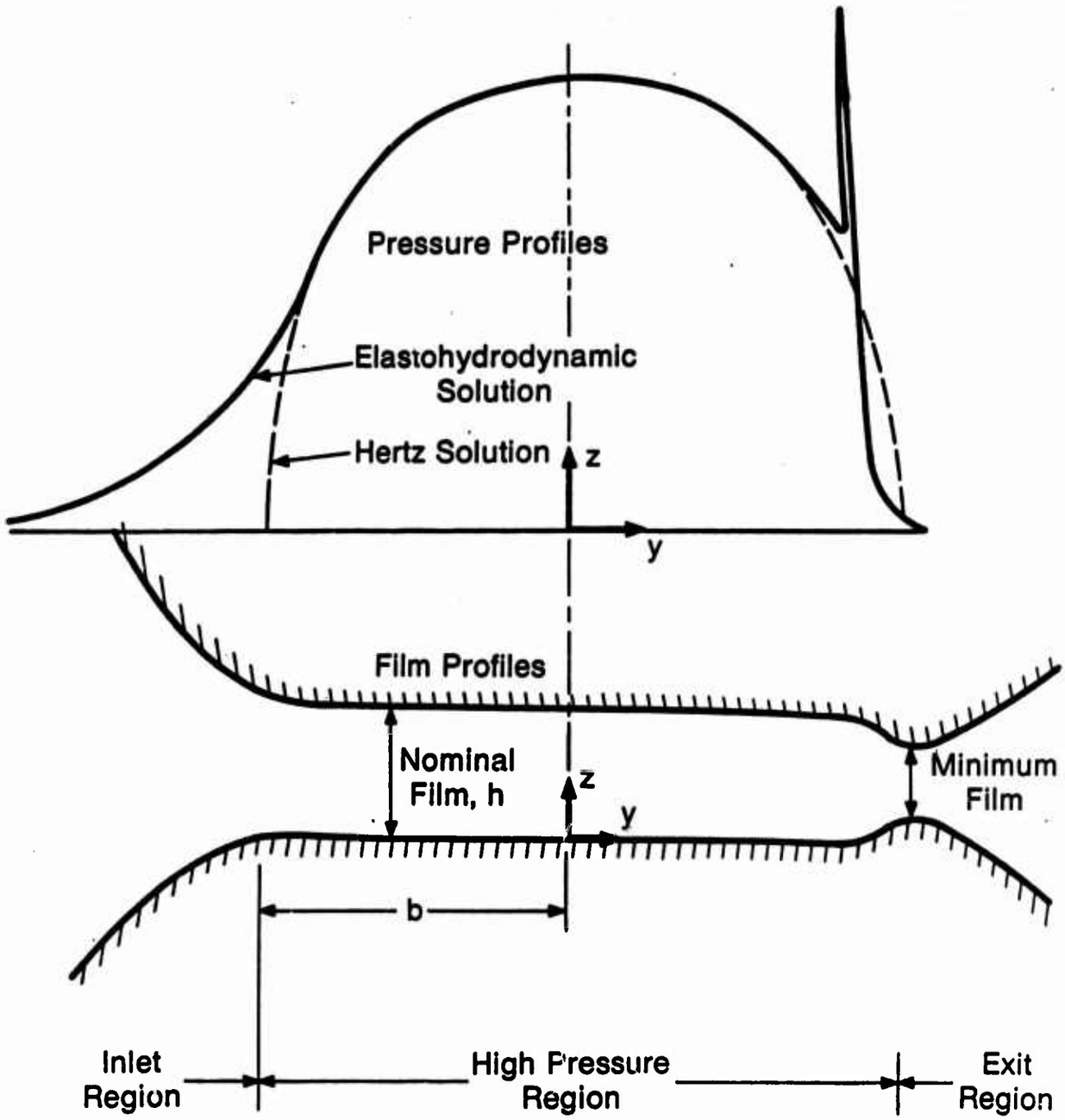

Figure 1. Schematic Representation of an Elastohydrodynamic Contact Zone

$$h = h_{iso}\,\phi_T \qquad (1)$$

where h_{iso} is the isothermal film thickness and ϕ_T is a thermal reduction factor to allow for the reduction in film thickness due to viscous heating in the inlet zone.

For an elliptical contact, the isothermal film thickness may be computed by the following formula, provided by Hamrock and Dowson [23]

$$\frac{h_{iso}}{R} = 2.69\frac{U^{0.67}G^{0.53}(1 - 0.61\ e^{-0.73k})}{W^{0.067}} \qquad (2)$$

where $R = \frac{R_1 R_2}{R_1 + R_2}$

$G = \alpha E'$

$\frac{1}{E'} = \frac{1}{2}\left\{\frac{1 - \nu_1^2}{E_1} + \frac{1 - \nu_2^2}{E_2}\right\}$

$U = \frac{\mu_0 \bar{U}}{E' R}$

$\bar{U} = (U_1 + U_2)/2$

$W = \frac{Q}{E'R}$

$k = \frac{a}{b}$

with
- a = Semi-major axis of the contact ellipse
- b = Semi-minor axis of the contact ellipse
- E = Elastic modulus of the interacting body
- Q = Applied load
- R = Radius in the rolling direction
- α = Pressure-Viscosity coefficient
- ν = Poisson's ratio
- μ_0 = Absolute viscosity

and the subscripts $_1$ and $_2$ denote the two elastic bodies in contact.

The thermal reduction factor, ϕ_T, may be determined from the numerical results tabulated by Smith et al [10], based on the work by Cheng and Sternlicht [24].

2.2 Computation of Traction

The computation of traction is based on a model originally presented by Kannel and Walowit [5] and later used by Gupta et al. [3]. The problem is basically formulated in terms of the following equations:

$$\text{Energy Equation:} \quad K\frac{\partial^2 T}{\partial z^2} = -\tau\,\dot{s} \tag{3}$$

$$\text{Geometric Compatibility:} \quad \frac{\partial u}{\partial z} = \dot{s}(\tau,p,T) \tag{4}$$

$$\text{Constitutive Equation:} \quad \dot{s}(\tau,p,T) = \frac{\tau}{\mu(p,T)} \tag{5}$$

where

K = thermal conductivity
T = absolute temperature
τ = shear stress
$\dot{s}$ = shear strain rate
u = lubricant velocity
p = pressure
μ = lubricant viscosity
z = coordinate across the film, as shown in figure 1.

With the nominal film thickness computed by equations (1) and (2), the applicable boundary conditions, for the solution of equations (3) to (5) are

$$\begin{aligned} z = 0: &\quad T = T_1 \text{ and } u = U_1 \\ z = h: &\quad T = T_2 \text{ and } u = U_2 \end{aligned} \tag{6}$$

Let the temperatures of the two contacting bodies be equal, i.e., $T_1=T_2=T_0$, and with μ_0 as the viscosity at reference temperature T_0, all the variables may be nondimensionalized as follows:

$$T^* = T/T_0, \quad \mu^* = \mu/\mu_0, \quad z^* = z/h \text{ and } U^* = u/\bar{U} \tag{7}$$

Equations (3-5) may now be combined to obtain the following governing equations:

$$\frac{\partial^2 T}{\partial z^2} = \frac{\tau \bar{U} h}{K T_0}\frac{\partial U}{\partial z} \tag{8}$$

and

$$\frac{\partial U}{\partial z} = \frac{h\tau}{\mu_0 U}\frac{1}{\mu} \tag{9}$$

where the asterisk has been dropped for brevity. Also note that μ is a function of pressure and temperature as defined in equation (5).

Integrating equation (8) with the first of boundary condition in (6) gives

$$\frac{\partial T}{\partial z} - \frac{\partial T}{\partial z}\bigg|_{z=0} = -\frac{\tau \bar{U} h}{K T_0}(U - U_1) \tag{10}$$

and the division of equation (10) by (9) results in the following governing equation

$$\frac{1}{\mu}\frac{\partial T}{\partial U} = \frac{\mu_0 \bar{U}}{h\tau}\frac{\partial T}{\partial z}\bigg|_{z=0} - \frac{\mu_0 \bar{U}^2}{K T_0}(U - U_1) \tag{11}$$

which may be integrated, through the lubricant film, with the boundary conditions in equation (6) to obtain

$$\frac{\partial T}{\partial z}\bigg|_{z=0} = \frac{h\tau \bar{U}(U_2 - U_1)}{2K T_0} \tag{12}$$

By substituting equation (12) in (11) and by denoting the viscosity as a function of pressure and temperature

$$\mu = f(p,T) \tag{14}$$

the governing equation through the lubricant film may be written as

$$\frac{\partial T}{\partial U} = \frac{\mu_0 \bar{U}^2}{K T_0}(1 - U)\, f(p,T) \tag{15}$$

Also, the shear stress through the film, is obtained by combining equation (4) and (5)

$$\tau = \frac{\mu_0 \bar{U}}{h}\int_{U_1}^{U_2} f(p,T)\, dU \tag{16}$$

Equations (15) and (16) are solved simultaneously to obtain the shear stress through the film. Equation (15) is first integrated to obtain a temperature-velocity relation, which when combined with (14) gives the viscosity-velocity relation required in (16).

For any arbitrary viscosity-pressure-temperature relation, equation (14), equations (15) and (16) may be, in general, solved numerically to obtain the shear stress at any point in the contact zone. The shear stress can then be integrated over the contact zone to obtain the total tractive force. A traction coefficient may then be defined, either in terms of the local stress ratio or the ratio of the total traction to applied normal force

$$\kappa_{local} = \tau/p$$
$$\kappa_{global} = F/Q \tag{17}$$

where F is the integrated traction force and Q is the applied normal contact load.

Since the slip velocity varies greatly in a typical rolling-element-to-race contact, the local traction coefficient is most suitable when applying the traction model to a rolling bearing. However, for the purpose of laboratory investigations to determine the model coefficients with single contacts, the global traction coefficient is significant.

It is clear from the above formulation that equation (14), which defines the pressure-viscosity relation of the lubricant, is the primary input to the traction model. The complexities associated with traction computation are directly related to the general form of this constitutive equation. The two most common forms of the pressure-temperature-viscosity relation are:

Type I relation: $$\frac{\mu}{\mu_o^*} = f(p,T) = \exp\{\alpha^* p + \beta^* T_o(1-T)\} \qquad (18)$$

Type II relation: $$\frac{\mu}{\mu_o^{**}} = f(p,T) = \exp\left\{\alpha^{**} p + \frac{\beta^{**}}{T_o}\left(\frac{1}{T} - 1\right)\right\} \qquad (19)$$

Smith et al. [1] and Walowit and Smith [2] used the type I relation, and they have shown that for such a relation a close form formula for traction computation in a rolling-sliding contact may be derived. In the case of type II relation, however, the integration is not quite straight-forward and a numerical approach is preferred, as shown by Gupta et al [3].

The basic difference in the two relations lies in their physical characteristics. With the increased thermal heating during increasing sliding velocity, the type I relation gives a diminishing traction coefficient in the high slip region. With the type II relation, however, the thermal effect tends to level off to an asymptotic value, which results in a corresponding steady value of the traction coefficient at high slip velocities.

Aside from the above formulation, some of the more recent work suggests alternate approaches to traction computation in a concentrated rolling-sliding contact. Some of the noted works are due to Johnson and Tevaariverk [25], Bair and Winer [26] and Trachman [6]. The adaptability of these models to military lubricants used in rolling bearing applications has yet to be investigated.

2.3 Regression Analysis for Model Coefficients

As discussed above, the determination of model coefficients, such as, μ_o^*, α^*, β^*, etc., is an important task in the develcpment of a traction model. In terms of the above type I or type II relations, perhaps the most direct method of determining the coefficients is to measure the viscosity as a function of both pressure and temperature and then curve-fit the data to appropriate relation. However, high-pressure viscometry has been a very difficult subject; therefore, a more semi-empirical approach, which consists of traction measurement in a single contact and derivation of model coefficient from a regression analysis of the traction data, has been more suitable. Although such an approach does not provide significant insight

into the physics of lubricant behavior, it does result in a realistic model for computation of traction in practical applications.

The apparatus used for the measurement of traction consists of two independently driven disks, loaded against each other, when the lubricant is fed through a jet. See schematic diagram in figure 2. The disks are normally crowned to simulate an elliptical contact of rolling bearing applications. The test rig at the AFWAL Aero Propulsion Laboratory (AFWAL/POSL), which is one of several such facilities, is used in the present investigation.

Analysis of the experimental traction data consists of first creating data subsets which represent traction-slip behavior as a function of contact pressure under fixed rolling velocity and operating temperature. Since a reliable measurement of disk temperature is quite difficult, the disk temperature is assumed to be equal to the inlet temperature. The traction behavior is now fitted to either the type I or type II relation and the model coefficients are derived by a least-squares regression analysis.

Consider the elliptical contact zone shown in figure 2 and assume the slip velocity to be constant over the contact area, as will the case in the test rig. Using the type I relation, equations (14) to (16) may be written as:

$$\mu = \mu_0 \exp \{\alpha^* p + \beta^* T_0 (1-T)\} \tag{20}$$

$$\frac{\partial T}{\partial U} = \frac{\mu_0 {}^* \bar{U}^2}{K T_0} (1-U) \exp \{\alpha^* p + \beta^* T_0 (1-T)\} \tag{21}$$

$$\tau = \frac{\mu_0 {}^* U}{h} \int_{U_1}^{U_2} \exp \{\alpha^* p + \beta^* T_0 (1-T)\} \, dU \tag{22}$$

Straight forward integration of equation (21) and (22) shall result in the following expression for the shear stress:

$$\tau = \frac{\mu_0 {}^* \bar{U}}{h \Lambda} (U_2 - U_1) \exp(\alpha^* p) \frac{\sinh^{-1} \Lambda}{\sqrt{1 + \Lambda^2}} \tag{23}$$

where

$$\Lambda^2 = \frac{\mu_0 {}^* \beta^* e^{\alpha^* p} \bar{U}^2 (U_2 - U_1)^2}{8K} \tag{24}$$

Since the slip is constant over the contact ellipse, the total tractive force, F, over the contact is written as

$$F = \int_0^1 \int_0^{2\pi} ab\tau \, d\theta \, r dr = 2\pi ab \int_0^1 \tau \, r dr \tag{25}$$

and the global traction coefficient, κ_{global}, written now simply as κ, is:

$$\kappa = \frac{F}{Q} = \frac{2\pi ab}{Q} \int_0^1 \tau \, r dr \tag{26}$$

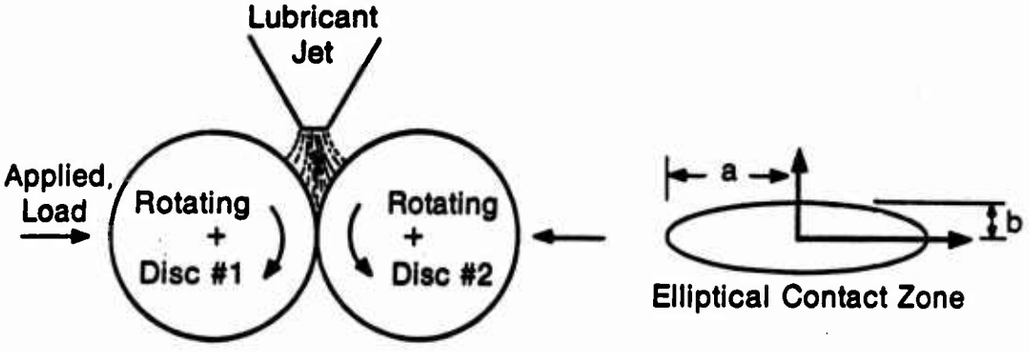

Figure 2. **Schematic Representation of a Rolling Disc Machine for Lubricant Traction Measurement**

where Q is the normal load and a and b are, respectively, the semi- major and minor axes of the contact ellipse.

Realizing that the pressure, p, in equations (23) and (24) is elliptical, with a maximum Hertz pressure, p_H,

$$p = p_H \sqrt{1 - r^2} \tag{27}$$

the traction coefficient may be reduced to the following algebraic equation:

$$\kappa = \frac{3}{\alpha^* p_H^2 h \Psi} \quad \frac{8K\mu_o^*}{\beta^*} \left\{ [\sinh^{-1}(\Psi e^{\rho})]^2 - \frac{1}{\rho} [f(\Psi e^{\rho}) - f(\Psi)] \right\} \tag{28}$$

where

$$\rho = \alpha^* p_H / 2, \qquad \Psi = \bar{U}(U_2 - U_1) \quad \frac{\mu_o^* \beta^*}{8K}, \quad \text{and}$$

$$f(\Psi) = \int_0^{\Psi} \frac{[\sinh^{-1}\psi]^2}{\psi} \, d\psi.$$

The integral $f(\Psi)$ may be computed numerically, and it may be tabulated over the expected range of Ψ.

For the purpose of regression analysis, the traction coefficient is further abbreviated as

$$\kappa = \lambda \, Y \, Z \tag{29}$$

where

$$\lambda = \frac{3}{2 \, p_H h} \quad \frac{8K\mu_o^*}{\beta^*}$$

$$Y = \frac{1}{\rho \, \Psi}$$

and $$Z = [\sinh^{-1}(\Psi e^{\rho})]^2 - \frac{1}{\rho} [f(\Psi e^{\rho}) - f(\Psi)]$$

If the measured traction coefficient for any data point i is κ_{mi}, then the squared deviation between the predicted and measured traction is defined as

$$L = \sum_{i=1}^{N} (\kappa_i - \kappa_{mi})^2 \tag{30}$$

The three variables with respect to which L has to be minimized are λ, ρ and Ψ. It is clear that for prescribed ρ and Ψ, the variation of L with λ is

linear; therefore, λ may be readily computed by conventional linear regression analysis. Variations with ρ and Ψ are nonlinear, and for computing these parameters the problem is set-up as:

$$\sum_{i=1}^{N} (\kappa_i - \kappa_{mi}) \frac{\partial \kappa_i}{\partial x_j} = G_j = 0, \quad j=1,2, \quad x_1=\Psi, \; x_2=\rho \tag{31}$$

and the Jacobian

$$\frac{\partial G_j}{\partial x_k} = \sum_{i=1}^{N} \left\{ \frac{\partial \kappa_i}{\partial \kappa_k} \frac{\partial \kappa_i}{\partial \kappa_j} + (\kappa_i - \kappa_{mi}) \frac{\partial^2 \kappa_i}{\partial x_j \partial x_k} \right\} \tag{32}$$

Once the various derivatives have been expressed in terms of derivatives of Y and Z, defined above, the set of two simultaneous equations (31) may be solved by conventional Newton-Raphson techniques.

A similar procedure can be used for the type II relation, but the complexity of the problem increases greatly because the entire problem is now solved numerically. However, the coefficients of the type I relation may be used to determine realistic first estimates for the type II model. Also, it must be noted that since the pressure-viscosity coefficient essentially influences the tractive behavior in the low slip region, it is quite reasonable to assume $\alpha^* = \alpha^{**}$. The other two coefficients are computed numerically.

The model coefficient, computed above, may be tabulated over the range of rolling speeds and operating temperatures. Appropriate values of these coefficients may then be used in bearing dynamics computer programs, such as ADORE, to determine the performance of the bearing.

In reality, the above process is less tedious than it appears, both in terms of data analysis and the subsequent use of the model in bearing dynamics computer programs. The analysis of the data has to be carried out only once, and all the coefficients may be tabulated for future use. The use of the model in ADORE is quite straight forward, at least with the type I relation.

It must be remembered that the computational efficiency of ADORE, and other bearing dynamics programs, greatly depends on the complexity of the traction model, since this model operates in the most inner loop of the program. The use of the type II model, where the shear stress is computed numerically, therefore, needs some caution. Also, with particular emphasis on computational simplicity other models [6,25,26] should be further explored. The regression analysis described above provides a generic approach for the computation of coefficient of any arbitrary model from the experimental traction data obtained over the expected range of operating conditions.

3. RESULTS

Based on the analytical formulation described in the preceding section, experimental traction data forms the basic foundation to the traction model development. For the present investigation, the data obtained at the AFWAL Aero Propulsion Laboratory for the MIL-L-7808 and MIL-L-23699-type military lubricants is considered, and the various coefficients for the type I and type II viscosity-pressure-temperature relations are derived. The model is then incorporated in the bearing dynamics computer program, ADORE, and the general slip behavior of a roller is simulated in a cylindrical roller bearing.

Most of the available data were obtained with a set of 76.20 mm (3.0 inch) diameter disks with a crown radius of 914.40 mm (36 inch); in one of the data sets the crown radius was set equal to the rolling radius to simulate a circular point contact. The inlet oil temperature was varied in the range of 290 to 366 °K; the rolling velocity was varied from 21 to 45 M/Sec; and the contact pressures ranged from 540 to 860 MPa with the 914.40 mm crowned disks and 1440 to 2050 MPa in the case of a circular point contact. In all cases the lubricant was fed through a jet and the inlet temperature was closely monitored. In some cases measurement of disk surface temperature was also attempted.

3.1 General Traction Behavior

The general traction behavior of most lubricants in an elastohydrodynamic contact is described in figure 3a. The traction coefficient first increases, almost linearly, with slip, it peaks to a maximum value, and then with the increasing thermal effect with higher slip velocities it begins to drop. The discussion presented in the preceding section clearly demonstrates that the analytical model considered herein preserves such a general behavior. In fact, figure 3a shows the fit of the model to actual traction data obtained at certain experimental conditions. See Appendix A for the explanation of the various symbols used in the computer-generated traction plots, such as, figure 3a, and others, throughout this report. The actual experimental points are marked with a square, while the solid line represents prediction of the model based on the type I relation. The results with the type II relation are similar. See figure 3b. Clearly, the fit between model predictions and experimental data is very good. Thus for any given traction-slip curve, the model coefficients may be derived to provide a close simulation of experimentally observed traction behavior.

Since the practical significance of a traction model lies in its predictive capabilities over a reasonably wide range of operating conditions, the close fit of the data shown in figures 3a and 3b, although necessary, does not provide sufficient confidence in the model predictions. Clearly the derivation and tabulation of model coefficients for each operating condition are impractical. Realistic objective of a model is to simulate the observed traction behavior over the entire range of data with one set of model coefficients. With such an ultimate objective, the regression analysis is carried out over the range of contact pressures at prescribed rolling velocity and inlet temperature. Although, the coefficients so derived may

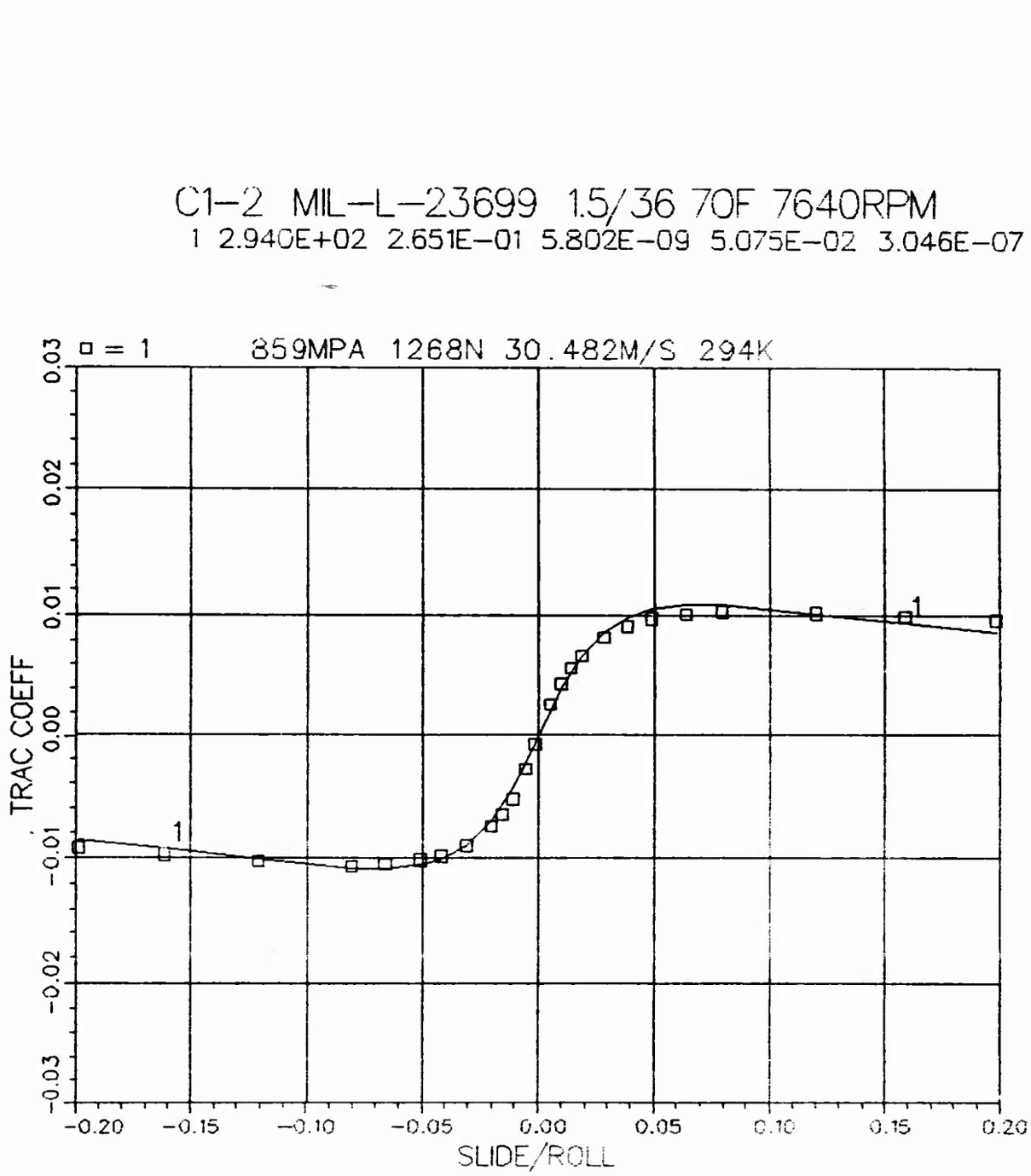

Figure 3a. Typical traction behavior and the predictions of the type I model.

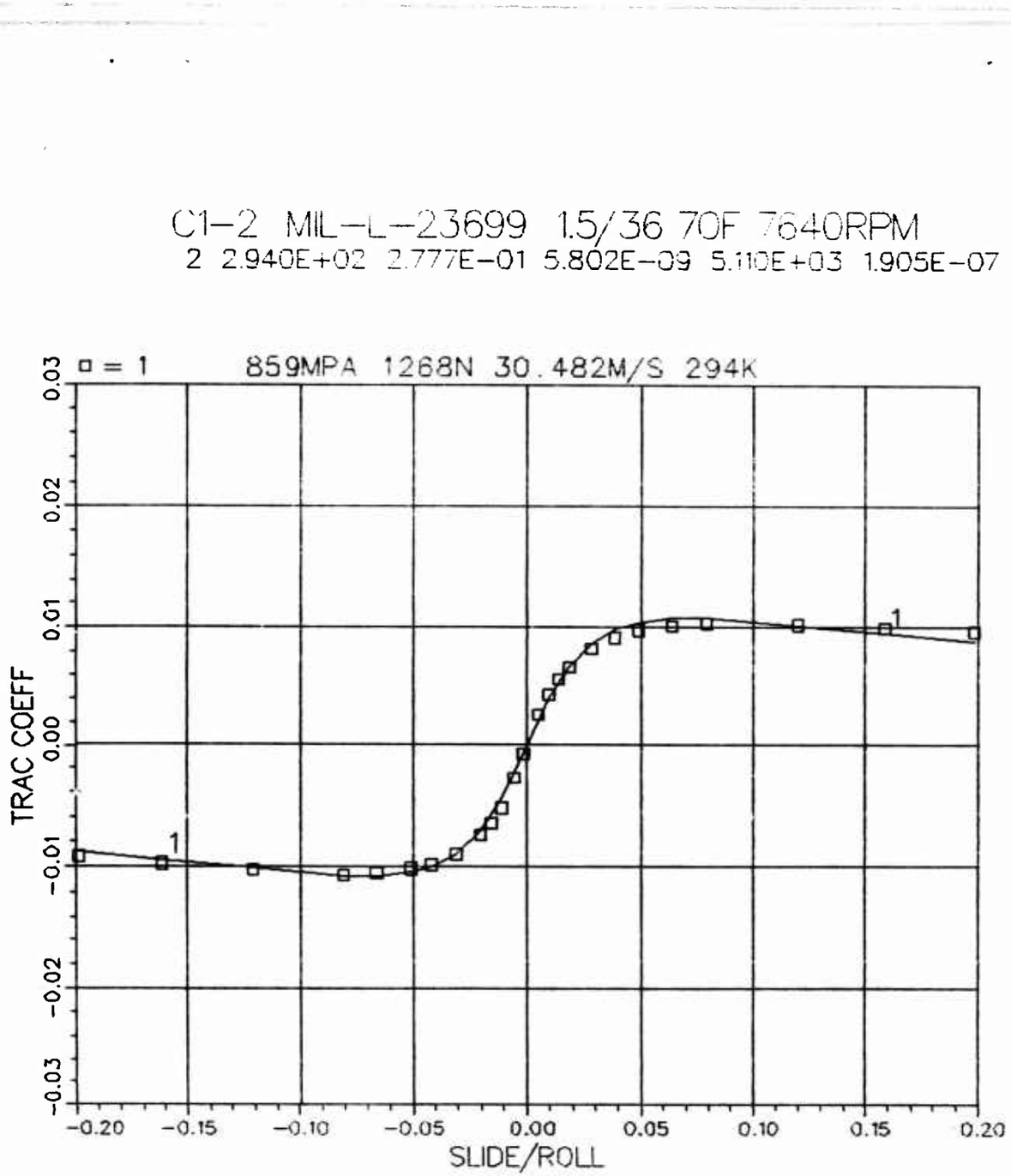

Figure 3b. General traction behavior and the predictions of the type II model.

be further curve-fitted to cover the variation over rolling velocity and temperature, they have a substantial significance in rolling bearings where, for a given application, the variations in rolling velocities and operating temperatures is not very large. Thus, as a first step to traction model development, the model coefficients in the present investigation are tabulated over the rolling velocities and inlet oil temperatures.

3.2 Traction Sensitivity to Model Coefficients

In order to establish some physical significance of each of the model coefficient, it is necessary to investigate the sensitivity of traction behavior to each model coefficient before presenting the results of the regression analysis carried out in the present investigation.

There are essentially three parameters of the models considered herein: the reference viscosity, μ_o* or μ_o**, the pressure viscosity coefficient, α* or α**; and the temperature-viscosity coefficient, β* or β**. Figures 4a and 4b show the variation in traction as a function of the reference viscosity for the type I and type II models respectively. As expected, the increase in viscosity results in a corresponding increase in traction for both types of models. The results of the pressure-viscosity coefficients are also similar, as seen in figures 5a and 5b. The temperature-viscosity parameter demonstrates, perhaps, the most interesting results; traction as a function of β* is shown in figure 6a while similar results as a function of β** for the type II model are shown in figure 6b. Note that at high slip velocities the type I model results in a relatively faster drop-off of traction coefficient compared to the type II model; this is primarily due to the thermal behavior of the two constitutive relations. At low slip, however, the two models are essentially identical when the pressure-viscosity coefficients for the two models are the same. In fact, it is the pressure-viscosity coefficient which essentially establishes the slope of the traction curve at low slip velocities, as discussed earlier.

The overall difference between the type I and type II relations is, therefore, only significant at high slip velocities. Under excessive slip, as the temperature of the lubricant increases, the effective viscosity continues to drop at a steady rate for the type I model; therefore the traction coefficient continues to drop. In the type II model, on the other hand, the rate at which the viscosity drops gradually slows down due to the inverse temperature effect; this results in a somewhat asymptotic behavior of the traction coefficient at very high slip velocities. Such a difference in behavior is seen in figure 7, where traction predictions by the two models are shown under identical operating conditions.

3.3 MIL-L-23699-Type Lubricant

The ambient properties of the MIL-L-23699-type lubricant are well documented in the literature. In the present investigation the data compiled by Gupta et al. [3] is used for the computation of film thickness. Also, based on the model correlations reported in this work the pressure-viscosity coefficient in the high pressure contact region, α* or α**, is assumed to be 5.8E-09 1/Pa.

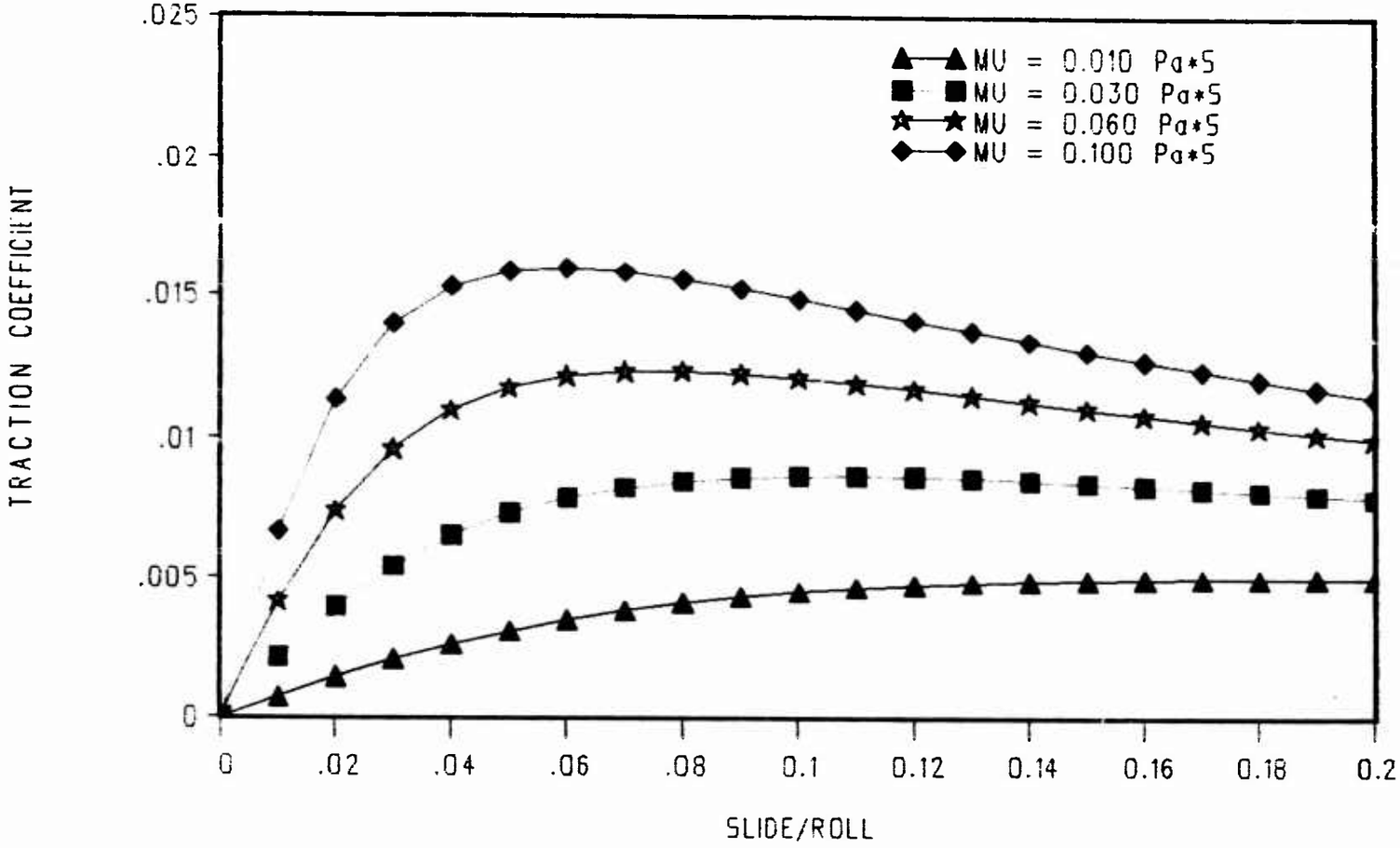

Figure 4a. The influence of reference viscosity, μ_o^* (MU), in the type I model.

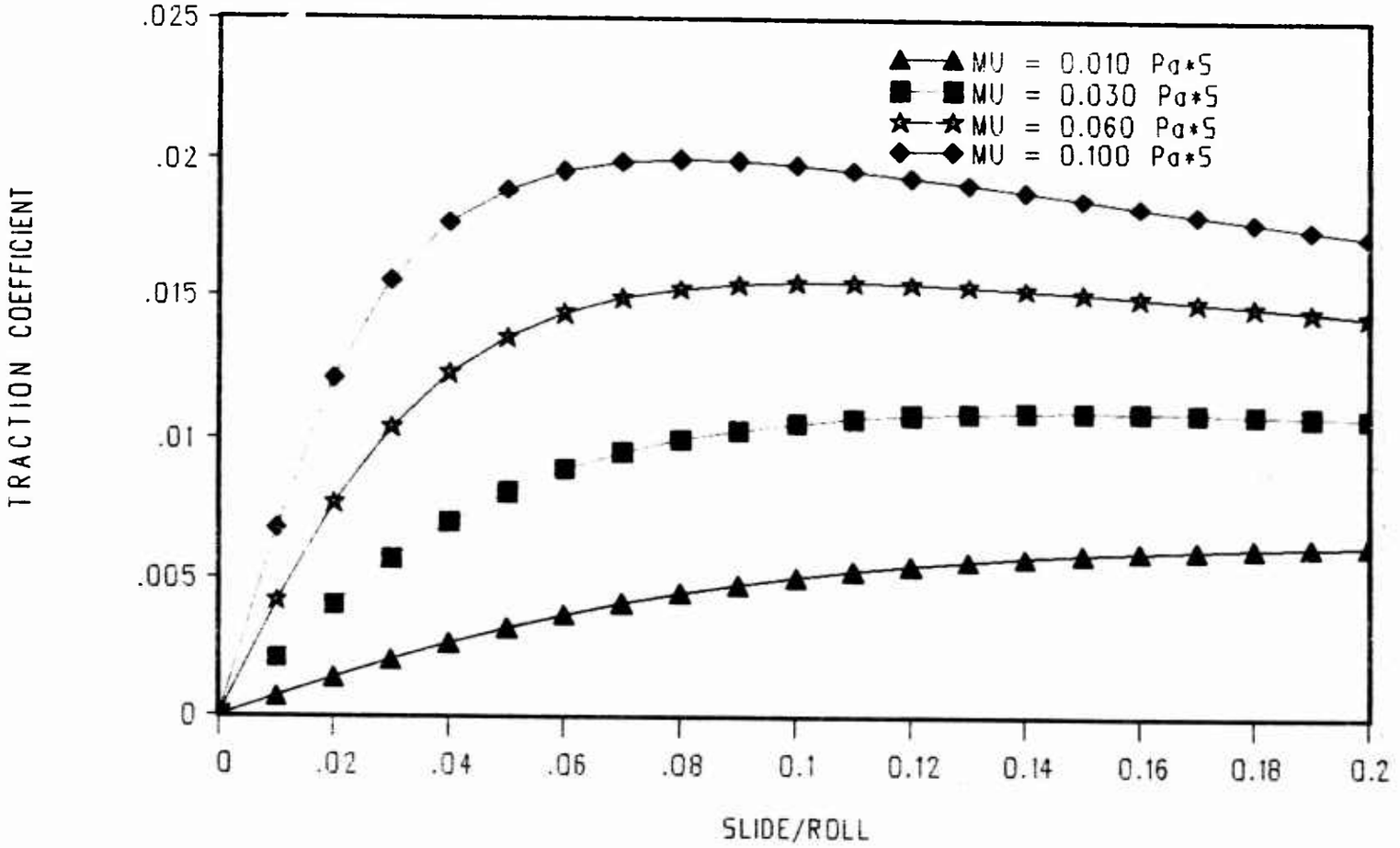

Figure 4b. The influence of reference viscosity, μ_o^{**}(MU), in the type II model.

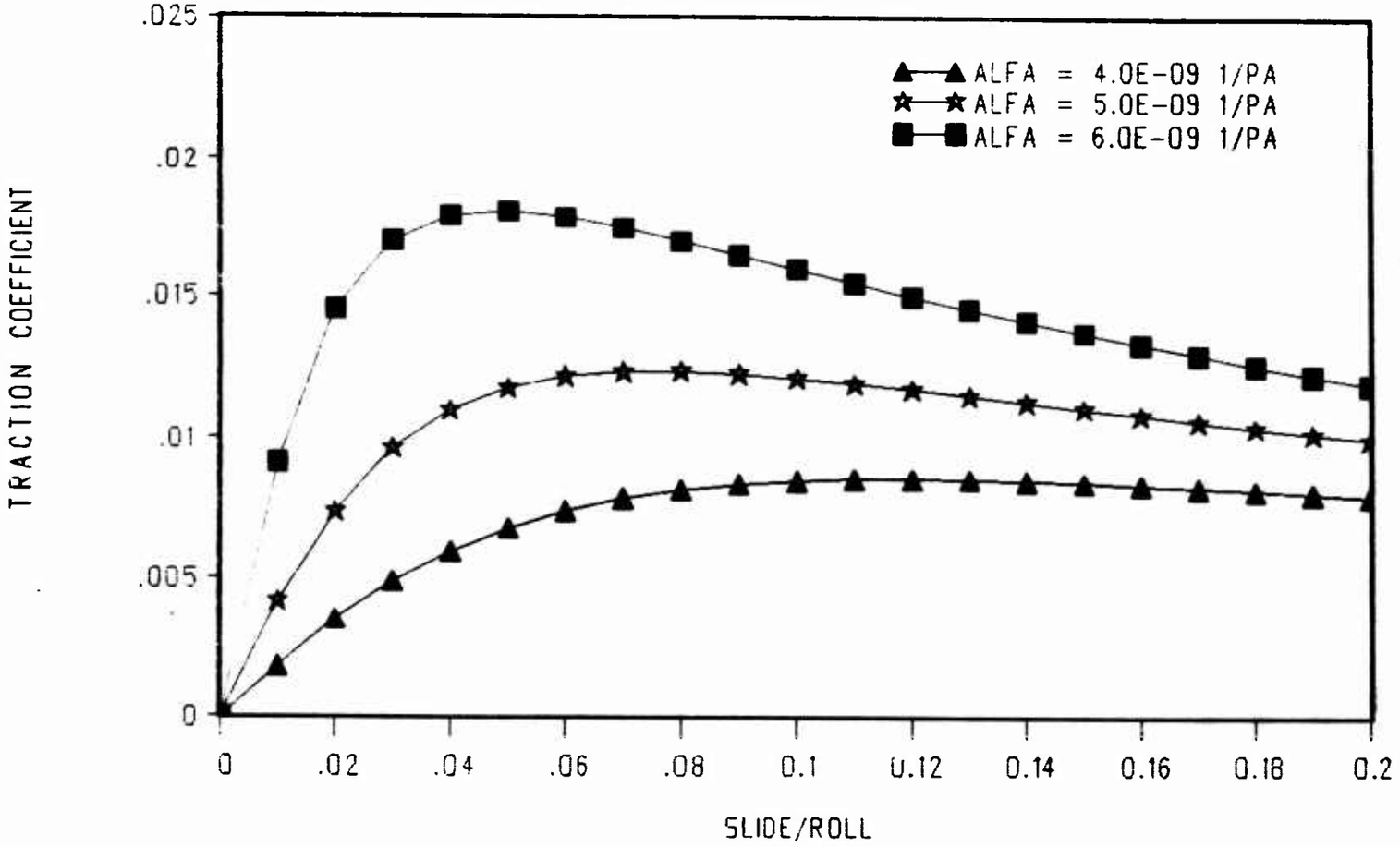

Figure 5a. The influence of pressure-viscosity coefficient, α^* (ALFA), in the type I model.

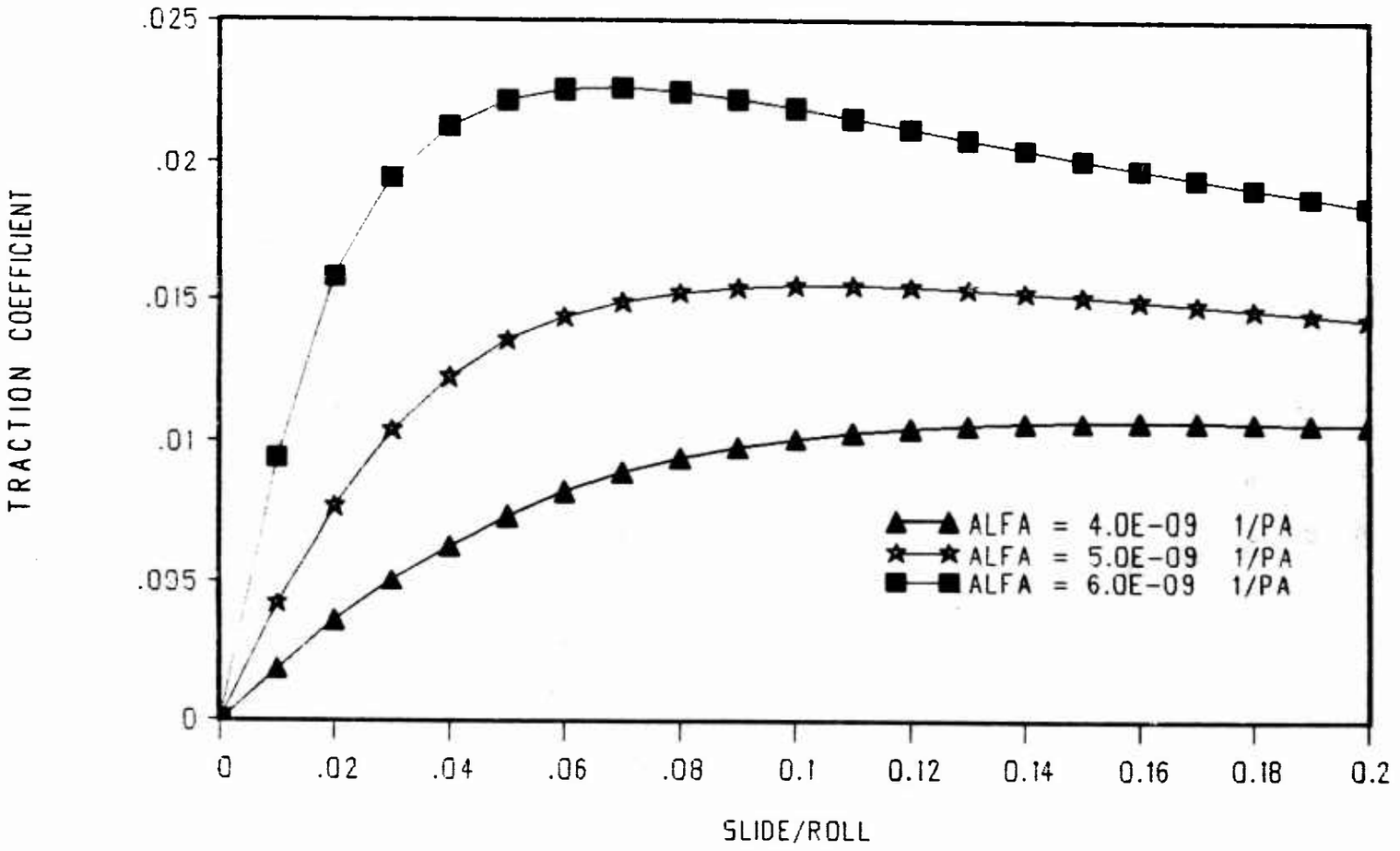

Figure 5b. The influence of pressure-viscosity coefficient, α^{**} (ALFA), in the type II model.

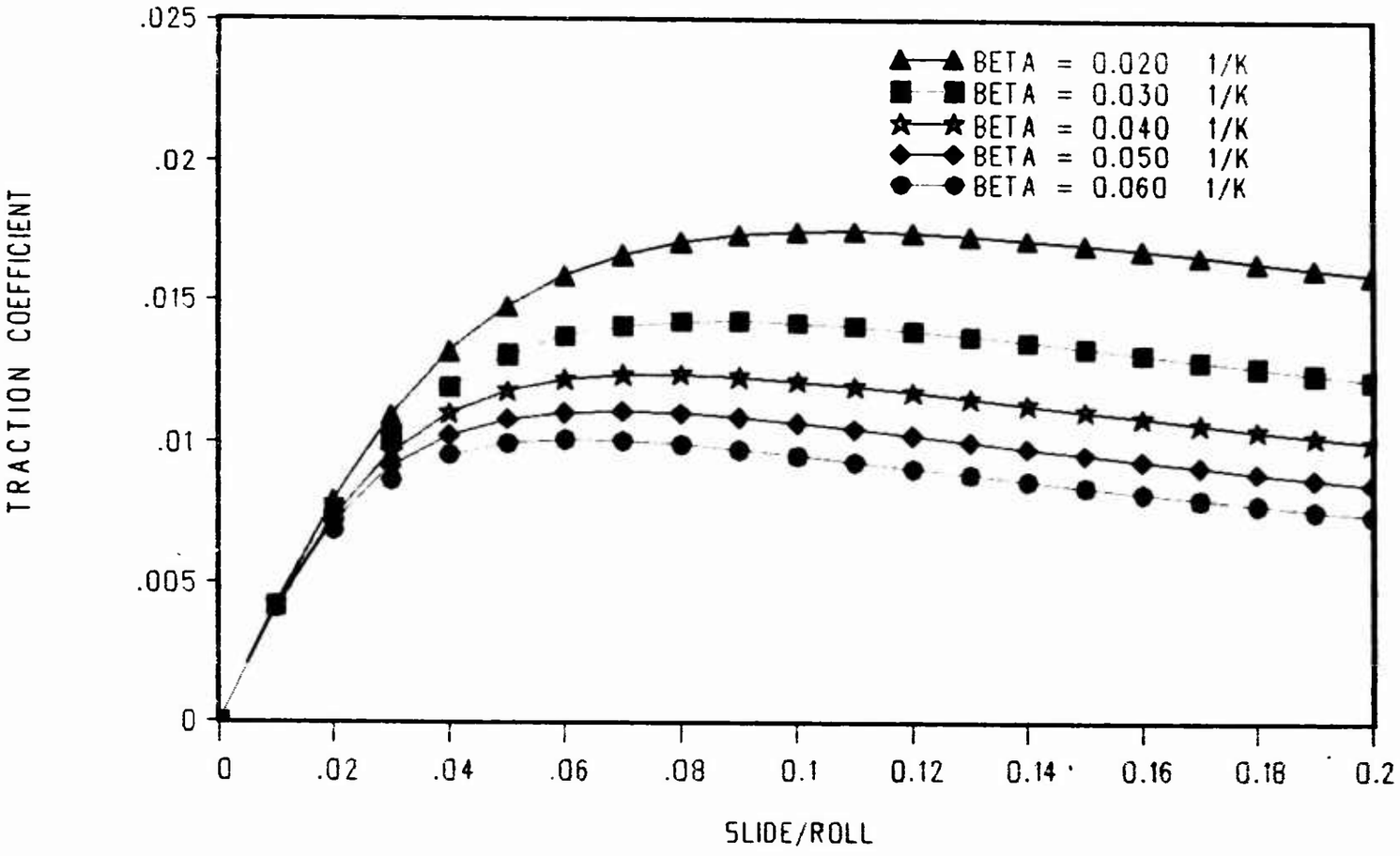

Figure 6a. The influence of temperature–viscosity coefficient, β^* (BETA), in the type I model.

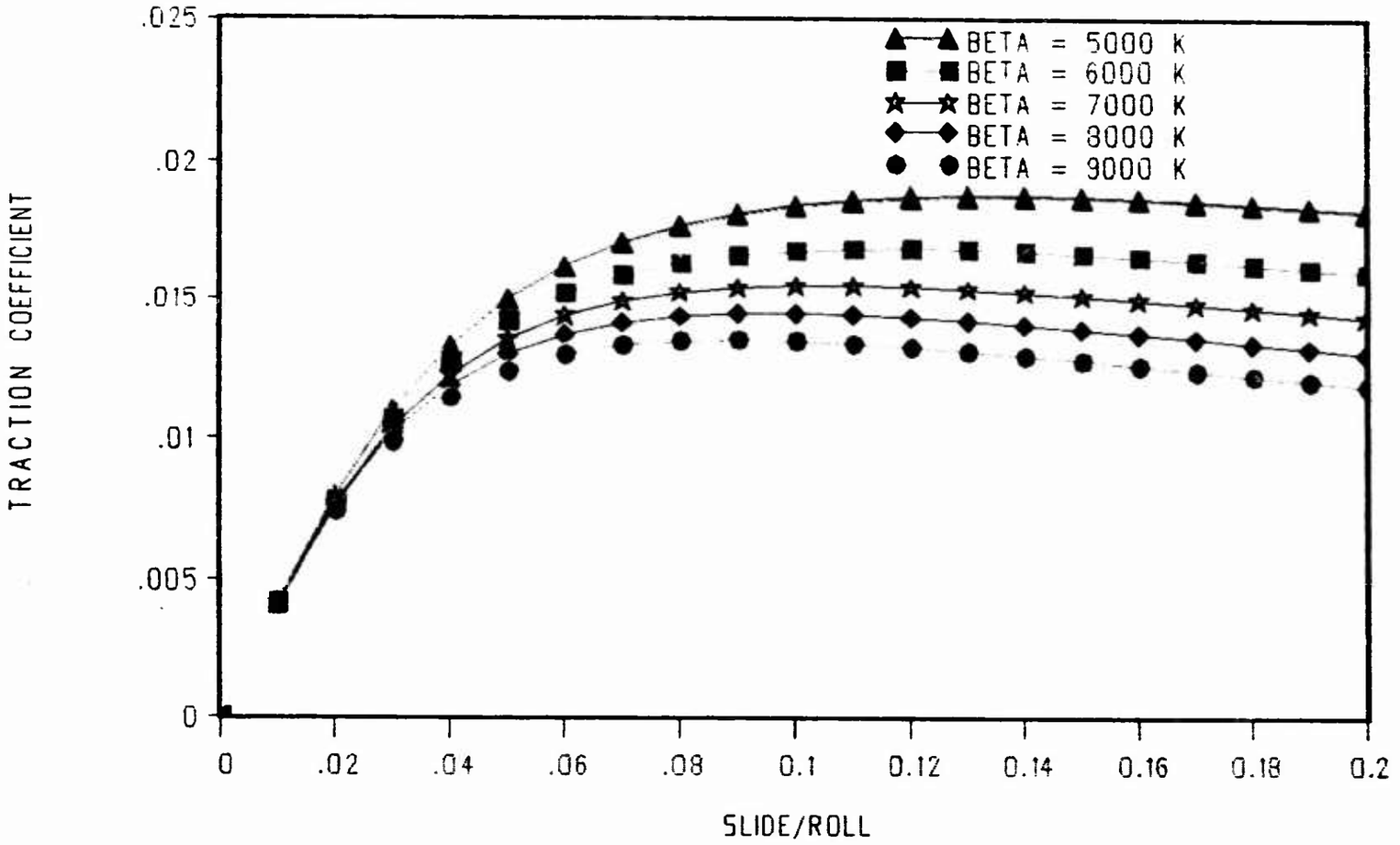

Figure 6b. The influence of temperature-viscosity coefficient, β^{**}(BETA), in the type II model.

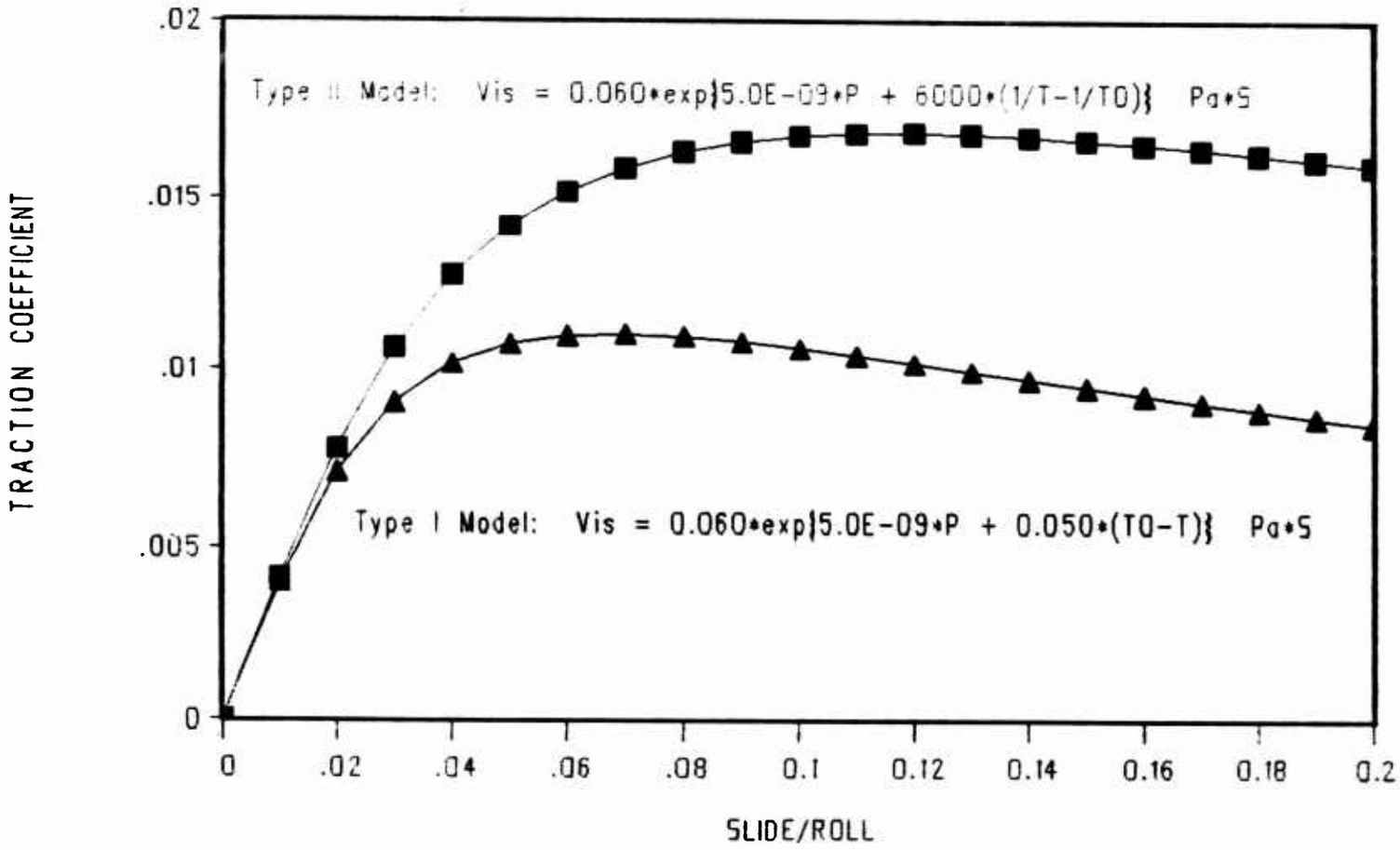

Figure 7. Comparison of the two models at a reference temperature, T_o, of 346 ° K.

Figures 8a and 8b show the experimental traction data (marked points) and model predictions (solid lines) for the type I and type II models respectively, at an inlet temperature of 344 °K and at a rolling speed of 30.5 M/Sec. Clearly, the fit between the data and model predictions is very good for both types of viscosity-pressure-temperature relations. The fit is also very good at the higher rolling speeds and higher inlet temperatures, figures 9a and 9b show the results at 366 °K inlet temperature and at a rolling speed of 45.5 M/Sec, which represents the extreme operating conditions of the available data. At the low end of inlet temperatures and rolling speeds, however, there is substantial difference between model predictions and experimental observations. As shown in figure 10a, the regression coefficients for the type I model provide a relatively good fit to the medium pressure data, it under-predicts traction at higher pressures and the predictions are higher than the experimental observations at lower pressures. With the type II relation, however, the regression analysis results in a fairly good fit at higher pressures, while the predictions are higher than the experimental observations at lower pressures, as shown in figure 10b.

On the whole correlations between the model predictions and experimental observations are equally good for both the type I and type II models. Plots for the entire data set are included with the model predictions in Appendix A and the model coefficients, computed from the regression analysis, are summarized in table 1.

A close examination of the coefficients tabulated in table 1 reveals that the reference viscosity parameters, μ_o^* and μ_o^{**}, generally decrease with both rolling speed and temperature. This is in complete agreement with the trends observed earlier by Gupta et al [3]. The variation in β^*, however, unlike the earlier data [3], does not appear to be significant; this suggests a further refinement in the model by carrying out the regression analysis over the viscosity parameter only. For the type II model, however, there is a noticeable variation in β^{**} as a function of rolling speed and temperature; it seems to decrease with rolling speed and increase with temperature. Such a trend is in agreement with the earlier data [3]. A rigorous quantitative comparison of the coefficients derived by Gupta et al [3] to those obtained under the present investigation is not quite straightforward because the disk temperature data is not available in the current data base. However, in view of the present observation that, at least for the type I relation, the traction model may be reduced to only a single viscosity parameter, it will be interesting to repeat the regression analysis of both the earlier and the current data with a fixed β^* and with the disk temperatures equated to the inlet temperature.

3.4 MIL-L-7808-Type Lubricant

The MIL-L-7808-type lubricant is, perhaps, the most widely used military lubricant and its rheological behavior has been studied by a number of investigators. In the present investigation, the ambient properties documented by Gupta et al. [3] are used for the film thickness computation and also, based on the parametric study reported in this work the pressure-viscosity coefficient in the high-pressure contact region is assumed to be 5.22E-09 1/Pa, as a baseline.

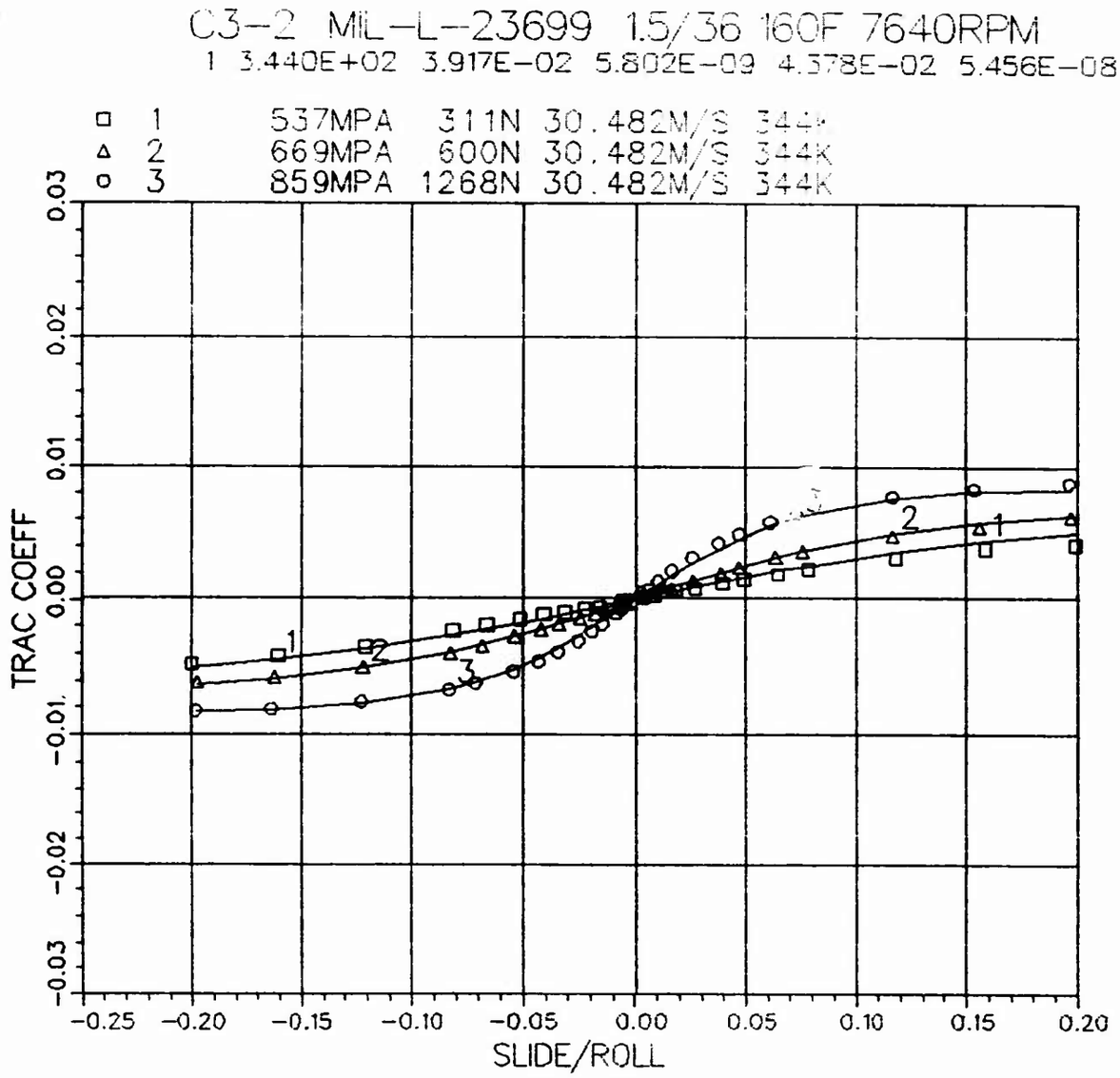

Figure 8a. Fit of the type I model to the MIL-L-23699 data at 344 ^{o}K and at a rolling speed of 30.5 meters/second.

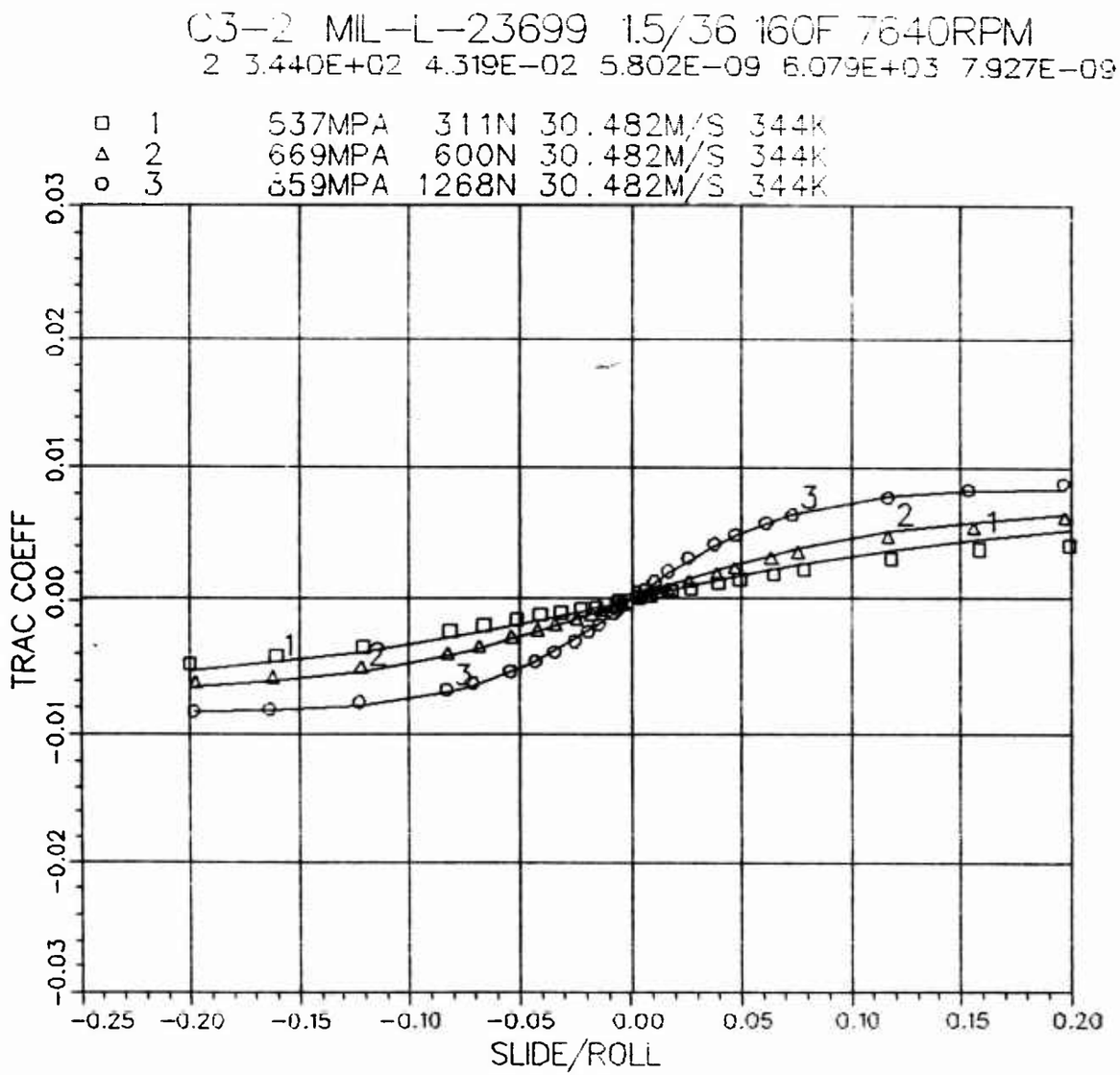

Figure 8b. Fit of the type II model to the MIL-L-23699 data at 344°K and at a rolling speed of 30.5 meters/second.

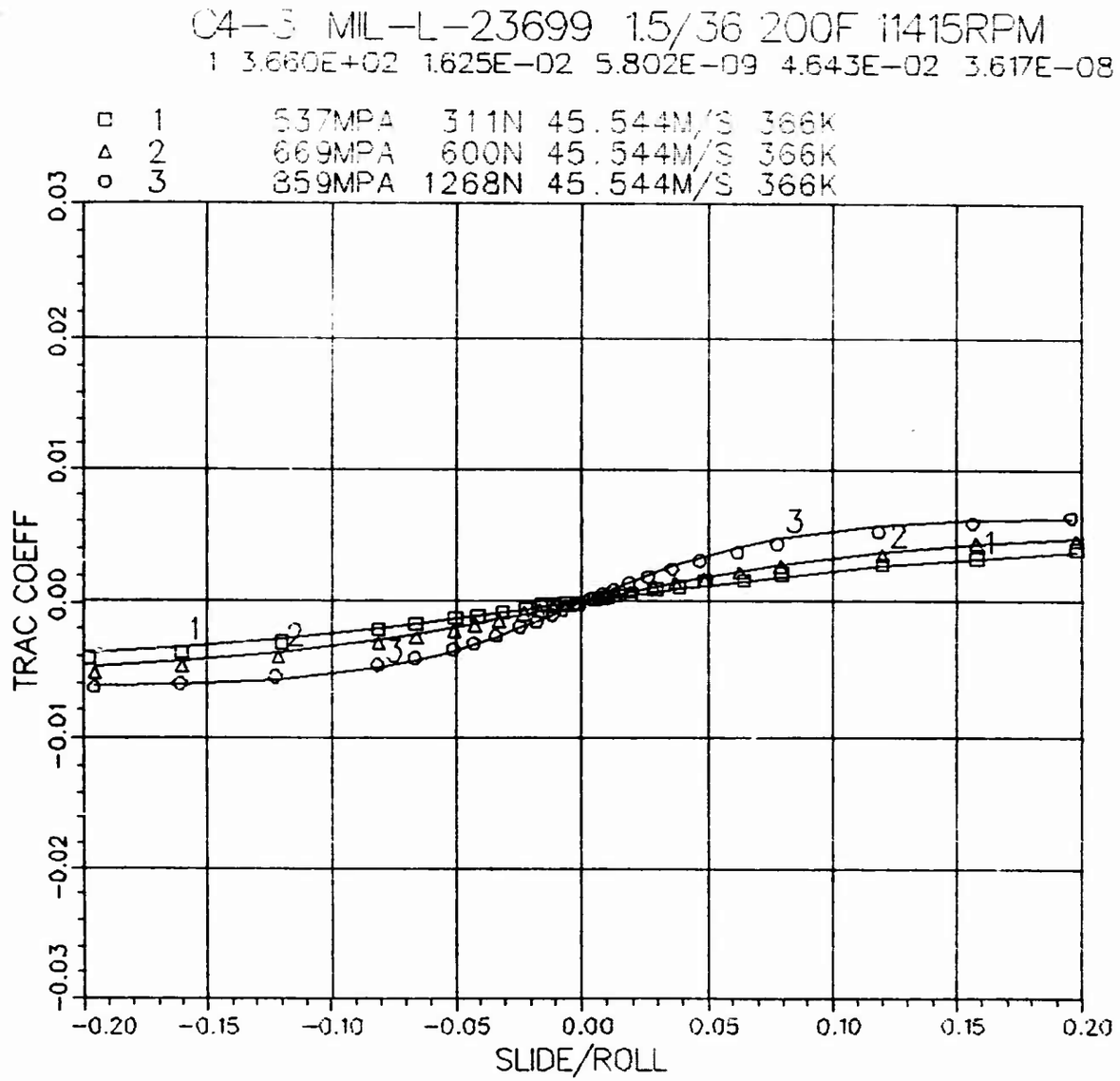

Figure 9a. Fit of the type I model to the MIL-L-23699 data at 366 ^{o}K and at a rolling speed of 45.5 meters/second.

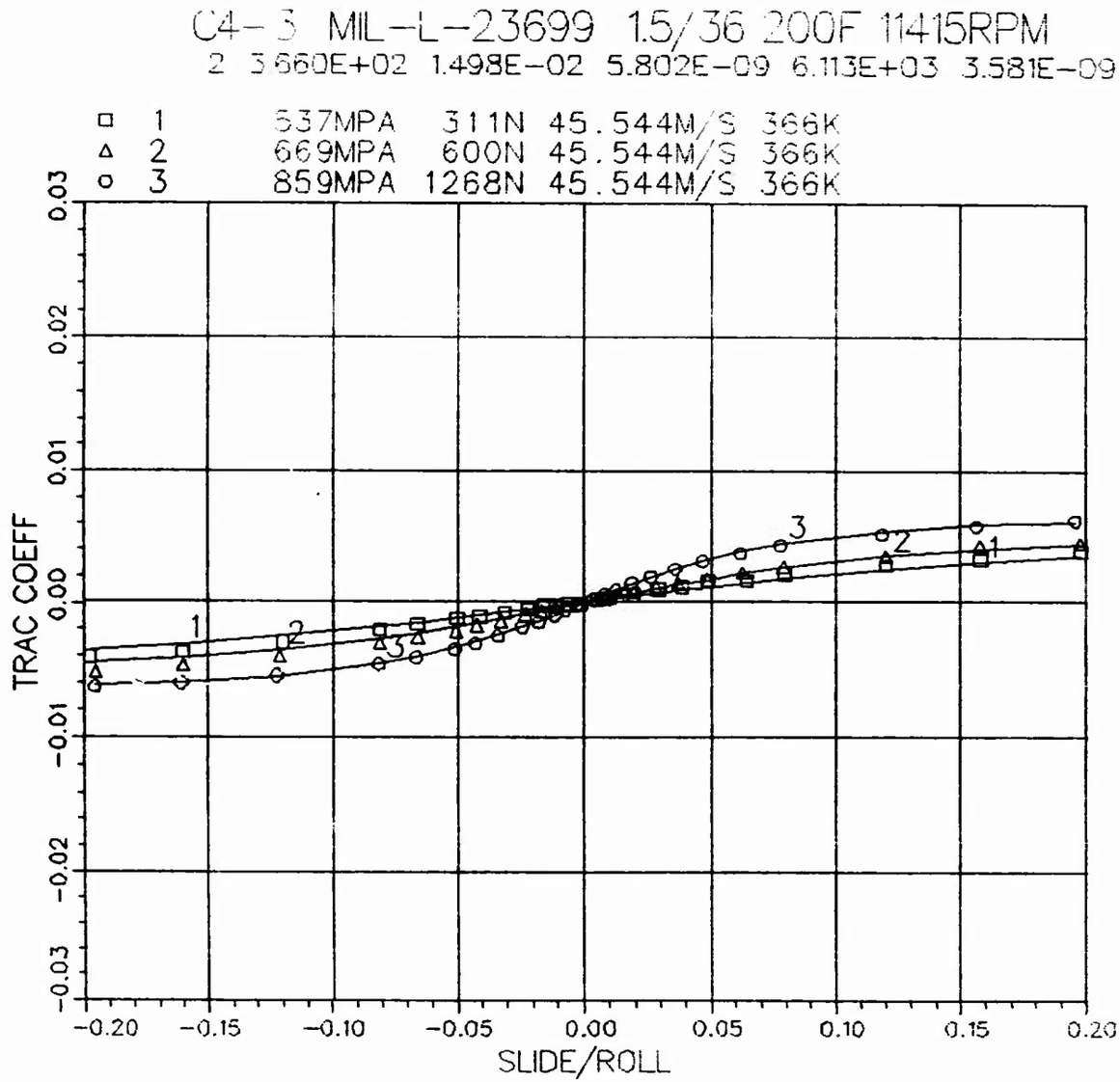

Figure 9b. Fit of the type II model to the MIL-L-23699 data at 366 ^{o}K and at rolling speed of 45.5 meters/second.

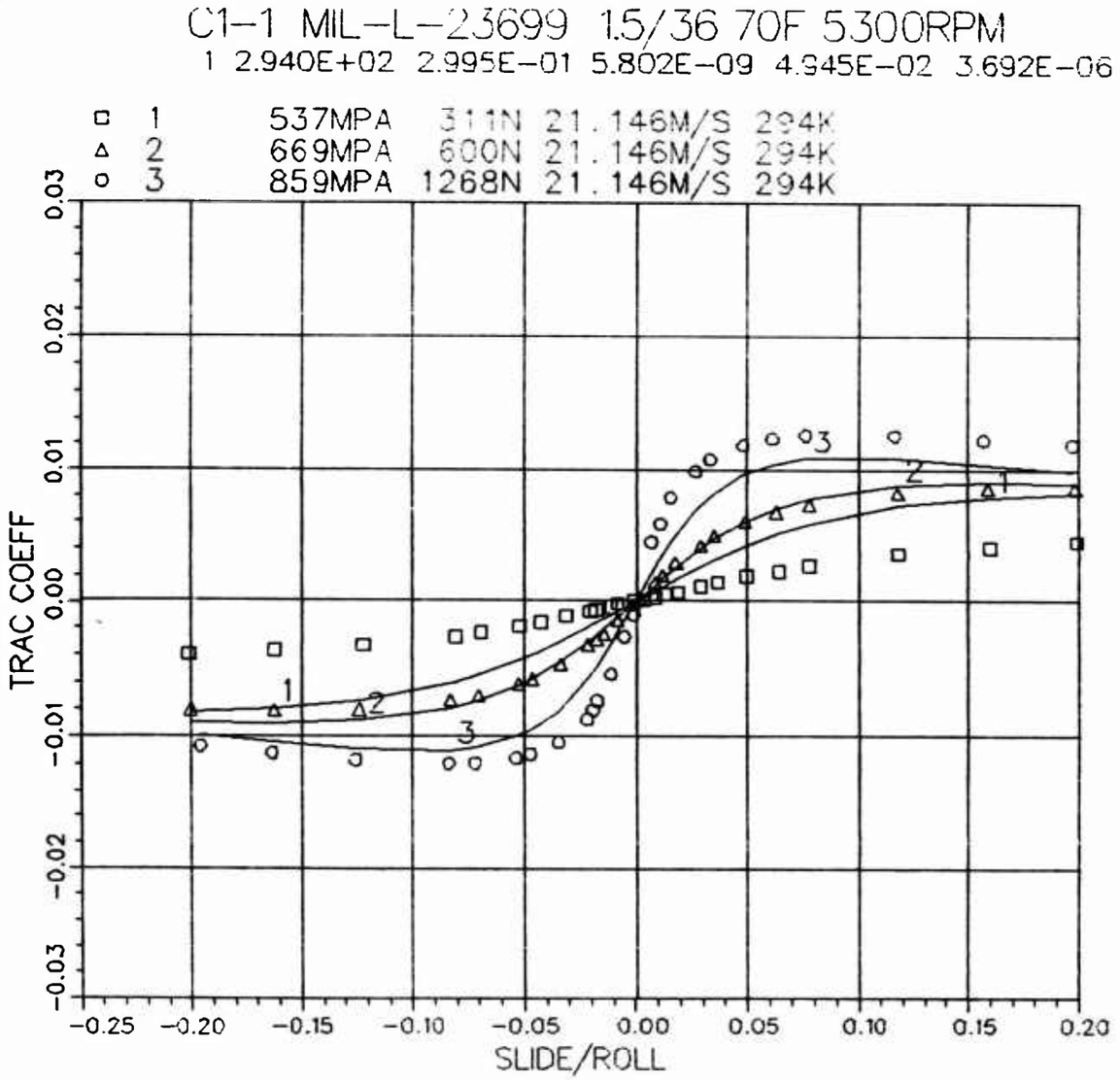

Figure 10a. Fit of the type I model to the MIL-L-23699 data at 294 ^{o}K and at a rolling speed of 21.15 meters/second.

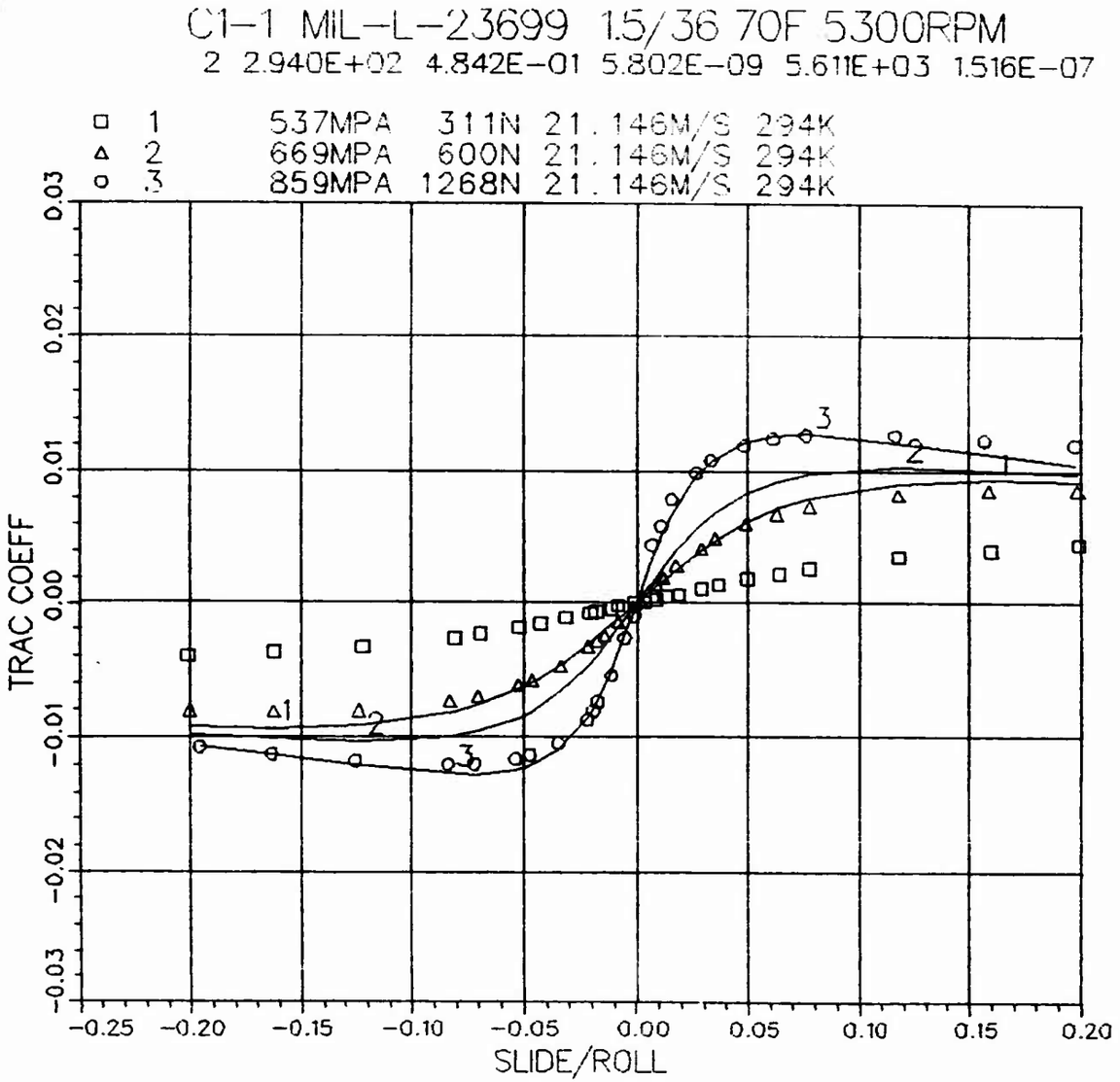

Figure 10b. Fit of the type I model to the MIL-L-23699 data at 294 ^{o}K and at a rolling speed of 21.15 meters/second.

Table 1

Model Coefficients for the MIL-L-23699 Lubricant

Cor elations at Inlet Temperature

$\alpha^* = \alpha^{**} = 5.802 \times 10^{-9}$ 1/Pa

Temp (°K)	Roll Velo (M/S)	μ_0^* (Pa.S)	β^* (1/°K)	μ_0^{**} (Pa.S)	β^{**} (°K)
294	21.146	0.2995	0.04945	0.4842	5611
294	30.482	0.2651	0.05075	0.2771	5110
294	45.544	0.07182	0.03998	0.09958	4348
322	21.146	0.1290	0.05621	0.1571	6851
322	30.482				
322	45.544	0.04668	0.04984	0.05358	5491
344	21.146	0.04634	0.04905	0.05646	7632
344	30.482	0.03917	0.04378	0.04319	6079
344	45.544	0.03103	0.04692	0.03215	5969
366	21.146	0.01915	0.06207	0.02058	9861
366	30.482	0.01752	0.04668	0.01896	7307
366	45.544	0.01625	0.04643	0.01498	6113

The model correlations are very similar to those observed for the MIL-L-23699 type lubricant. The fit between the data and model predictions is extremely good throughout the entire range of operating conditions, except for the few data sets obtained at the lowest inlet temperature. Figures 11a and 11b show the fits at an inlet temperature of 322 °K and at the high end of rolling speeds, 45.5 M/Sec, for the type I and type II models respectively. The fit at the higher temperature of 344 °K is shown in figures 12a and 12b, respectively for the two types of viscosity-pressure-temperature relations. At the lower inlet temperature, 294 °K, similar to the MIL-L-23699 type lubricant, the type I model seems to better fit the data at medium pressures, while the type II relation fits better at higher pressures, as seen in figures 13a and 13b. A worthy observation here is the fact that there is a definite bias in this set of experimental data, i.e., the traction coefficients at the positive slip velocities are different from those at the corresponding negative value of slip velocities, particularly at the high end of contact pressures. One of the factors contributing to this difference in traction is the different rolling speed at the corresponding points on the positive and negative sides of the data, due to the fact that the variation in slip is obtained by varying the velocity of only one of the disks. However, the difference seen in figures 13a and 13b, cannot be fully accounted for by the varying rolling speed alone. Perhaps, the torque measurement and calibration systems, and the general nature of power dissipation in the support bearings, particularly at lower oil temperatures, need further examination.

Based on the above discussion it may be concluded that except for the data obtained at the low end of inlet temperatures, there is a good agreement between the model predictions and experimental observations. The computer plots for the entire range of data along with model predictions, for both the type I and type II models, are included in Appendix A. The model coefficients, computed from the regression analysis, are summarized in table 2.

The trends of the various model parameters are similar to those discussed above for the MIL-L-23699 lubricant and they are in good agreement to those obtained earlier by Gupta et al. [3], except that the variation in the temperature-viscosity parameter, β^*, is not significant in the current data. Based on this finding it is necessary to repeat the regression analysis with fixed β^* for both the earlier and current data. Also, the disk temperature in the earlier data should be set equal to the inlet temperature for a one to one comparison with the current data.

3.5 Effect of Contact Geometry

All of the experimental data discussed above was obtained with a set of crowned disk specimens, with a rolling radius of 38.10 mm and a crown radius of 914.40 mm. Thus the shape of the contact zone was a relatively narrow ellipse which simulates either a closely conformed ball/race contact in a ball bearing or a roller/race line contact in cylindrical roller bearings. With the objective of investigating the influence of contact geometry one set of traction data, for the MIL-L-7808-type lubricant, was obtained with spherical disks, where the crown radius is set equal to the rolling radius; thus, a circular point contact is simulated.

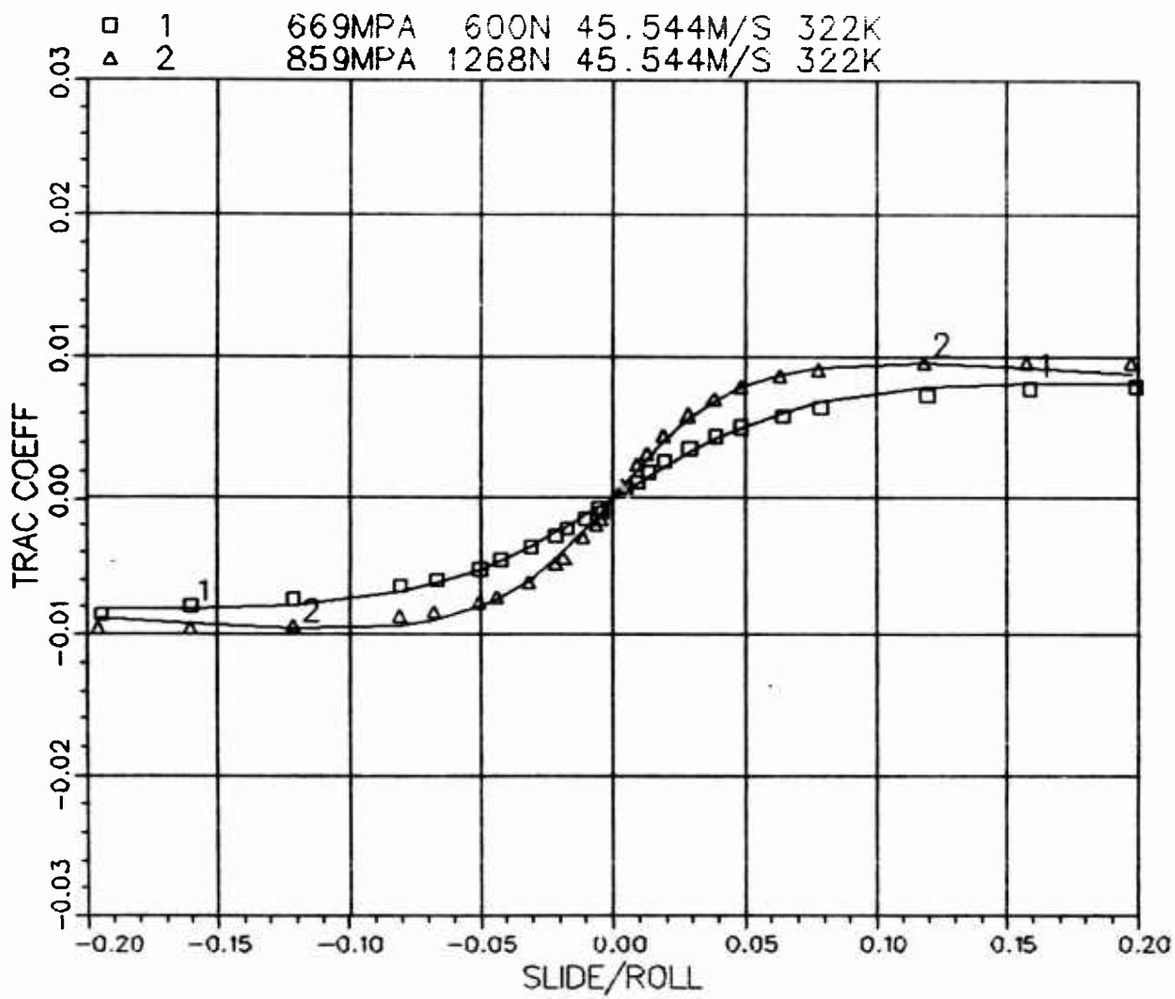

Figure 11a. Fit of the type I model to the MIL-L-7808 data at 322 ^{o}K and at a rolling speed of 45.5 meters/second.

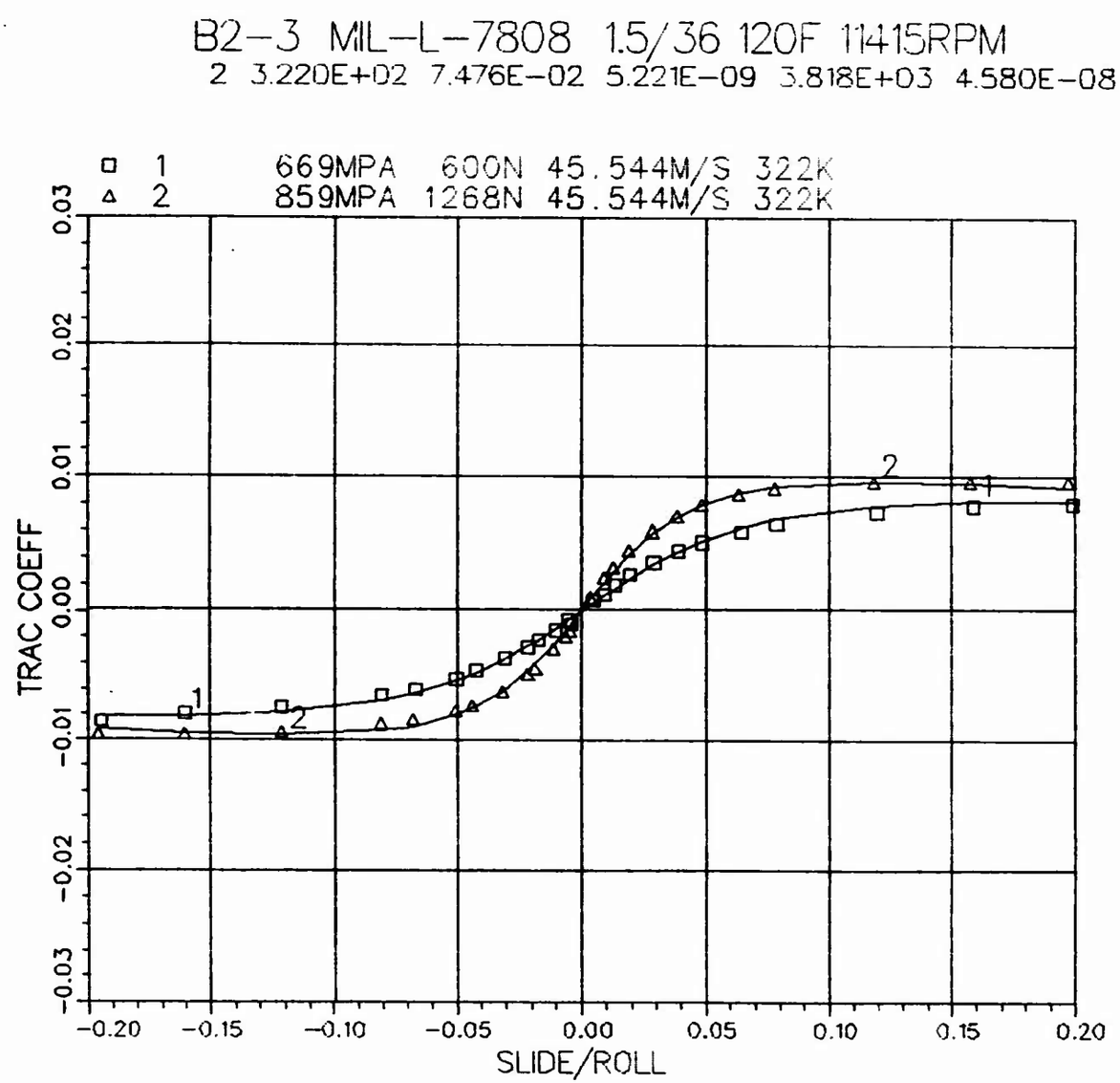

Figure 11b. Fit of the type II model to the MIL-L-7808 data at 322 ^{o}K and at a rolling speed of 45.5 meters/second.

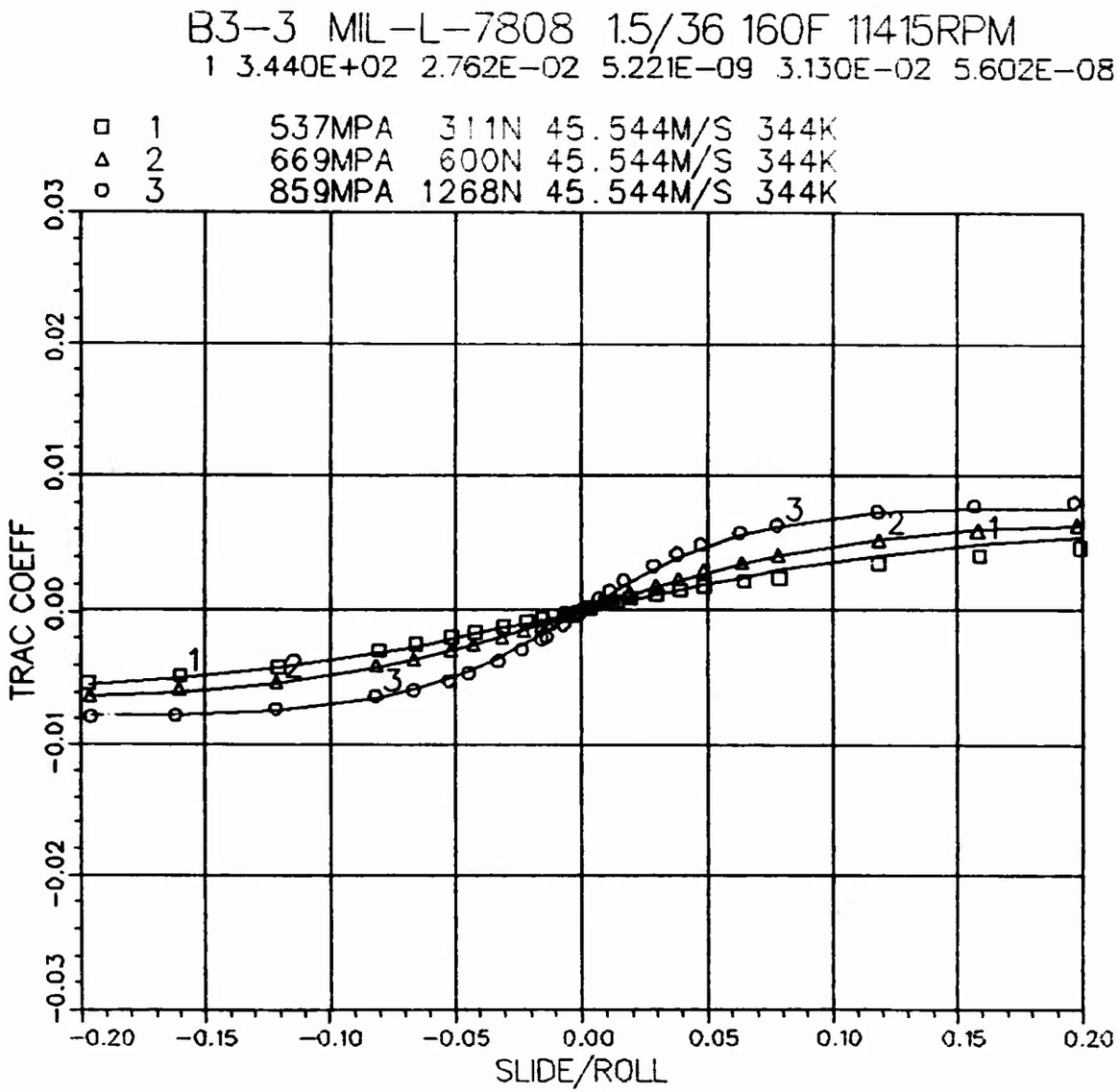

Figure 12a. Fit of the type I model to the MIL-L-7808 data at 344 ^{o}K and at a rolling speed of 45.5 meters/second.

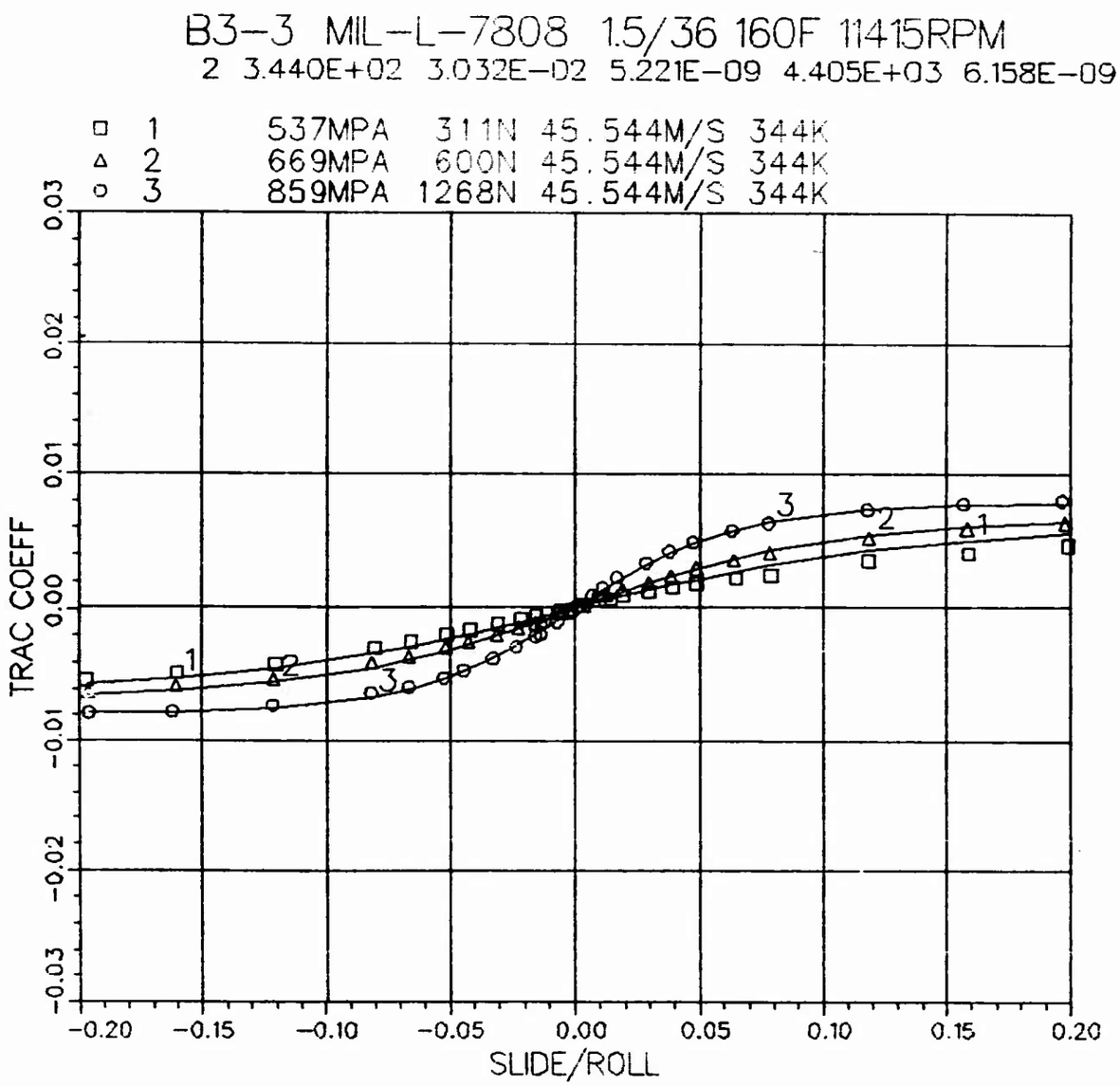

Figure 12b. Fit of the type II model to the MIL-L-7808 data at 344 ^{o}K and at a rolling speed of 45.5 meters/second.

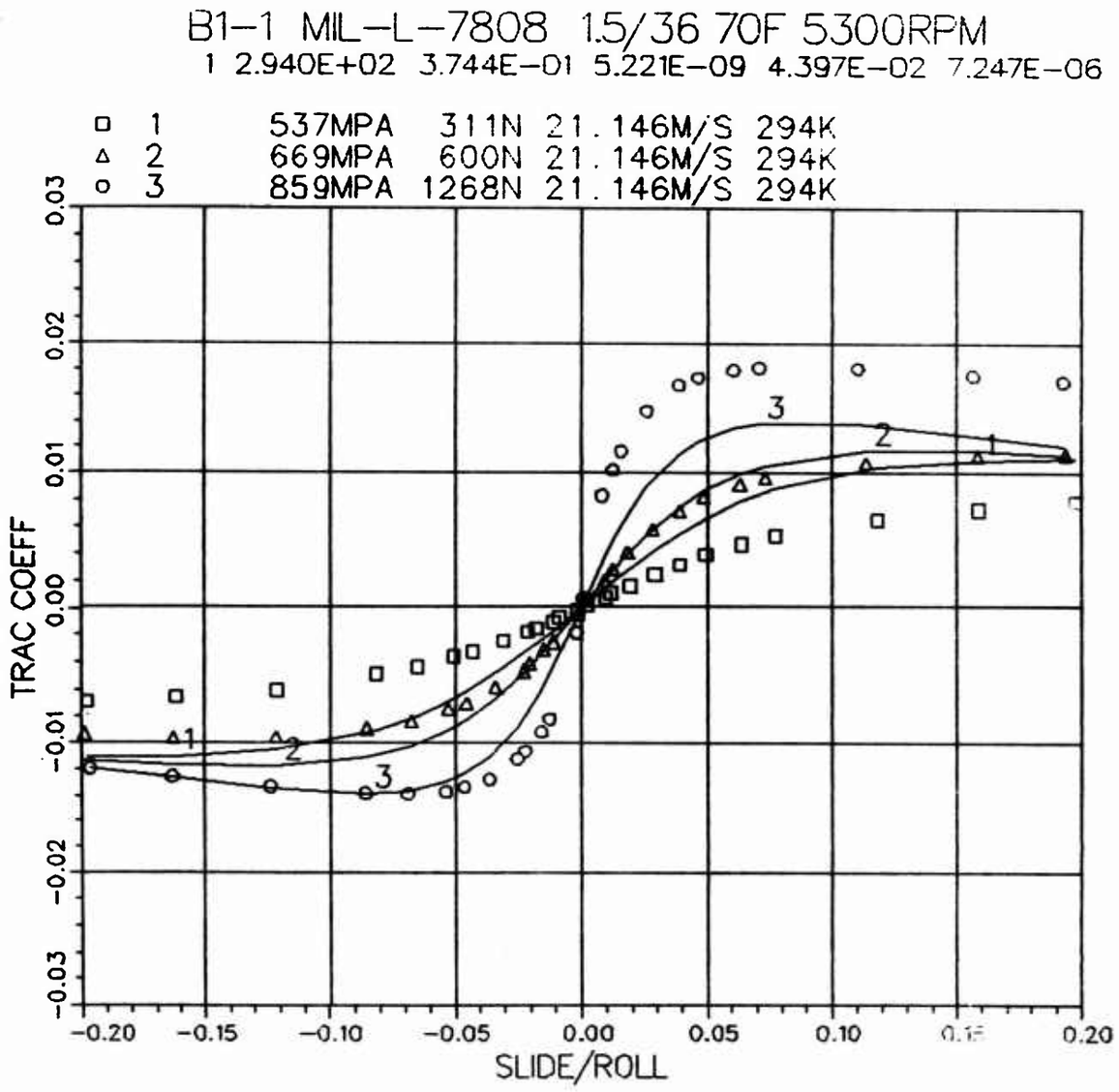

Figure 13a. Fit of the type I model to the MIL-L-7808 data at 294 ^{o}K and at a rolling speed of 21.15 meters/second.

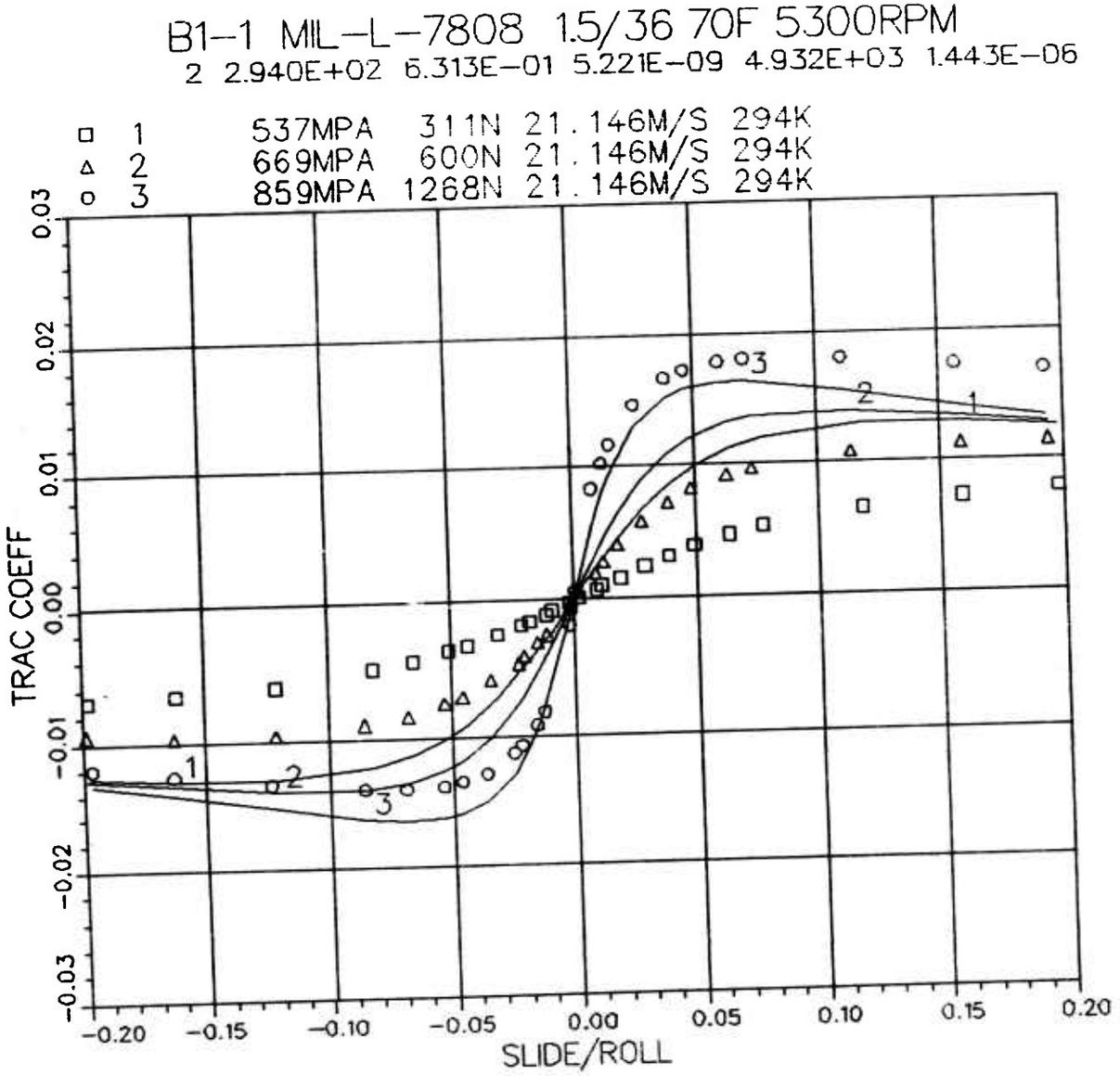

Figure 13b. Fit of the type II model to the MIL-L-7808 data at 294 ^{o}K and at a rolling speed of 21.15 meters/second.

Table 2

Model Coefficients for the MIL-L-7808 Lubricant

Correlations at Inlet Temperature

$\alpha^* = \alpha^{**} = 5.221 \times 10^{-9}$ 1/Pa

Temp (°K)	Roll Velo (M/S)	μ_o^* (Pa.S)	β^* (1/°K)	μ_o^{**} (Pa.S)	β^{**} (°K)
294	21.146	0.3744	0.04397	0.6313	4932
294	30.482	0.2289	0.04243	0.4060	4812
294	45.544	0.1013	0.03855	0.1558	4187
322	21.146	0.1084	0.04341	0.1591	6117
322	30.482	0.08075	0.03579	0.1047	4743
322	45.544	0.07136	0.03138	0.07476	3818
344	21.146	0.04119	0.05071	0.04771	7231
344	30.482	0.03073	0.03554	0.03712	5448
344	45.544	0.02762	0.03130	0.03032	4405

Figures 14a and 14b show a typical set of traction data and its correlations with the type I and type II models. It is seen that the type I model fits the experimental behavior fairly well, although the fit is not as good as that observed earlier for the elliptical contact data. Note the rather high slope of the traction curve, which results from the relatively high contact stresses in the point contact data. Under the very high contact stress the predictions of the type II model are somewhat questionable, particularly with regard to computation of thermal reduction factor for the lubricant film, the viscous shear heating in the high-pressure contact zone, and the positive traction slope in the high slip region, as seen in figure 14b.

The computed model coefficients for this set of data are tabulated in table 3 and the traction curves are included in Appendix A. Similar to the elliptical contact data, discussed above, the coefficients in table 3 are computed with the assumption that the surface temperature of the disks is equal to the inlet temperature. The general trends of the coefficients are quite similar to those discussed above for the line contact data. However, in view of the substantially increased scatter between the experimental data and model predictions, particularly in terms of the very high traction slopes at low slip rates and very high contact pressures, it is necessary to modify the model to allow for viscoelastic effects, after ensuring the repeatability of the data. Such refinements may be based on the more recent work by Johnson and Tevaariverk [26], and by Bair and Winer [27].

Since the point contact data includes some measurement of disk temperatures, the regression analysis is repeated with the actual disk temperatures; the resulting coefficients are tabulated in table 4. Although the scatter between the experimental data and the model predictions, see the data set plots in Appendix A, is relatively unchanged, there is a rather erratic change in the model coefficients. The jump in the viscosity parameters at 322 °K, in table 4, suggests possible experimental discrepancies in the temperature data.

3.6 Rolling Bearing Performance Modeling

The significance of the traction model lies in the prediction of component behavior and the simulation of practical mechanical systems where the lubricant is used in practice. For the purpose of illustration, the model coefficients computed above for the type I model are input to the bearing dynamics computer model, ADORE, and the slip characteristics of a roller in a cylindrical roller bearing are investigated as the roller travels through the load zone in the radial loaded bearing. Figure 15 shows the length of simulation and the normal load variation as the roller travels from a relatively unloaded state to the maximum load state and then exits out of the load zone.

As the roller travels through such varying contact loads, the tractive forces at the roller/race interaction, which are derived from the lubricant traction model, determine the acceleration of the roller; hence roller slip or skid is very closely coupled to the lubricant traction behavior. Figure 16a shows the simulated behavior under the type I model at 294 °K. The operating conditions at the roller/race interface, particularly the rolling speed, are within the range of experimental data used to derive the model

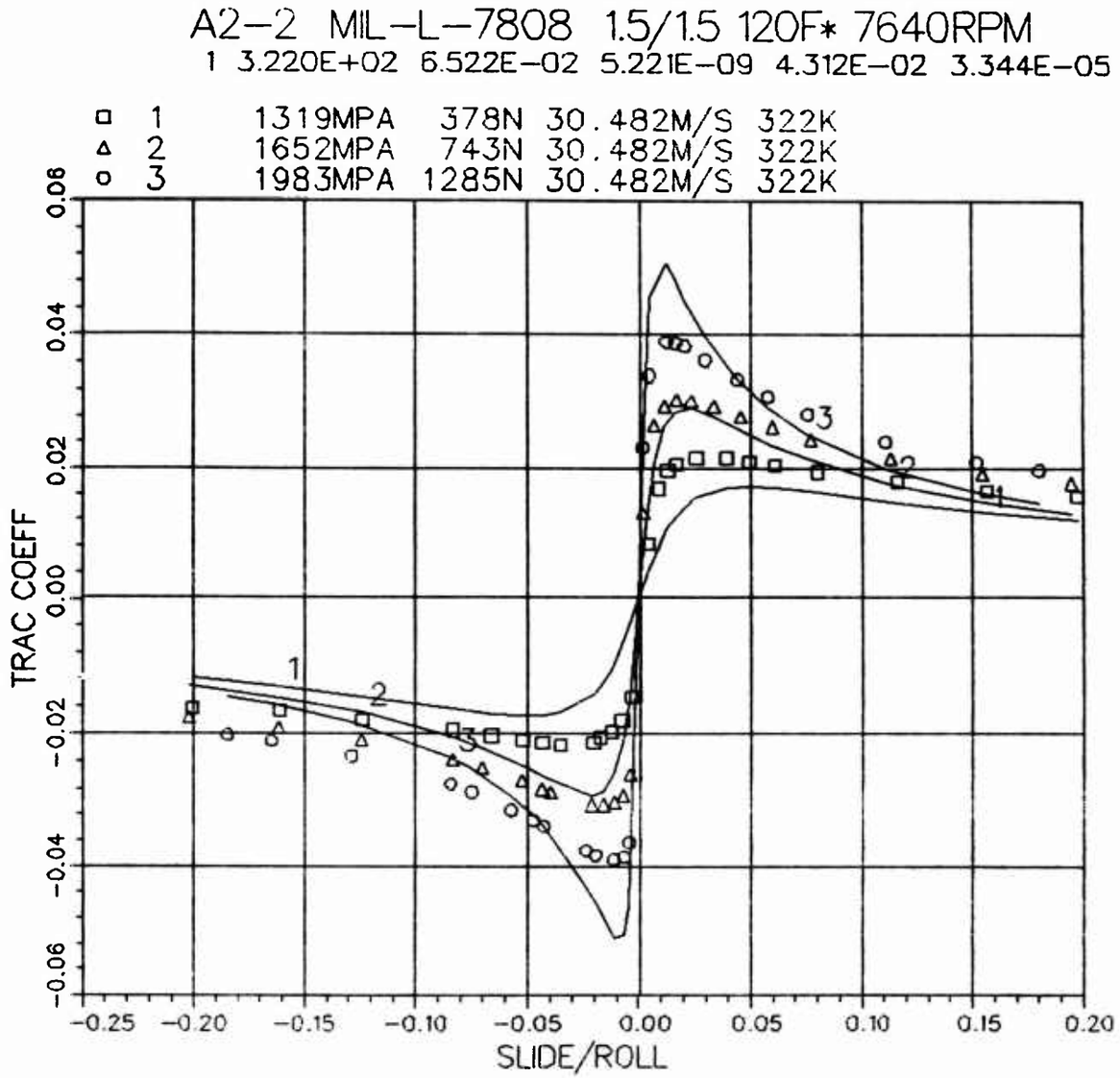

Figure 14a. Typical correlation of the type I model to the high-pressure circular contact traction data obtained with the MIL-L-7808 lubricant.

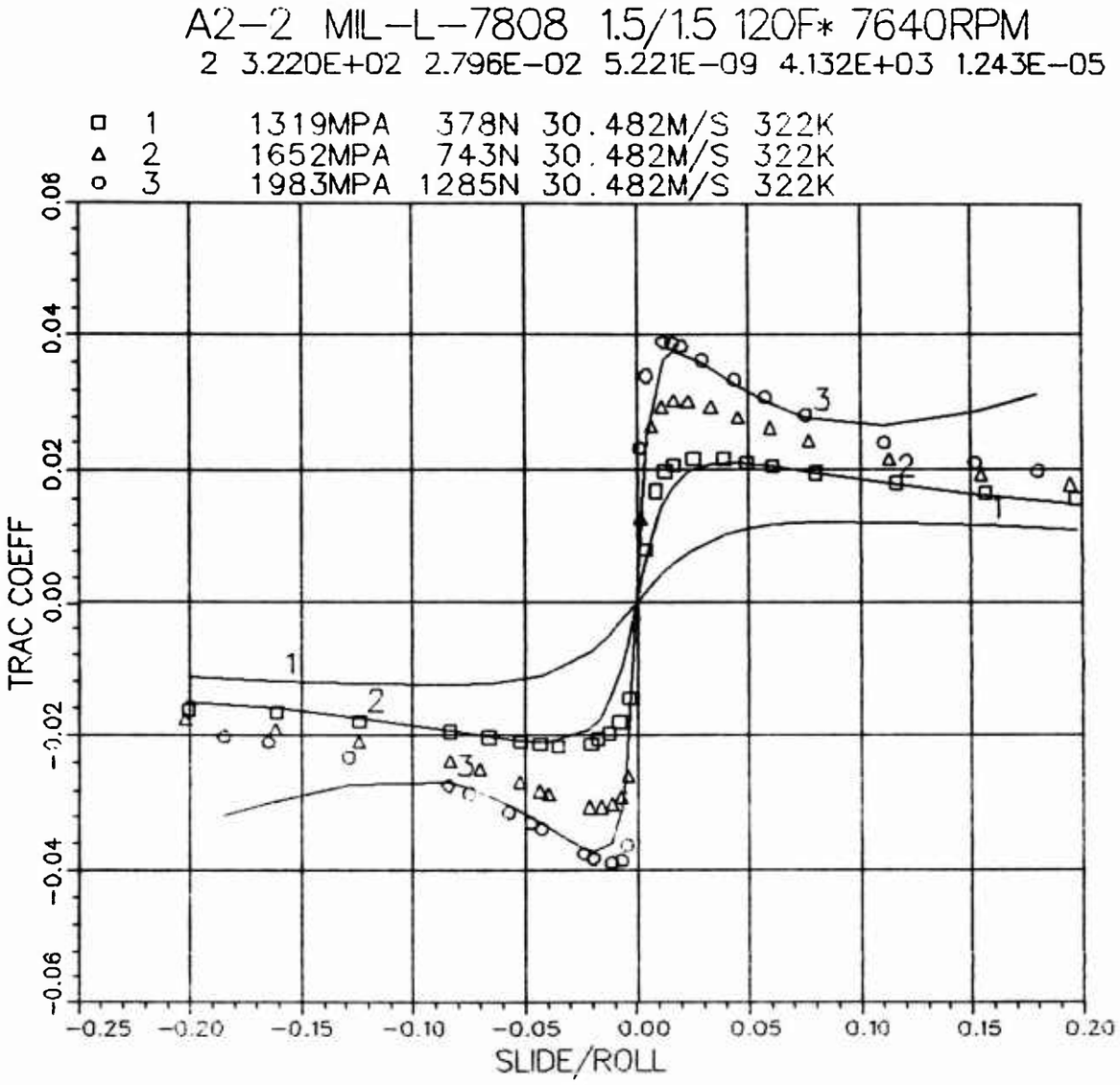

Figure 14b. Typical correlation of the type II model to the high-pressure circular contact traction data obtained with the MIL-L-7808 lubricant.

Table 3

Model Coefficients for the MIL-L-7808 Lubricant

Point Contact Data

Correlations at Inlet Temperature

$\alpha^* = \alpha^{**} = 5.221 \times 10^{-9}$ 1/Pa

Temp (°K)	Roll Velo (M/S)	μ_o^* (Pa.S)	β^* (1/°K)	μ_o^{**} (Pa.S)	β^{**} (°K)
294	21.146	0.1317	0.04559	0.06474	4019
294	30.482	0.03520	0.01755	0.01925	2273
294	45.544	0.02477	0.02878	0.005355	2832
322	21.146	0.07780	0.05270	0.03988	5305
322	30.482	0.06522	0.04312	0.02796	4132
322	45.544	0.06168	0.04114	0.01542	3420
344	21.146				
344	30.482				
344	45.544	0.01655	0.03636	0.009870	4611

Table 4

Model Coefficients for the MIL-L-7808 Lubricant

Point Contact Data

Correlations at Disk Temperature

$\alpha^* = \alpha^{**} = 5.802 \times 10^{-9}$ 1/Pa

Temp (°K)	Roll Velo (M/S)	μ_o^* (Pa.S)	β^* (1/°K)	μ_o^{**} (Pa.S)	β^{**} (°K)
294	21.146	0.1928	0.04473	0.1049	4268
294	30.482	0.04486	0.01780	0.02547	2397
294	45.544	0.04363	0.02891	0.09967	3114
322	21.146	0.3280	0.03505	0.2063	3934
322	30.482	0.2331	0.03236	0.1558	3461
322	45.544	0.2345	0.03567	0.05930	3304
344	21.146				
344	30.482				
344	45.544	0.09320	0.02583	0.1026	3732

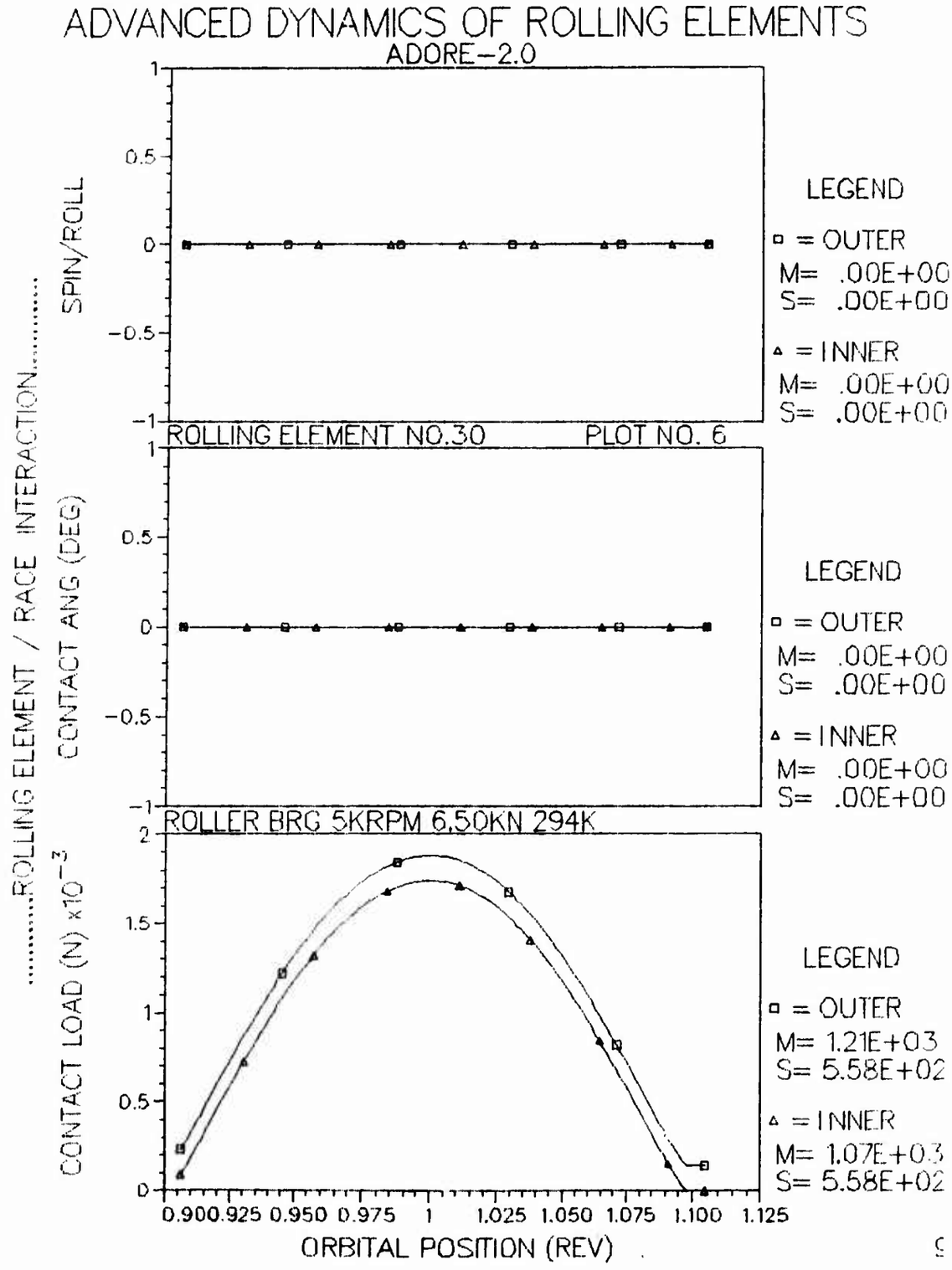

Figure 15. Typical roller/race load variation in a radially loaded cylindrical roller bearing.

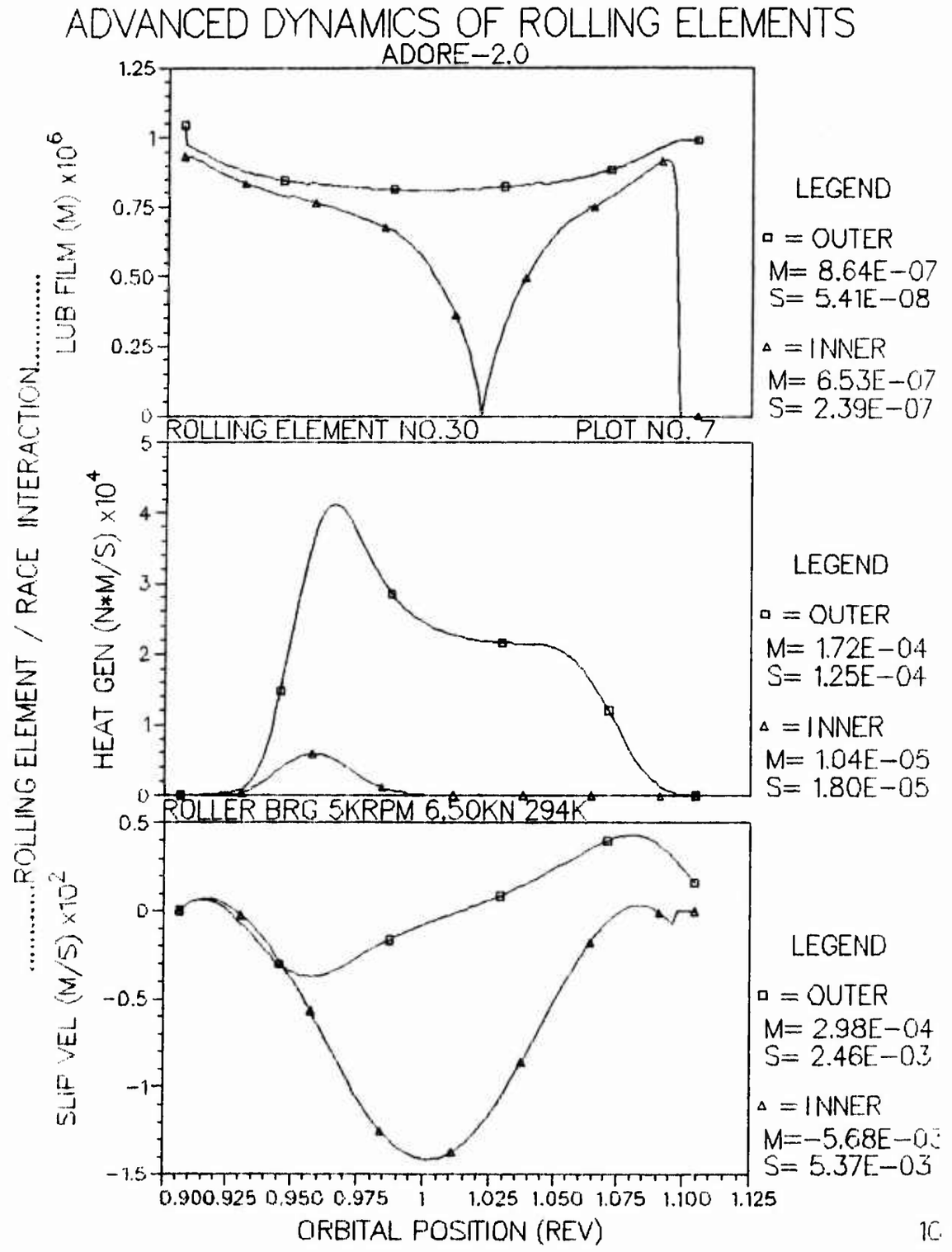

Figure 16a. The simulation of roller/race slip with the MIL-L-7808, type I lubricant model at 294°K.

coefficients. As the load on the roller increases, it demands a definite traction force from the lubricant in order to maintain a rolling configuration at both races. Thus the slip on the driving race, which is the inner race in the present case, begins to increase in search of increasing traction; the slip will normally increase until the required acceleration is met. With a liquid-lubricated bearing, the increasing slip results in a reduction in film thickness due to shear heating of the lubricant. This in turn results in a reduction in traction through the film, but it increases the probability of metal contact as the film thickness approaches the rms surface roughness of the interacting surfaces. Such a mechanism for the MIL-L-7808 lubricant is clearly seen in figure 16a. It is seen that since the lubricant traction force is always less than that required to keep the roller in a rolling state, the slip at the roller to inner race interface increases to a maximum when the roller reaches the maximum load. The thermal effect in the lubricant film through this slippage reduces the film thickness to almost zero under the maximum load. Note that since the solutions shown in figure 16a do not include any metal contact and are strictly based on fluid traction, the contact losses, particularly at the inner race, may be greatly under estimated.

If the operating temperature is increased to 344 °K, the upper limit of experimental data, both the lubricant film thickness and traction further reduce but the general behavior of roller remains unchanged. This is shown in figure 16b, which is qualitatively similar to figure 16a.

A practical question which arises from the above discussion concerns the determination of optimum lubricant behavior for acceptable bearing performance. It is necessary that the lubricant provide adequate traction to prevent excessive skid on the roller, yet the traction should be small enough to keep the heat generation in the bearing within reasonable limits. A realistic modeling of lubricant behavior is, therefore, extremely important. To establish this point a bit further, consider the traction curve of figure 17, which provides somewhat larger tractions than those observed with the MIL-L-7808 lubricant. Under such a behavior, the traction forces, as the roller begins to slip, rapidly meet the roller acceleration requirements; and since the traction response at the outer and inner races is identical under the hypothetical model, the roller slip rates and traction coefficients adjust such that the heat generated at the outer and inner race interactions are almost equal. Such a behavior is shown in figure 18. It is also seen that the slip rates in figure 18 are lower than those shown in figures 16a and 16b; however, the heat generated at roller/race contact is significantly larger due to higher traction coefficients, which implies that certain optimization of the lubricant properties is necessary. Such an optimization can be easily performed by carrying out a parametric evaluation of the roller motion as a function of the coefficients of the traction model. Thus the development of a traction model is significant for the design and performance simulation of mechanical components, such as rolling bearings.

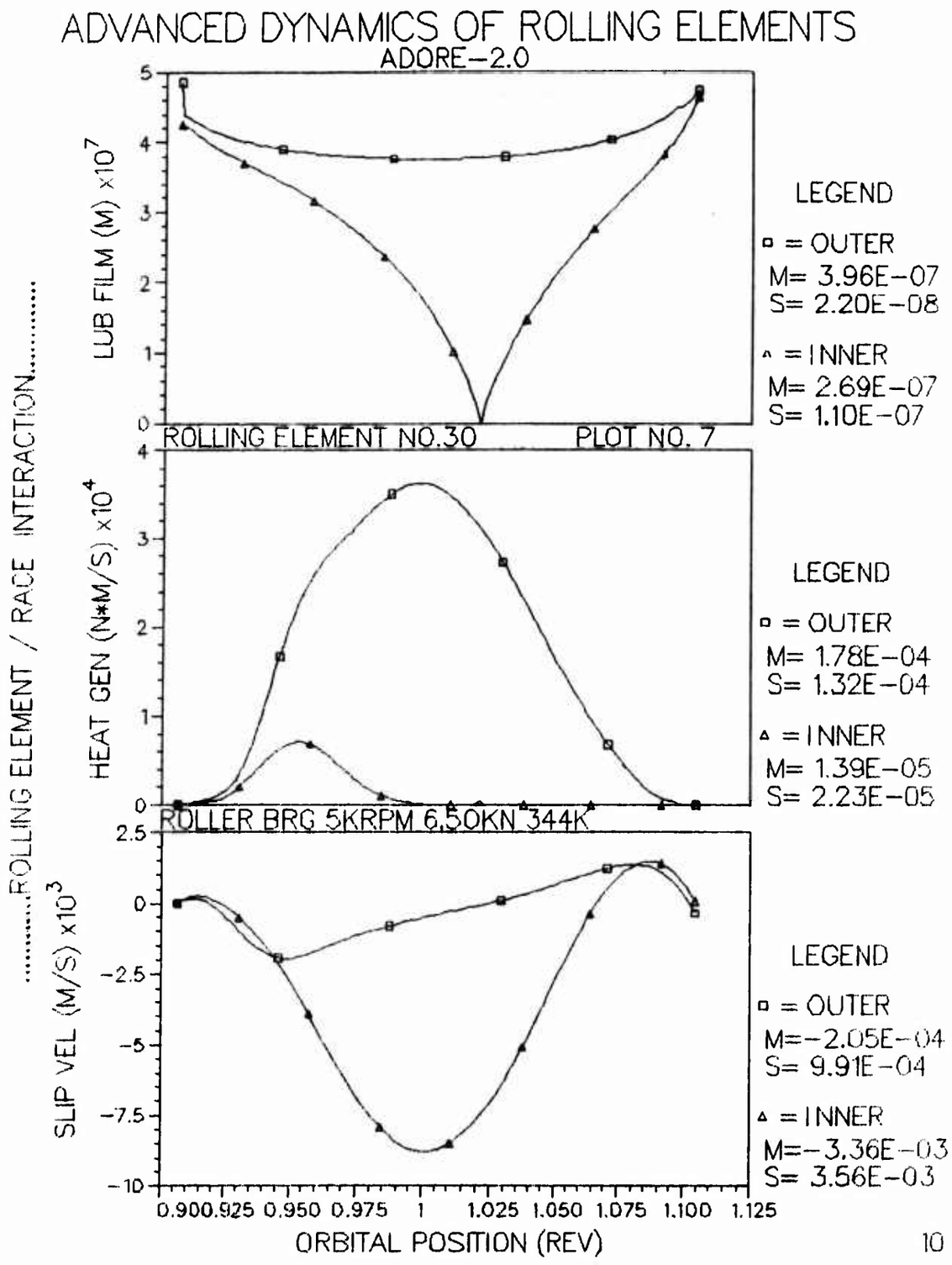

Figure 16b. The simulation of roller/race slip, in a cylindrical roller bearing, with the MIL-L-7808, type I traction model at 344 ^{o}K.

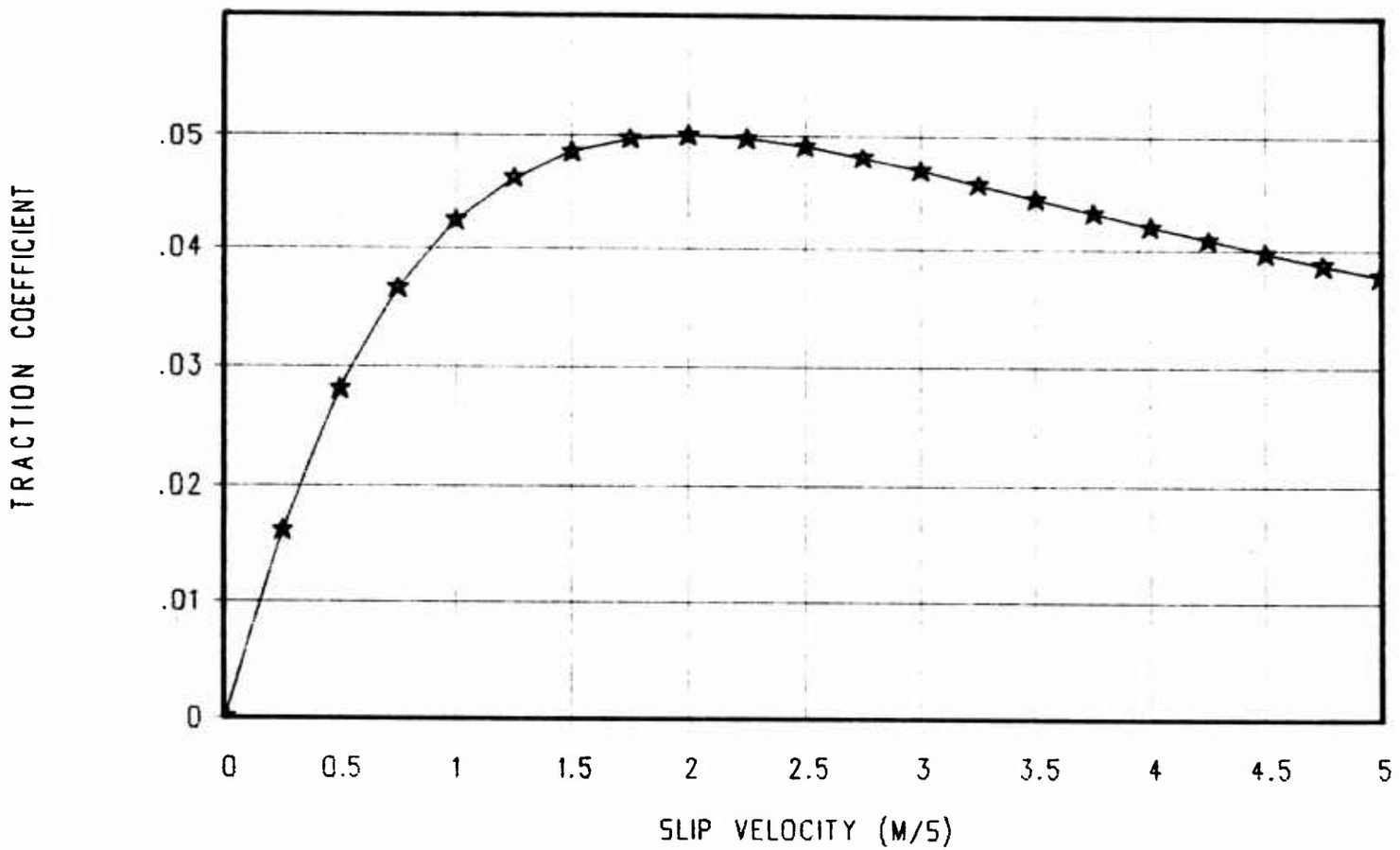

Figure 17. A hypothetical traction–slip curve.

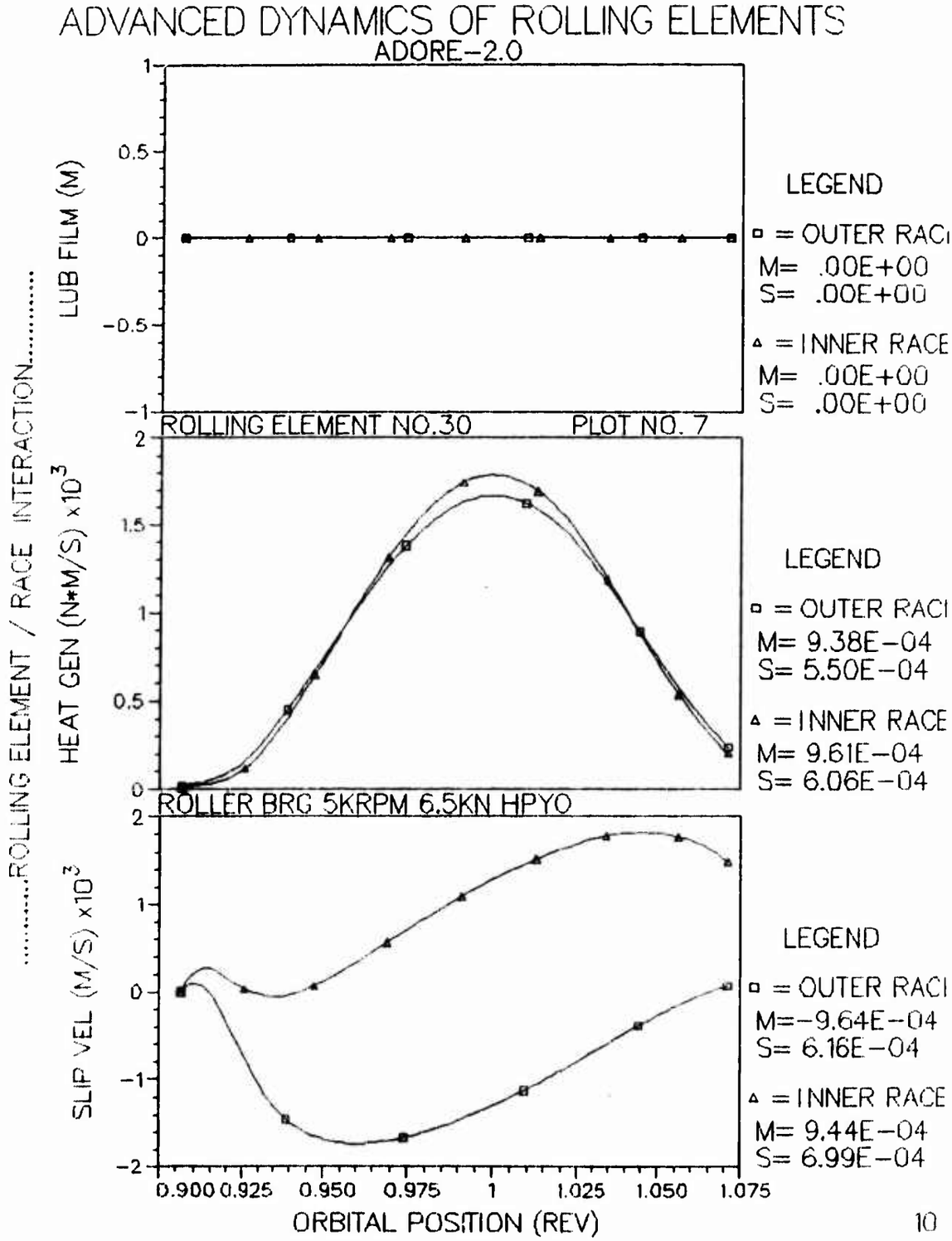

Figure 18. The simulation of roller/race slip in a cylindrical roller bearing with the hypothetical traction model shown in figure 17.

4. CONCLUSIONS

The feasibility of a traction model, based on viscosity-pressure-temperature constitutive relations in the high-pressure zone of elastohydrodynamic contacts, is demonstrated for two military lubricants meeting MIL-L-23699 and MIL-L-7808 specifications. The model predictions are shown to agree fairly well with the experimental data obtained at the AFWAL Aero Propulsion Laboratory, with cylindrical disk specimens resulting in an elliptical contact.

Among the two types of viscosity-pressure-temperature relations, type I with exponential variation in viscosity with pressure and temperature, and type II with the viscosity varying exponentially with pressure and inverse temperature, the regression coefficients for the type I model indicate that the entire variation may be represented by a variation in a reference viscosity parameter; thus a greatly simplified relation for traction may be obtained. Also, since the mathematical simplicity of the type I relation allows for an effective incorporation of the traction model in sophisticated component models, such as the advanced bearing dynamics computer code ADORE, it offers significant potential for the performance simulation of practical components as a function of lubricant behavior and, therefore, the development of lubricants for advanced applications.

In the case of very high pressure circular contacts, noticeable scatter between the experimental data and model predictions is observed, particularly in terms of modeling the rather high traction slope in the very low slip region. This, to some extent, suggests a viscoelastic behavior of the lubricant. Further model refinements to allow for such physical behavior are therefore necessary for applications with extremely high contact pressures.

The close coupling between the lubricant behavior and component performance is demonstrated by modeling the roller slip as a function of lubricant behavior in a cylindrical roller bearing. It is demonstrated that the development of a realistic traction model is vital to the selection of optimum lubricant behavior for a given application.

5. RECOMMENDATIONS FOR FUTURE DEVELOPMENTS

The findings of the present investigation demonstrate the feasibility of the overall approach to traction model development through a least-squared regression fit of a physical model to actual traction data. However, the ultimate development of a model for military applications requires significant further development. Based on the conclusions of the present work, some of the specific tasks requiring further development are listed below:

1. The regression analysis for the type I relation should be repeated for the present data with the entire variation in traction modeled in terms of the variation of the reference viscosity parameter. A similar analysis should be carried out for other sets of data available for similar lubricants. If such an analysis results in acceptable correlations then a significant simplification in the rheological model may be accomplished, and this will contribute to a substantial improvement in the computing effort required to model component behavior as a function of lubricant properties.

2. The traction model should be extended to include viscoelastic effects. Appropriate modifications to the regression analysis should then be made to allow for the computation of model coefficients from laboratory traction data. This will significantly improve traction predictions at very high contact pressures and in the low slip region.

3. Although the isothermal film thickness can be easily computed from the available formulae, the computation of thermal reduction factors becomes questionable as the available numerical solutions are extrapolated to very high slip velocities, which are sometimes encountered in roller bearings. Also, in ball bearings, when the ball/cage collisions are severe, excessive ball/race slip or skid is encountered. Thus some refinements in the thermal model for the elastohydrodynamic film thickness are necessary to improve the predictions at high slip velocities.

4. Some of the very recent research has established that the lubricant film thickness in elastohydrodynamic contacts should also be modified to allow for the surface roughness of the interacting surfaces. The development of "roughness factors", based on the available numerical solutions, is therefore, proposed.

5. Since both the film thickness and lubricant behavior in the high-pressure contact zone play an important role in the prediction of traction, it will be desirable to carryout simple experiments where the film thickness and traction may be measured simalteneously. The optical rig at the AFWAL Aero Propulsion Laboratory may be used to obtain such experimental data.

6. Fundamental measurements of lubricant rheology are vital to realistic physical interpretation of the model coefficients. For example, significant physical justification to the pressure-viscosity coefficients, derived from regression analysis of the traction data, may be obtained if the high-pressure viscosity data is available. Indeed,

high-pressure viscometry is a difficult task, however, the recent developments at the AFWAL Aero Propulsion Laboratory provide substantial advancements of such techniques. It is, therefore, suggested that the model coefficients should be compared to the high-pressure viscometry data and appropriate correlations should be developed.

7. The maximum rolling speeds and operating temperatures at which most of the available traction data was obtained are well below the actual conditions in high-speed rolling bearings used in a wide range of military applications. The models developed on the basis of such data have to be greatly extrapolated when they are actually used in bearing performance modeling. Experimental work to extend the operating range of the traction experiments is therefore necessary. Perhaps traction measurements with larger diameter disks, compared to the current 76 mm diameter disks, will be desirable if the maximum disk speed is an experimental limitation.

8. The recent traction data obtained at the AFWAL Aero Propulsion Laboratory for heavily loaded circular point contact is, perhaps, the first data set of its kind. Such data are indeed necessary over a wider range of contact geometry in order to establish the effect of the ellipticity parameters on traction and resulting behavior of a bearing. Also, some of traction experiments with varying geometry may be carried out under controlled misalignment to simulate the effect of spin velocities normal to the contact. The present traction rig at the AFWAL Aero Propulsion Laboratory apparently has such a capability; therefore, such experiments may not be very difficult.

9. After establishing adequate validation of a traction model on the basis of actual traction data obtained with single contacts, it is essential to prove the significance of the model in component modeling. The modeling of bearing performance for prescribed traction models, and comparison of the bearing performance predictions to bearing test data, is therefore necessary. Such test data has been obtained for high-speed ball bearings at the AFWAL Aero Propulsion Laboratory. However, due to a combined slip and spin of the balls, the kinematics of a ball/race contact is extremely complex, and a validation of the traction model for such bearings requires extensive analytical modeling of the contact. The validation, therefore, results in a number of questions with regard to both contact modeling and applicability of traction models developed from greatly simplified contacts. Perhaps experiments with cylindrical roller bearings, where the roller/race contacts are practically free of any spin normal to the contact and the slip is fairly uniform over the contact, at least for carefully aligned bearings, may provide validation of a traction model on a more fundamental level. Once such a validation of the model has been established, it may be applied on a "point-to-point basis" to a rather complex ball/race contact, and the validation of the model with the ball bearing data shall become significantly meaningful.

10. The ultimate outcome of any analytical model of a mechanical component is normally judged in terms of the accuracy of overall performance and life predictions. With a validated traction model the understanding of

shear stresses, film thicknesses and the overall tribological interaction of mating surfaces in practical components, such as rolling bearings, shall be significantly enhanced. The current life prediction models can, therefore, be reliably updated to allow for surface-originated fatigue and asperity interactions in heavily loaded high-speed bearings.

6. REFERENCES

1. Smith, R.L., Walowit, J.A. and McGrew, J.M., "Elastohydrodynamic Traction Coefficients of 5P4E Polyphenyl Ether", Journal of Lubrication Technology, vol 97, pp 353-362 (1972).

2. Walowit, J.A. and Smith, R.L., "Traction Characteristics of MIL-L-7808 Oil", Journal of Lubrication Technology, vol 98, pp 607-612.

3. Gupta, P.K., Flamand, L., Berthe, D. and Godet, M., "On the Traction Behavior of Several Lubricants", Journal of Lubrication Technology, vol 103, pp 55-64 (1981).

4. Kannel, J.W., Bell, J.C. and Allen, C.M., "A Study of the Influence of Lubricant on High-Speed Rolling Contact Bearing Performance", Technical Report ASD-TR-61-643, Part III, Wright-Patterson Air Force Base, Ohio, (1963).

5. Kannel, J.W. and Walowit, J.A., "Simplified Analysis for Tractions Between Rolling-Sliding Elastohydrodynamic Contacts", Journal of Lubrication Technology, vol 93, pp 39-46 (1971).

6. Trachman, E.G., "A Simplified Technique for Predicting Traction in Elastohydrodynamic Contacts", ASLE Trans, vol 21, pp 33-62 (1978).

7. Trachman, E.G. and Cheng, H.S.,"Thermal and non-Newtonian Effects on Traction in Elastohydrodynamic Contacts", Proc. Instn. of Mech. Engrs., London, Second Symposium on Elastohydrodynamic Lubrication, pp 142-148 (1972).

8. Kannel, J.W. and Dow, T.A., "The Relation Between Pressure and Temperature in Rolling-Sliding EHD Contact", ASLE Trans, vol 23, pp 262-268 (1980).

9. Nagaraj, H.S. and Gupta, P.K., "EHD Traction Data for a Traction Fluid", MTI Technical Report #MTI 78TR143, Mechanical Technology Incorporated, Latham, N.Y. (1978).

10. Smith, R.L., Walowit, J.A., Gupta, P.K. and McGrew J.M., "Research on Elastohydrodynamic Lubrication of High-Speed Rolling-Sliding Contacts", U.S. Air Force Technical Report #AFAPL-TR-71-54, Air Force Aero Propulsion Laboratory, Wright-Patterson Air Force Base, Ohio, (1971).

11. Walters, C.T., "The Dynamics of Ball Bearings", Journal of Lubrication Technology, vol. 93F, pp 1-10 (1971).

12. Gupta, P.K., "Transient Ball Motion and Skid in Ball Bearings", Journal of Lubrication Technology, vol 93F, pp 261-269 (1975).

13. Gupta, P.K., "DREB: A New Tool For Rolling Bearing Performance Simulation", ASME Paper #78-DE-15, Presented at the 1978 Design Engineering Conference, Chicago, Illinois, (1978).

14. Gupta, P.K., "Dynamics of Rolling Element Bearings, Parts I to IV", Journal of Lubrication Technology, vol 101, pp 293-326 (1979).

15. Gupta, P.K., "Interactive Graphic Simulation of Rolling Element Bearings, Phase I: Low Frequency Phenomena and RAPIDREB Development", Air Force Technical Report #AFWAL-TR-81-4148, Air Force Materials Laboratory, Wright-Patterson Air Force Base, Ohio, (1981).

16. Gupta, P.K., "Simulation of Low-Frequency Components in the Dynamic Response of a Ball Bearing", Advances in Computer Aided Bearing Design, ASME Pub, Proc. ASLE/ASME Lubrication Conference, (1982).

17. Gupta, P.K., Dill, J.F. and Bandow, H.E., "Dynamics of Rolling Element Bearings: Experimental Validation of DREB and RAPIDREB Computer Programs", Presented at the 1984 ASME/ASLE Lubrication Conference, San Diego, California, To be published in Journal of Lubrication Technology.

18. Brown, P.F., Carrono, M.J., Dobek, L.J., McFadden, R.J., Miner, J.R. and Robinson, J.D., "Main Shaft High-Speed Cylincrical Roller Bearings for Gas Turbine Engines, Parts I to IV", Report #NAPC-PE-60C, prepared for Naval Air Propulsion Center, Trenton, New Jersey and Air Force Aero Propulsion Laboratory, Wright-Patterson Air Force Base, Ohio, (1980).

19. Gupta, P.K., ADVANCED DYNAMICS OF ROLLING ELEMENTS, Springer-Verlag, Inc., 1984.

20. Dill, J.F. and Gupta, P.K., "Ball Bearing Response to an Unbalanced Load", AIAA Paper #83-1129, Presented at the AIAA/ASME 19th Joint Propulsion Conference, June 27-29, Seattle, Washington, (1983).

21. Gupta, P.K., Dill, J.F. and Bandow, H.E., "Parametric Evaluation of a Solid-Lubricated Ball Bearing", ASLE Paper #83-LC-1B-1, Presented at the 1983 ASLE/ASME Lubricantion Conference, Hartford, Conn., To be Published in ASLE Trans.

22. Bandow, H.E., Gray, S. and Gupta, P.K., "Performance Simultion of a Solid Lubricated Ball Bearing", To be presented at the 1985 ASLE Spring Meeting, Las Vegas, Nevada, May 1985.

23. Hamrock, B.J. and Dowson, D., BALL BEARING LUBRICATION: THE ELASTOHYDRODYNAMICS OF ELLIPTICAL CONTACTS, John Wiley, 1981.

24. Cheng, H.S. and Sternlicht, B., "A Numerical Solution for the Pressure, Temperature, and Film Thickness between Two Infinitely Long Lubricated Rolling and Sliding Cylinders Under Heavy Loads", J. Basic Engrg., ASME Trans., vol 92, pp 155-162, 1970.

25. Johnson, K.L. and Tevaariverk, J.L., "Shear Behavior of EHD Oil Films", Proc. Royal Soc. London, A356, pp 215, 1977.

26. Bair, S. and Winer, W.O., "A Rheological Model for EHD Contacts based on Primary Laboratory Data", J. Lub Tech., ASME Trans., vol 101, no. 3, pp 258, 1979.

Appendix A

TRACTION DATA

The data obtained at the AFWAL Aero Propulsion Laboratory and used in the present investigation for the development of traction model coefficients is documented in this Appendix. The data sets are identified by set numbers A, B and C, for the different lubricants and contact configurations as follows:

Set A: MIL-L-7808 lubricant (Code 077-11), Circular Contact.
Set B: MIL-L-7808 lubricant (Code 077-11), Elliptical Contact.
Set C: MIL-L-23699 lubricant (Code 077-15), Elliptical Contact.

The data is documented in terms of selected experimental data points, indicated by various markers, and model predictions, indicated by solid lines, in the graphs included in this Appendix. The various symbols and text format on each graph is explained by the following labels, indicated in bold face on a typical graph shown on the next page.

1. Data set number assigned as follows:
   First Digit: A, B or C indicating lubricant type as shown above.
   Second Digit: 1, 2, 3 or 4 indicating operating temperature number.
   Third Digit: 1, 2 or 3 indicating rolling speed number.

2. Lubricant name.
3. Disk radius (inch) in rolling direction.
4. Crown radius (inch).
5. Inlet Temperature (°F).
6. Disk rpm under pure rolling.
7. Model type 1 or 2.
8. Reference temperature (°K) used in the model.
9. Viscosity parameter (Pa.S), μ_0* or μ_0**.
10. Pressure-viscosity coefficient (1/Pa), α* or α**.
11. Temperature-viscosity coefficient, β* (1/°K) or β** (°K).
12. SSD for the regression fit.
13. Marker identifying the experimental data.
14. Solid line number corresponding to model predictions.
15. Hertz contact pressure (MPa).
16. Contact load (N).
17. Rolling velocity (M/S).
18. Inlet temperature (°K).
19. Traction coefficient.
20. Slide/Roll ratio.

For data set A, two sets of plots are included. In the first set, label #5, inlet temperature (°F), includes an asterisk (*), which means that the model correlations were obtained with the disk temperature set equal to the inlet temperature. In the second set, which is without the asterisk on label #5, the correlations were obtained with actual disk temperature data included in the experimental data set. All correlations for data sets B and C were obtained with the disk temperature set equal to the inlet temperature.

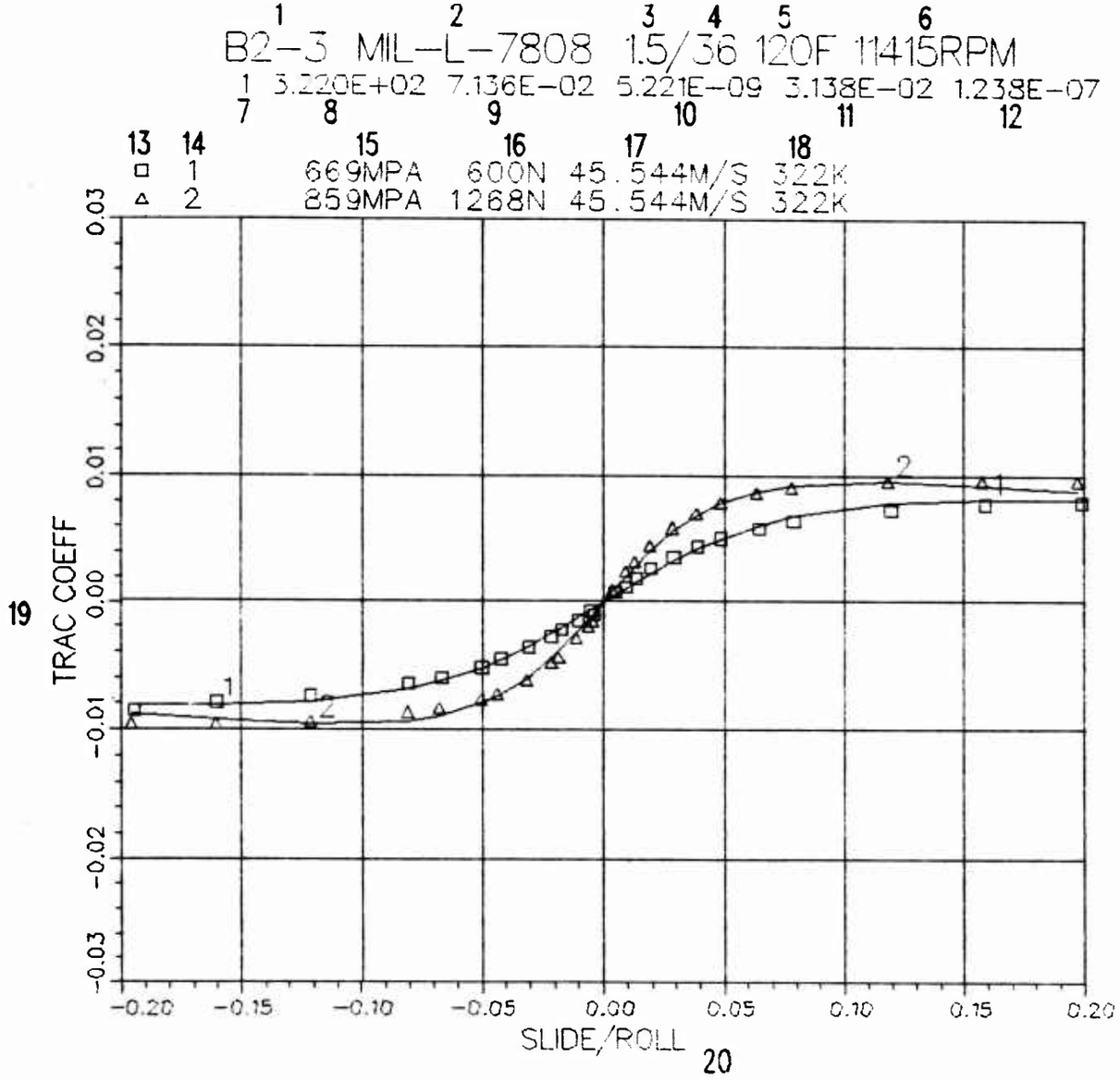

LIST OF SYMBOLS USED IN THE COMPUTER GENERATED TRACTION CURVE

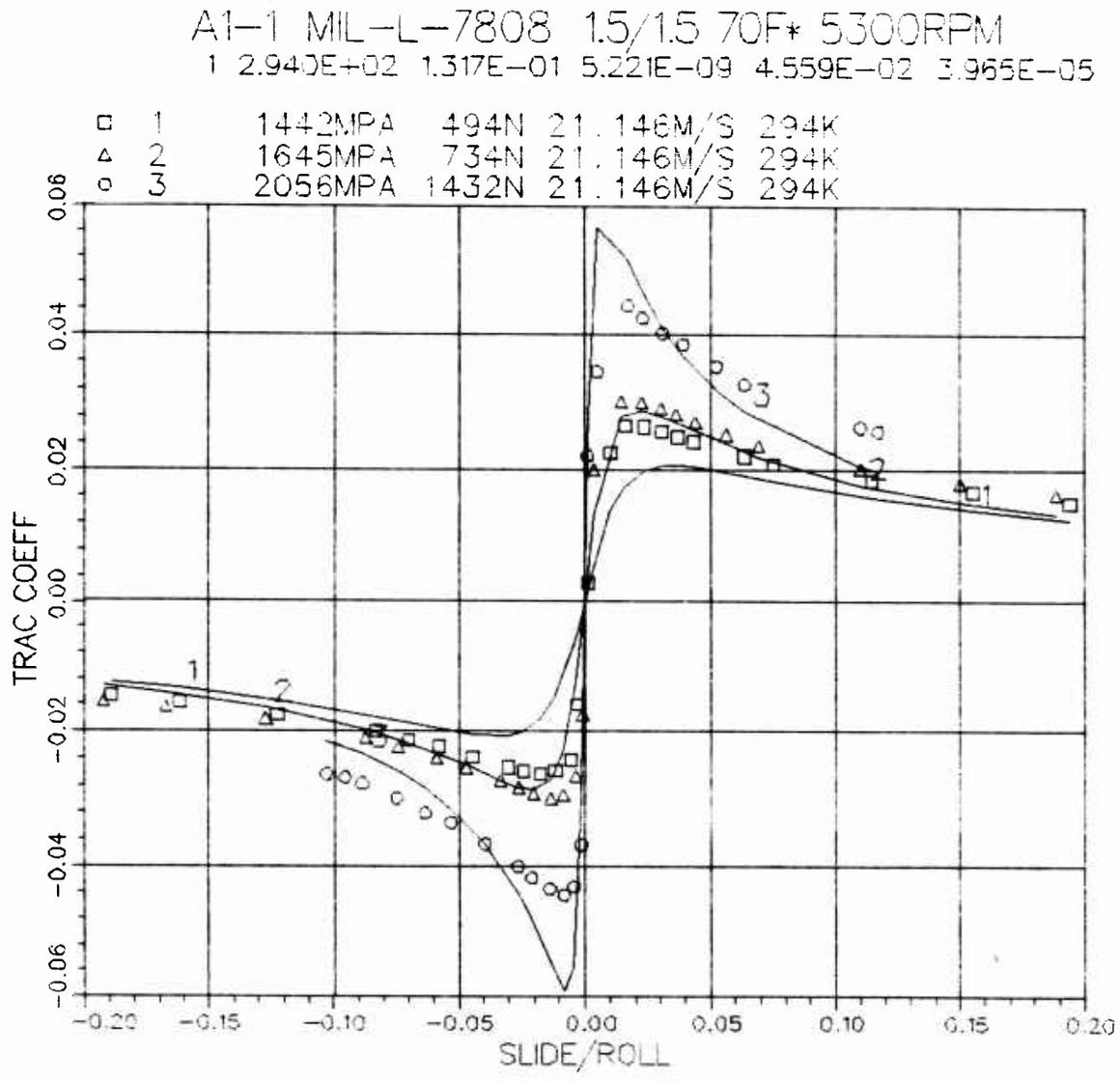
A1-1 MIL-L-7808 1.5/1.5 70F* 5300RPM
1 2.940E+02 1.317E-01 5.221E-09 4.559E-02 3.965E-05
1 1442MPA 494N 21.146M/S 294K
2 1645MPA 734N 21.146M/S 294K
3 2056MPA 1432N 21.146M/S 294K
TRAC COEFF
0.06
0.04
0.02
0.00
-0.02
-0.04
-0.06
-0.20
-0.15
-0.10
-0.05
0.00
0.05
0.10
0.15
0.20
SLIDE/ROLL

A1-1 MIL-L-7808 1.5/15 70F* 5300RPM

2 2.940E+02 6.474E-02 5.221E-09 4.019E+03 1.321E-05

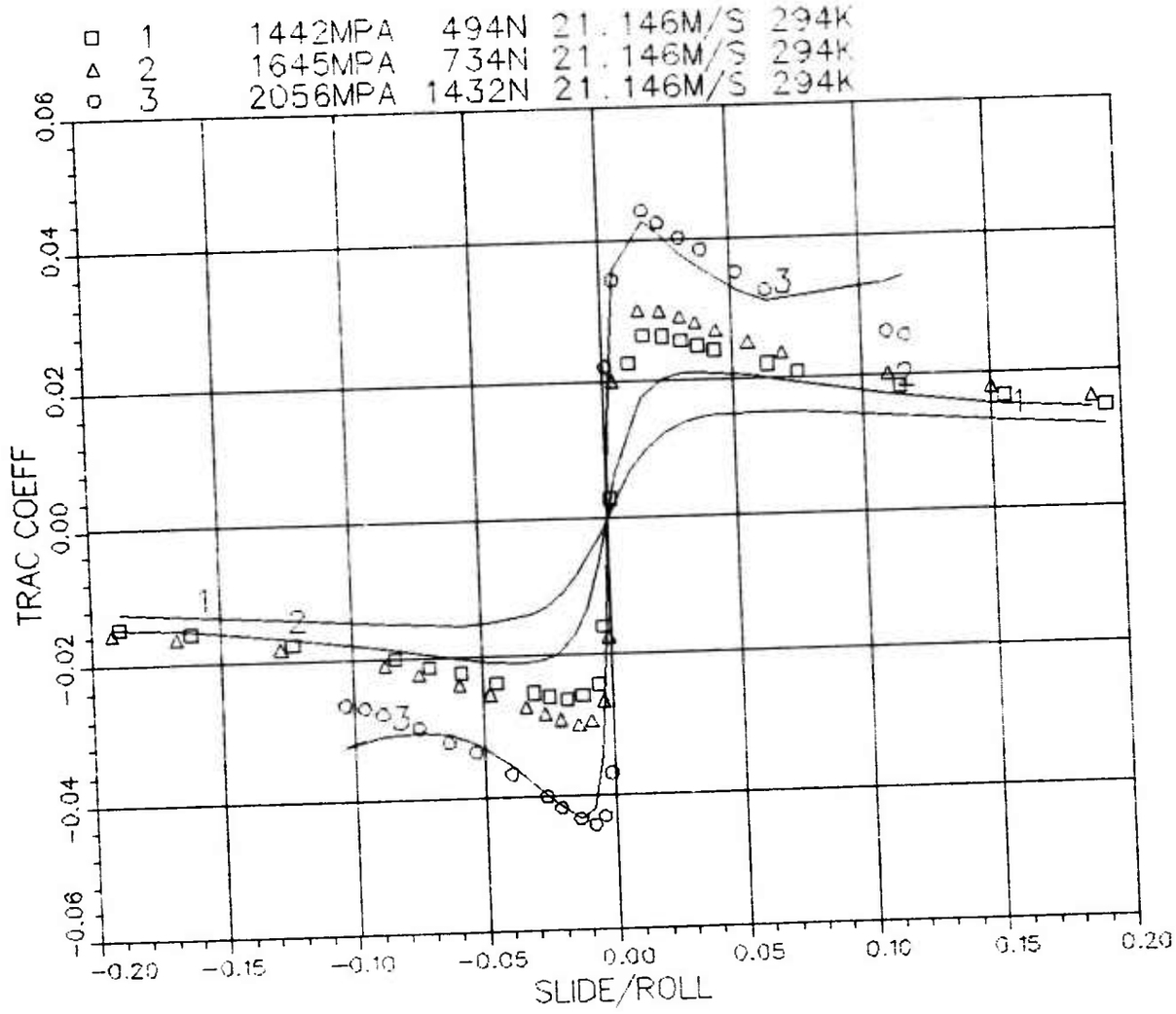

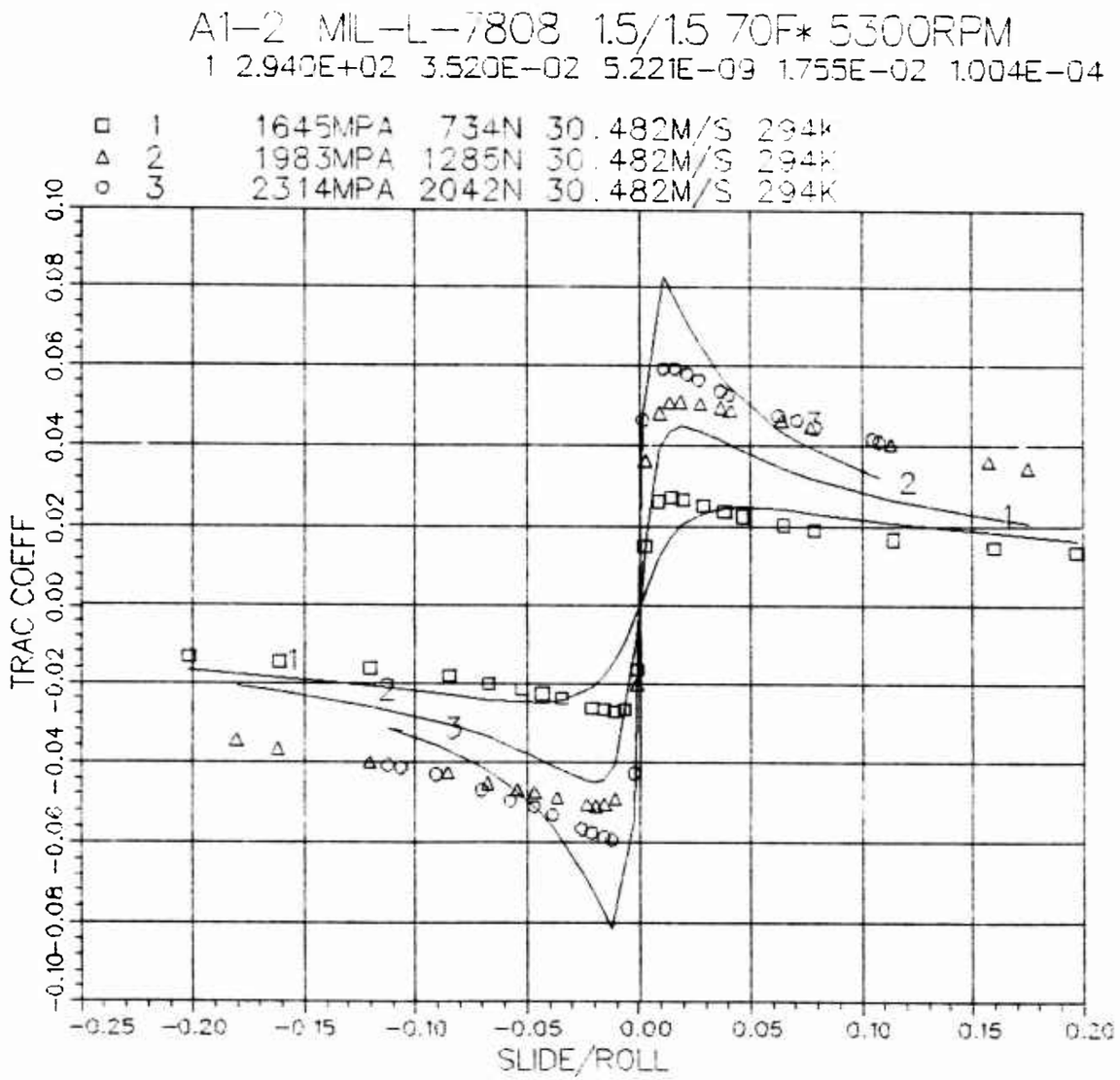
A1-2 MIL-L-7808 1.5/1.5 70F* 5300RPM
1 2.940E+02 3.520E-02 5.221E-09 1.755E-02 1.004E-04
□ 1 1645MPA 734N 30.482M/S 294K
△ 2 1983MPA 1285N 30.482M/S 294K
○ 3 2314MPA 2042N 30.482M/S 294K
TRAC COEFF
SLIDE/ROLL
0.10
0.08
0.06
0.04
0.02
0.00
-0.02
-0.04
-0.06
-0.08
-0.10
-0.25
-0.20
-0.15
-0.10
-0.05
0.00
0.05
0.10
0.15
0.20

A1-2 MIL-L-7808 1.5/1.5 70F* 5300RPM

2 2.940E+02 1.925E-02 5.221E-09 2.273E+03 1.719E-05

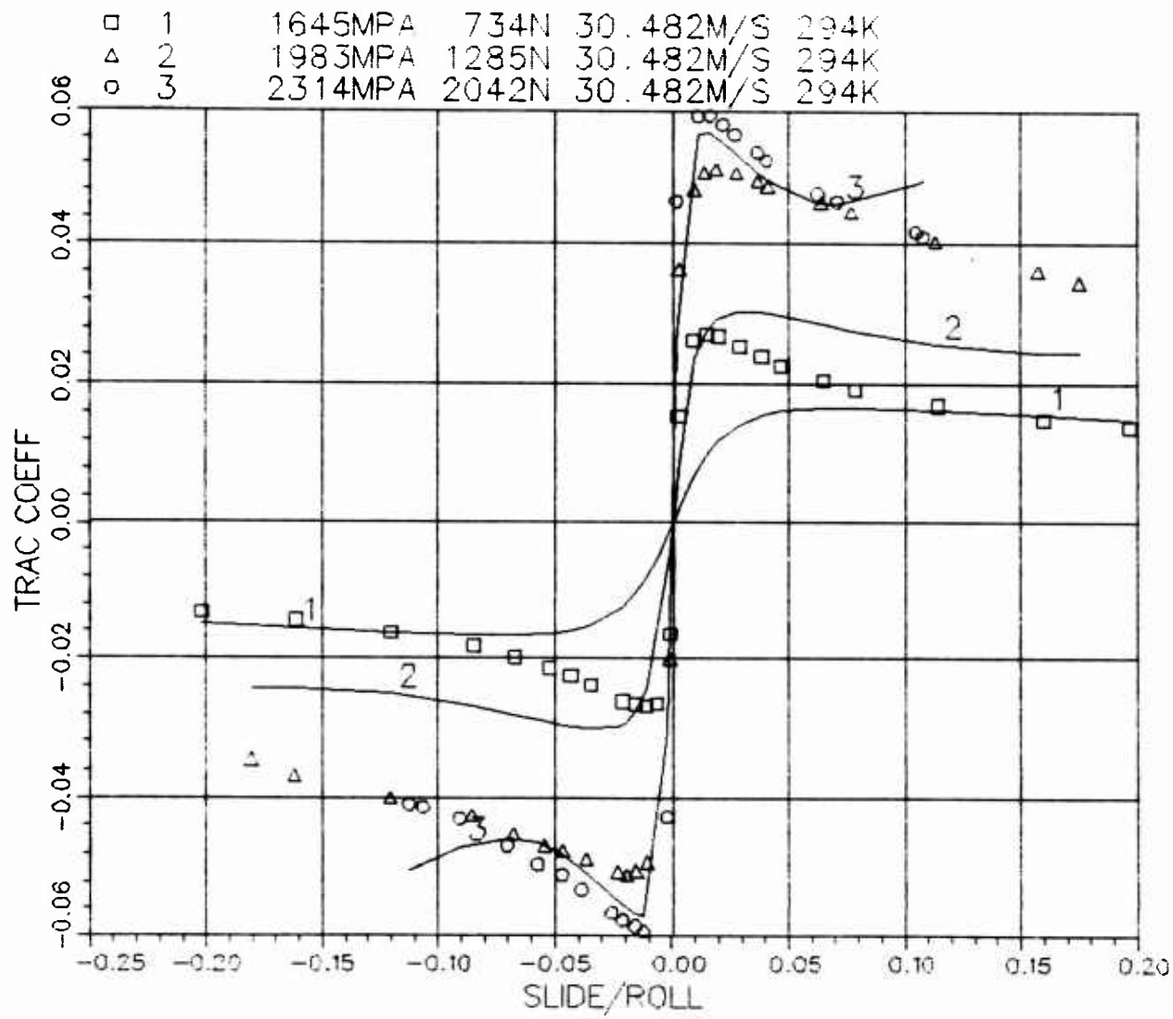

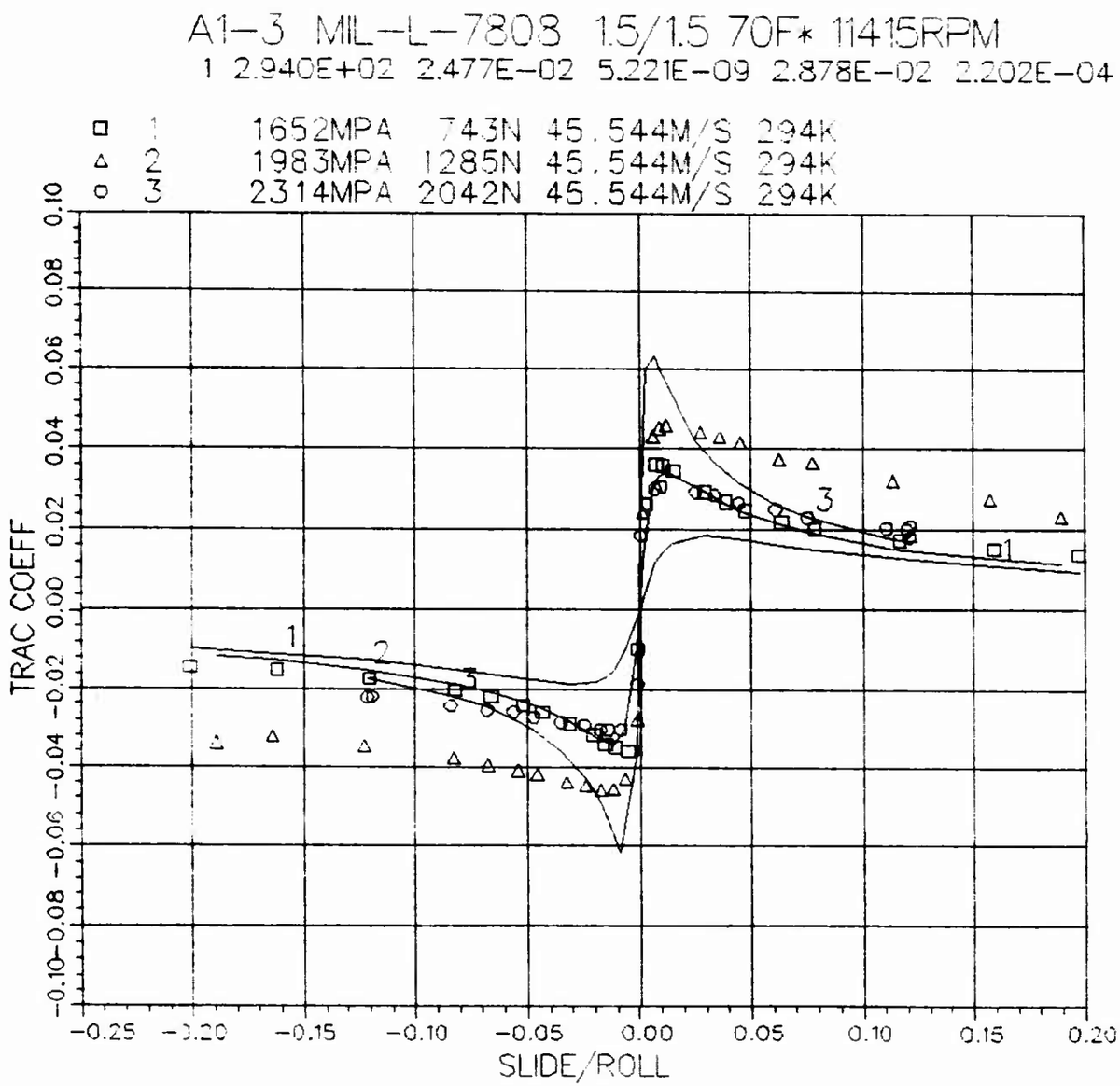
A1-3 MIL-L-7808 1.5/1.5 70F* 11415RPM
1 2.940E+02 2.477E-02 5.221E-09 2.878E-02 2.202E-04
1 1652MPA 743N 45.544M/S 294K
2 1983MPA 1285N 45.544M/S 294K
3 2314MPA 2042N 45.544M/S 294K
TRAC COEFF
SLIDE/ROLL
0.10
0.08
0.06
0.04
0.02
0.00
-0.02
-0.04
-0.06
-0.08
-0.10
-0.25
-0.20
-0.15
-0.10
-0.05
0.00
0.05
0.10
0.15
0.20

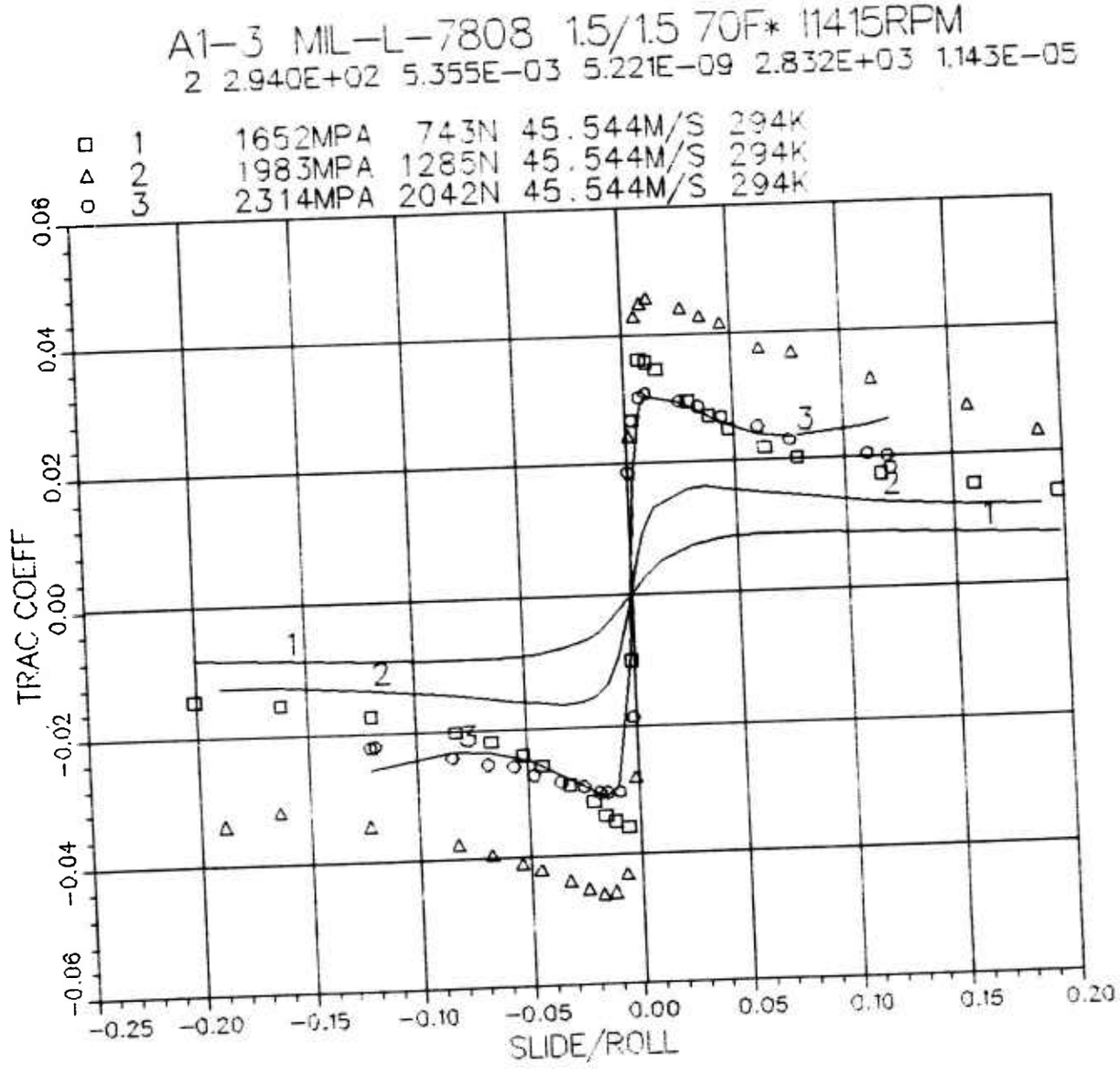
A1-3 MIL-L-7808 1.5/1.5 70F* 11415RPM
2 2.940E+02 5.355E-03 5.221E-09 2.832E+03 1.143E-05
1 1652MPA 743N 45.544M/S 294K
2 1983MPA 1285N 45.544M/S 294K
3 2314MPA 2042N 45.544M/S 294K
TRAC COEFF
SLIDE/ROLL
0.06
0.04
0.02
0.00
-0.02
-0.04
-0.06
-0.25
-0.20
-0.15
-0.10
-0.05
0.00
0.05
0.10
0.15
0.20

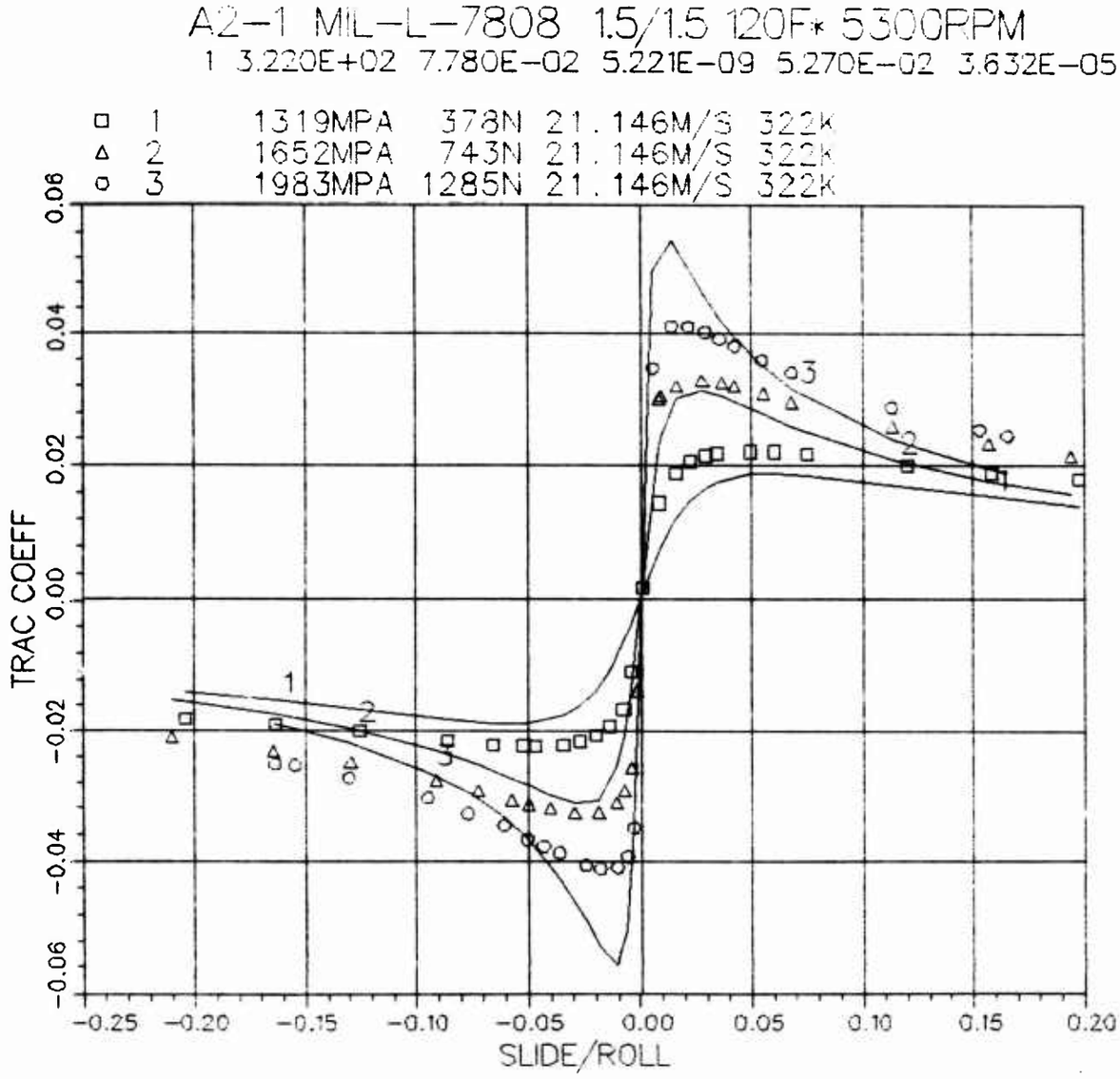
A2-1 MIL-L-7808 1.5/1.5 120F* 5300RPM
1 3.220E+02 7.780E-02 5.221E-09 5.270E-02 3.632E-05
1 1319MPA 378N 21.146M/S 322k
2 1652MPA 743N 21.146M/S 322k
3 1983MPA 1285N 21.146M/S 322k
TRAC COEFF
SLIDE/ROLL
0.06
0.04
0.02
0.00
-0.02
-0.04
-0.06
-0.25
-0.20
-0.15
-0.10
-0.05
0.00
0.05
0.10
0.15
0.20

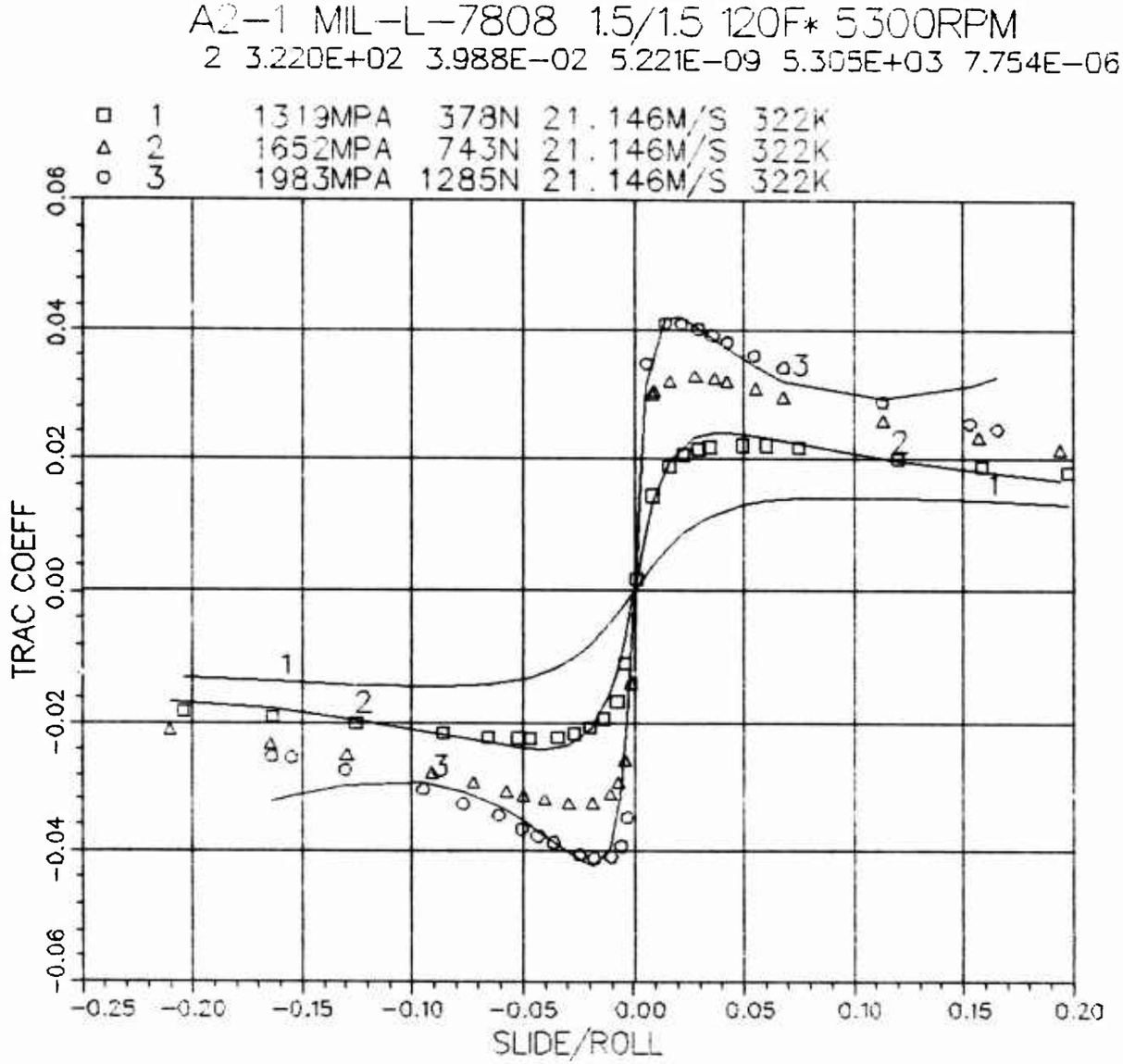
A2-1 MIL-L-7808 1.5/1.5 120F* 5300RPM
2 3.220E+02 3.988E-02 5.221E-09 5.305E+03 7.754E-06
1 1319MPA 378N 21.146M/S 322K
2 1652MPA 743N 21.146M/S 322K
3 1983MPA 1285N 21.146M/S 322K
TRAC COEFF
SLIDE/ROLL
0.06
0.04
0.02
0.00
-0.02
-0.04
-0.06
-0.25
-0.20
-0.15
-0.10
-0.05
0.00
0.05
0.10
0.15
0.20

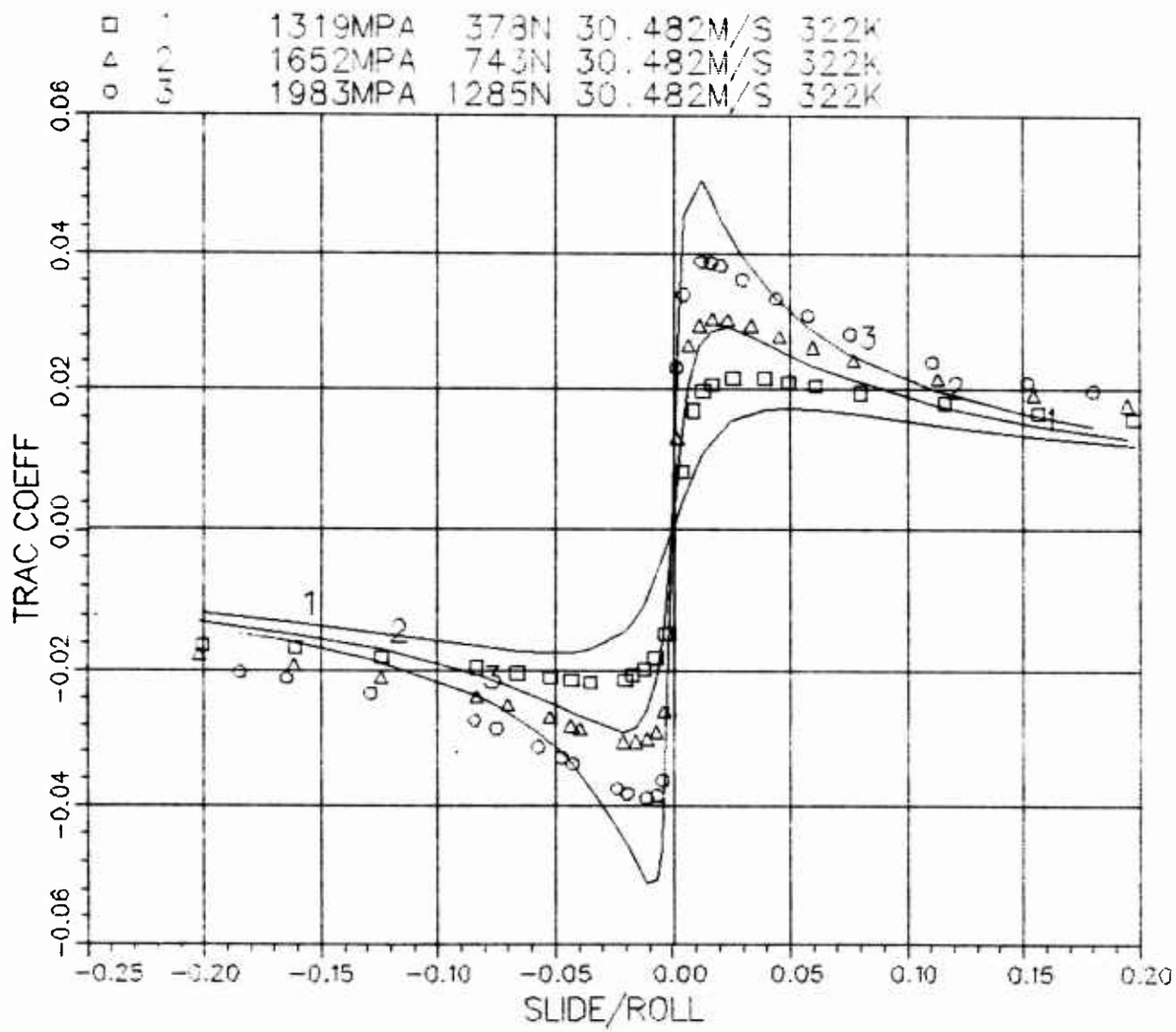
A2-2 MIL-L-7808 1.5/1.5 120F* 7640RPM
1 3.220E+02 6.522E-02 5.221E-09 4.312E-02 3.344E-05
1319MPA 378N 30.482M/S 322K
1652MPA 743N 30.482M/S 322K
1983MPA 1285N 30.482M/S 322K
TRAC COEFF
SLIDE/ROLL
0.06
0.04
0.02
0.00
-0.02
-0.04
-0.06
-0.25
-0.20
-0.15
-0.10
-0.05
0.00
0.05
0.10
0.15
0.20

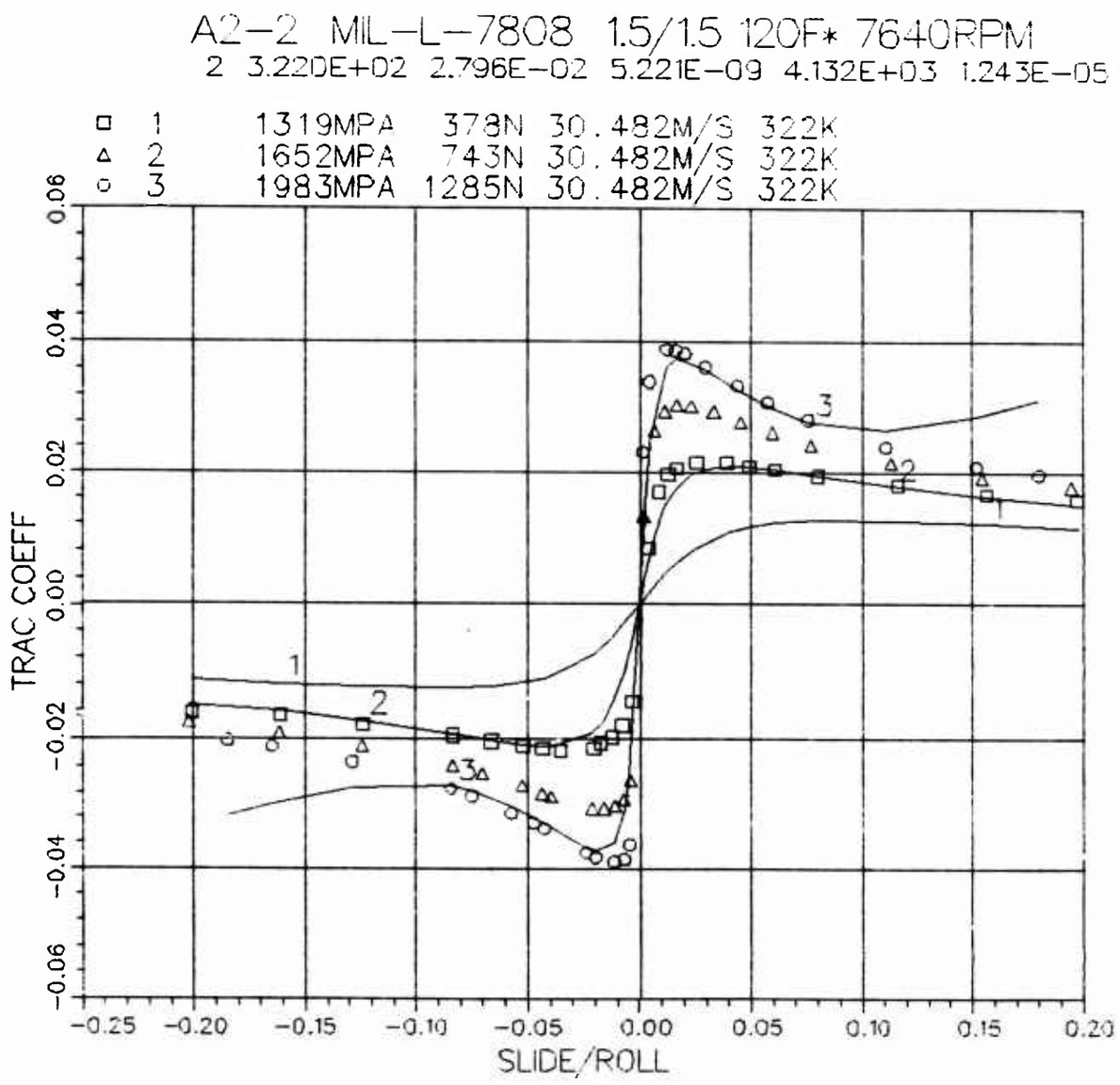
A2-2 MIL-L-7808 1.5/1.5 120F* 7640RPM
2 3.220E+02 2.796E-02 5.221E-09 4.132E+03 1.243E-05
1 1319MPA 378N 30.482M/S 322K
2 1652MPA 743N 30.482M/S 322K
3 1983MPA 1285N 30.482M/S 322K
TRAC COEFF
0.06
0.04
0.02
0.00
-0.02
-0.04
-0.06
-0.25 -0.20 -0.15 -0.10 -0.05 0.00 0.05 0.10 0.15 0.20
SLIDE/ROLL

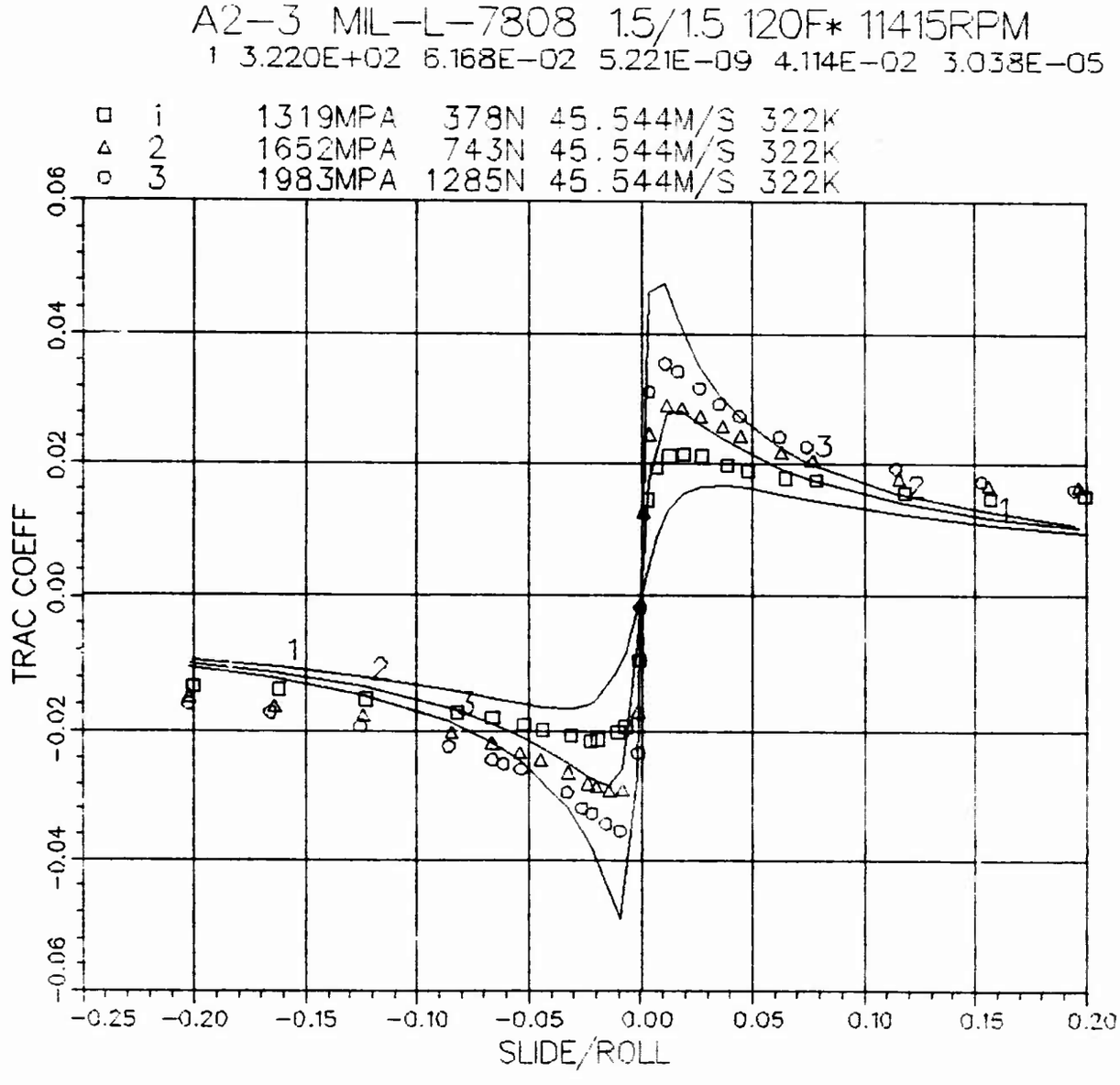
A2-3 MIL-L-7808 1.5/1.5 120F* 11415RPM
1 3.220E+02 6.168E-02 5.221E-09 4.114E-02 3.038E-05
1 1319MPA 378N 45.544M/S 322K
2 1652MPA 743N 45.544M/S 322K
3 1983MPA 1285N 45.544M/S 322K
TRAC COEFF
SLIDE/ROLL
0.06
0.04
0.02
0.00
-0.02
-0.04
-0.06
-0.25
-0.20
-0.15
-0.10
-0.05
0.00
0.05
0.10
0.15
0.20

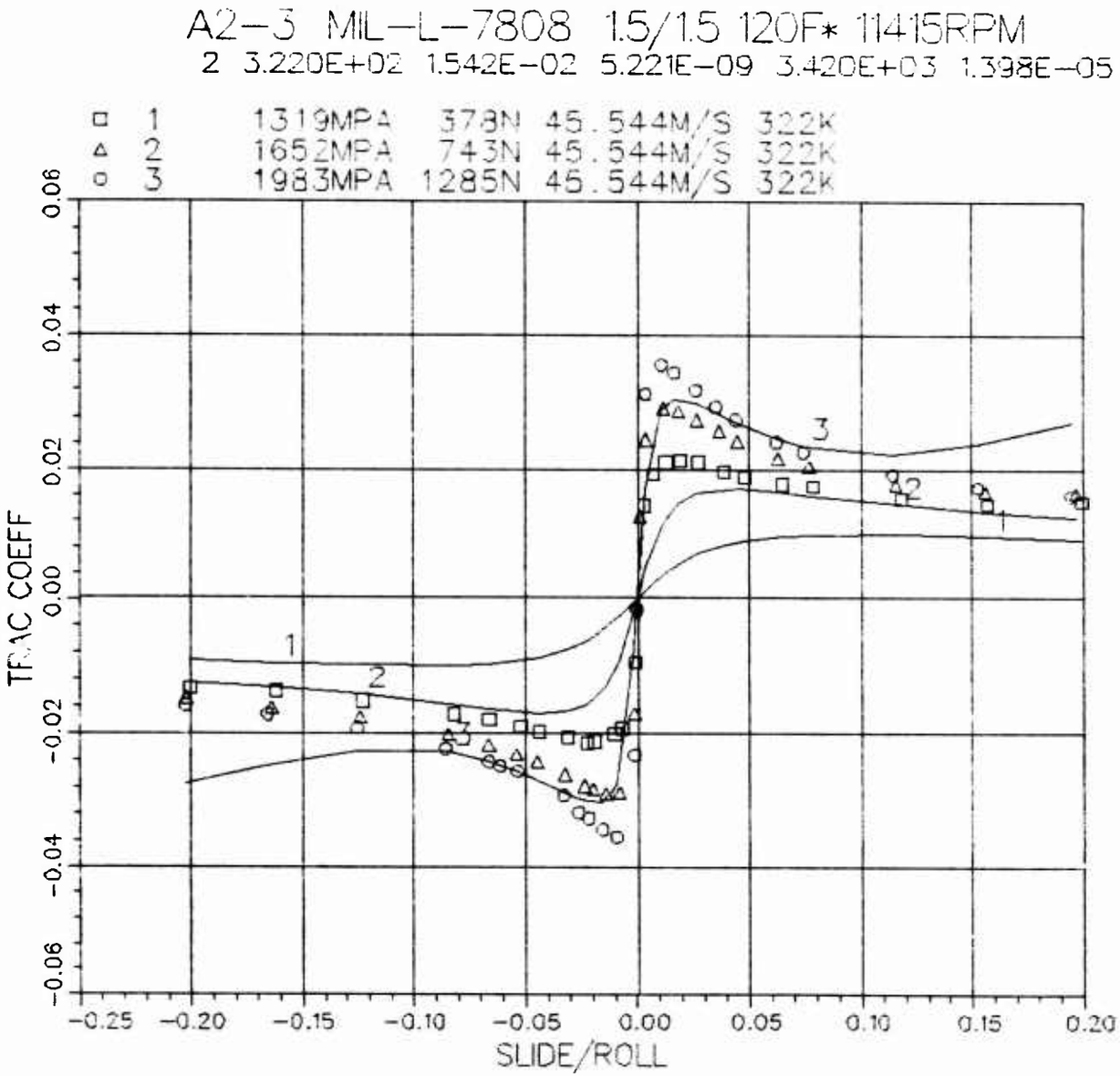
A2-3 MIL-L-7808 1.5/1.5 120F* 11415RPM
2 3.220E+02 1.542E-02 5.221E-09 3.420E+03 1.398E-05
1 1319MPA 378N 45.544M/S 322K
2 1652MPA 743N 45.544M/S 322K
3 1983MPA 1285N 45.544M/S 322K
TRAC COEFF
SLIDE/ROLL
0.06
0.04
0.02
0.00
-0.02
-0.04
-0.06
-0.25
-0.20
-0.15
-0.10
-0.05
0.00
0.05
0.10
0.15
0.20

A3-3 MIL-L-7808 1.5/1.5 160F* 11415RPM

1 3.440E+02 1.655E-02 5.221E-09 3.636E-02 1.828E-05

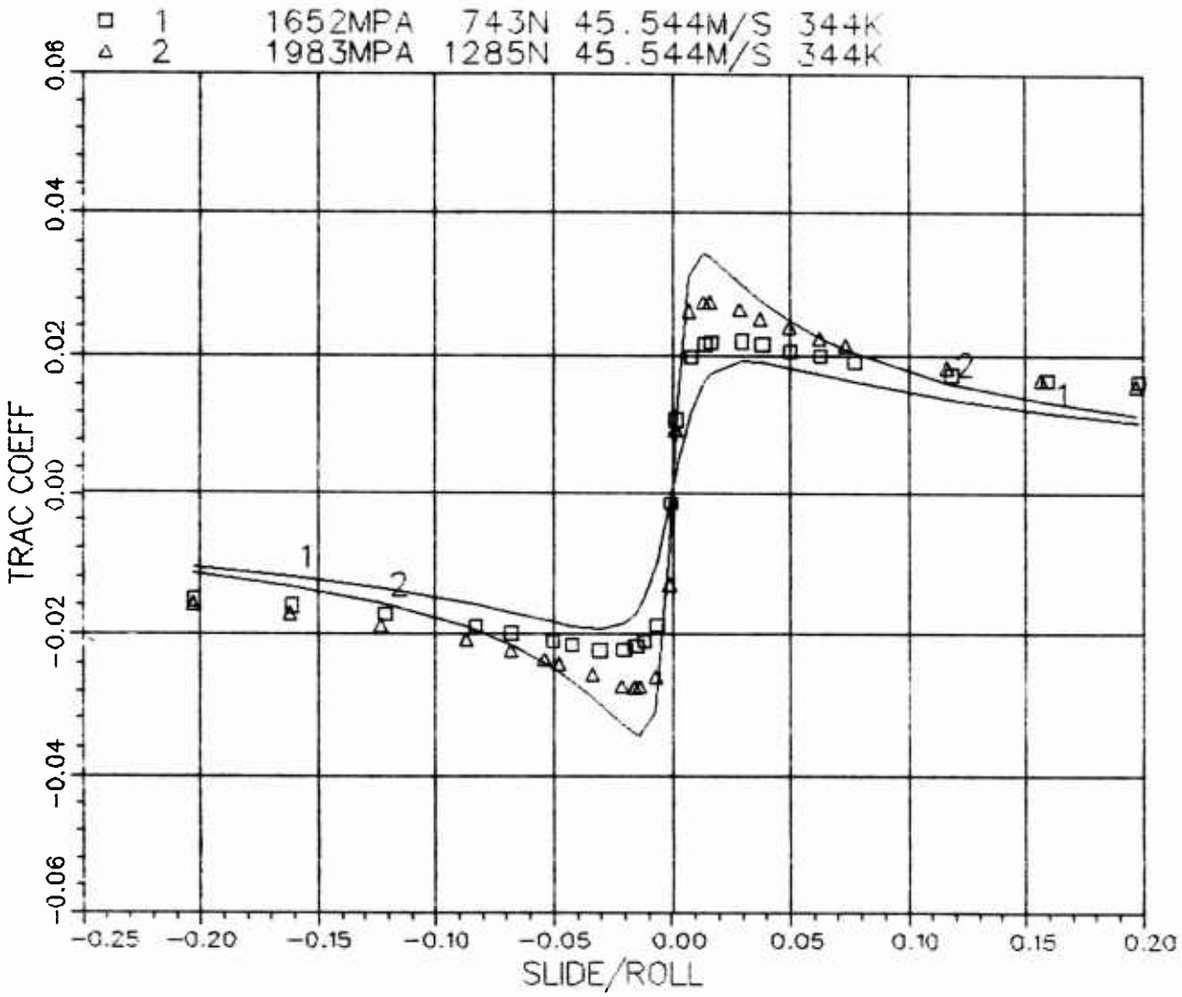

A3-3 MIL-L-7808 1.5/1.5 160F* 11415RPM

2 3.440E+02 9.870E-03 5.221E-09 4.611E+03 5.779E-06

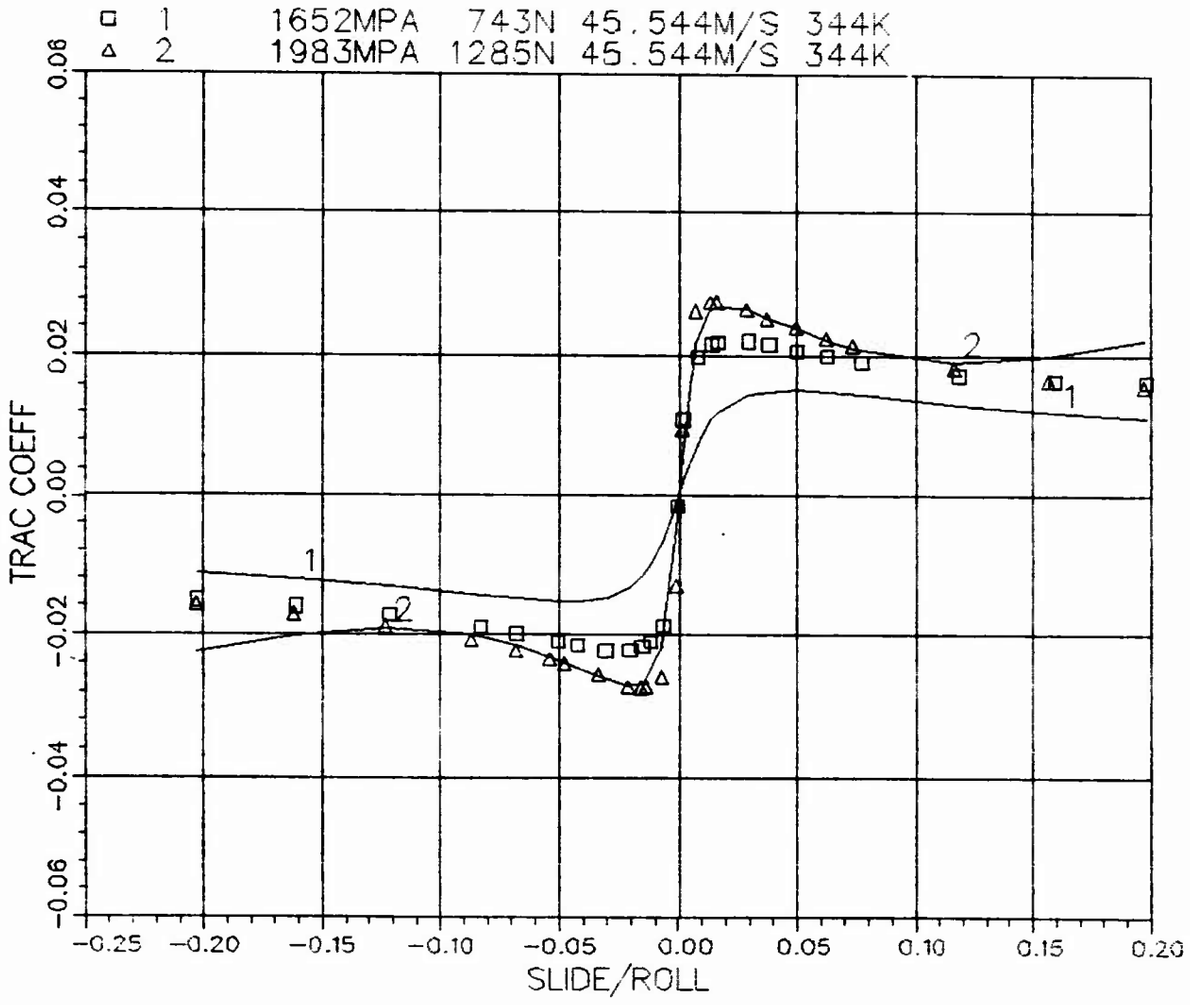

A1-1 MIL-L-7808 1.5/1.5 70F 5300RPM

1 2.940E+02 1.928E-01 5.221E-09 4.473E-02 3.303E-05

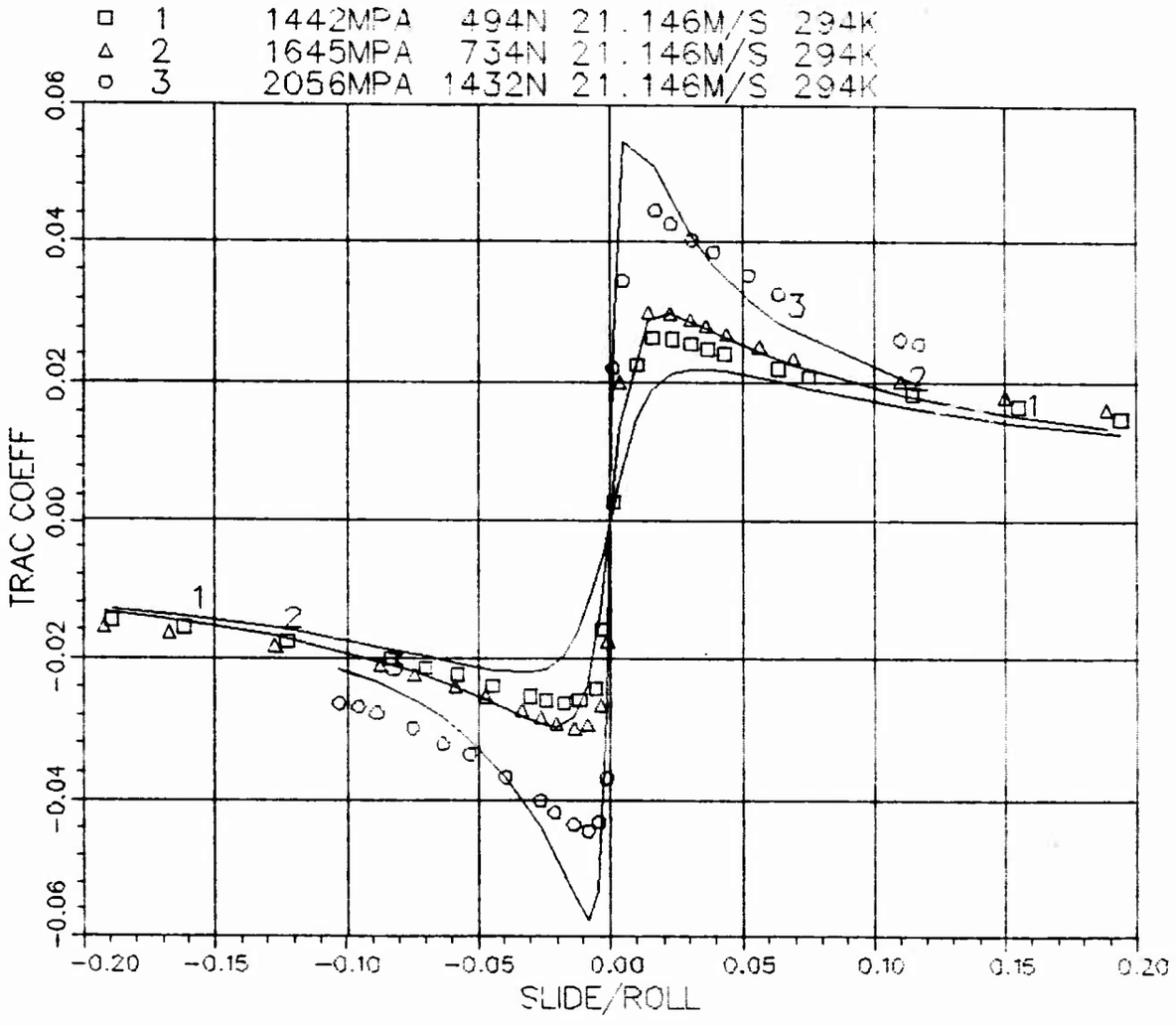

A1-1 MIL-L-7808 1.5/1.5 70F 5300RPM

2 2.940E+02 1.049E-01 5.221E-09 4.268E+03 1.305E-05

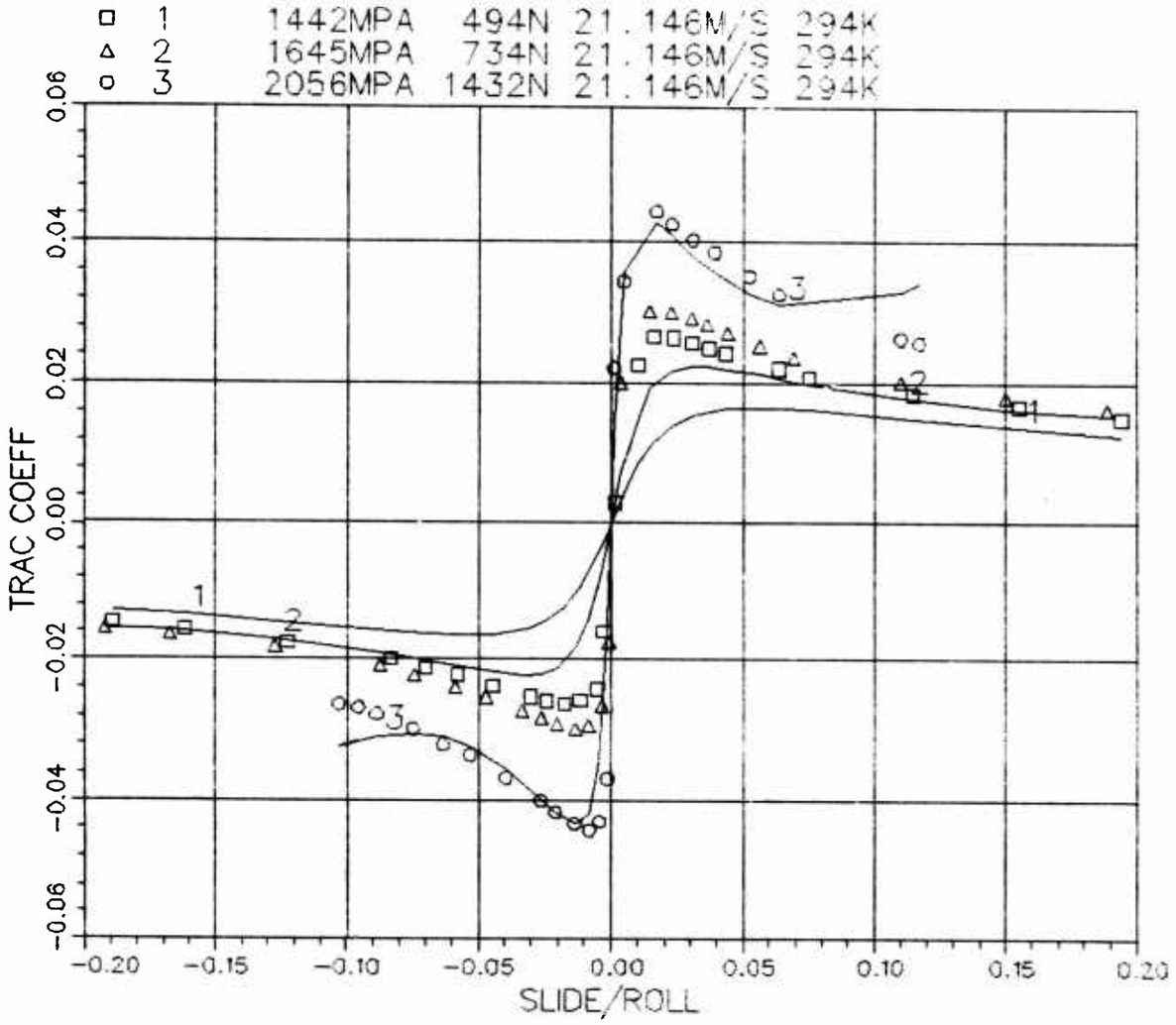

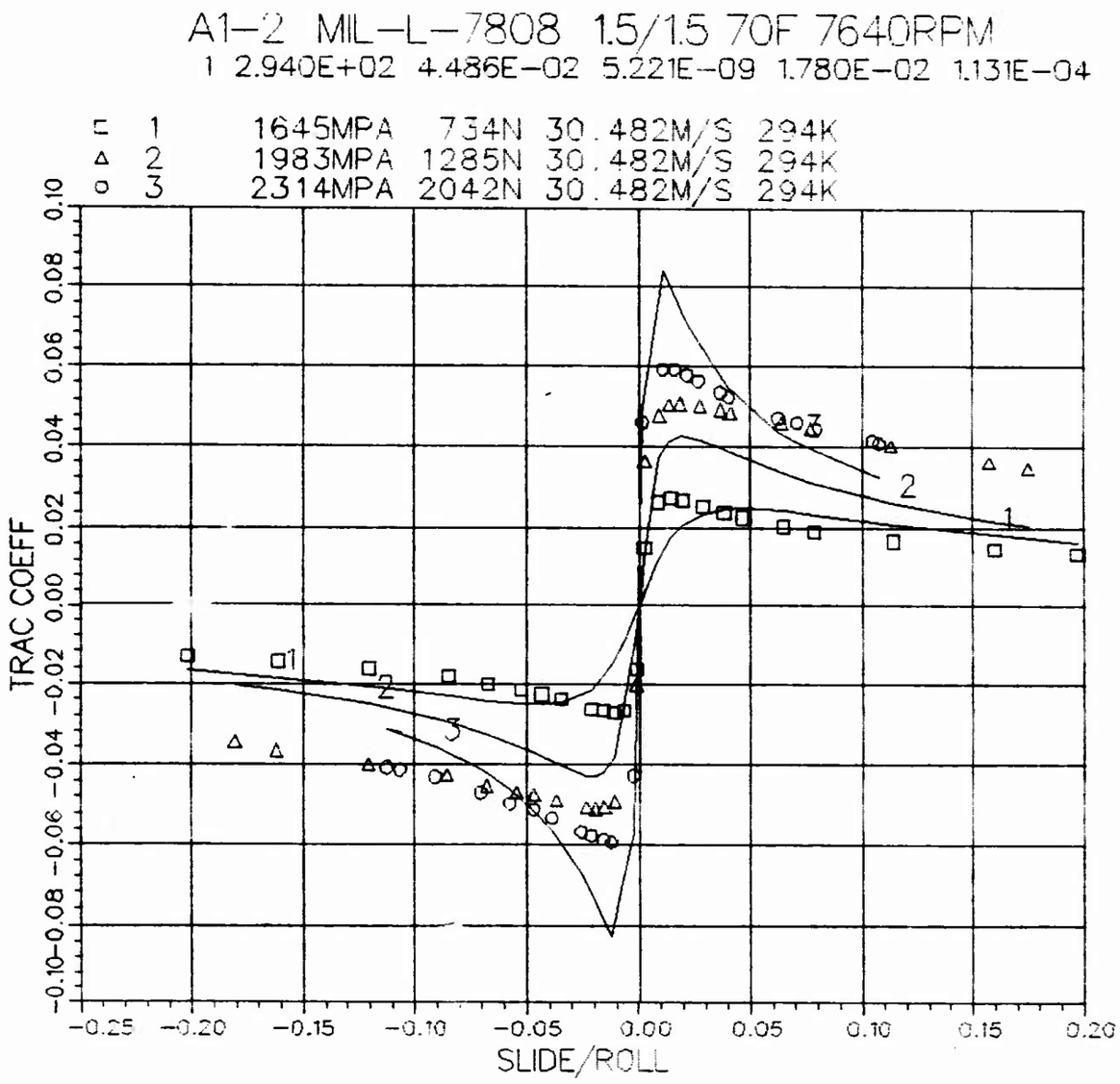
A1-2 MIL-L-7808 1.5/1.5 70F 7640RPM
1 2.940E+02 4.486E-02 5.221E-09 1.780E-02 1.131E-04
1 1645MPA 734N 30.482M/S 294K
2 1983MPA 1285N 30.482M/S 294K
3 2314MPA 2042N 30.482M/S 294K
TRAC COEFF
SLIDE/ROLL
0.10
0.08
0.06
0.04
0.02
0.00
-0.02
-0.04
-0.06
-0.08
-0.10
-0.25
-0.20
-0.15
-0.10
-0.05
0.00
0.05
0.10
0.15
0.20

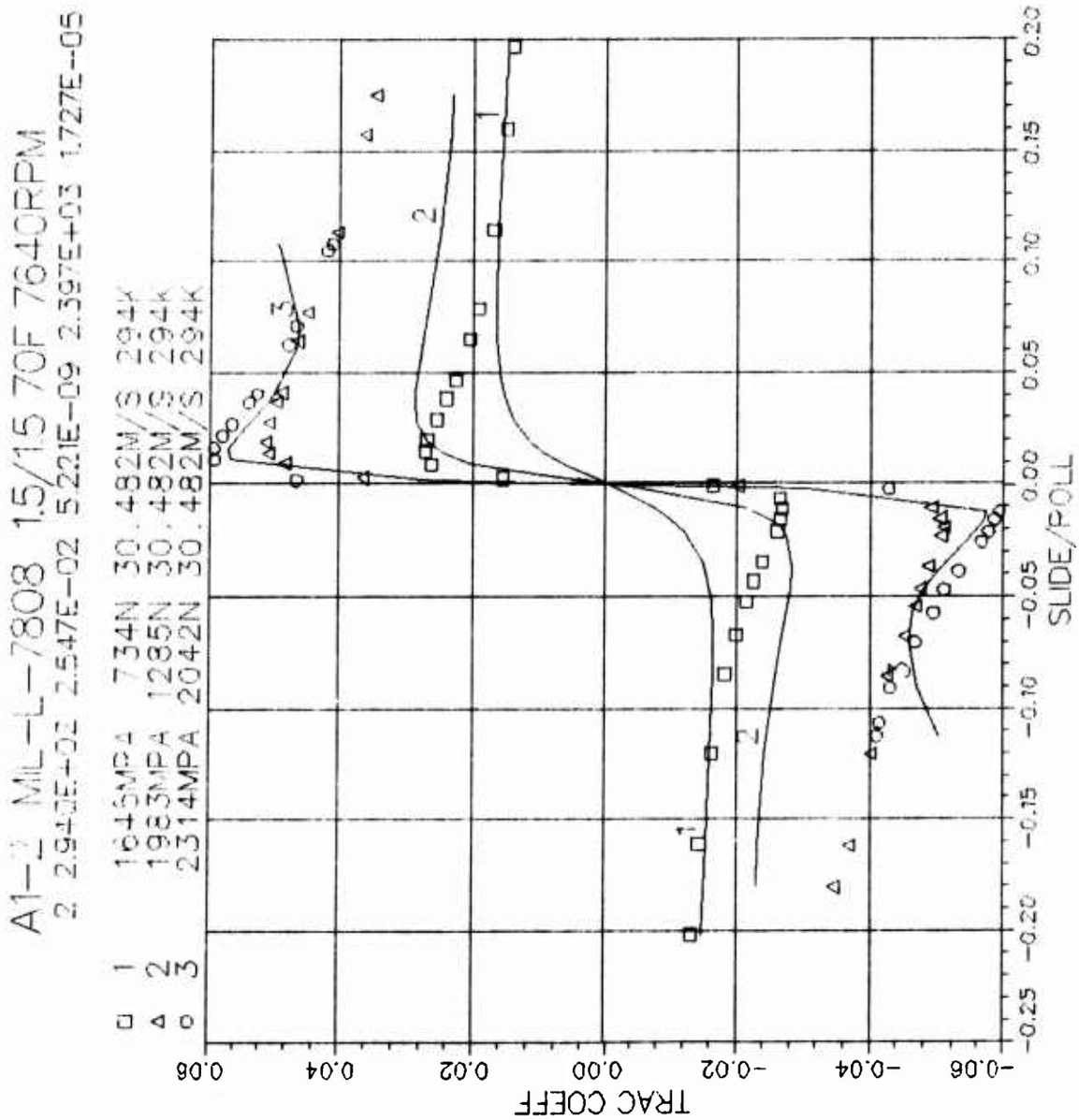
A1-[illegible] MIL-L-7808 1.5/15 70F 7640RPM
2 2.943E+02 2.547E-02 5.221E-09 2.397E+03 1.727E-05
1 1645MPA 734N 30.482M/S 294K
2 1983MPA 1285N 30.482M/S 294K
3 2314MPA 2042N 30.482M/S 294K
TRAC COEFF
SLIDE/ROLL
0.06
0.04
0.02
0.00
-0.02
-0.04
-0.06
0.20
0.15
0.10
0.05
0.00
-0.05
-0.10
-0.15
-0.20
-0.25

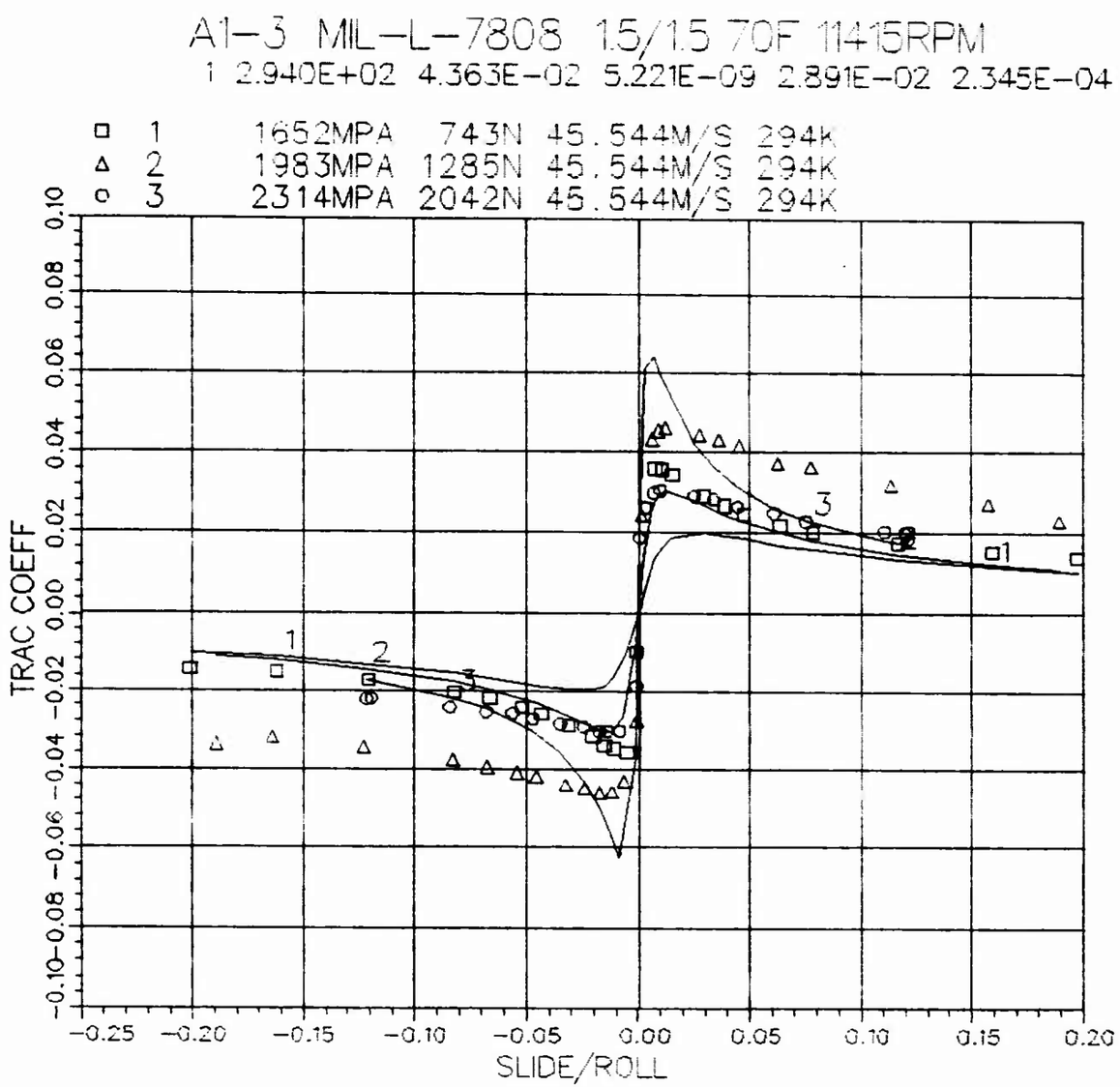
A1-3 MIL-L-7808 1.5/1.5 70F 11415RPM
1 2.940E+02 4.363E-02 5.221E-09 2.891E-02 2.345E-04
1 1652MPA 743N 45.544M/S 294K
2 1983MPA 1285N 45.544M/S 294K
3 2314MPA 2042N 45.544M/S 294K
TRAC COEFF
SLIDE/ROLL
0.10
0.08
0.06
0.04
0.02
0.00
-0.02
-0.04
-0.06
-0.08
-0.10
-0.25
-0.20
-0.15
-0.10
-0.05
0.00
0.05
0.10
0.15
0.20

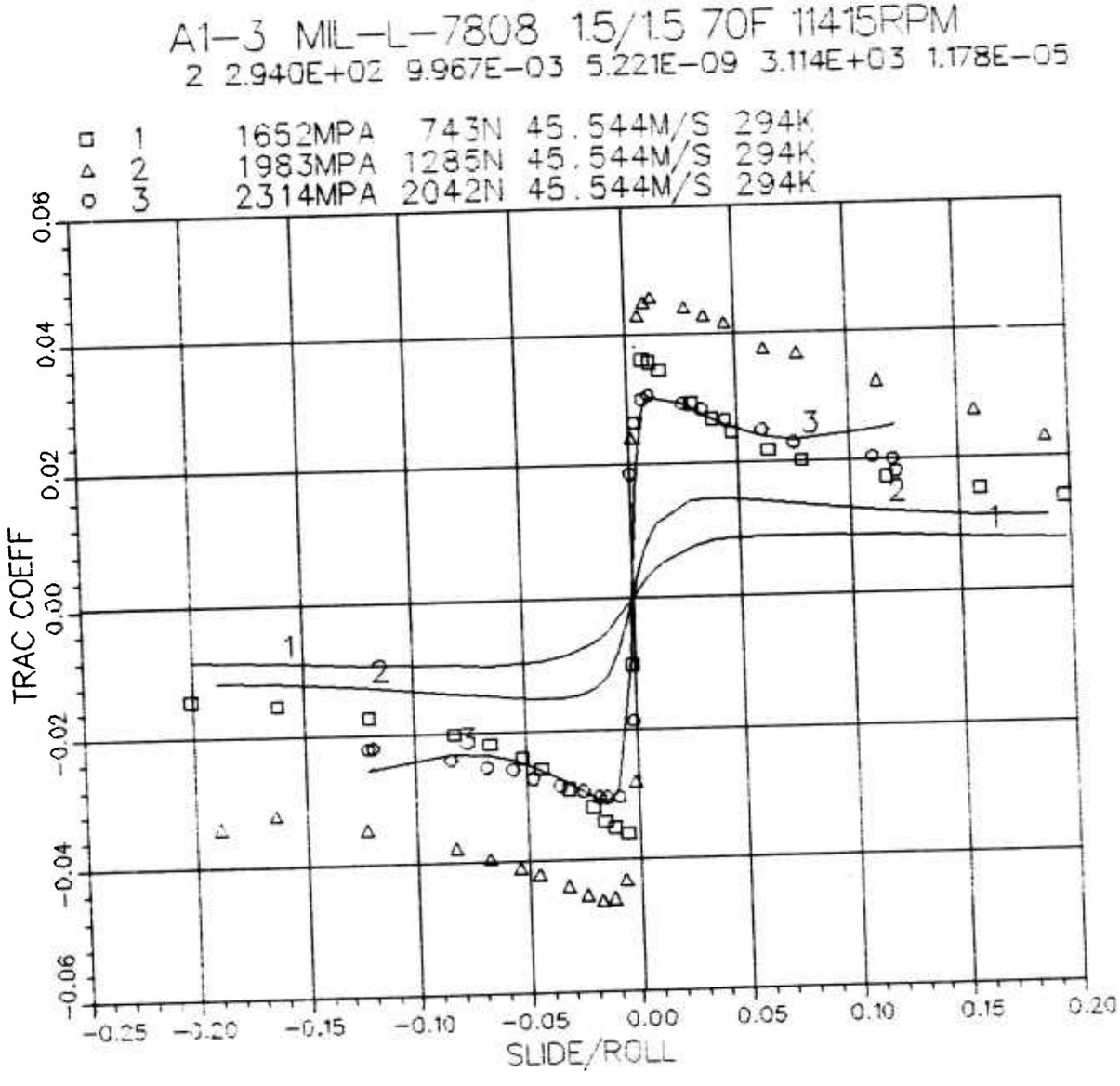
A1-3 MIL-L-7808 1.5/1.5 70F 11415RPM
2 2.940E+02 9.967E-03 5.221E-09 3.114E+03 1.178E-05
1 1652MPA 743N 45.544M/S 294K
2 1983MPA 1285N 45.544M/S 294K
3 2314MPA 2042N 45.544M/S 294K
TRAC COEFF
SLIDE/ROLL
0.06
0.04
0.02
0.00
-0.02
-0.04
-0.06
-0.25
-0.20
-0.15
-0.10
-0.05
0.00
0.05
0.10
0.15
0.20

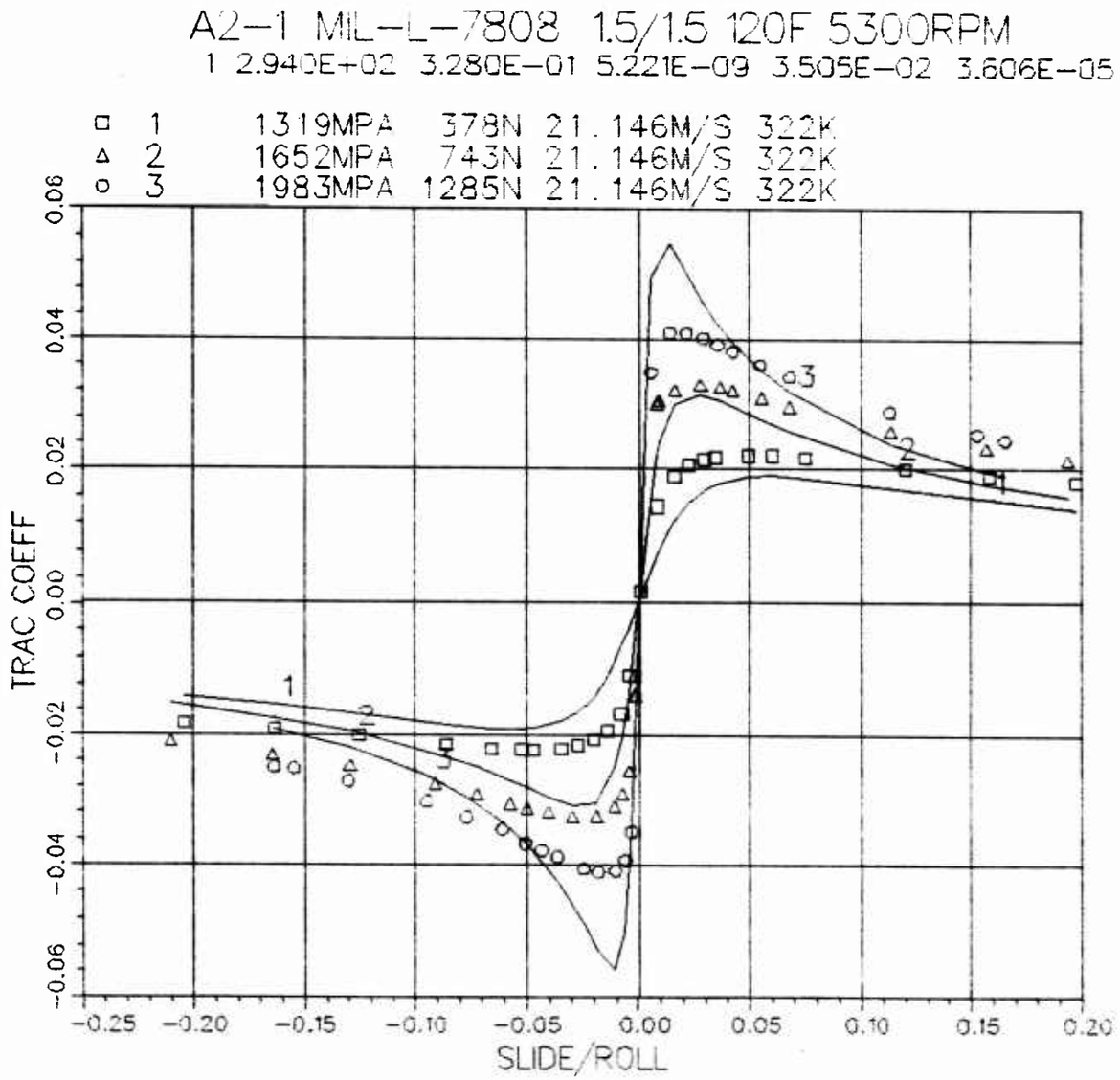
A2-1 MIL-L-7808 1.5/1.5 120F 5300RPM
1 2.940E+02 3.280E-01 5.221E-09 3.505E-02 3.606E-05
1 1319MPA 378N 21.146M/S 322K
2 1652MPA 743N 21.146M/S 322K
3 1983MPA 1285N 21.146M/S 322K
TRAC COEFF
SLIDE/ROLL
0.06
0.04
0.02
0.00
-0.02
-0.04
-0.06
-0.25
-0.20
-0.15
-0.10
-0.05
0.00
0.05
0.10
0.15
0.20

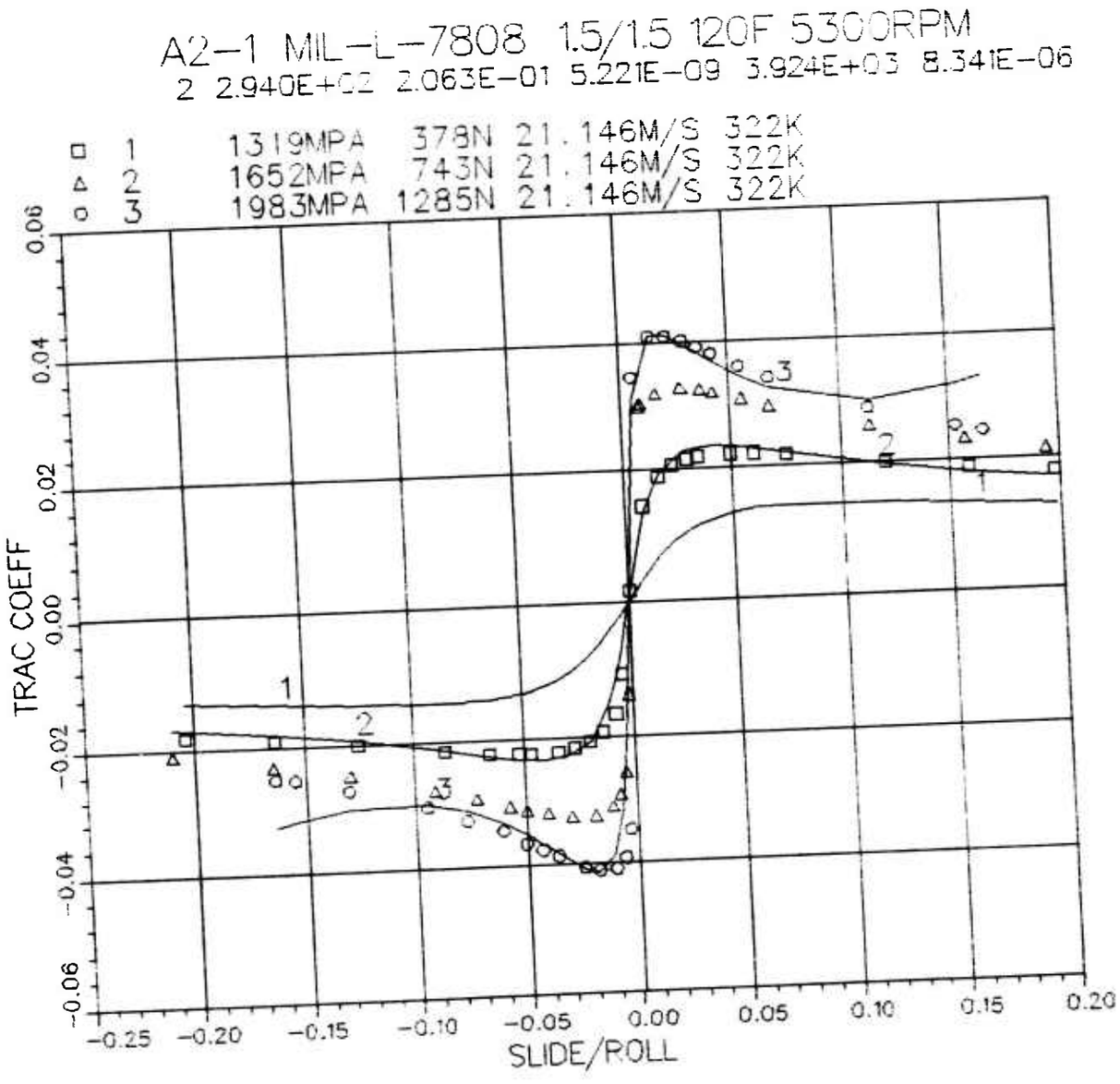
A2-1 MIL-L-7808 1.5/1.5 120F 5300RPM
2 2.940E+02 2.063E-01 5.221E-09 3.924E+03 8.341E-06
1 1319MPA 378N 21.146M/S 322K
2 1652MPA 743N 21.146M/S 322K
3 1983MPA 1285N 21.146M/S 322K
TRAC COEFF
SLIDE/ROLL
0.06
0.04
0.02
0.00
-0.02
-0.04
-0.06
-0.25
-0.20
-0.15
-0.10
-0.05
0.00
0.05
0.10
0.15
0.20

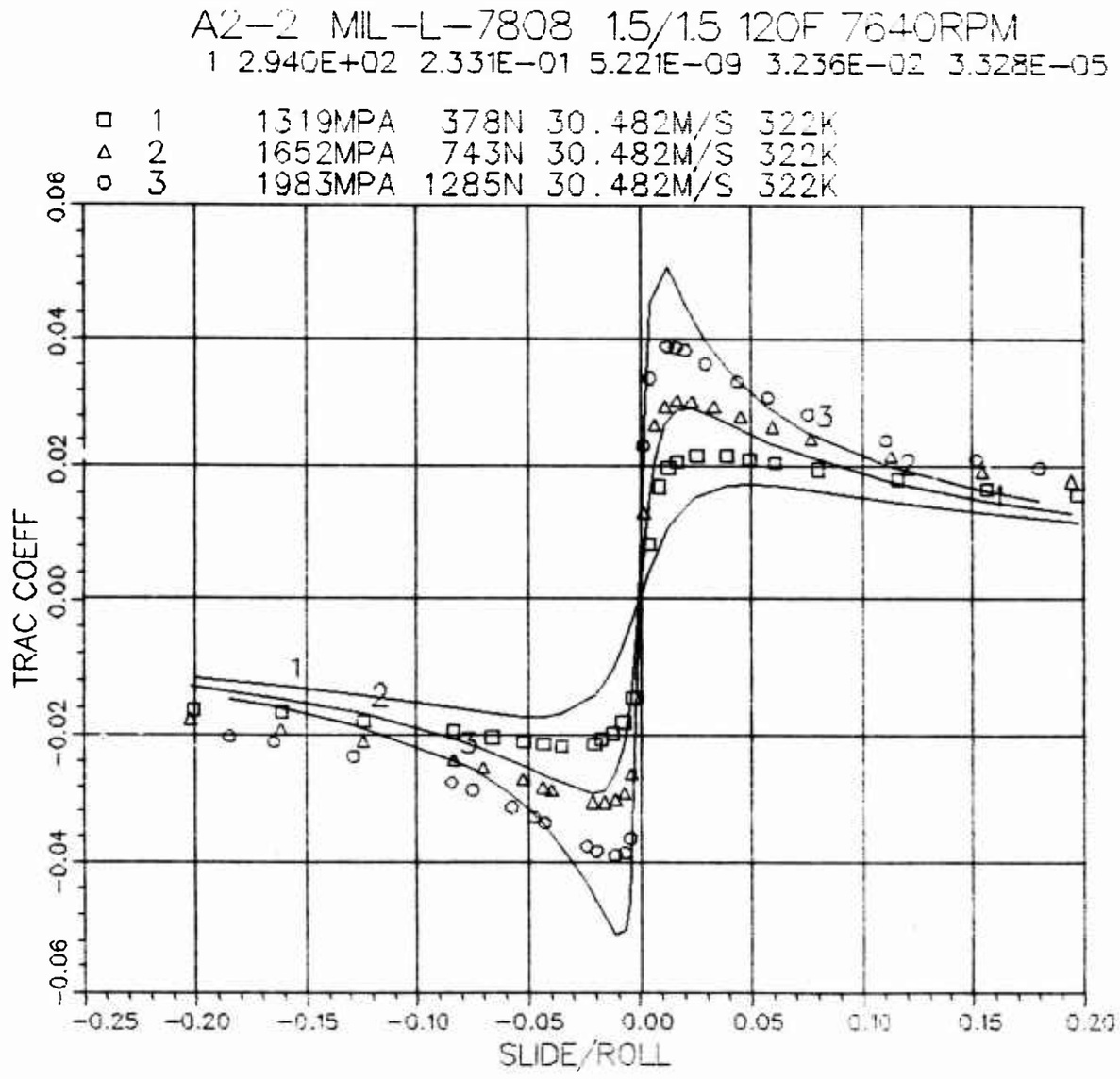
A2-2 MIL-L-7808 1.5/1.5 120F 7640RPM
1 2.940E+02 2.331E-01 5.221E-09 3.236E-02 3.328E-05
1 1319MPA 378N 30.482M/S 322K
2 1652MPA 743N 30.482M/S 322K
3 1983MPA 1285N 30.482M/S 322K
TRAC COEFF
SLIDE/ROLL
0.06
0.04
0.02
0.00
-0.02
-0.04
-0.06
-0.25
-0.20
-0.15
-0.10
-0.05
0.00
0.05
0.10
0.15
0.20

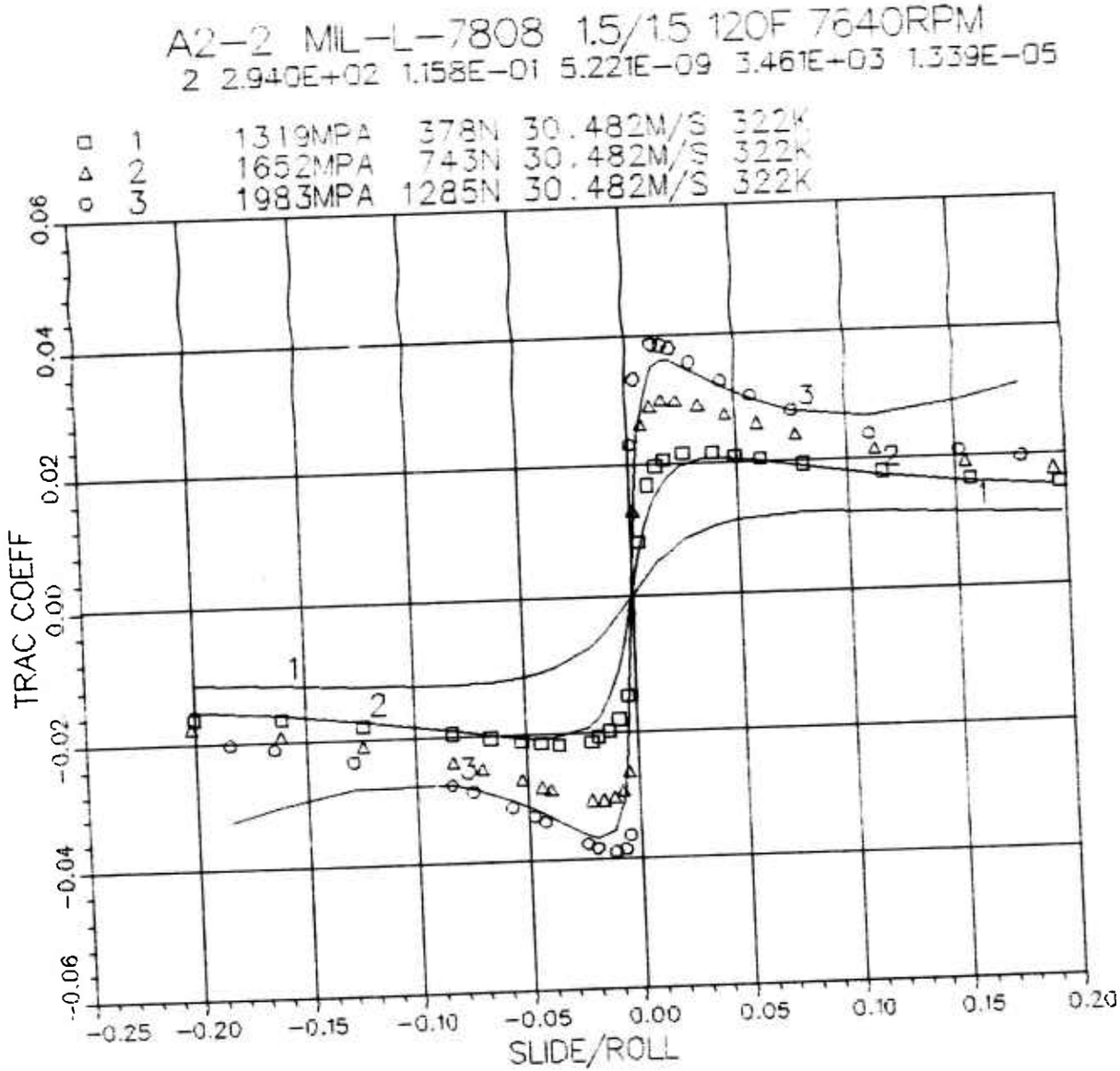
A2-2 MIL-L-7808 1.5/1.5 120F 7640RPM
2 2.940E+02 1.158E-01 5.221E-09 3.461E+03 1.339E-05
1 1319MPA 378N 30.482M/S 322K
2 1652MPA 743N 30.482M/S 322K
3 1983MPA 1285N 30.482M/S 322K
TRAC COEFF
SLIDE/ROLL
0.06
0.04
0.02
0.00
-0.02
-0.04
-0.06
-0.25
-0.20
-0.15
-0.10
-0.05
0.00
0.05
0.10
0.15
0.20

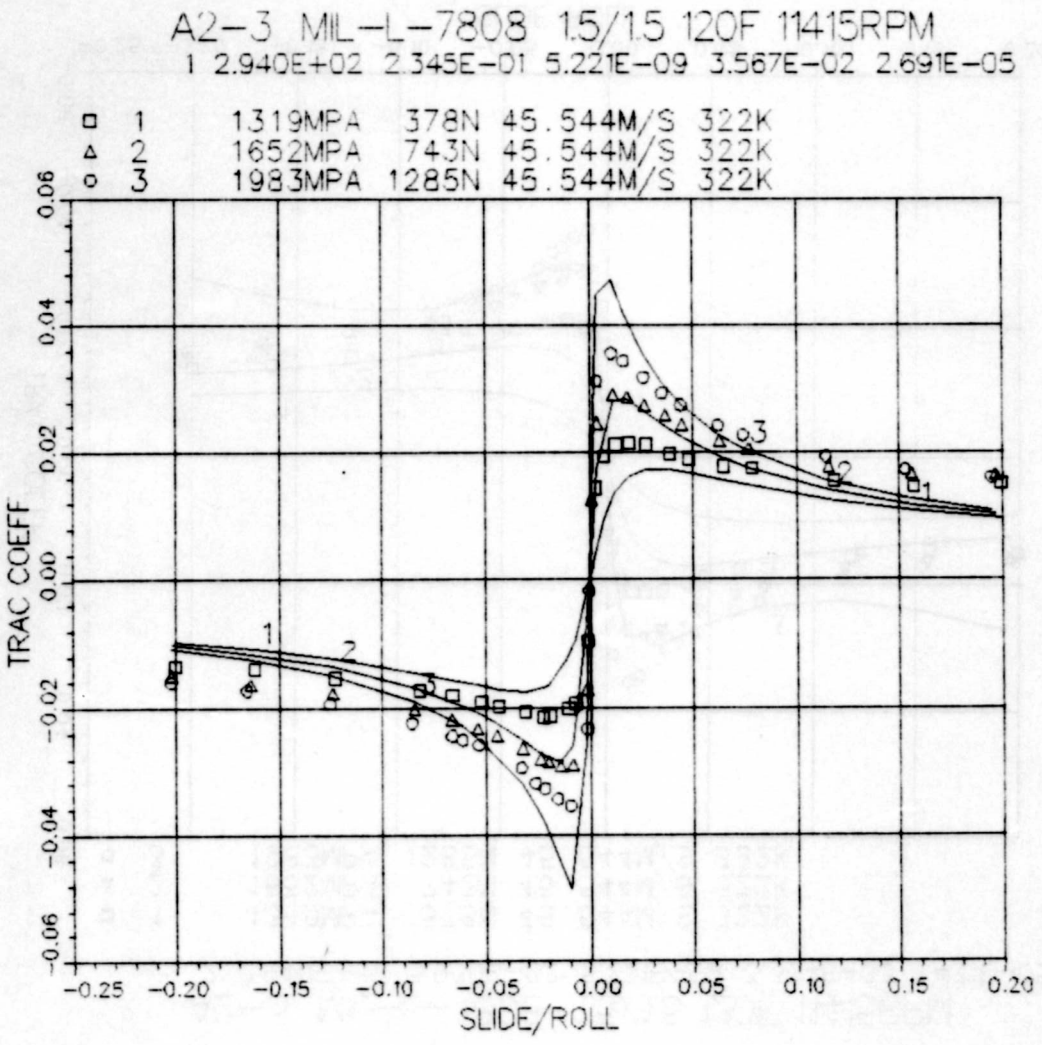
A2-3 MIL-L-7808 1.5/1.5 120F 11415RPM
1 2.940E+02 2.345E-01 5.221E-09 3.567E-02 2.691E-05
1 1319MPA 378N 45.544M/S 322K
2 1652MPA 743N 45.544M/S 322K
3 1983MPA 1285N 45.544M/S 322K
TRAC COEFF
SLIDE/ROLL
0.06
0.04
0.02
0.00
-0.02
-0.04
-0.06
-0.25
-0.20
-0.15
-0.10
-0.05
0.00
0.05
0.10
0.15
0.20

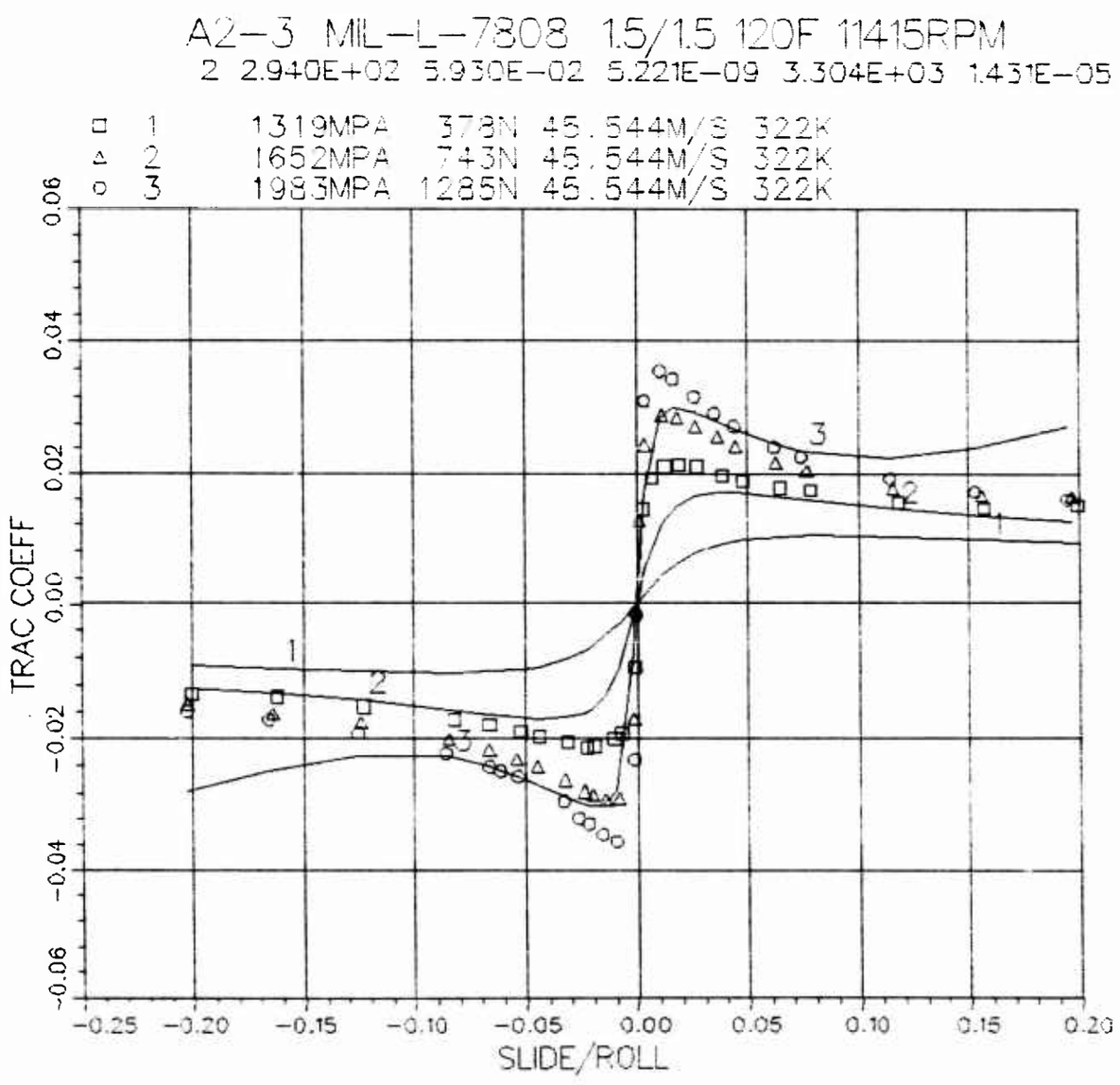
A2-3 MIL-L-7808 1.5/1.5 120F 11415RPM
2 2.940E+02 5.930E-02 5.221E-09 3.304E+03 1.431E-05
1 1319MPA 378N 45.544M/S 322K
2 1652MPA 743N 45.544M/S 322K
3 1983MPA 1285N 45.544M/S 322K
TRAC COEFF
0.06
0.04
0.02
0.00
-0.02
-0.04
-0.06
-0.25 -0.20 -0.15 -0.10 -0.05 0.00 0.05 0.10 0.15 0.20
SLIDE/ROLL

A3-3 MIL-L-7808 1.5/1.5 160F 11415RPM

1 2.940E+02 9.320E-02 5.221E-09 2.583E-02 1.860E-05

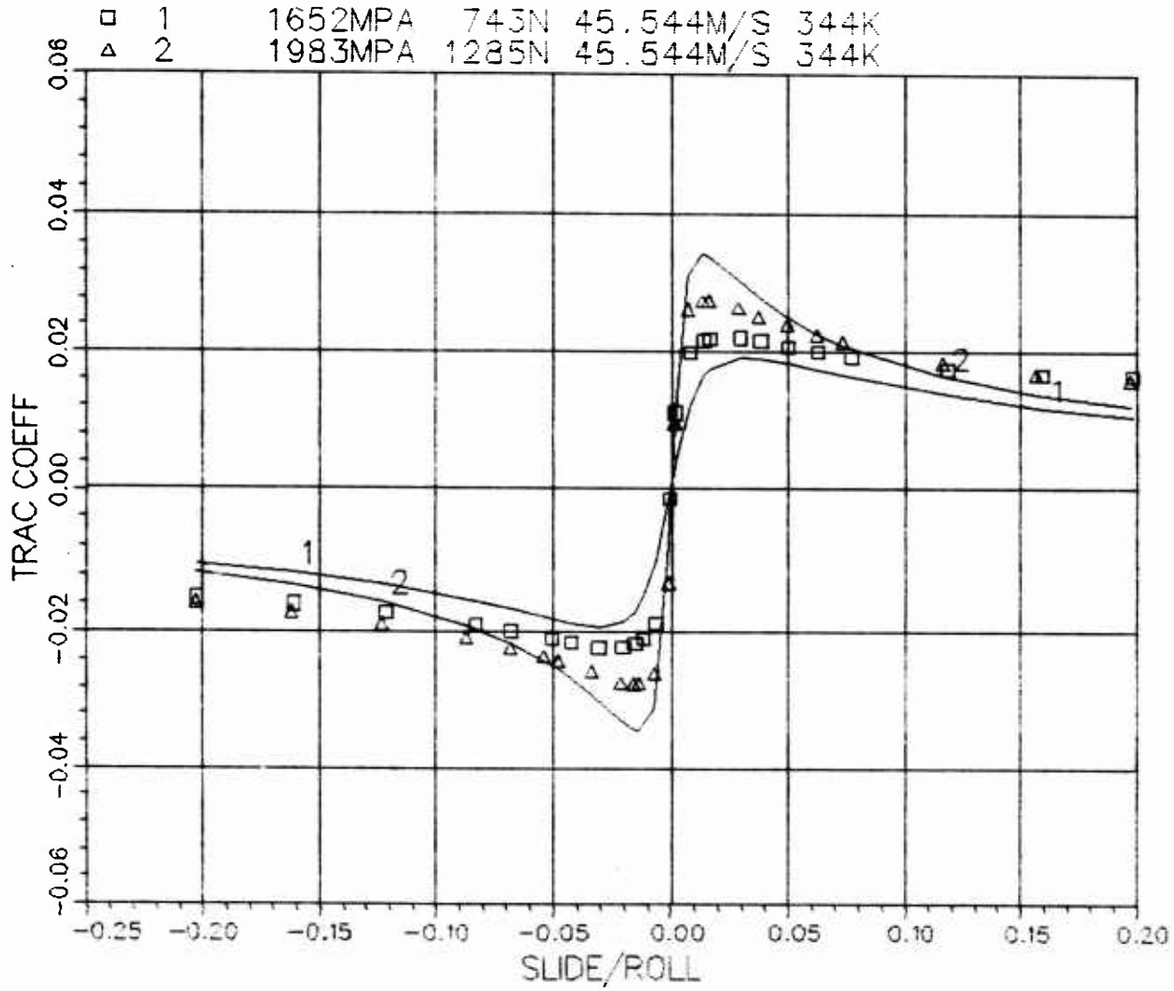

A3-3 MIL-L-7808 1.5/1.5 160F 11415RPM
2 2.940E+02 1.026E-01 5.221E-09 3.732E+03 6.347E-06

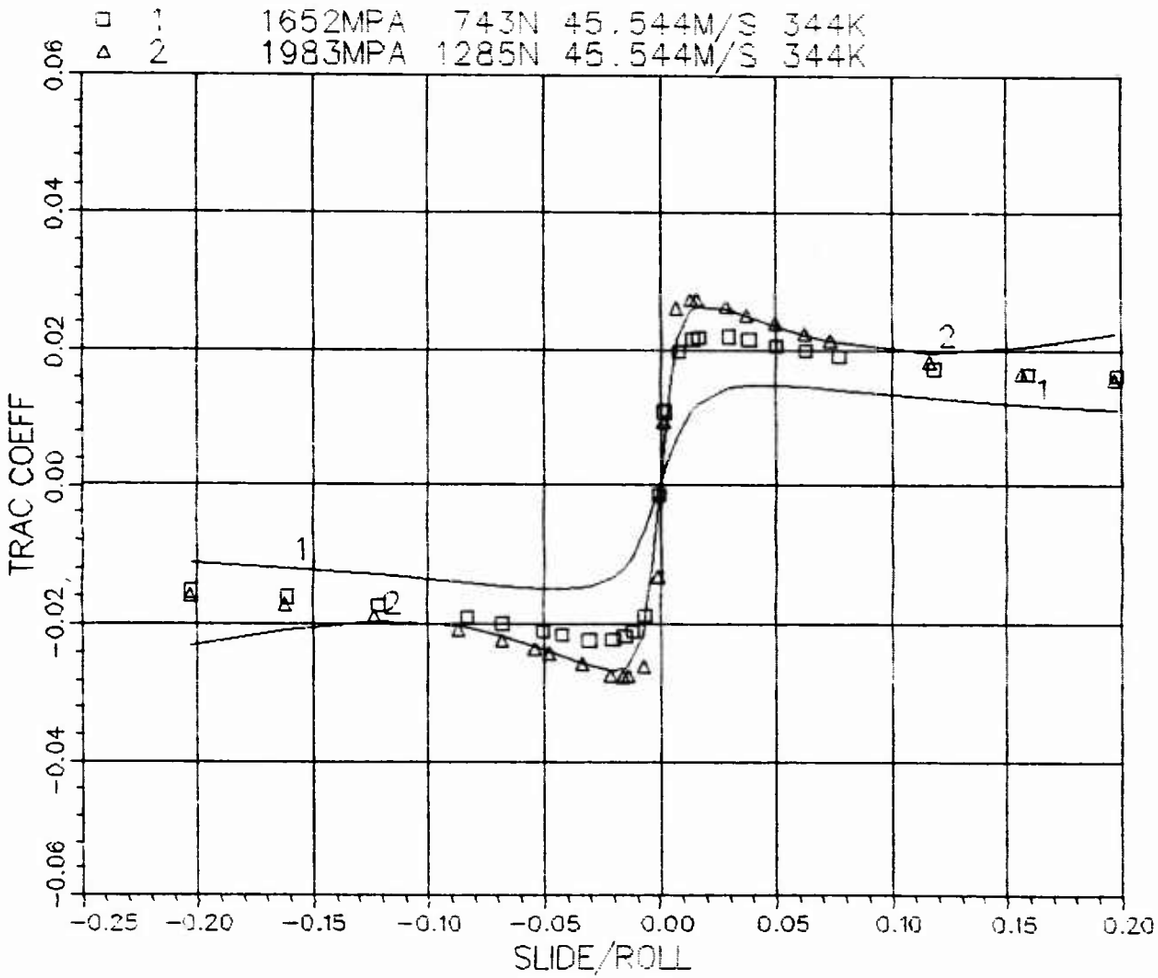

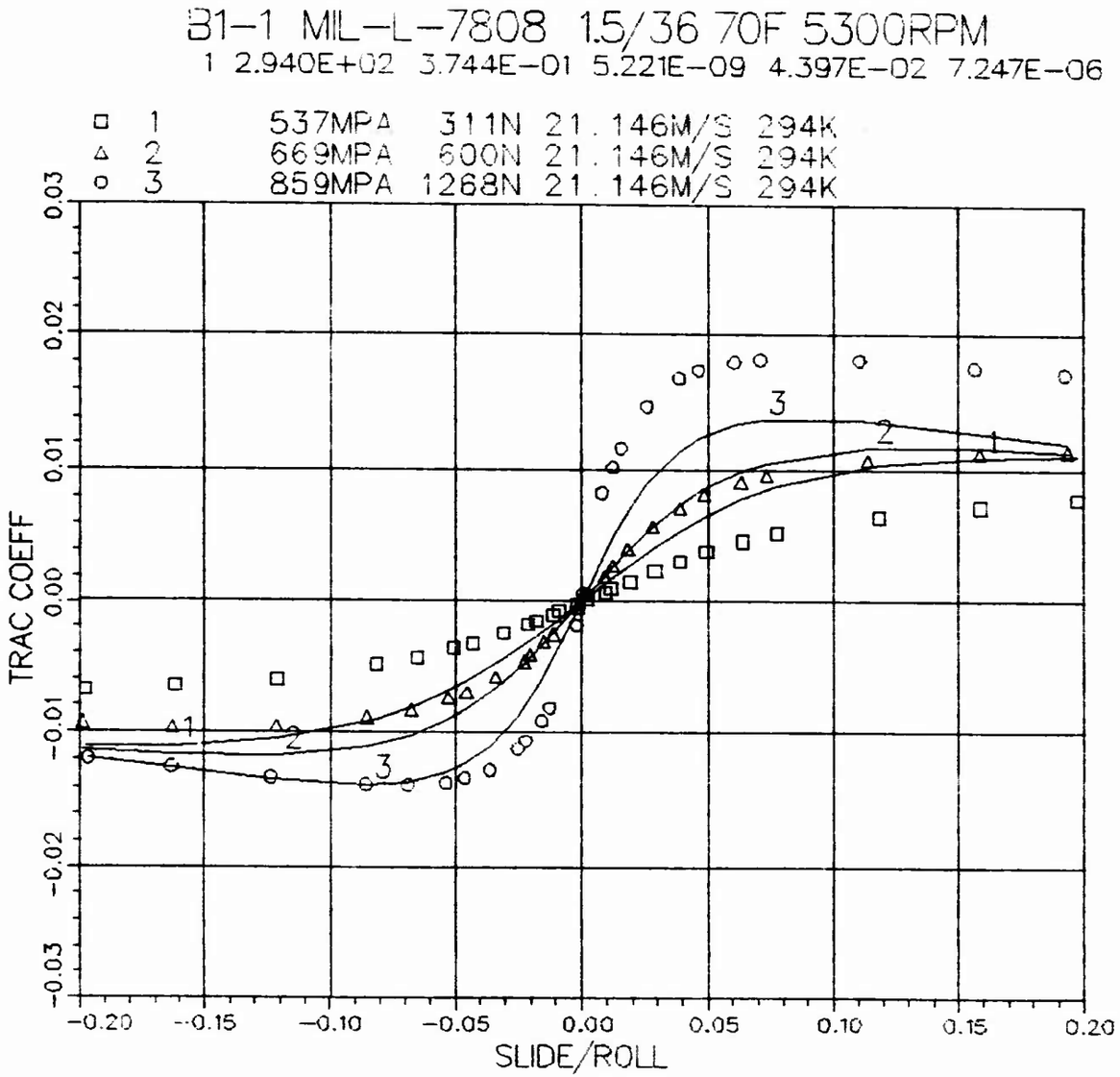
B1-1 MIL-L-7808 1.5/36 70F 5300RPM
1 2.940E+02 3.744E-01 5.221E-09 4.397E-02 7.247E-06
1 537MPA 311N 21.146M/S 294K
2 669MPA 600N 21.146M/S 294K
3 859MPA 1268N 21.146M/S 294K
TRAC COEFF
SLIDE/ROLL
0.03
0.02
0.01
0.00
-0.01
-0.02
-0.03
-0.20
-0.15
-0.10
-0.05
0.00
0.05
0.10
0.15
0.20

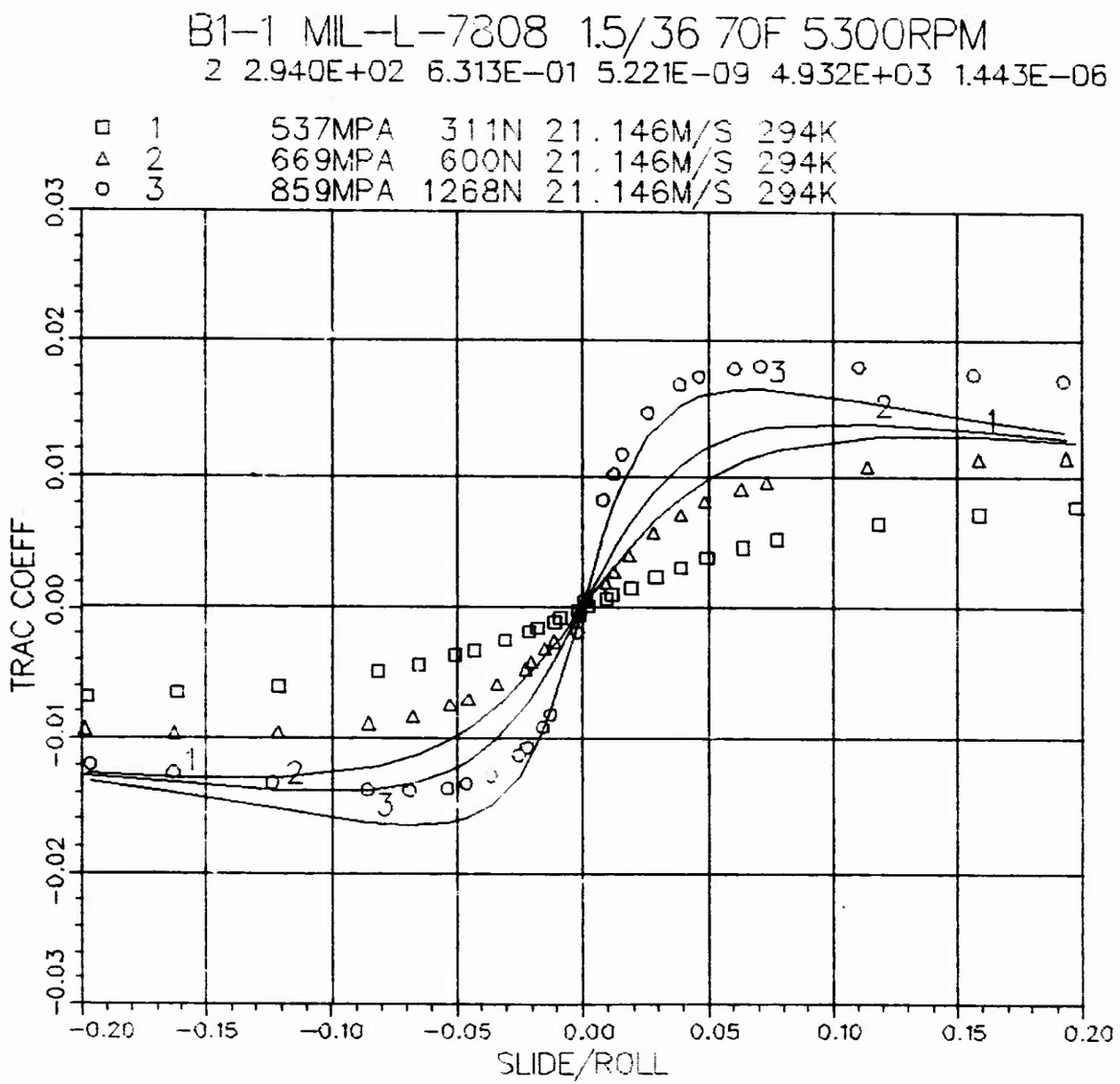
B1-1 MIL-L-7808 1.5/36 70F 5300RPM
2 2.940E+02 6.313E-01 5.221E-09 4.932E+03 1.443E-06
1 537MPA 311N 21.146M/S 294K
2 669MPA 600N 21.146M/S 294K
3 859MPA 1268N 21.146M/S 294K
TRAC COEFF
SLIDE/ROLL
0.03
0.02
0.01
0.00
-0.01
-0.02
-0.03
-0.20
-0.15
-0.10
-0.05
0.00
0.05
0.10
0.15
0.20

B1-2 MIL-L-7808 1.5/36 70F 7640RPM

1 2.940E+02 2.289E-01 5.221E-09 4.243E-02 5.109E-06

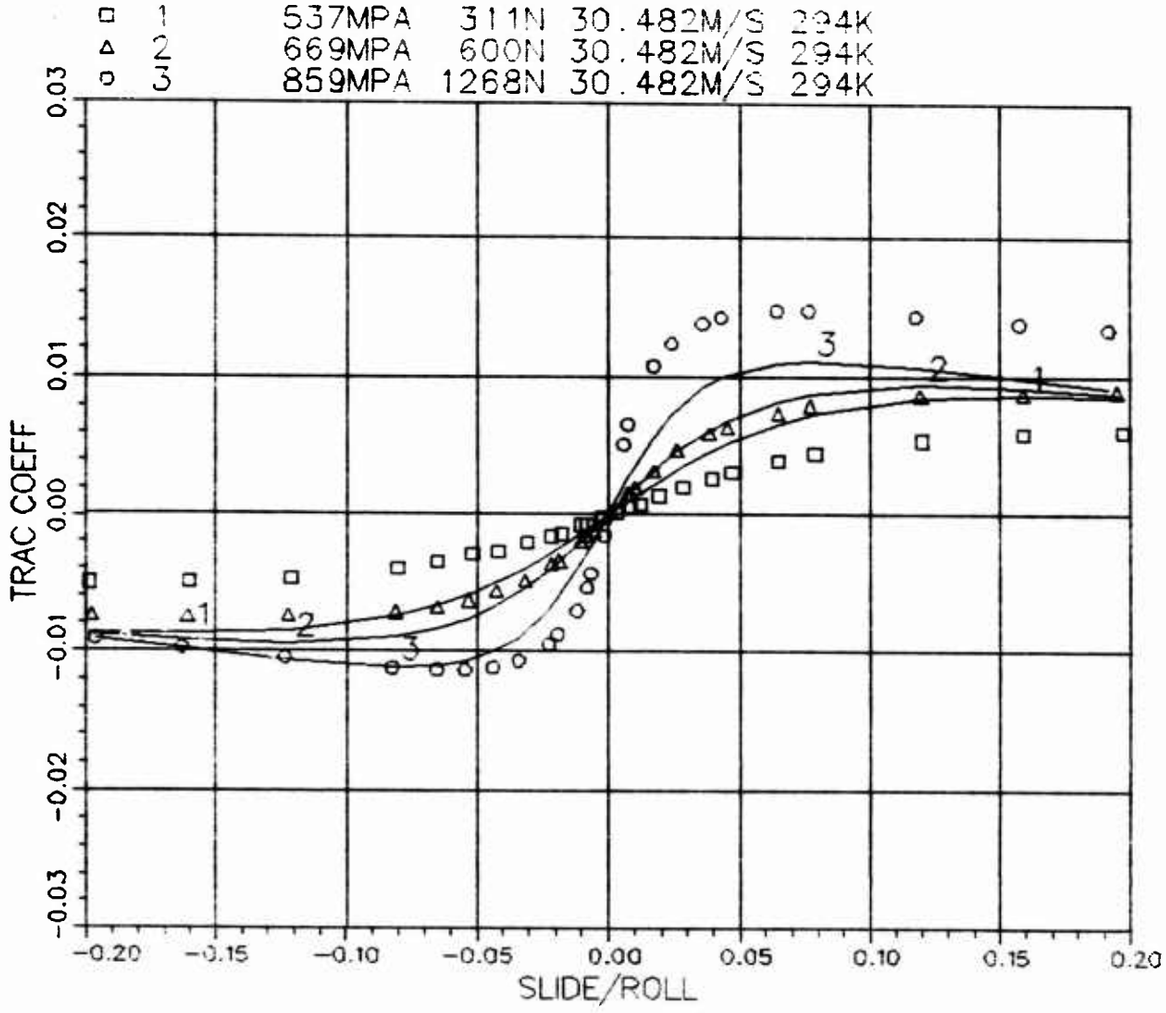

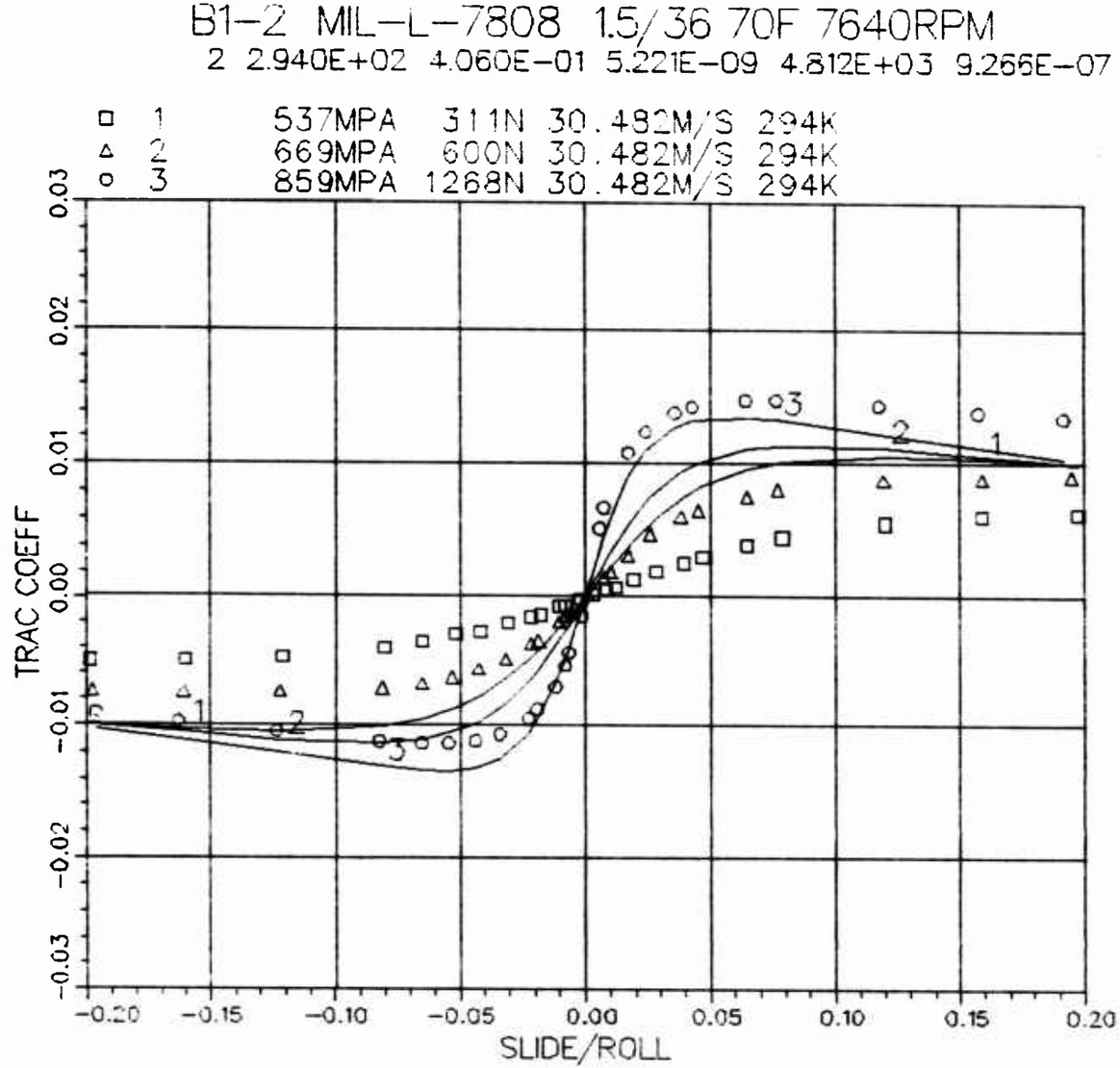
B1-2 MIL-L-7808 1.5/36 70F 7640RPM
2 2.940E+02 4.060E-01 5.221E-09 4.812E+03 9.266E-07
1 537MPA 311N 30.482M/S 294K
2 669MPA 600N 30.482M/S 294K
3 859MPA 1268N 30.482M/S 294K
TRAC COEFF
SLIDE/ROLL
0.03
0.02
0.01
0.00
-0.01
-0.02
-0.03
-0.20
-0.15
-0.10
-0.05
0.00
0.05
0.10
0.15
0.20

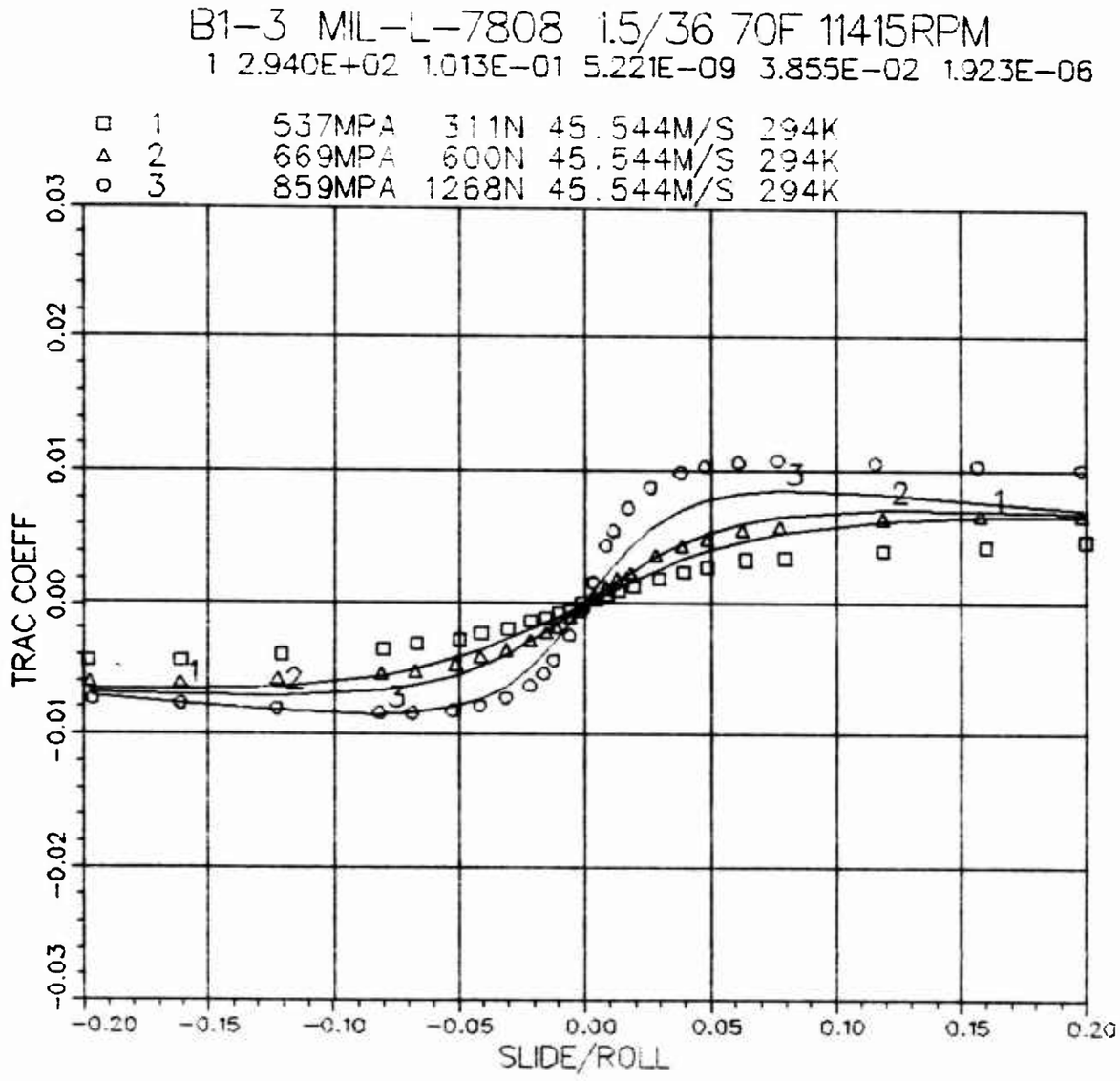
B1-3 MIL-L-7808 1.5/36 70F 11415RPM
1 2.940E+02 1.013E-01 5.221E-09 3.855E-02 1.923E-06
1 537MPA 311N 45.544M/S 294K
2 669MPA 600N 45.544M/S 294K
3 859MPA 1268N 45.544M/S 294K
TRAC COEFF
0.03
0.02
0.01
0.00
-0.01
-0.02
-0.03
-0.20
-0.15
-0.10
-0.05
0.00
0.05
0.10
0.15
0.20
SLIDE/ROLL

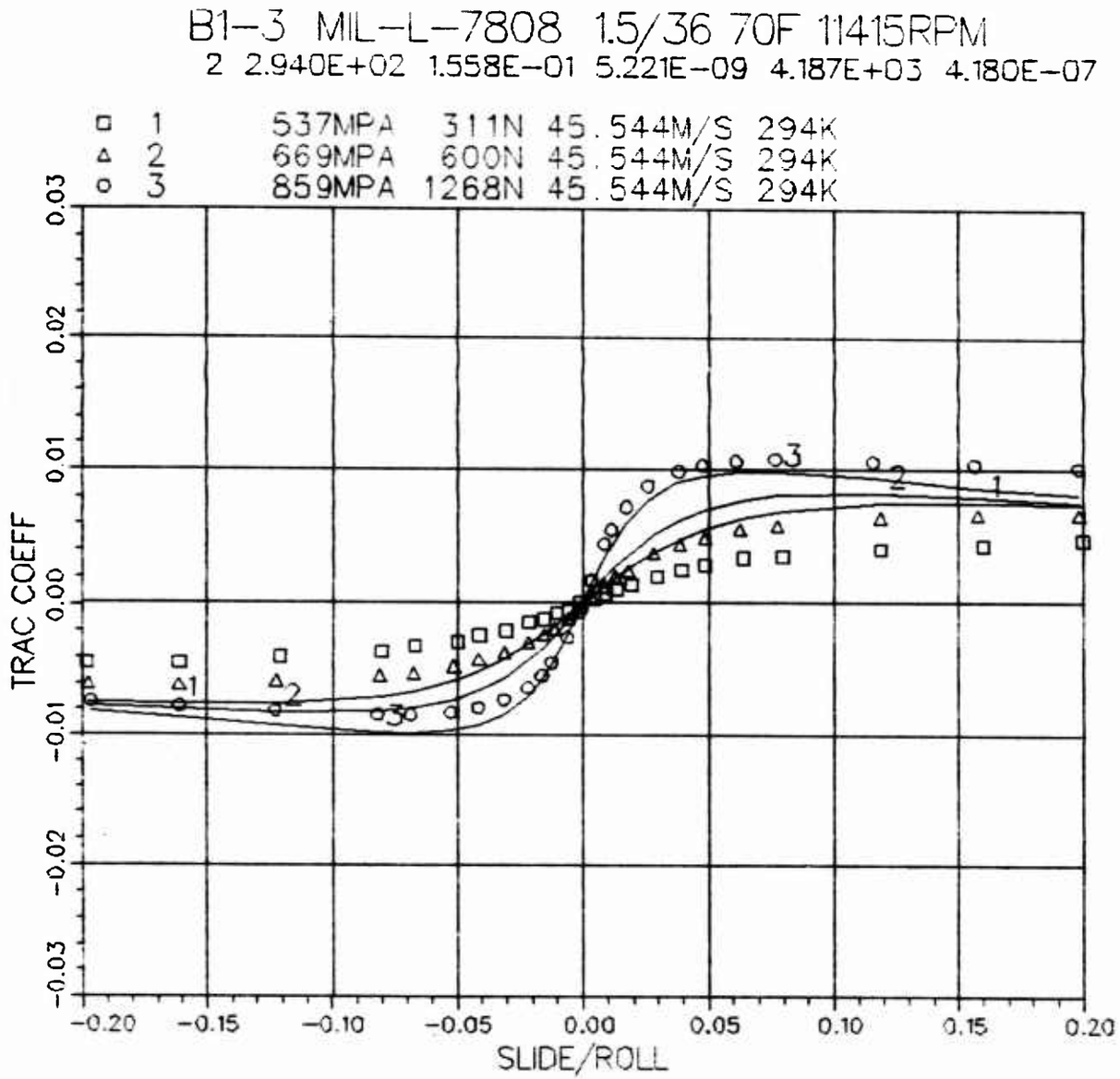
B1-3 MIL-L-7808 1.5/36 70F 11415RPM
2 2.940E+02 1.558E-01 5.221E-09 4.187E+03 4.180E-07
1 537MPA 311N 45.544M/S 294K
2 669MPA 600N 45.544M/S 294K
3 859MPA 1268N 45.544M/S 294K
TRAC COEFF
SLIDE/ROLL
0.03
0.02
0.01
0.00
-0.01
-0.02
-0.03
-0.20
-0.15
-0.10
-0.05
0.00
0.05
0.10
0.15
0.20

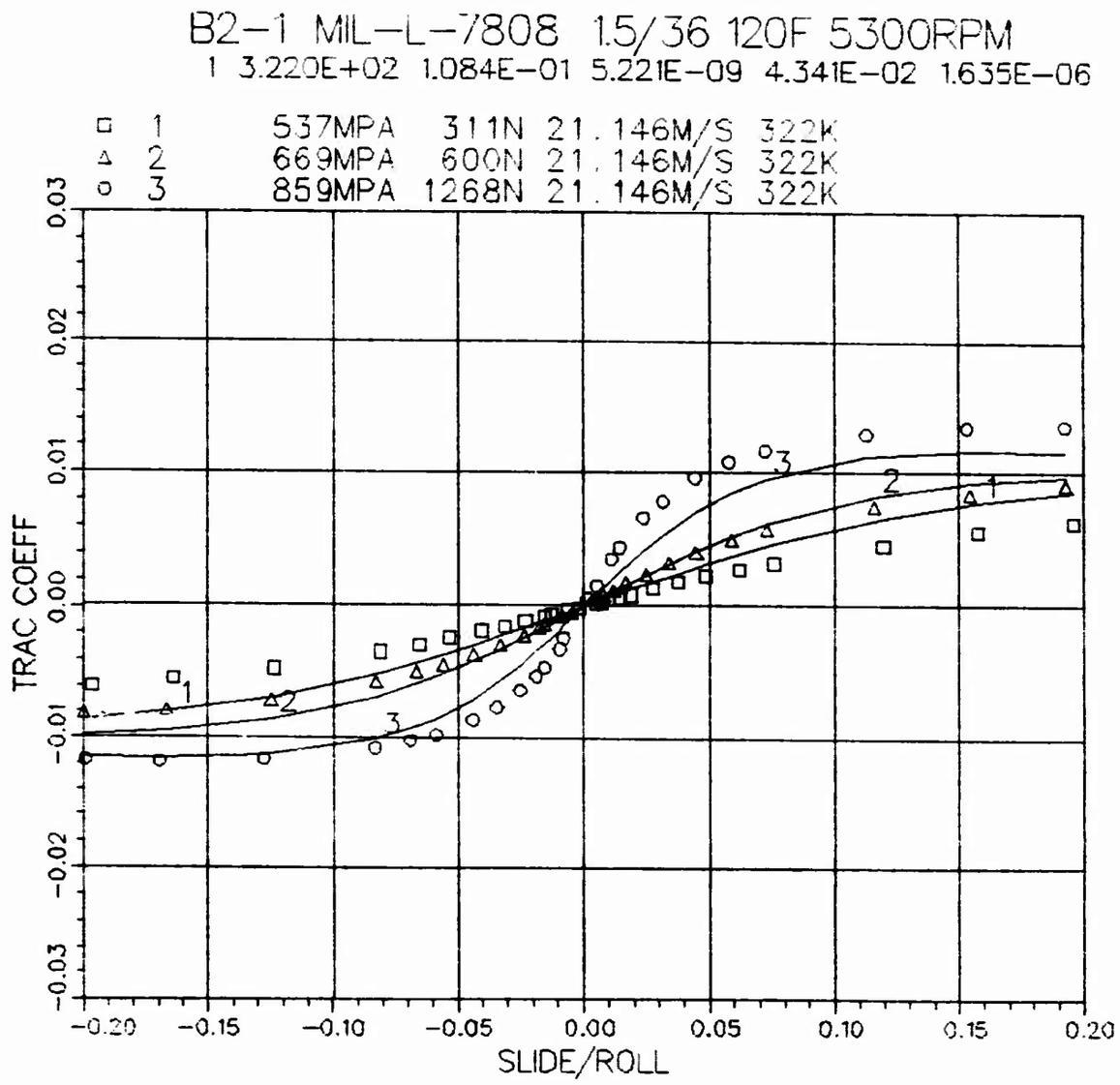
B2-1 MIL-L-7808 1.5/36 120F 5300RPM
1 3.220E+02 1.084E-01 5.221E-09 4.341E-02 1.635E-06
1 537MPA 311N 21.146M/S 322K
2 669MPA 600N 21.146M/S 322K
3 859MPA 1268N 21.146M/S 322K
TRAC COEFF
SLIDE/ROLL
0.03
0.02
0.01
0.00
-0.01
-0.02
-0.03
-0.20
-0.15
-0.10
-0.05
0.00
0.05
0.10
0.15
0.20

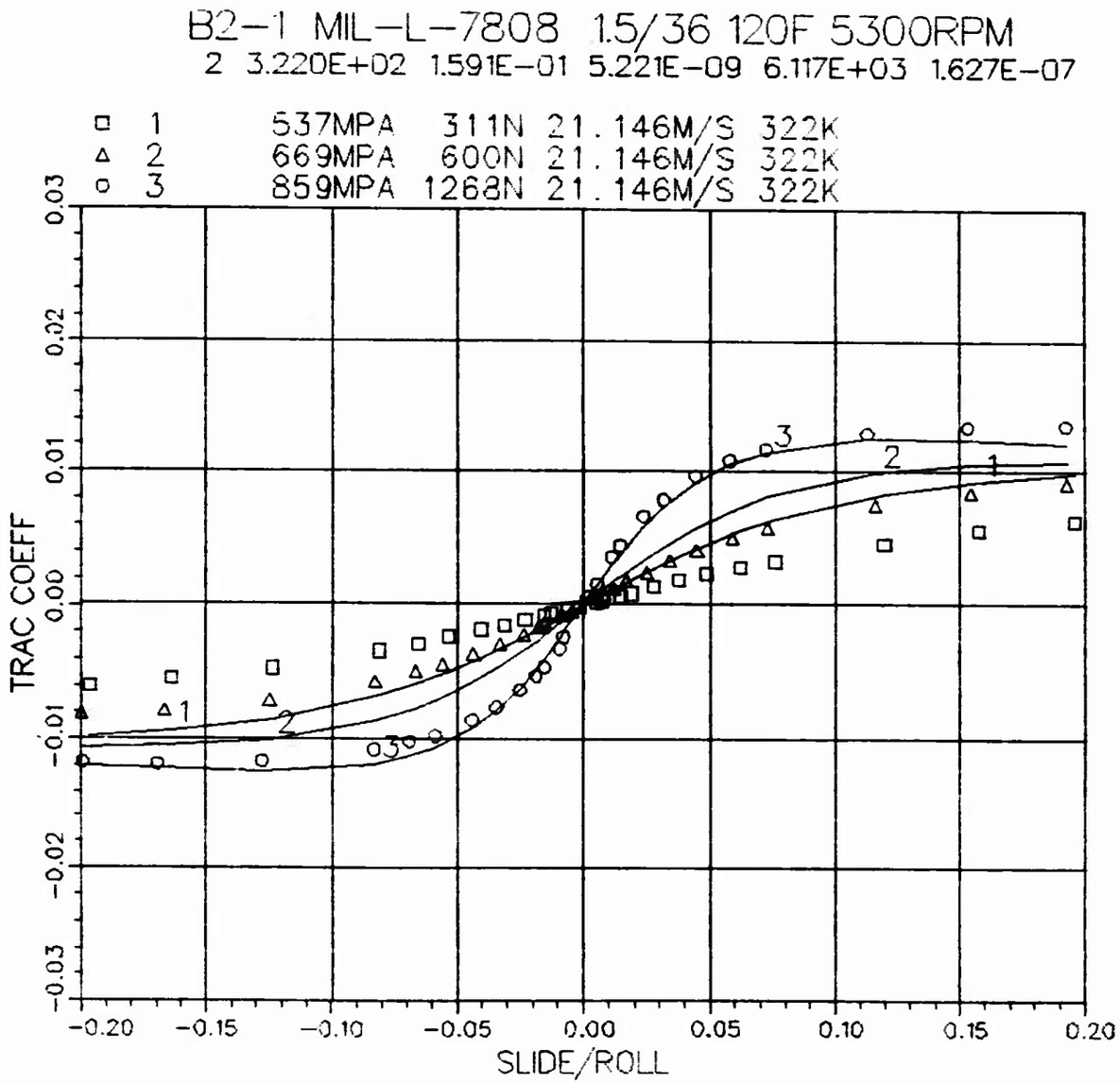
B2-1 MIL-L-7808 1.5/36 120F 5300RPM
2 3.220E+02 1.591E-01 5.221E-09 6.117E+03 1.627E-07
1 537MPA 311N 21.146M/S 322K
2 669MPA 600N 21.146M/S 322K
3 859MPA 1268N 21.146M/S 322K
TRAC COEFF
SLIDE/ROLL
0.03
0.02
0.01
0.00
-0.01
-0.02
-0.03
-0.20
-0.15
-0.10
-0.05
0.00
0.05
0.10
0.15
0.20

B2-2 MIL-L-7808 1.5/36 120F 7640RPM

1 3.220E+02 8.075E-02 5.221E-09 3.579E-02 5.531E-07

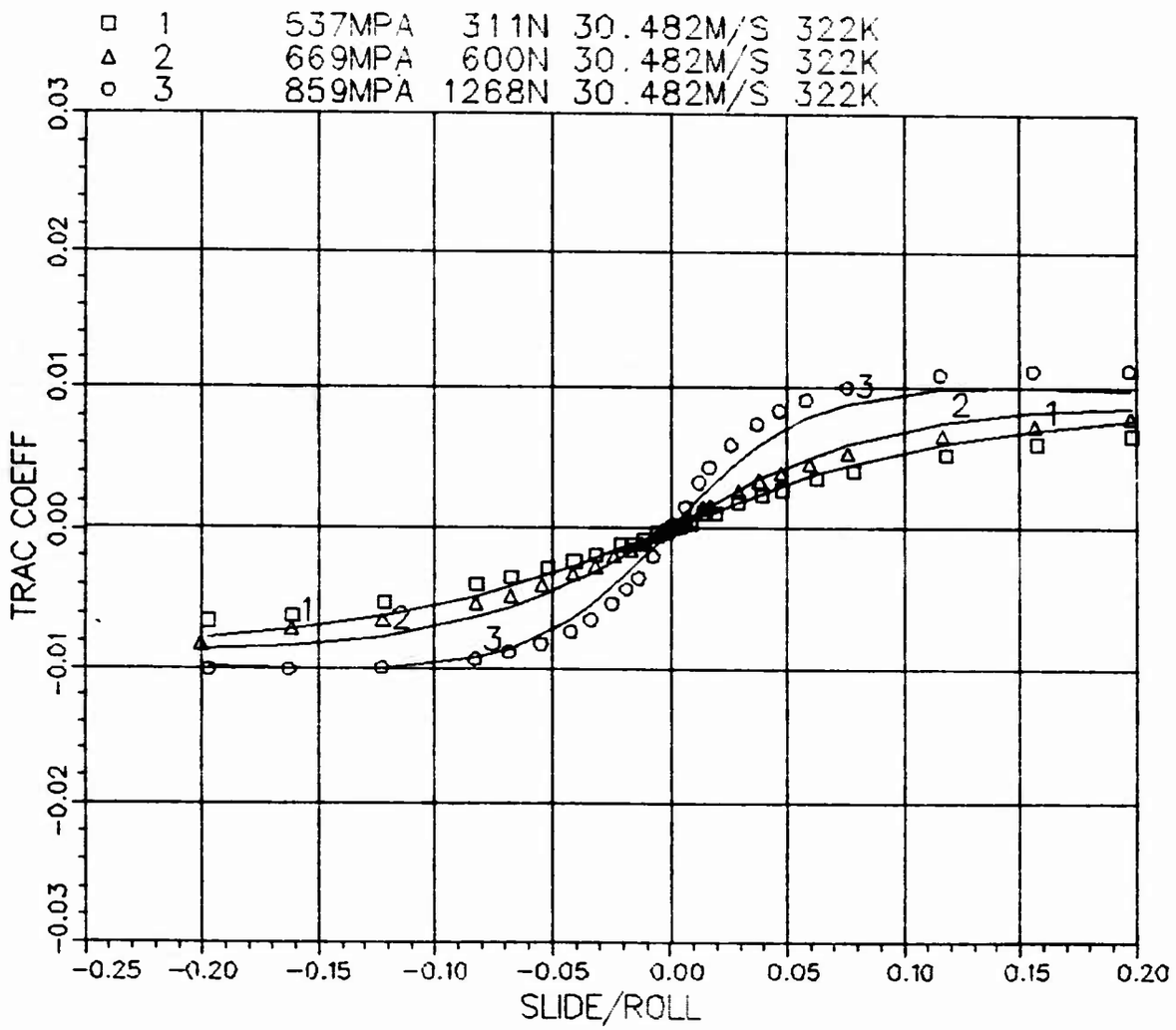

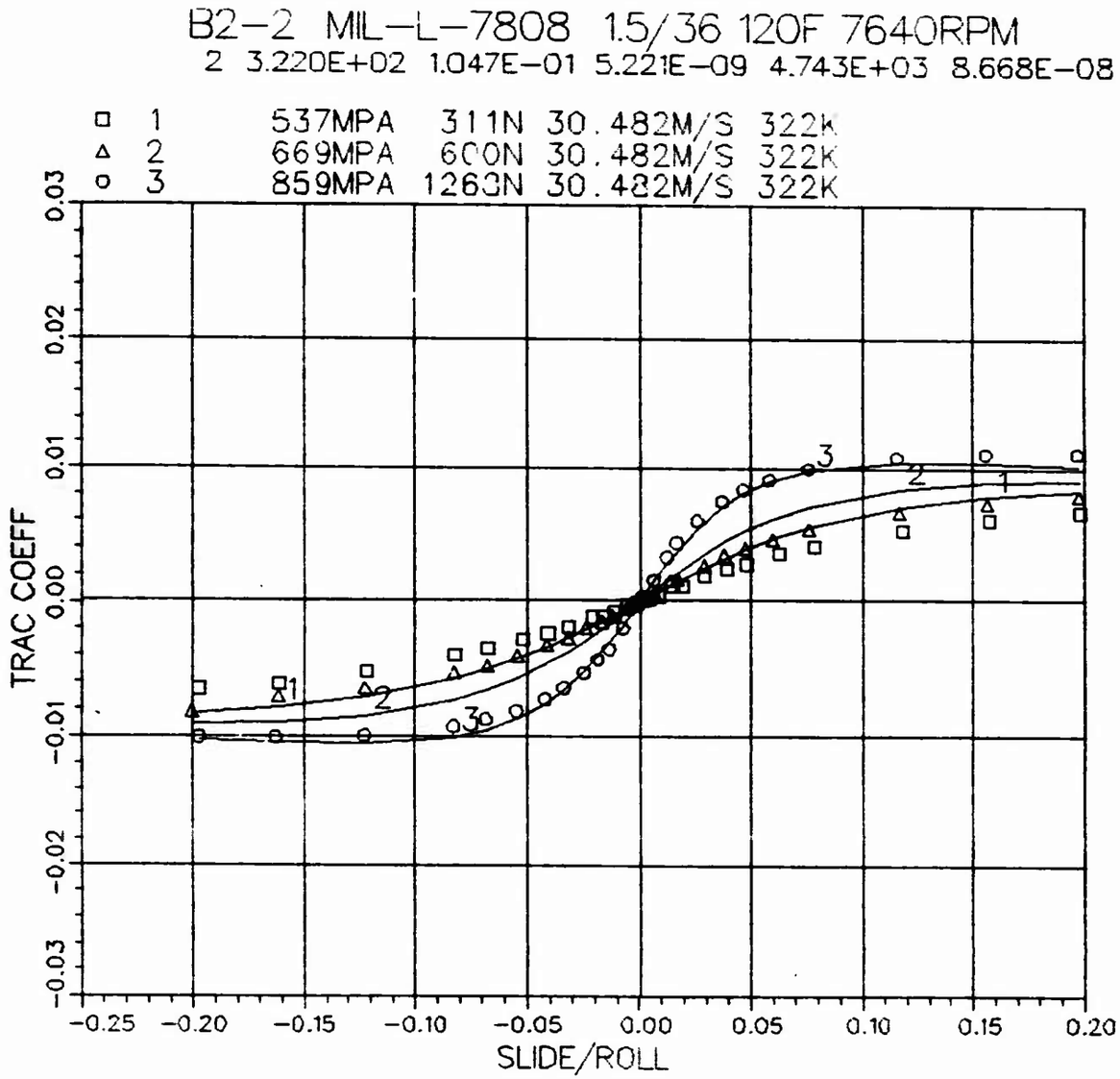
B2-2 MIL-L-7808 1.5/36 120F 7640RPM
2 3.220E+02 1.047E-01 5.221E-09 4.743E+03 8.668E-08
1 537MPA 311N 30.482M/S 322K
2 669MPA 600N 30.482M/S 322K
3 859MPA 1260N 30.482M/S 322K
TRAC COEFF
SLIDE/ROLL
0.03
0.02
0.01
0.00
-0.01
-0.02
-0.03
-0.25
-0.20
-0.15
-0.10
-0.05
0.00
0.05
0.10
0.15
0.20

B2-3 MIL-L-7808 1.5/36 120F 11415RPM

1 3.220E+02 7.136E-02 5.221E-09 3.138E-02 1.238E-07

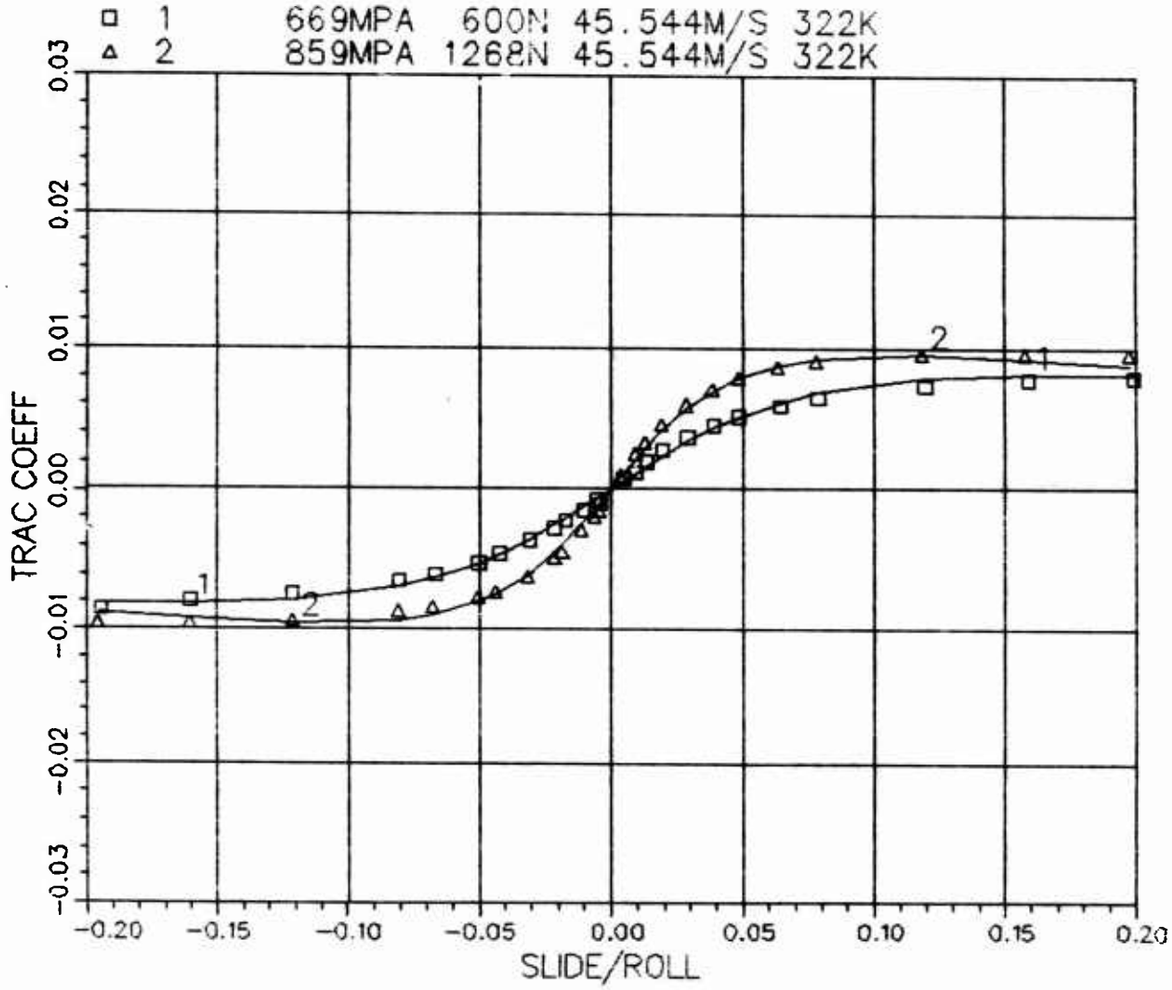

B2-3 MIL-L-7808 1.5/36 120F 11415RPM

2 3.220E+02 7.476E-02 5.221E-09 3.818E+03 4.580E-08

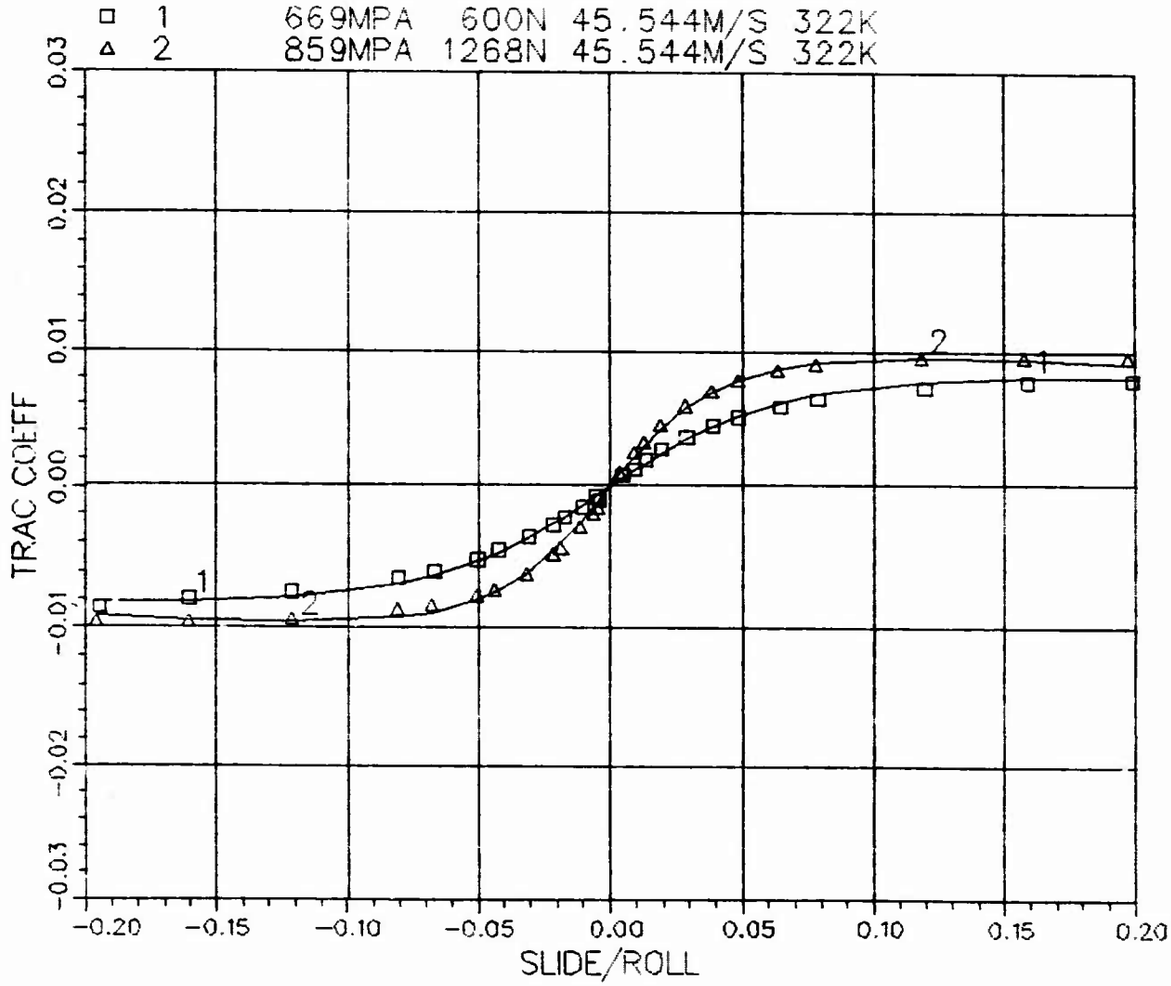

B3-1 MIL-L-7808 1.5/36 160F 5300RPM

1 3.440E+02 4.119E-02 5.221E-09 5.071E-02 2.797E-07

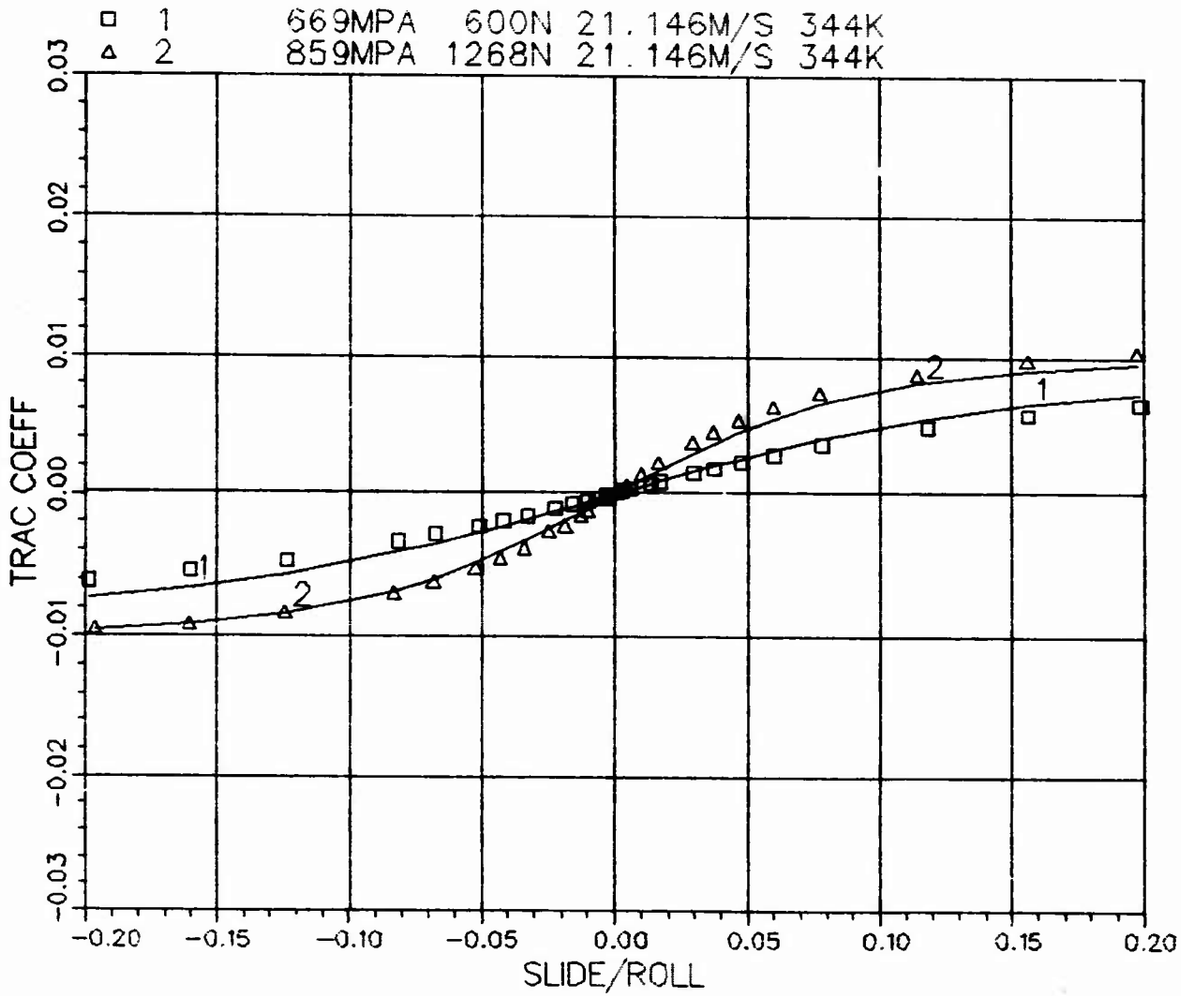

B3-1 MIL-L-7808 1.5/36 160F 5300RPM

2 3.440E+02 4.771E-02 5.221E-09 7.231E+03 6.042E-08

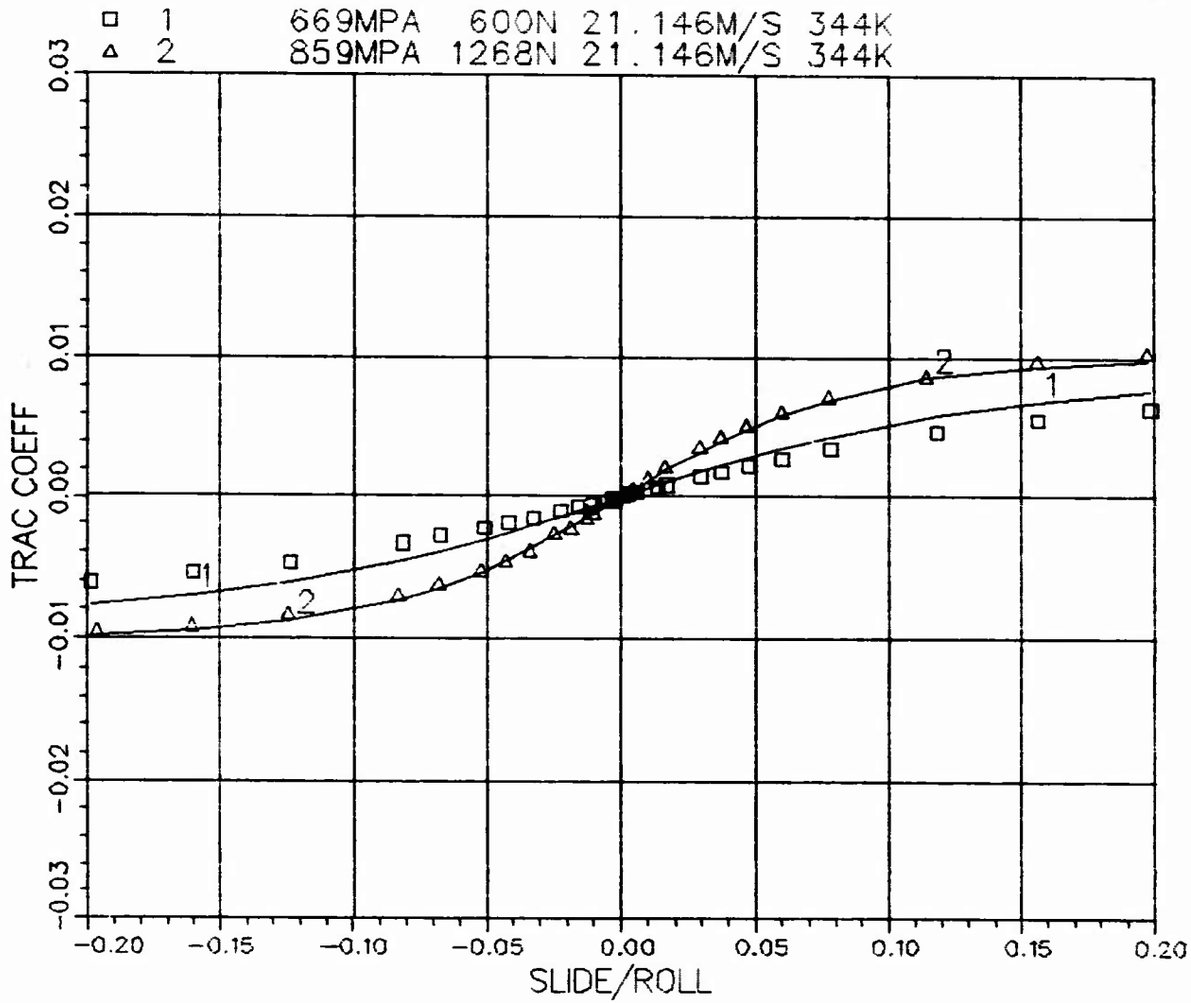

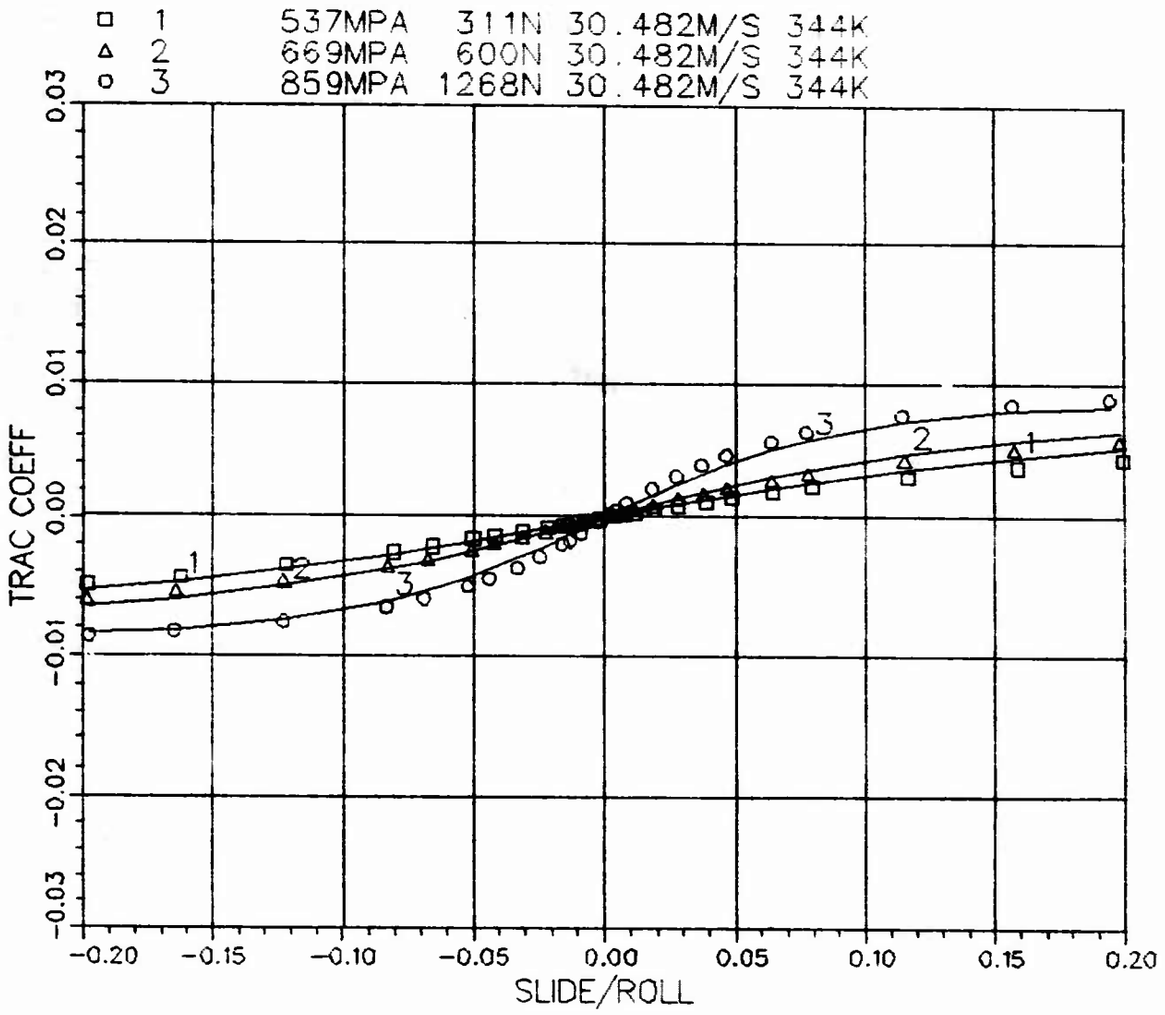
B3-2 MIL-L-7808 1.5/36 160F 7640RPM
1 3.440E+02 3.073E-02 5.221E-09 3.554E-02 1.377E-07
1 537MPA 311N 30.482M/S 344K
2 669MPA 600N 30.482M/S 344K
3 859MPA 1268N 30.482M/S 344K
TRAC COEFF
SLIDE/ROLL
0.03
0.02
0.01
0.00
-0.01
-0.02
-0.03
-0.20
-0.15
-0.10
-0.05
0.00
0.05
0.10
0.15
0.20

B3-2 MIL-L-7808 .5/36 160F 7640RPM

2 3.440E+02 3.712E-02 5.221E-09 5.448E+03 1.044E-08

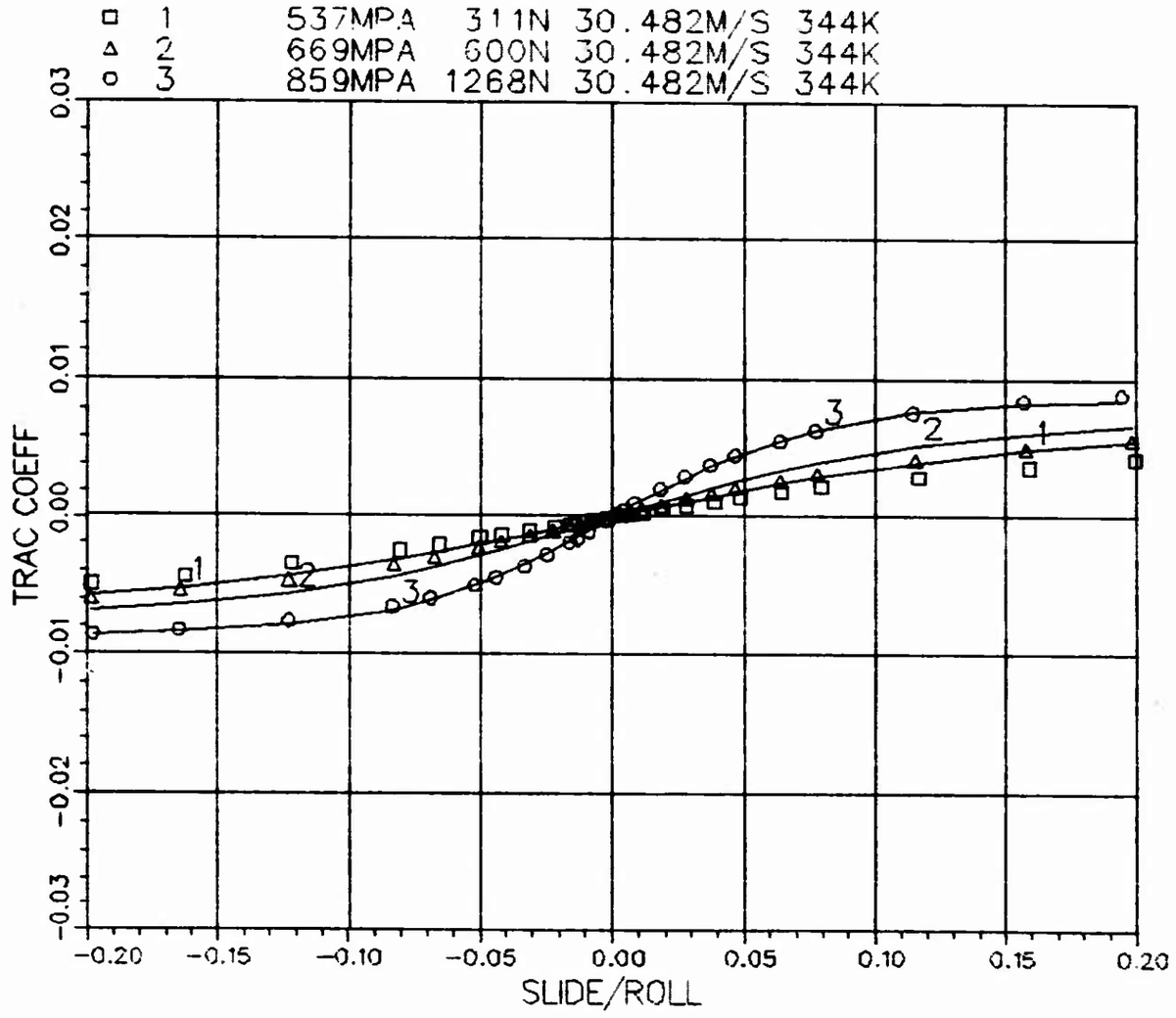

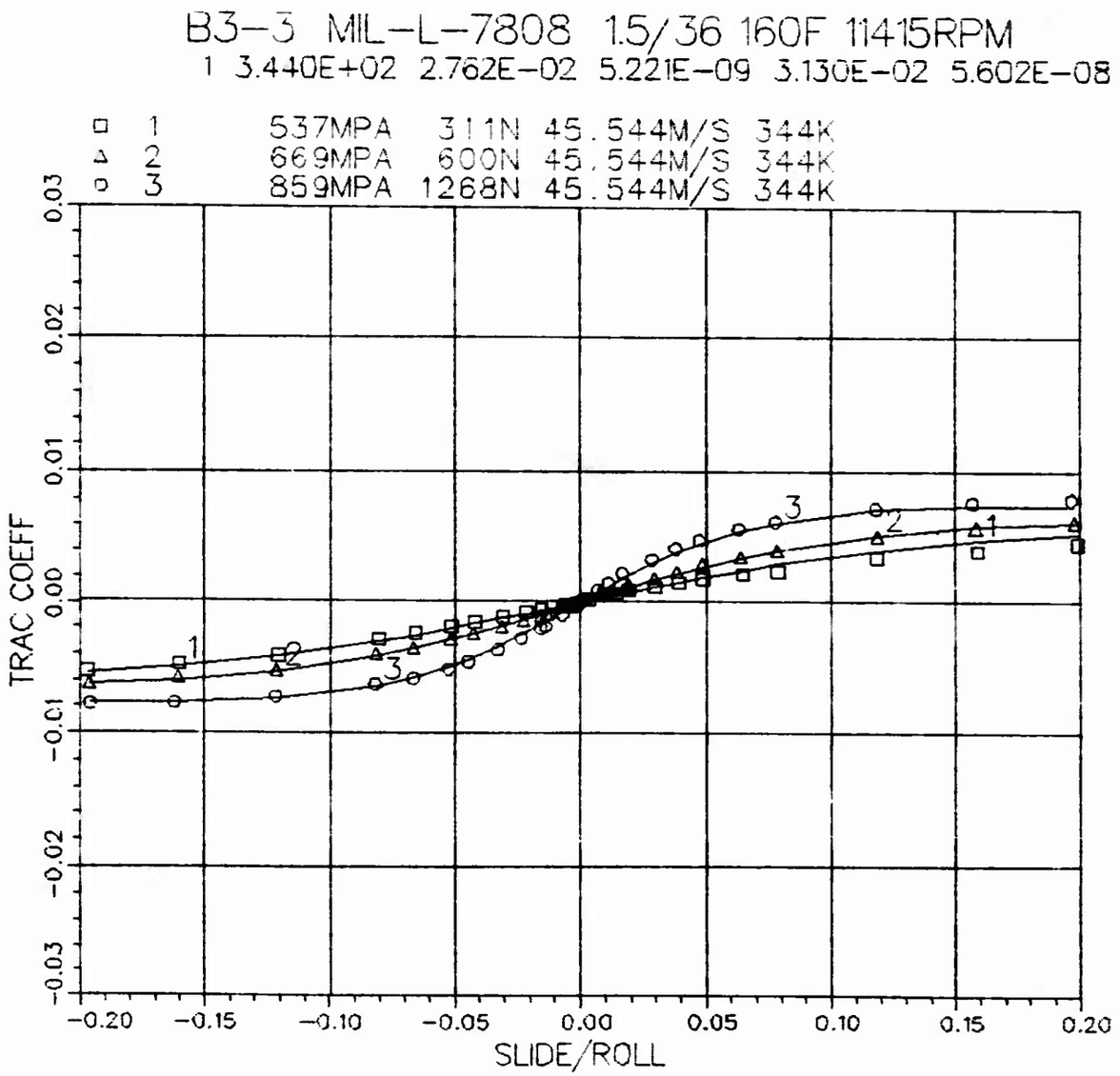
B3-3 MIL-L-7808 1.5/36 160F 11415RPM
1 3.440E+02 2.762E-02 5.221E-09 3.130E-02 5.602E-08
1 537MPA 311N 45.544M/S 344K
2 669MPA 600N 45.544M/S 344K
3 859MPA 1268N 45.544M/S 344K
TRAC COEFF
SLIDE/ROLL
0.03
0.02
0.01
0.00
-0.01
-0.02
-0.03
-0.20
-0.15
-0.10
-0.05
0.00
0.05
0.10
0.15
0.20

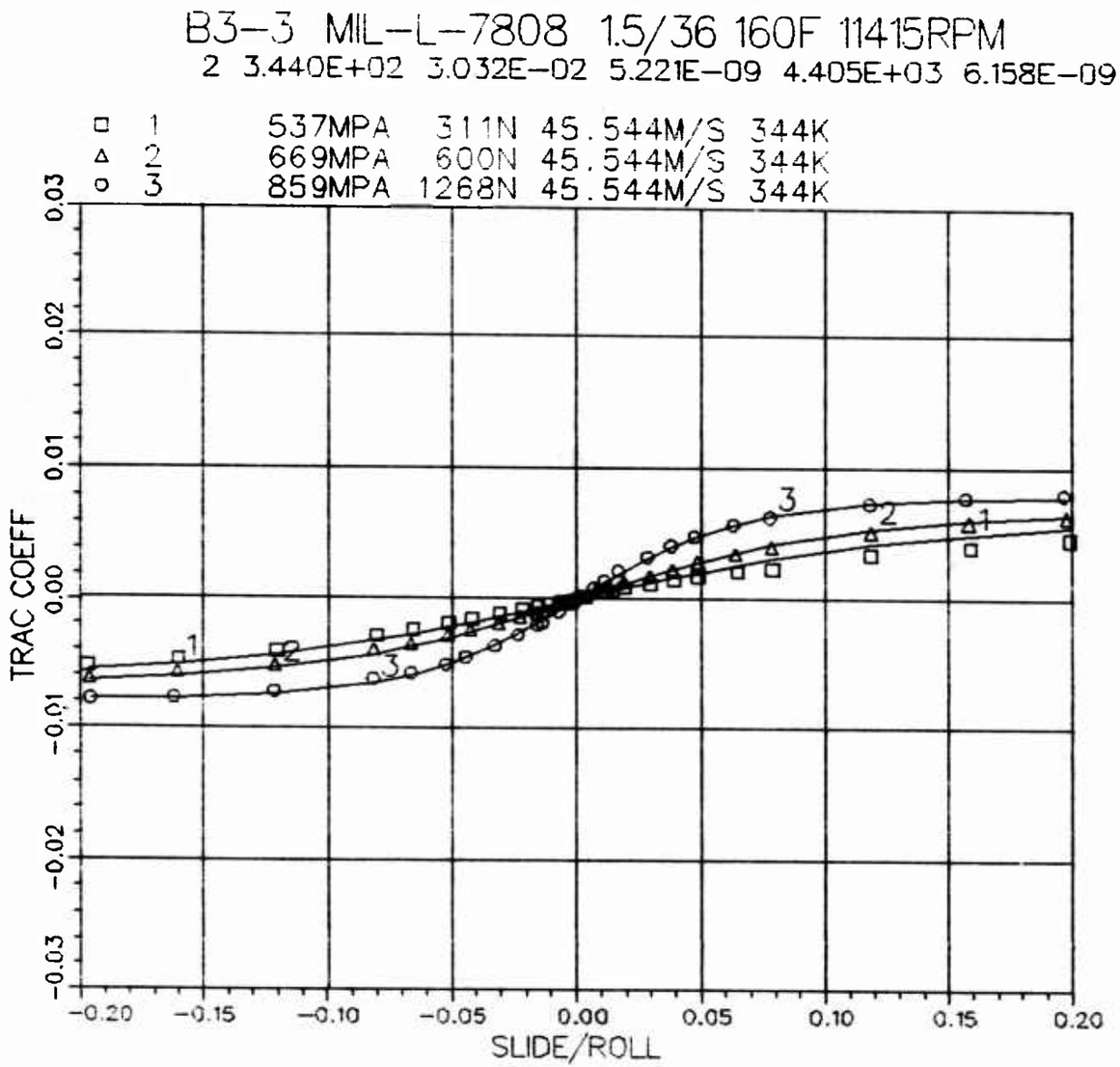
B3-3 MIL-L-7808 1.5/36 160F 11415RPM
2 3.440E+02 3.032E-02 5.221E-09 4.405E+03 6.158E-09
1 537MPA 311N 45.544M/S 344K
2 669MPA 600N 45.544M/S 344K
3 859MPA 1268N 45.544M/S 344K
TRAC COEFF
0.03
0.02
0.01
0.00
-0.01
-0.02
-0.03
-0.20
-0.15
-0.10
-0.05
0.00
0.05
0.10
0.15
0.20
SLIDE/ROLL

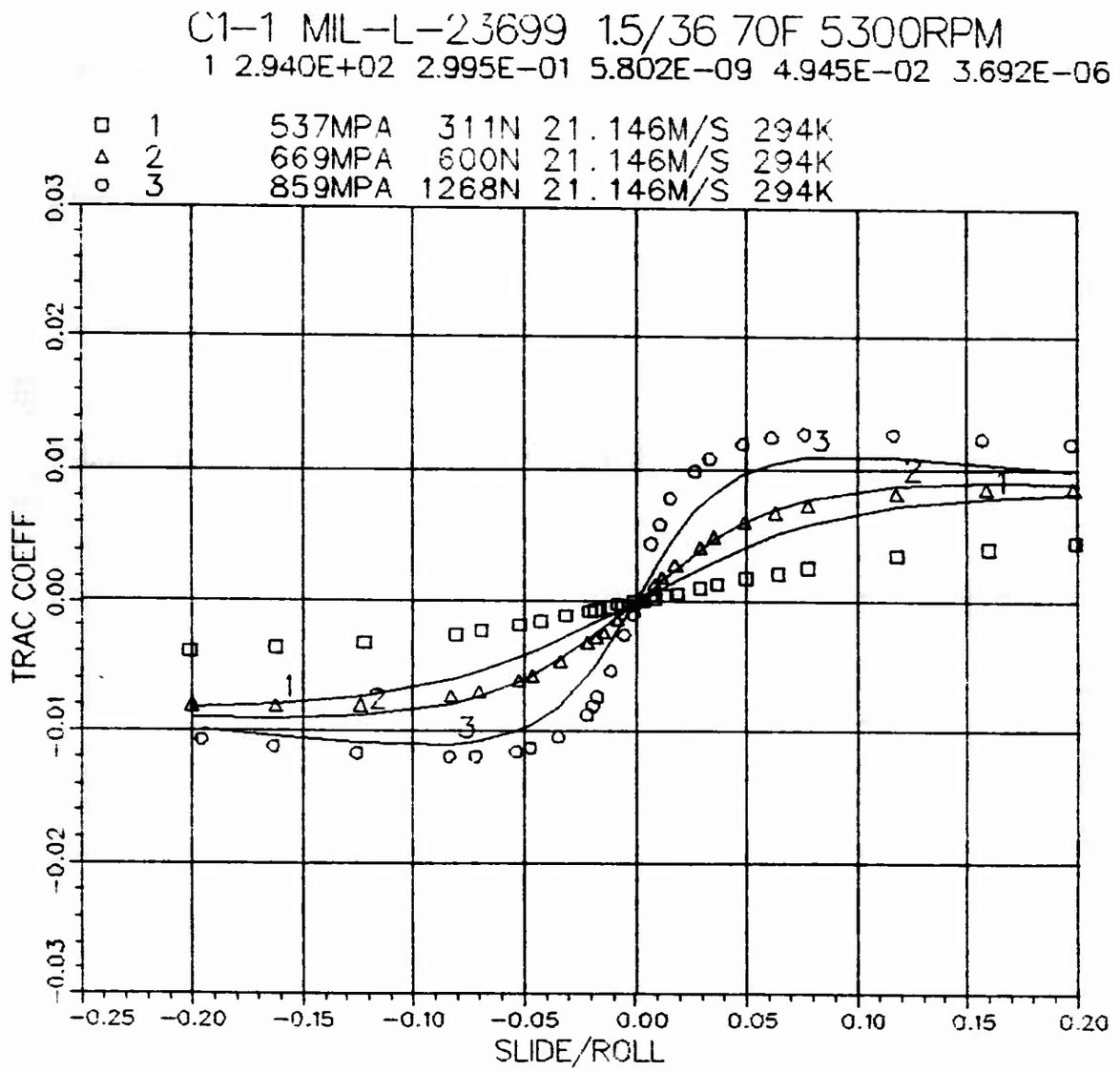
C1-1 MIL-L-23699 1.5/36 70F 5300RPM
1 2.940E+02 2.995E-01 5.802E-09 4.945E-02 3.692E-06
1 537MPA 311N 21.146M/S 294K
2 669MPA 600N 21.146M/S 294K
3 859MPA 1268N 21.146M/S 294K
TRAC COEFF
0.03
0.02
0.01
0.00
-0.01
-0.02
-0.03
-0.25 -0.20 -0.15 -0.10 -0.05 0.00 0.05 0.10 0.15 0.20
SLIDE/ROLL

C1-1 MIL-L-23699 1.5/36 70F 5300RPM

2 2.940E+02 4.842E-01 5.802E-09 5.611E+03 1.516E-07

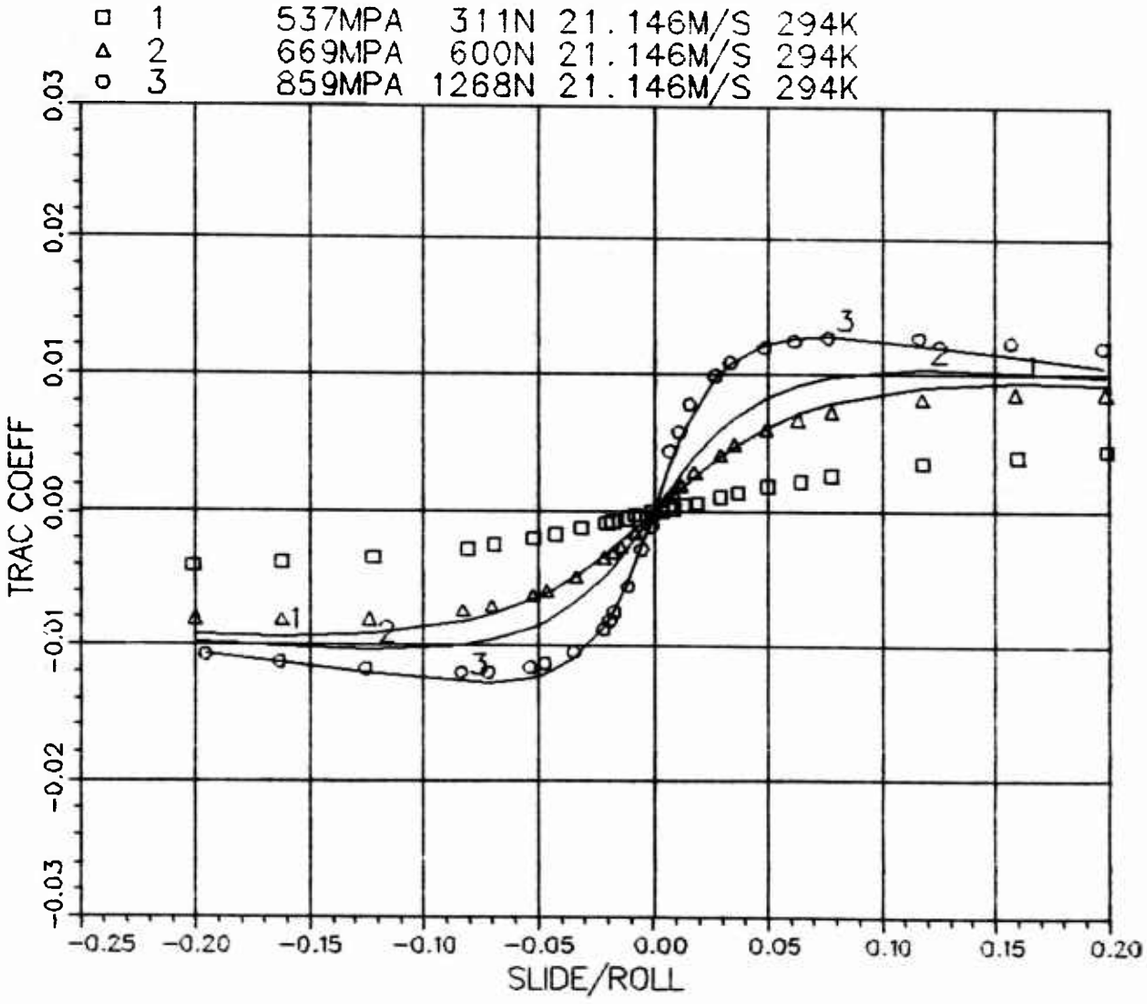

C1-2 MIL-L-23699 1.5/36 70F 7640RPM

1 2.940E+02 2.651E-01 5.802E-09 5.075E-02 3.046E-07

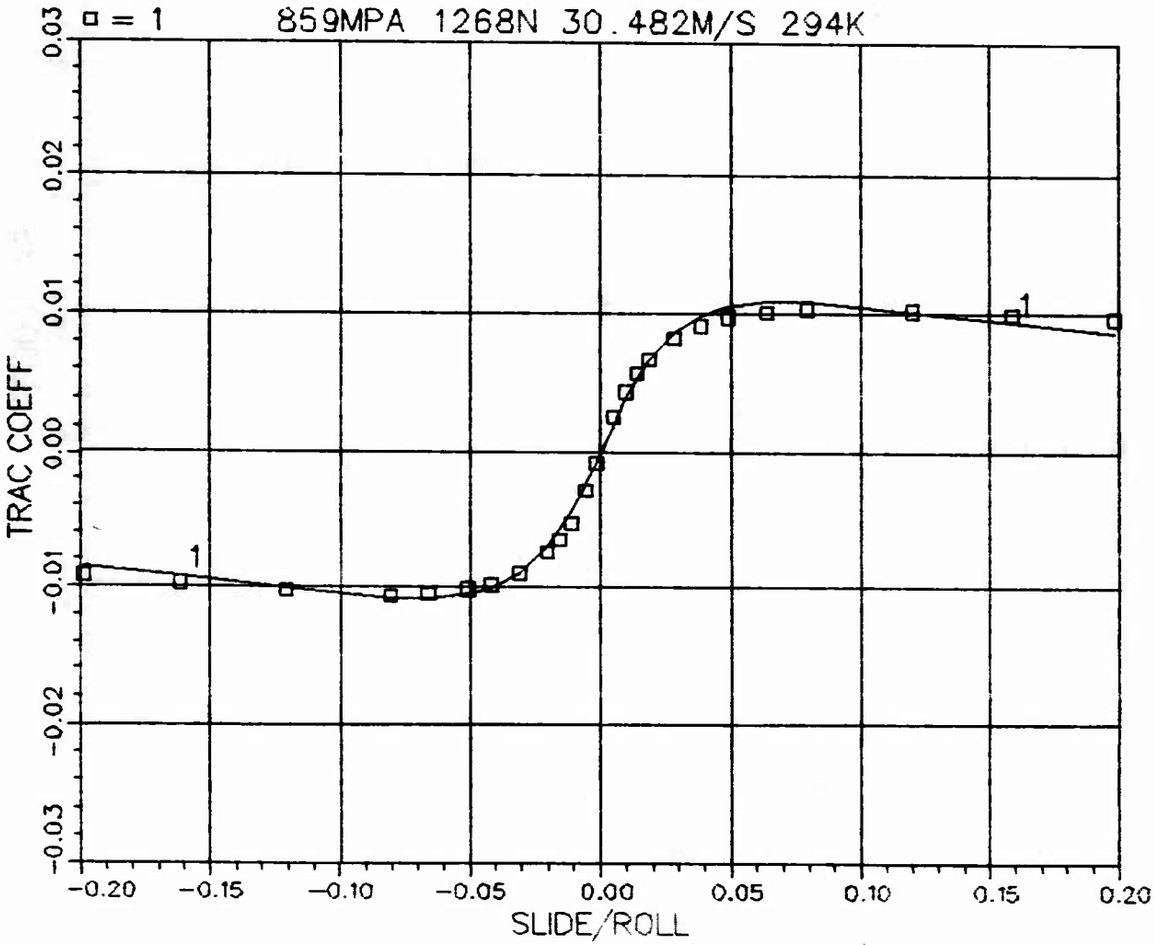

C1-2 MIL-L-23699 1.5/36 70F 7640RPM

2 2.940E+02 2.777E-01 5.802E-09 5.110E+03 1.905E-07

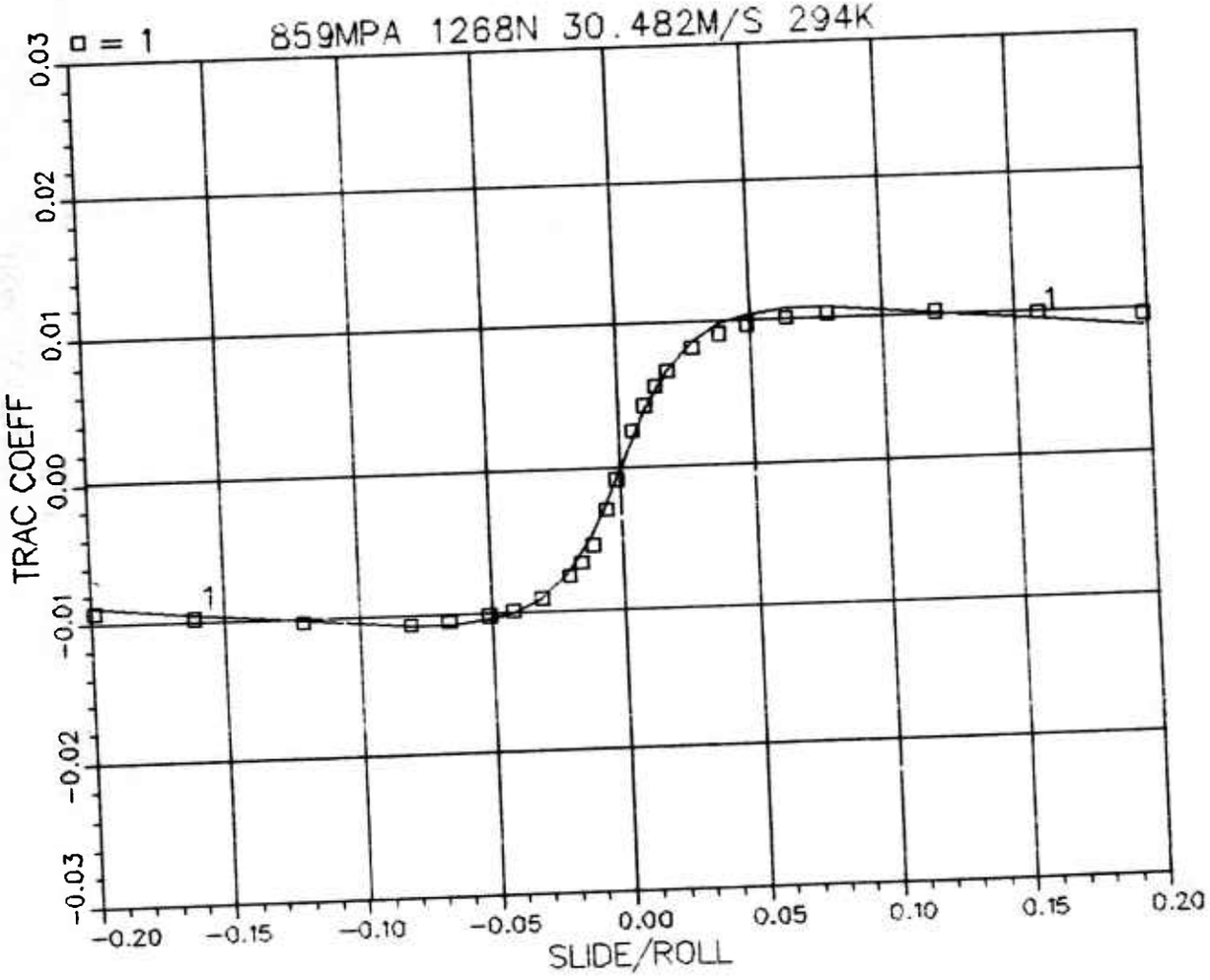

C1-3 MIL-L-23699 1.5/26 70F 11415RPM

1 2.940E+02 7.182E-02 5.802E-09 3.998E-02 6.326E-07

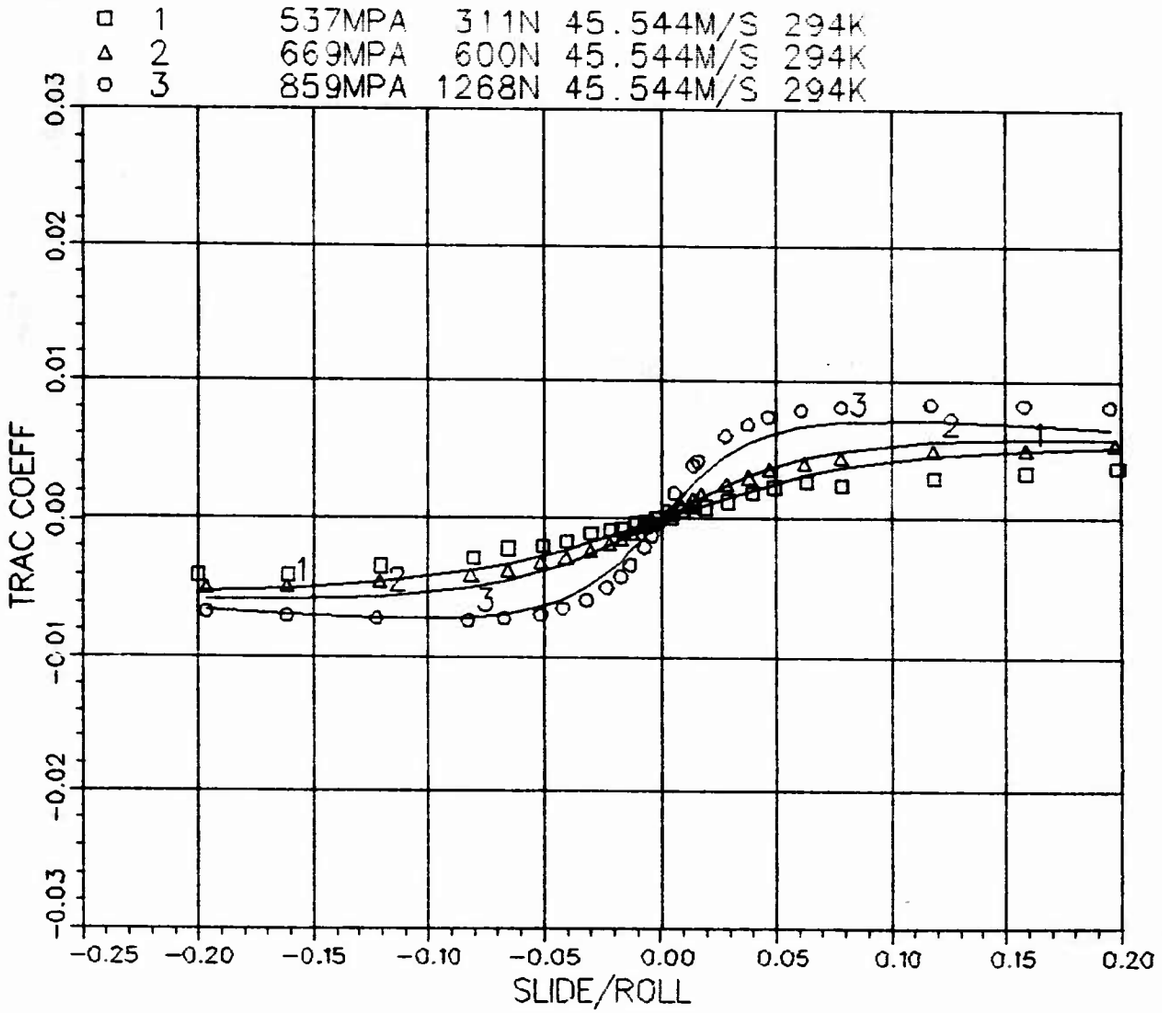

C1-3 MIL-L-23699 1.5/26 70F 11415RPM

2 2.940E+02 9.958E-02 5.802E-09 4.348E+03 7.631E-08

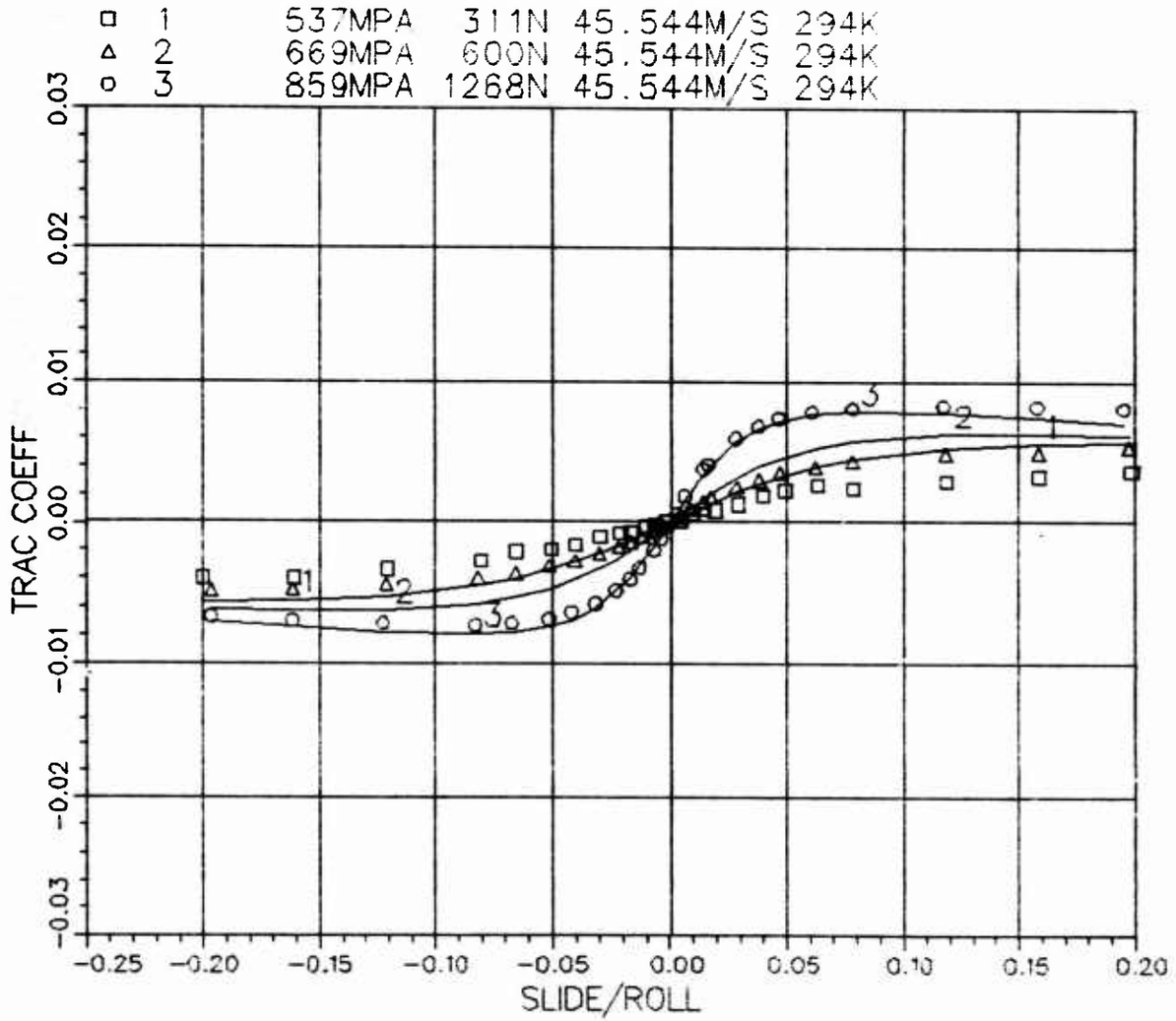

C2-1 MIL-L-23699 1.5/36 120F 5300RPM

1 3.220E+02 1.290E-01 5.802E-09 5.621E-02 8.101E-07

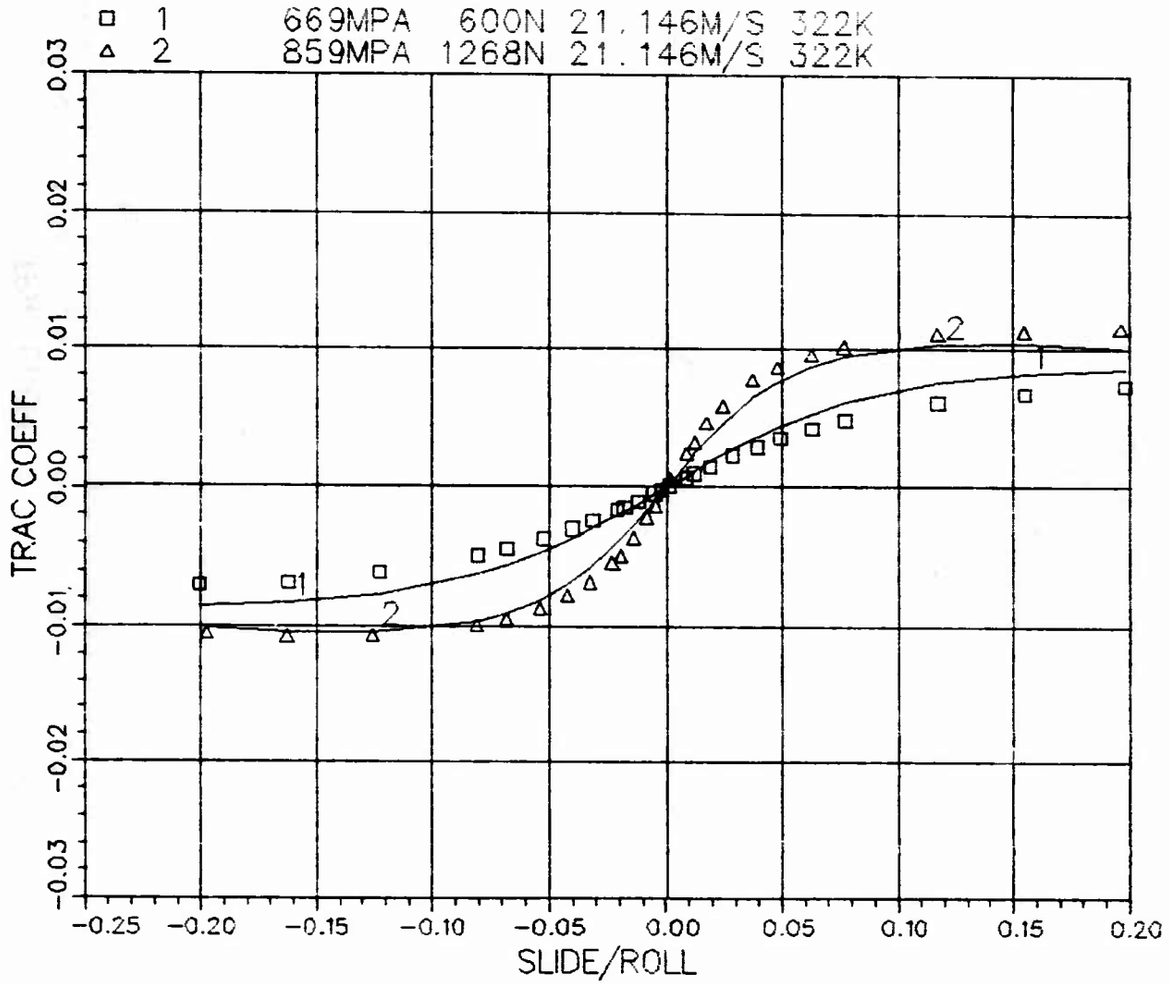

C2-1 MIL-L-23699 1.5/36 120F 5300RPM

2 3.220E+02 1.571E-01 5.802E-09 6.851E+03 1.108E-07

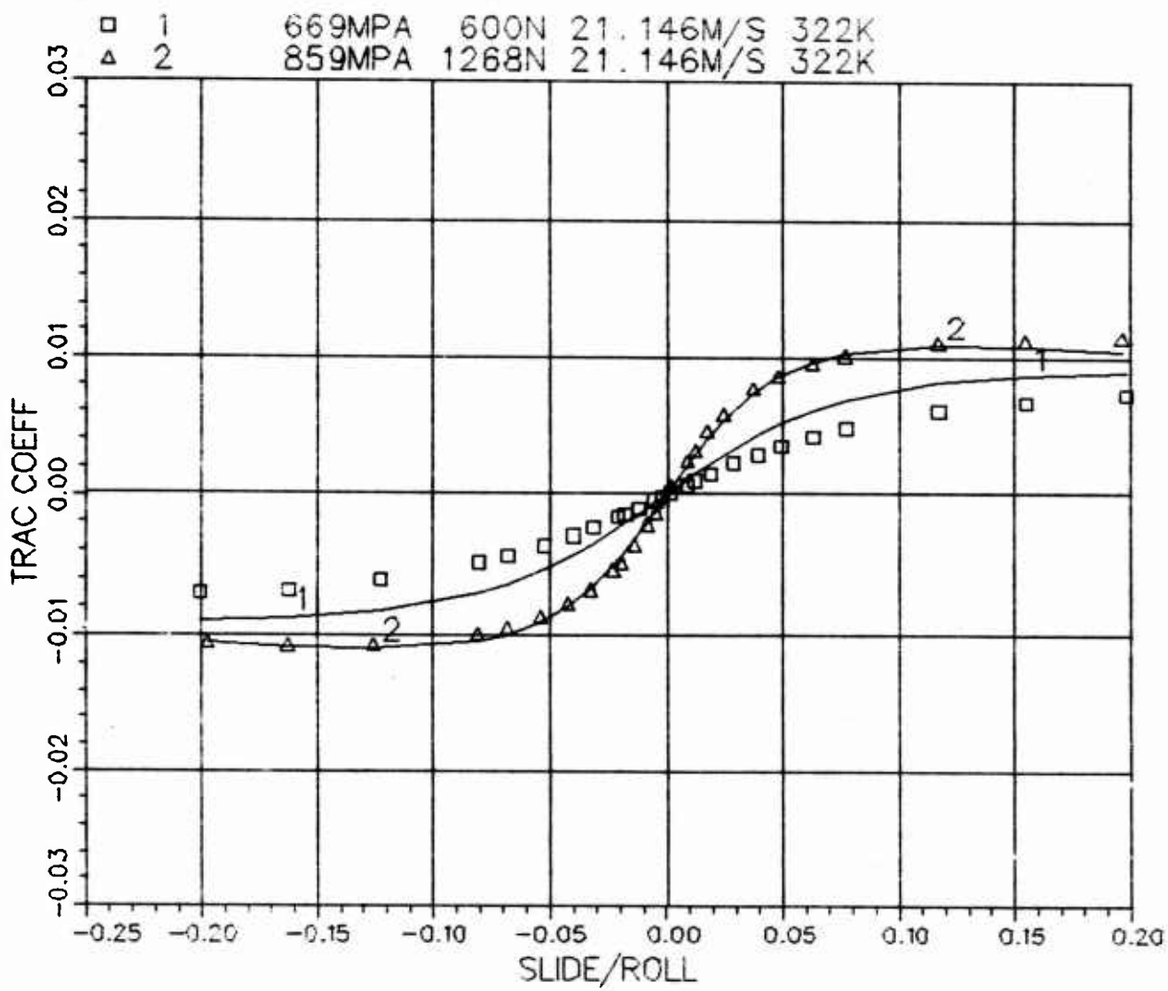

C2-3 MIL-L-23699 1.5/1.6 120F 11415RPM

1 3.220E+02 4.668E-02 5.802E-09 4.984E-02 1.769E-07

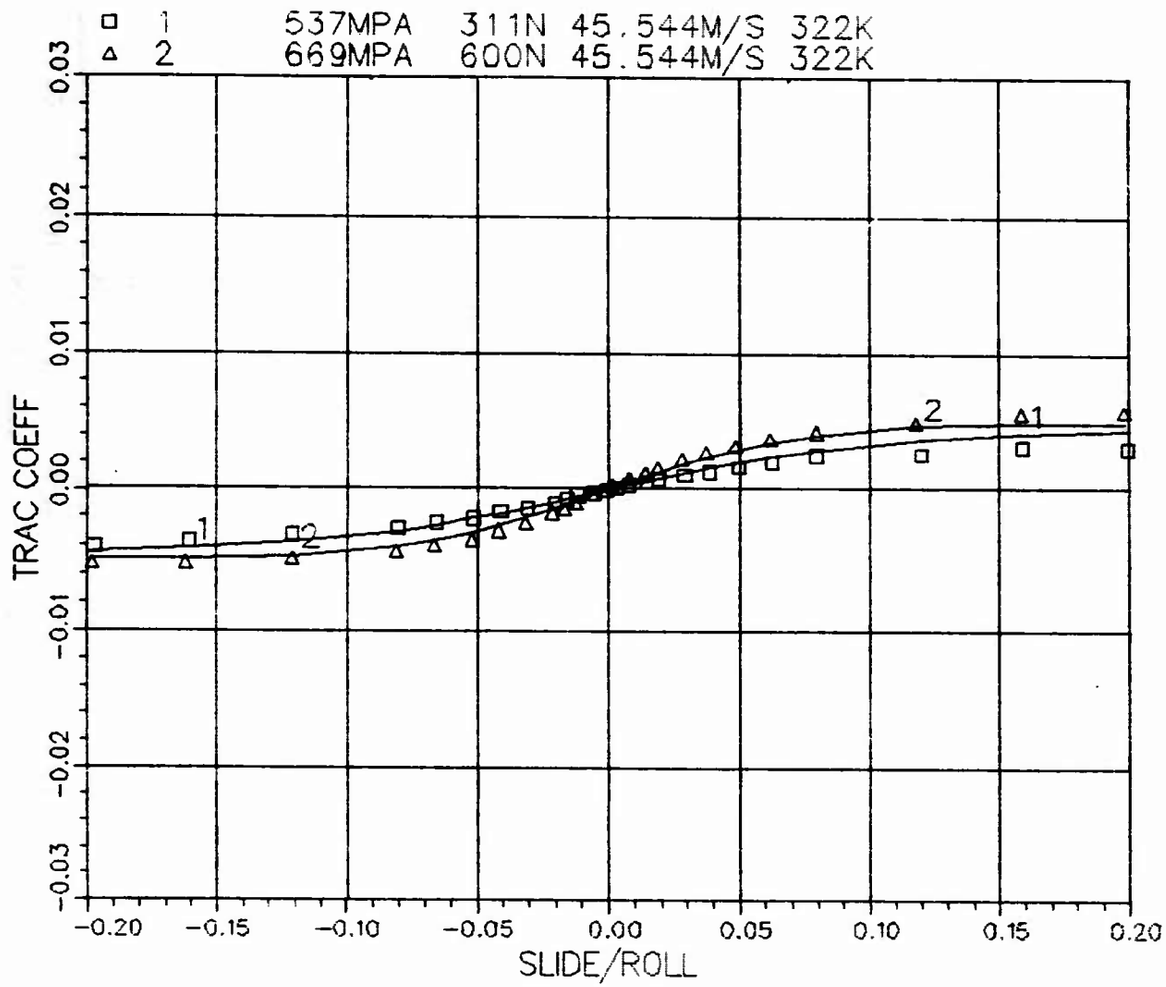

C2-3 MIL-L-23699 1.5/1.6 120F 11415RPM

2 3.220E+02 5.358E-02 5.802E-09 5.491E+03 2.176E-08

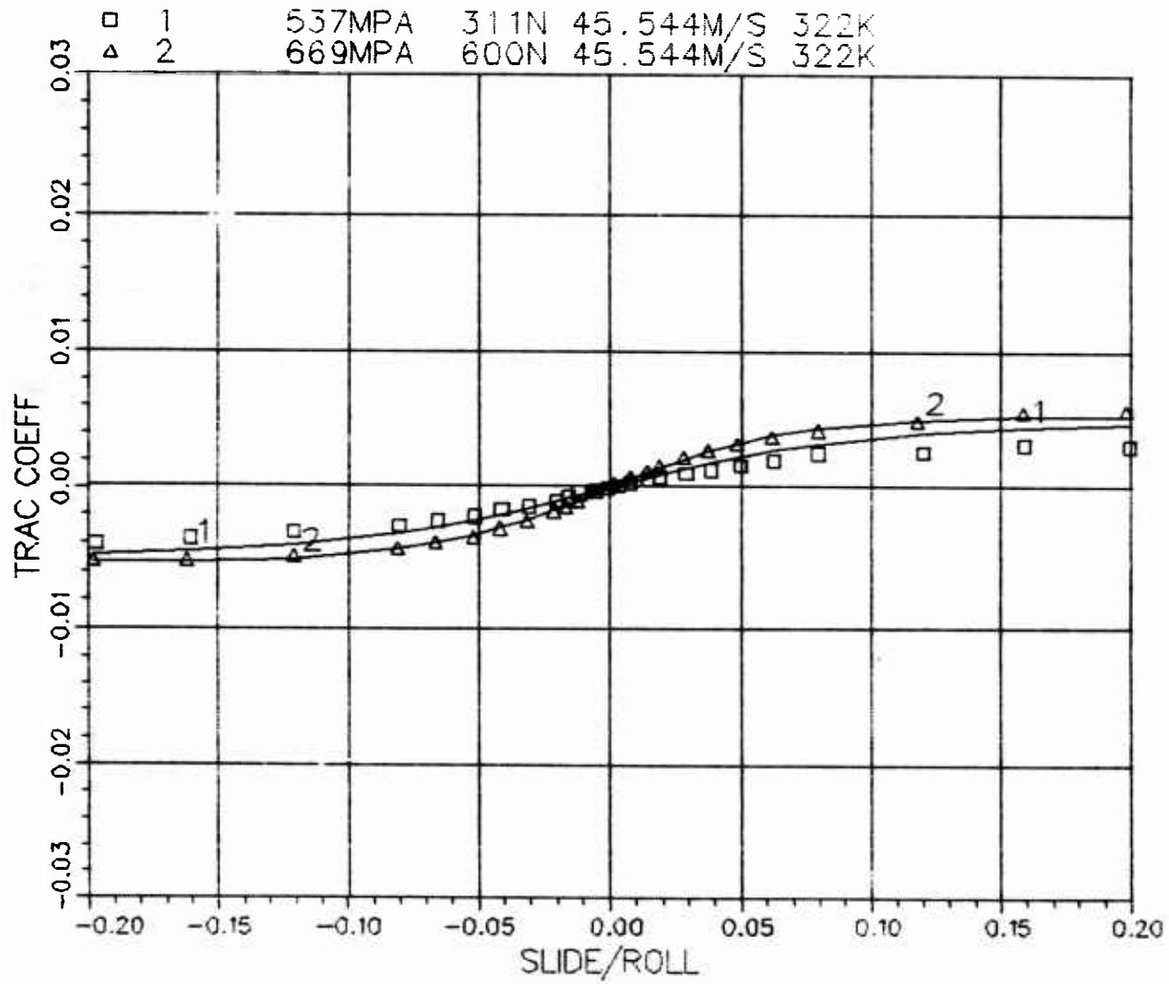

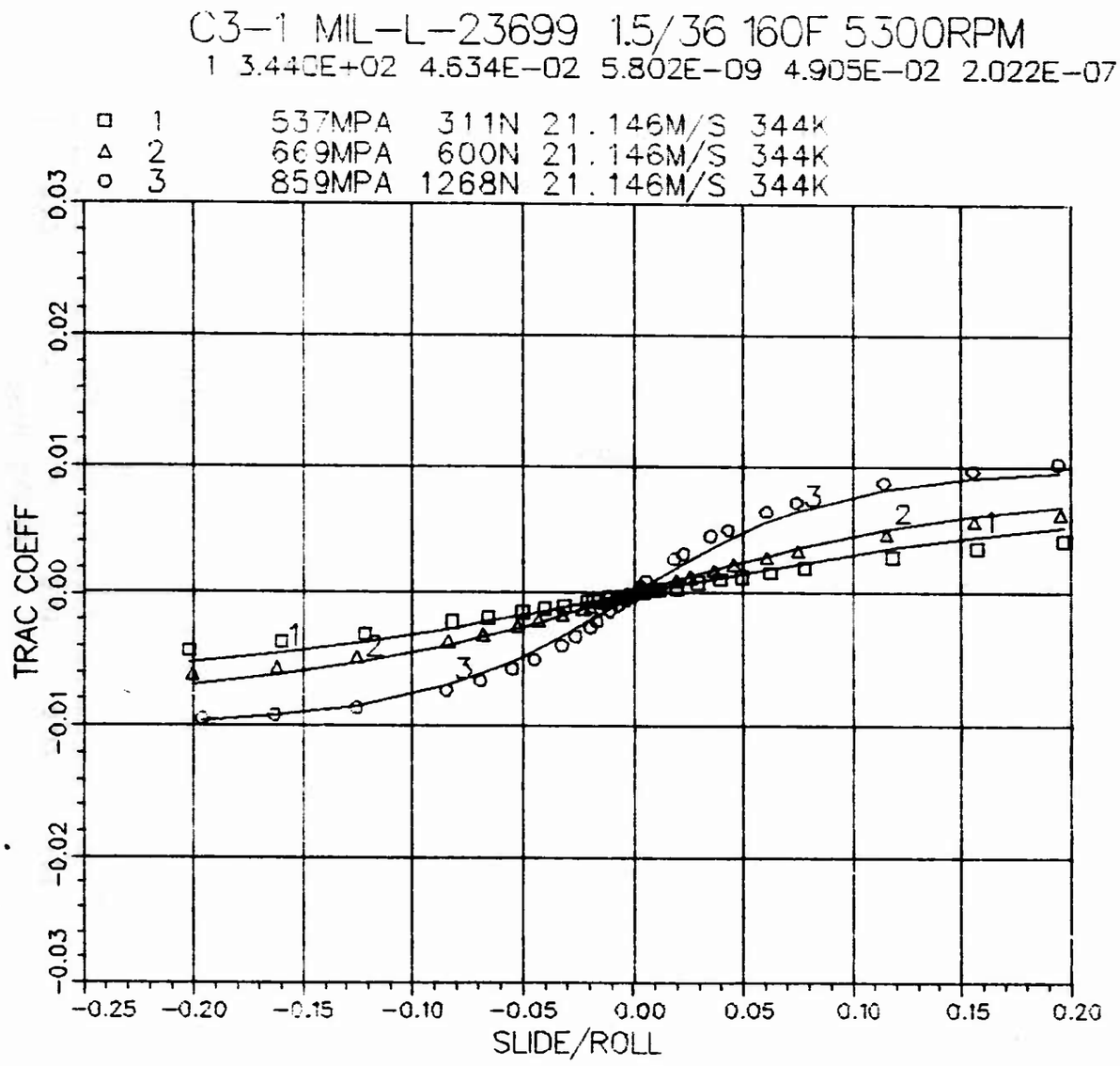
C3-1 MIL-L-23699 1.5/36 160F 5300RPM
1 3.440E+02 4.634E-02 5.802E-09 4.905E-02 2.022E-07
1 537MPA 311N 21.146M/S 344K
2 669MPA 600N 21.146M/S 344K
3 859MPA 1268N 21.146M/S 344K
TRAC COEFF
SLIDE/ROLL
0.03
0.02
0.01
0.00
-0.01
-0.02
-0.03
-0.25
-0.20
-0.15
-0.10
-0.05
0.00
0.05
0.10
0.15
0.20

C3-1 MIL-L-23699 1.5/36 160F 5300RPM

2 3.440E+02 5.646E-02 5.802E-09 7.632E+03 1.963E-08

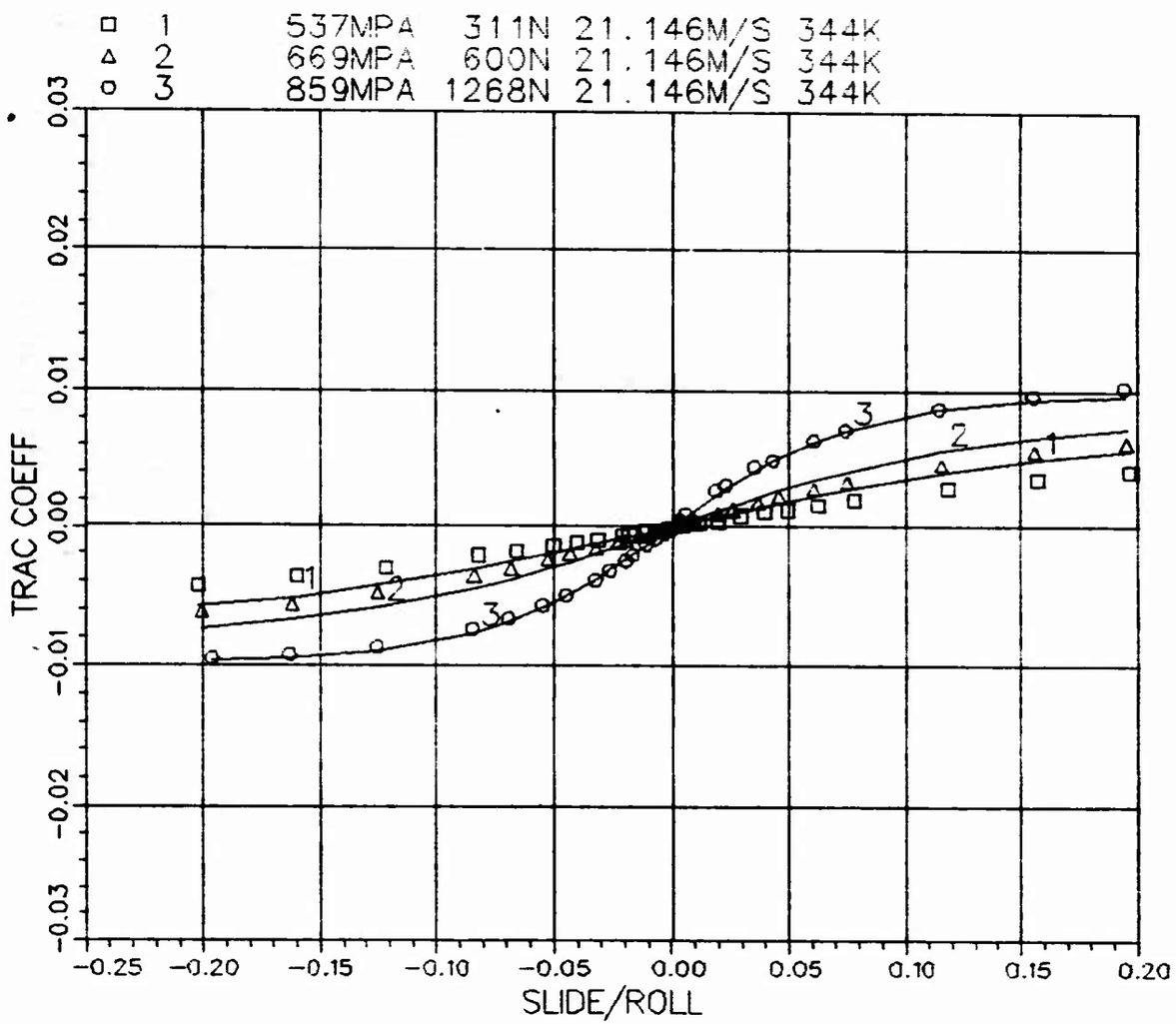

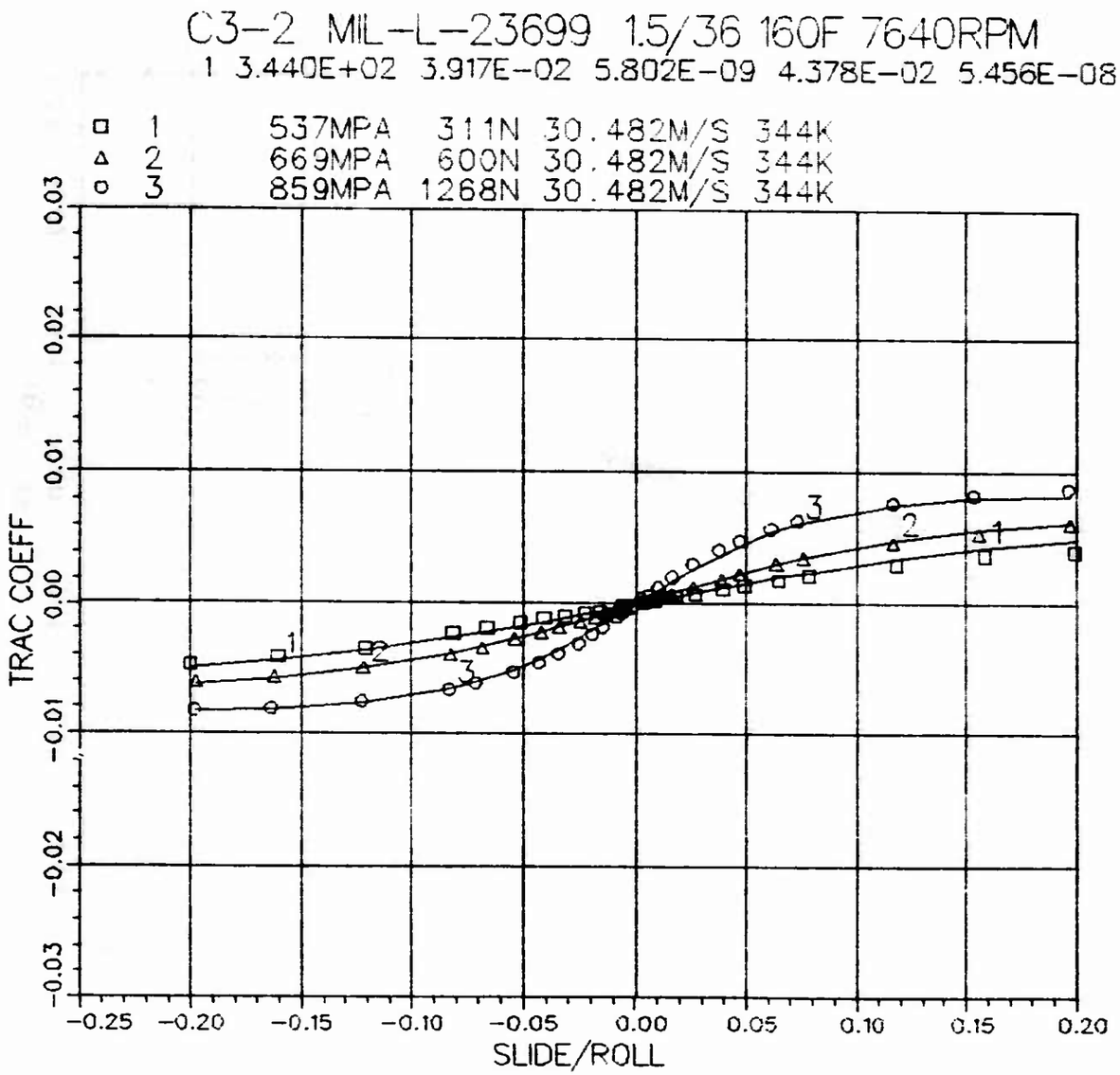
C3-2 MIL-L-23699 1.5/36 160F 7640RPM
1 3.440E+02 3.917E-02 5.802E-09 4.378E-02 5.456E-08
1 537MPA 311N 30.482M/S 344K
2 669MPA 600N 30.482M/S 344K
3 859MPA 1268N 30.482M/S 344K
TRAC COEFF
0.03
0.02
0.01
0.00
-0.01
-0.02
-0.03
-0.25 -0.20 -0.15 -0.10 -0.05 0.00 0.05 0.10 0.15 0.20
SLIDE/ROLL

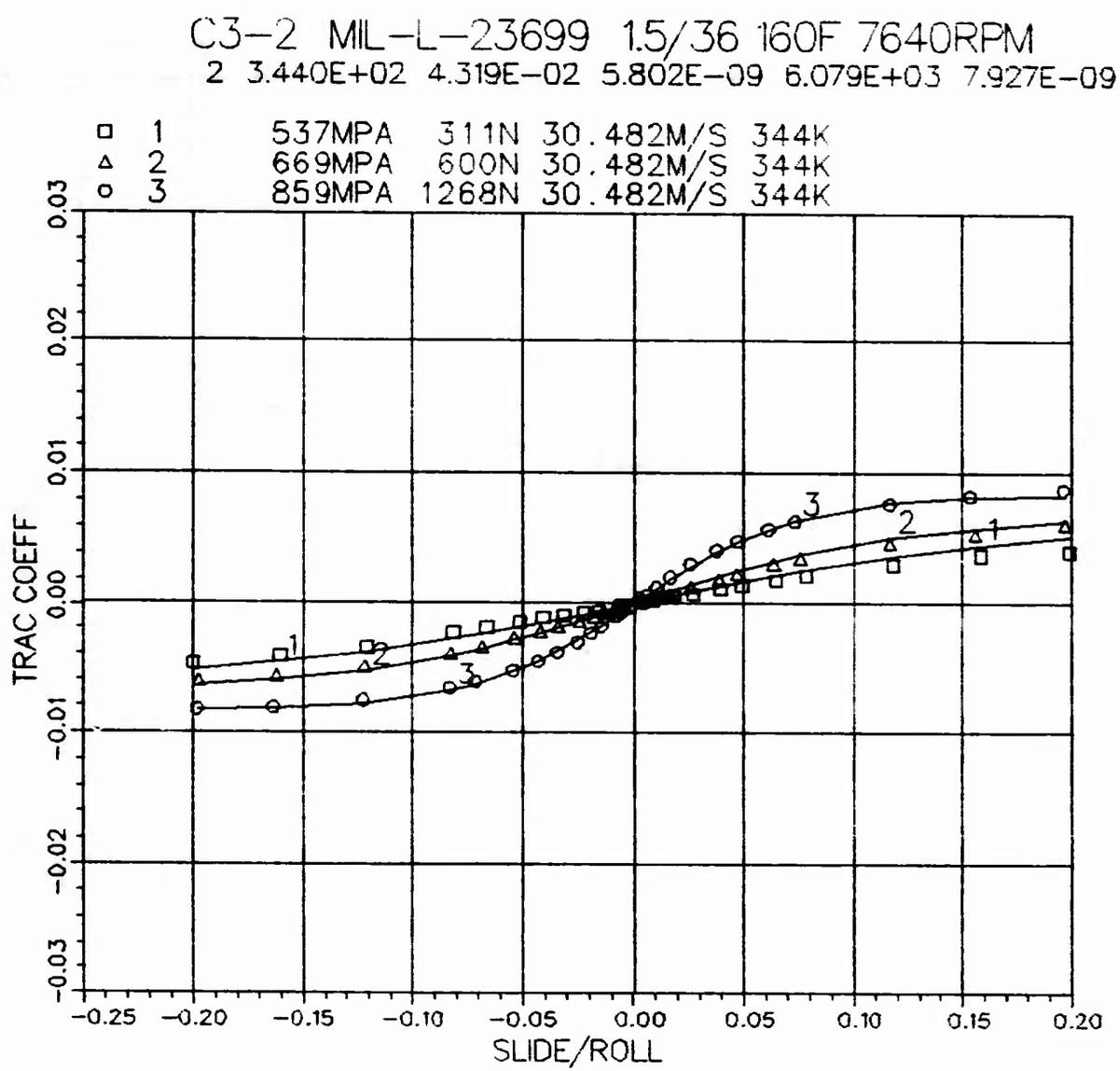
C3-2 MIL-L-23699 1.5/36 160F 7640RPM
2 3.440E+02 4.319E-02 5.802E-09 6.079E+03 7.927E-09
□ 1 537MPA 311N 30.482M/S 344K
△ 2 669MPA 600N 30.482M/S 344K
○ 3 859MPA 1268N 30.482M/S 344K
TRAC COEFF
0.03
0.02
0.01
0.00
-0.01
-0.02
-0.03
-0.25
-0.20
-0.15
-0.10
-0.05
0.00
0.05
0.10
0.15
0.20
SLIDE/ROLL

C3-3 MIL-L-23699 1.5/36 160F 11415RPM

1 3.440E+02 3.103E-02 5.802E-09 4.692E-02 2.954E-08

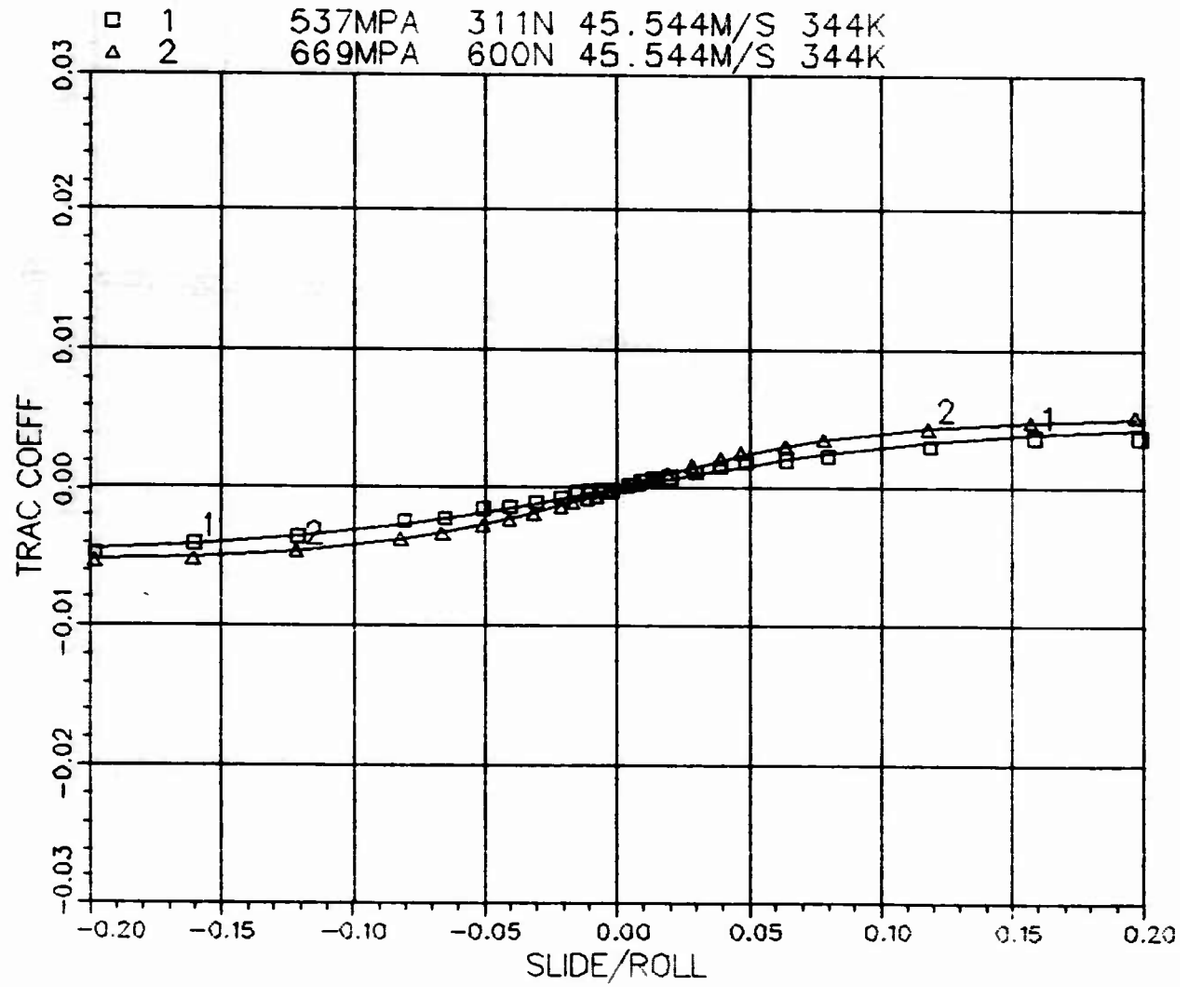

C3-3 MIL-L-23699 1.5/36 160F 11415RPM

2 3.440E+02 3.215E-02 5.802E-09 5.969E+03 3.567E-09

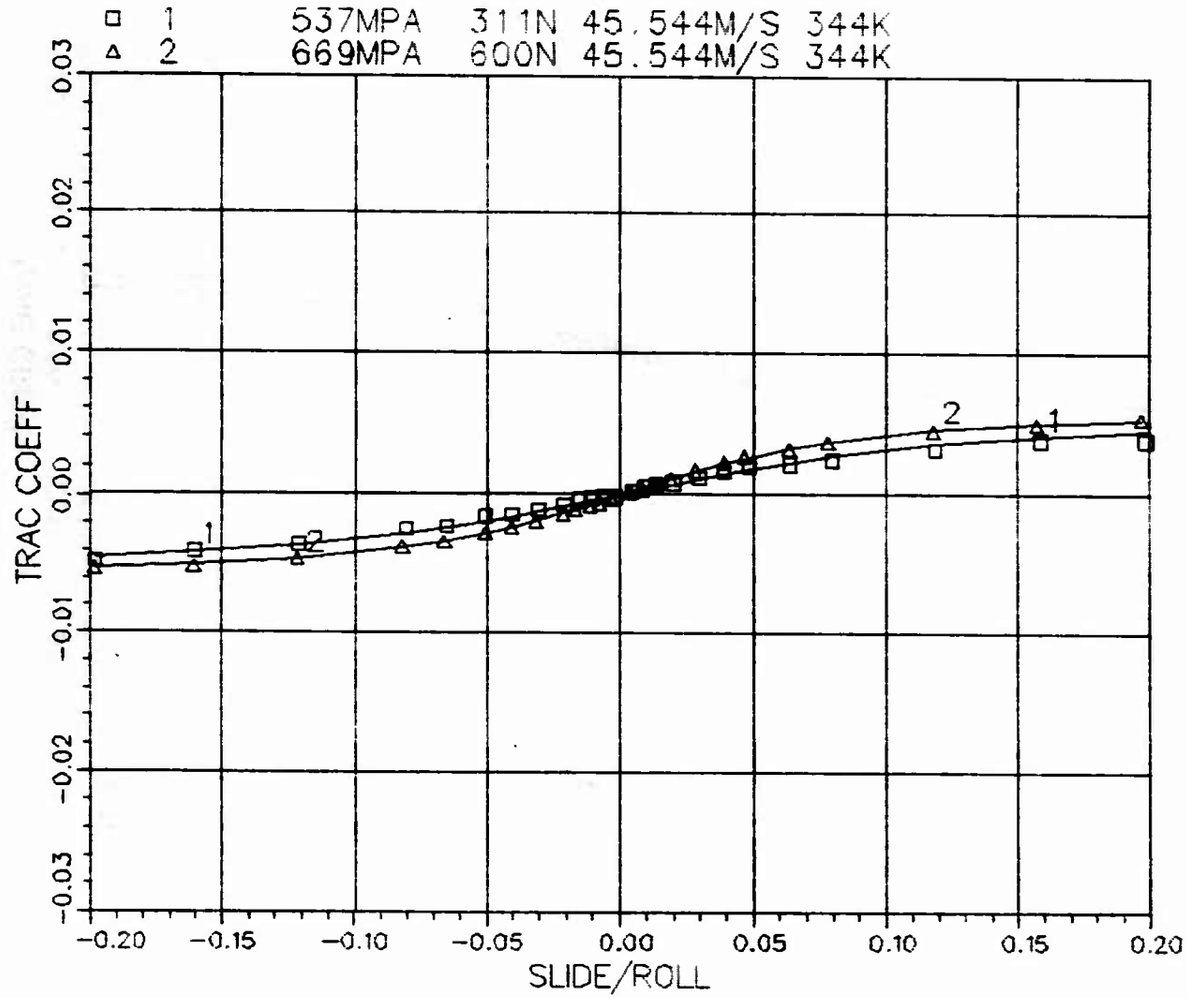

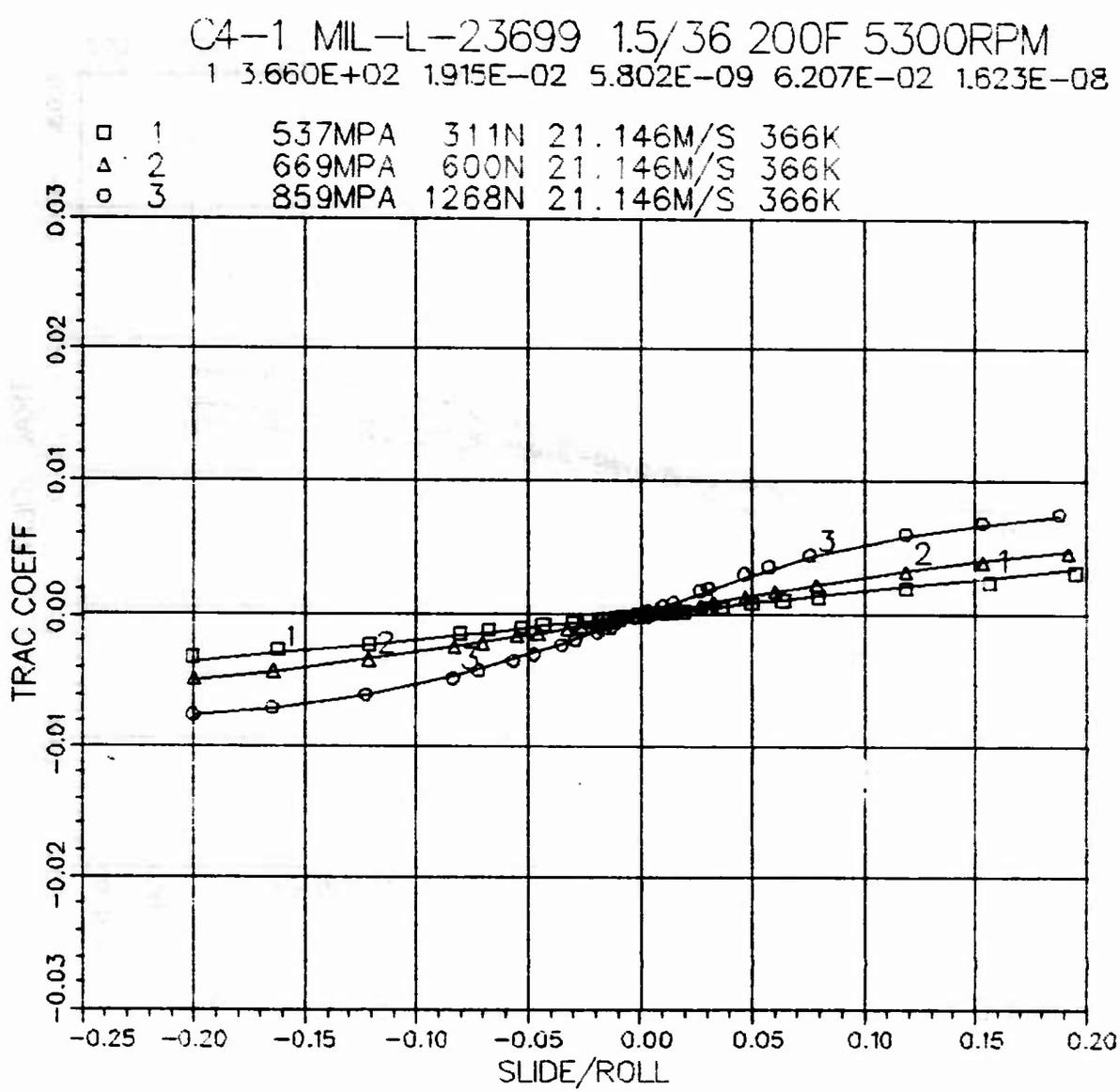
C4-1 MIL-L-23699 1.5/36 200F 5300RPM
1 3.660E+02 1.915E-02 5.802E-09 6.207E-02 1.623E-08
1 537MPA 311N 21.146M/S 366K
2 669MPA 600N 21.146M/S 366K
3 859MPA 1268N 21.146M/S 366K
TRAC COEFF
SLIDE/ROLL
0.03
0.02
0.01
0.00
-0.01
-0.02
-0.03
-0.25
-0.20
-0.15
-0.10
-0.05
0.00
0.05
0.10
0.15
0.20

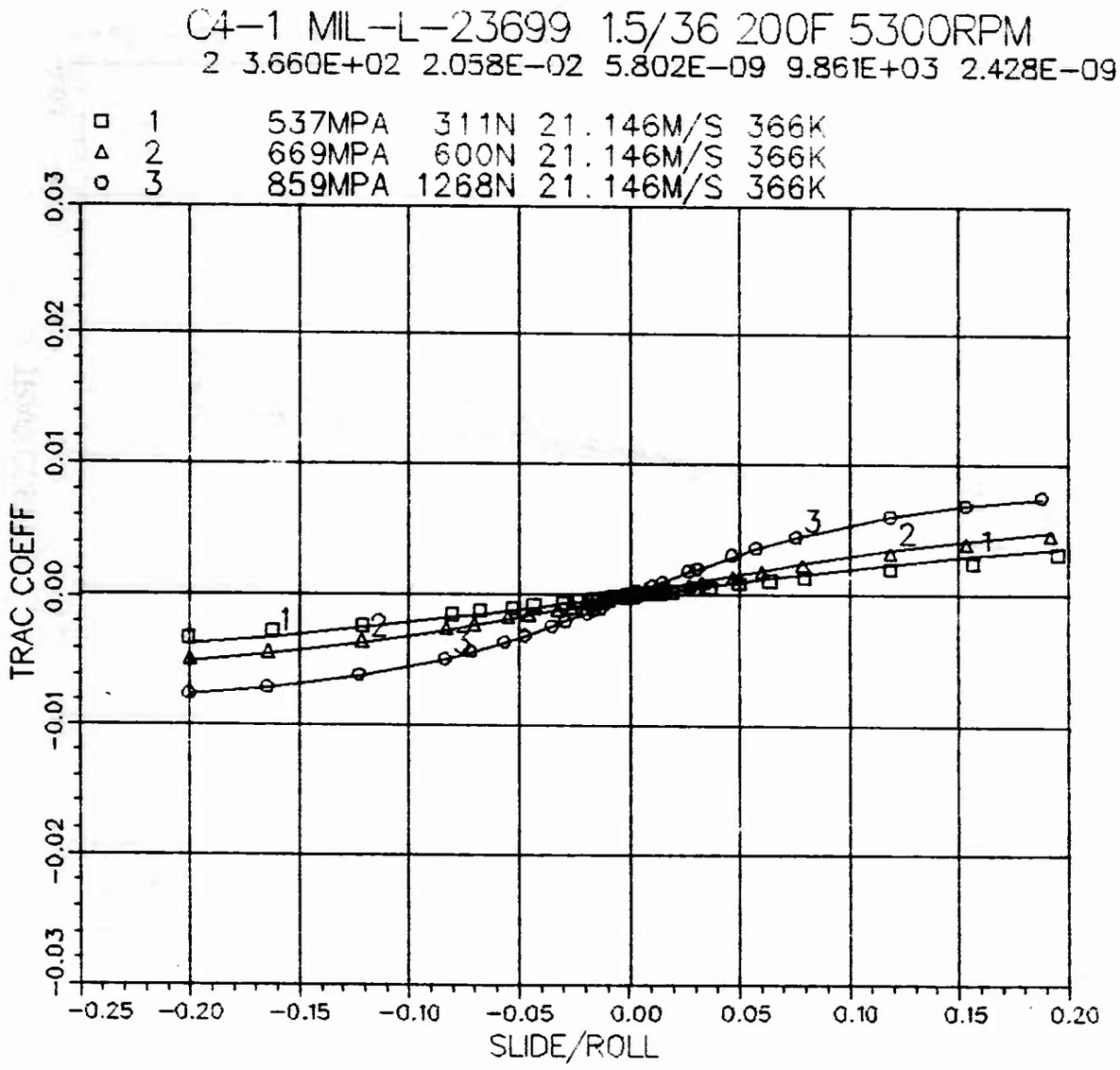
C4-1 MIL-L-23699 1.5/36 200F 5300RPM
2 3.660E+02 2.058E-02 5.802E-09 9.861E+03 2.428E-09
1 537MPA 311N 21.146M/S 366K
2 669MPA 600N 21.146M/S 366K
3 859MPA 1268N 21.146M/S 366K
TRAC COEFF
SLIDE/ROLL
0.03
0.02
0.01
0.00
-0.01
-0.02
-0.03
-0.25
-0.20
-0.15
-0.10
-0.05
0.00
0.05
0.10
0.15
0.20

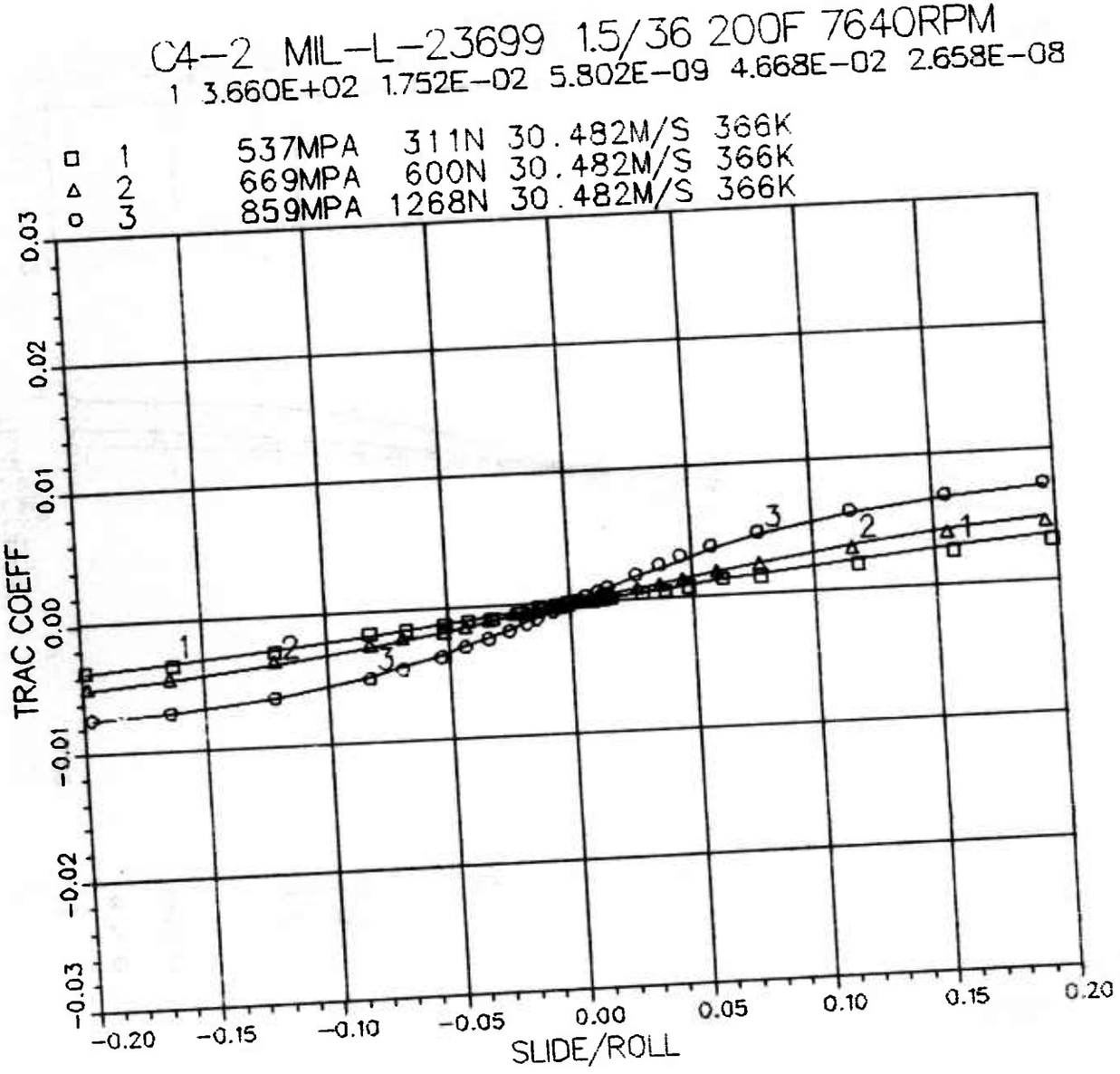
C4-2 MIL-L-23699 1.5/36 200F 7640RPM
1 3.660E+02 1.752E-02 5.802E-09 4.668E-02 2.658E-08
□ 1 537MPA 311N 30.482M/S 366K
△ 2 669MPA 600N 30.482M/S 366K
○ 3 859MPA 1268N 30.482M/S 366K
TRAC COEFF
SLIDE/ROLL
0.03
0.02
0.01
0.00
-0.01
-0.02
-0.03
-0.20
-0.15
-0.10
-0.05
0.00
0.05
0.10
0.15
0.20

C4-2 MIL-L-23699 1.5/36 200F 7640RPM

2 3.660E+02 1.896E-02 5.802E-09 7.307E+03 2.390E-09

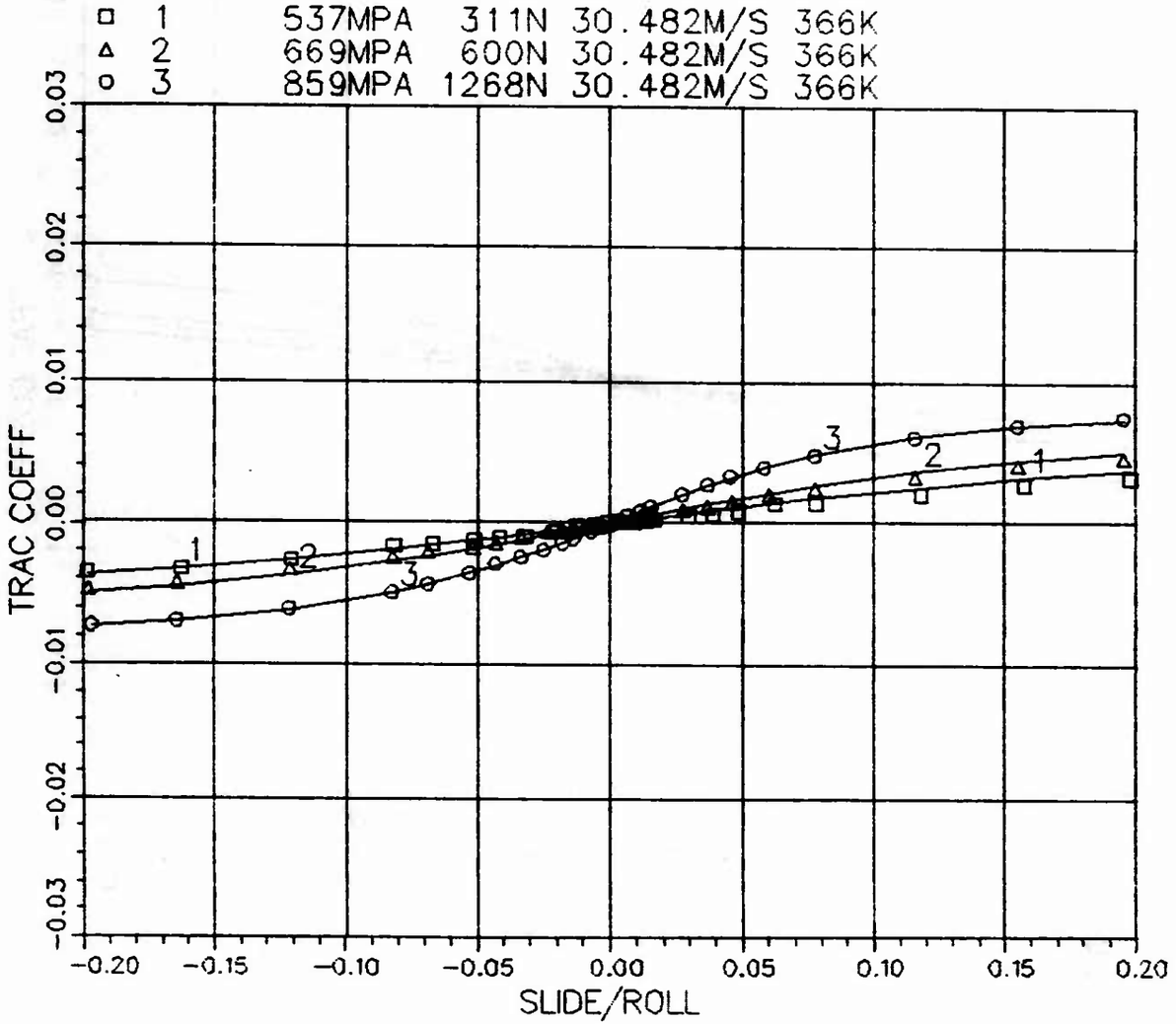

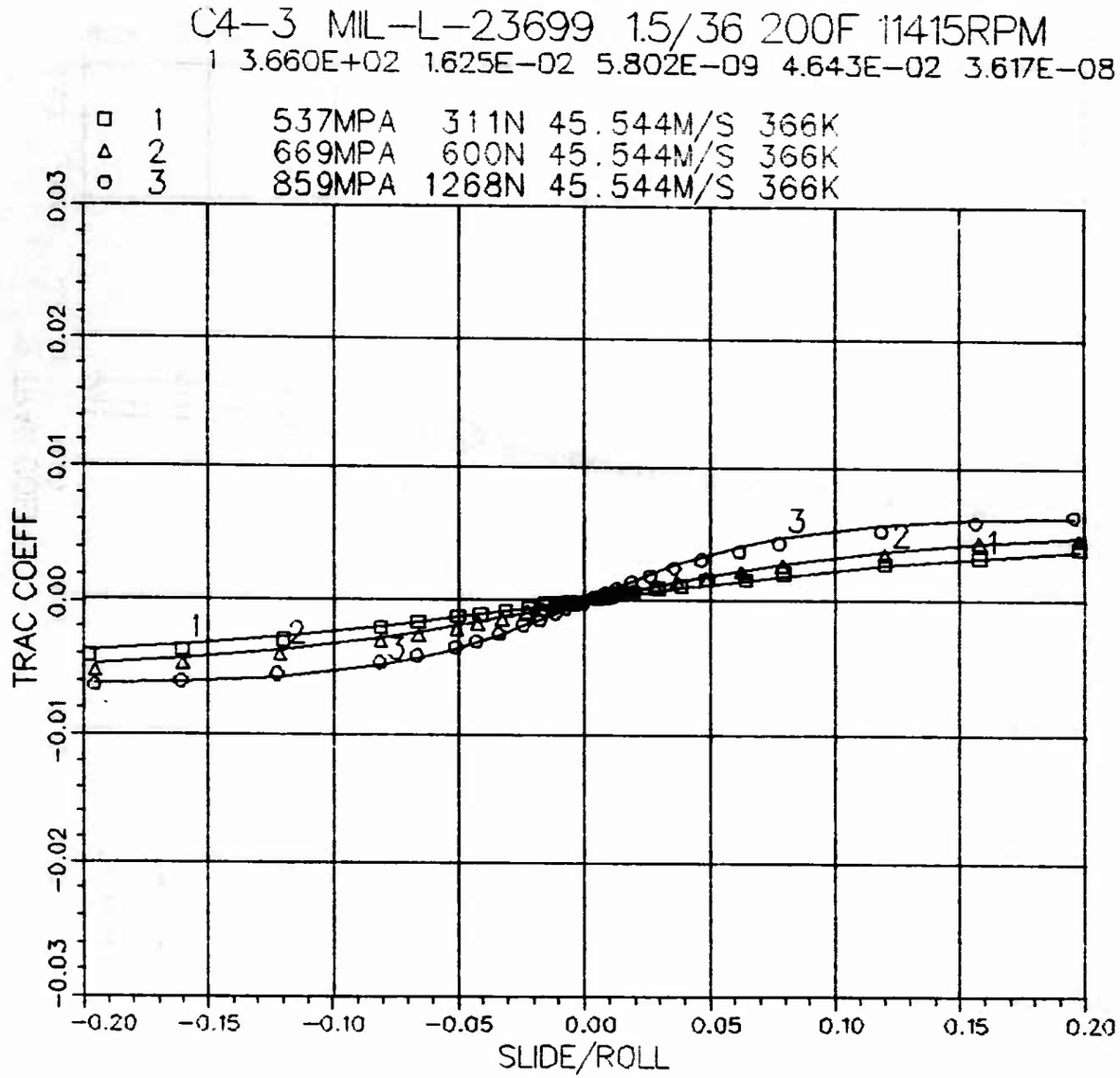
C4-3 MIL-L-23699 1.5/36 200F 11415RPM
1 3.660E+02 1.625E-02 5.802E-09 4.643E-02 3.617E-08
1 537MPA 311N 45.544M/S 366K
2 669MPA 600N 45.544M/S 366K
3 859MPA 1268N 45.544M/S 366K
TRAC COEFF
0.03
0.02
0.01
0.00
-0.01
-0.02
-0.03
-0.20
-0.15
-0.10
-0.05
0.00
0.05
0.10
0.15
0.20
SLIDE/ROLL

*U.S.Government Printing Office: 1987 — 748-061/60686

C4—3 MIL—L—23699 1.5/36 200F 11415RPM

2 3.660E+02 1.498E—02 5.802E—09 6.113E+03 3.581E—09

□	1	537MPA	311N	45.544M/S	366K
△	2	669MPA	600N	45.544M/S	366K
○	3	859MPA	1268N	45.544M/S	366K